Julius-Maximilians-Universität Würzburg

Function and regulation of phospholipase D in blood platelets: *in vitro* and *in vivo* studies in mice

Funktion und Regulation von Phospholipase D in Thrombozyten: *in vitro* und *in vivo* Studien in Mäusen

Doctoral thesis for a doctoral degree

at the Graduate School of Life Sciences

Section Biomedicine

submitted by

Ina Thielmann

from

Flensburg

Würzburg, 2014

Submitted on: ……………………………………………………………………………………

Members of the *Promotionskomitee*:

Chairperson: Prof. Dr. Thomas Dandekar

Primary Supervisor: Prof. Dr. Bernhard Nieswandt

Supervisor (Second): PD Dr. Heike Hermanns

Supervisor (Third): Prof. Dr. Manfred Gessler

Date of Public Defence: ………………………………………………………………

Date of Receipt of Certificates: …………………………………………………….

Summary

Platelet activation and aggregation are crucial for primary hemostasis but can also result in occlusive thrombus formation. Agonist induced platelet activation involves different signaling pathways leading to the activation of *phospholipases* (PL) which produce second messengers. While the role of PLCs in platelet activation is well established, less is known about the relevance of PLDs. In the current study, the function and regulation of PLD in platelets was investigated using genetic and pharmacological approaches.

In the first part of this thesis, adhesion, activation and aggregation of platelets from mice lacking PLD2 or both PLD1 and PLD2 were analyzed *in vitro* and *in vivo*. While the absence of PLD2 resulted in slightly reduced PLD activity in platelets, it had no detectable effect on the platelet function *in vitro* and *in vivo*. However, the combined deficiency of both PLD isoforms resulted in defective α-granule release and protection in a model of ferric chloride induced arteriolar thrombosis, effects that were not observed in mice lacking only one PLD isoform. These results revealed, for the first time, redundant roles of PLD1 and PLD2 in platelet α-granule secretion and indicate that this may be relevant for pathological thrombus formation. Thus, PLD might represent a promising target for antithrombotic therapy.

Thus, this hypothesis was tested more directly in the second part of this thesis. The effects of pharmacological inhibition of PLD activity on hemostasis, thrombosis and thrombo-inflammatory brain infarction in mice were assessed. Treatment of platelets with the reversible, small molecule PLD inhibitor *5-Fluoro-2-indolyl des-chlorohalopemide* (FIPI) led to a specific blockade of PLD activity that was associated with reduced α-granule release and integrin activation. Mice that received FIPI at a dose of 3 mg/kg displayed reduced occlusive thrombus formation upon chemical injury of carotid arteries or mesenterial arterioles. Similarly, FIPI-treated mice had smaller infarct sizes and significantly better motor and neurological function 24 hours after transient middle cerebral artery occlusion. This protective effect was not associated with major intracerebral hemorrhage or prolonged tail bleeding times. Thus, pharmacological PLD inhibition might represent a safe therapeutic strategy to prevent arterial thrombosis or ischemic stroke.

After revealing a central role for PLD in thrombo-inflammation, the regulation of PLD activity in platelets was analyzed in the last part of the thesis. Up to date, most studies made use of inhibitors potentially exerting off-target effects and consequently PLD regulation is discussed controversially. Therefore, PLD activity in mice genetically lacking potential modulators of PLD activity was determined to address these controversies. These studies revealed that PLD is tightly regulated during initial platelet activation. While integrin outside-in signaling and G_i signaling was dispensable for PLD activation, it was found that PLC dependent pathways were relevant for the regulation of PLD enzyme activity.

Zusammenfassung

Thrombozytenaktivierung und -aggregation sowie die anschließende Thrombusbildung sind essentielle Prozesse während der primären Hämostase. Andererseits kann unkontrollierte Thrombozytenaktivierung zum Gefäßverschluss und somit zu Schlaganfall oder Herzinfarkt führen.

Verschiedene Signalwege, die für die Thrombozytenaktivierung von Bedeutung sind, führen zur Aktivierung von *Phospholipasen* (PL), die daraufhin sekundäre intrazelluläre Botenstoffe generieren. Während die Rolle von PLCs für die Thrombozytenaktivierung bekannt ist, ist die Relevanz der PLDs noch ungeklärt. Die vorliegende Arbeit untersucht die Funktion und Regulation von PLD in der Thrombozytenaktivierung und Thrombusbildung mittels genetisch veränderter Mäuse.

Im ersten Teil der Arbeit wurde die Adhäsion, Aktivierung und Aggregation von *Pld2*$^{-/-}$ und *Pld1*$^{-/-}$/*Pld2*$^{-/-}$ Thrombozyten *in vitro* und *in vivo* untersucht. Es konnte gezeigt werden, dass die Abwesenheit von PLD2 zu einer verminderten PLD Aktivität in Thrombozyten führte. Dies hatte allerdings keinen erkennbaren Effekt auf die Funktion der Thrombozyten *in vitro* und *in vivo*. Die PLD doppel-defizienten Thrombozyten hingegen wiesen Defekte bei der Sekretion der α-Granula auf, was zur Bildung von instabilen FeCl$_3$-induzierten Thromben in einem *in vivo* Thrombosemodell führte. Diese Effekte waren in den einzeldefizienten Mäusen nicht vorhanden, was auf redundante Funktionen von PLD1 und PLD2 in diesem Prozess schließen lässt. Interessanterweise wurden keine hämostatischen Defekte durch die Doppeldefizienz hervorgerufen. Die vorliegenden Ergebnisse zeigen, dass PLD eine neue potentielle antithrombotische Zielstruktur darstellt.

Diese Hypothese wurde im zweiten Teil der Arbeit weiter überprüft. Der Effekt einer PLD Hemmung durch den reversiblen PLD Inhibitor *5-Fluoro-2-indolyl des-chlorohalopemide* (FIPI) auf Hämostase und Thrombose wurde untersucht. Es konnte gezeigt werden, dass die Behandlung von Mäusen mit FIPI zu einer spezifischen Blockade von PLD führte, die die α-Degranulierung und Integrinaktivierung, im ähnlichen Ausmaß wie in den doppeldefizienten Mäusen, beeinträchtigte. Des Weiteren zeigten Mäuse, die mit 3 mg/kg FIPI behandelt wurden, starke Defekte in der arteriellen Thrombusbildung in Makro- und Mikrogefäßen. FIPI vermittelte PLD Inhibition führte außerdem zu einem Schutz der Mäuse in einem Modell des ischämischen Schlaganfalls, ohne intrazerebrale Blutungen hervorzurufen. Diese Ergebnisse etablieren FIPI als potentiellen antithrombotischen Wirkstoff für eine effektive und sichere Behandlung von kardio- und zerebrovaskulären Erkrankungen.

Da PLD eine zentrale Rolle während der Thrombusbildung hat, wurde im letzten Teil der Arbeit auf die Regulation von PLD während der Thrombozytenaktivierung eingegangen. Bisherige Studien verwendeten häufig Inhibitoren, die zu unspezifischen Effekten führen können. Daher

wird die Regulation von PLD in der Literatur kontrovers diskutiert. Die Untersuchung der PLD Aktivität in verschiedenen knockout Mauslinien stellt einen nützlichen Ansatz dar, um die kontrovers diskutierte PLD Regulation aufzuklären. Zu diesem Zweck wurde die PLD Aktivität in genetisch veränderten Mäusen, denen potentielle Regulatoren von PLD fehlen, gemessen. Im Zuge diesen Untersuchungen konnte gezeigt werden, dass integrinabhängige- und G_i-vermittelte Signalwege keinen Einfluss auf die Regulation von PLD hatten, während PLC vermittelte Signale von Bedeutung waren.

Table of contents

1 Introduction

1.1 Platelets

Platelets are small, anucleated, discoid-shaped cell fragments that are released from *bone marrow* (BM) *megakaryocytes* (MKs). Protrusions, reaching into the sinusoidal vessels of the BM, are shed off by shear forces generated by the blood stream and get further fragmented into platelets [1]. This process is permanently maintained to balance the normal clearing of aged platelets by macrophages in the liver and spleen, keeping the platelet concentration at constant levels of 150,000-450,000/µl in humans and approximately 1,000,000/µl in mice. Human platelets have a lifespan of 7-10 days, whereas murine platelets circulate for approximately 5 days. With a diameter of 3-4 µm (1-2 µm in mice) they are the smallest cells in the blood. Their main function is to monitor the integrity of the vascular system. In addition to platelets, efficient hemostasis requires a functional coagulation system with its central product thrombin mediating the conversion of fibrinogen into fibrin and acting as a powerful platelet activator. The coagulation cascade can be initiated by *tissue factor* (TF), which is exposed upon vascular injury, or by negatively charged surfaces via the 'contact-activation' pathway (intrinsic coagulation) initiated by the activation of *coagulation factor* (F)XII.

Even though the vast majority of platelets is cleared without undergoing activation, platelets are capable of responding rapidly to damage of endothelial layers of the vessel wall by forming a plug that prevents excessive blood loss. The exposure of *extracellular matrix* (ECM) proteins, such as collagens and laminins, leads to initial platelet adhesion and activation. Subsequently, soluble mediators are released and secreted by activated platelets leading to the activation and recruitment of additional platelets at the injury site facilitating thrombus formation. However, under pathologic conditions, such as a rupture of an atherosclerotic plaque, the exposure of ECM proteins upon endothelial injury can cause an uncontrolled platelet reaction. This can lead to thrombotic events resulting in the obstruction of blood flow, the loss of oxygen supply and subsequent tissue damage, as seen in myocardial infarction and ischemic stroke [2]. Since these pathologies are the leading causes of death and disability in the developed world, there is a particular demand for the development of effective and safe antithrombotic therapies for the prophylaxis and treatment of ischemic cardio- and cerebrovascular diseases [3, 4].

Maintaining the balance of sealing a wound on the one hand and uncontrolled thrombotic events on the other hand requires a tight regulation of diverse activating and inhibitory platelet receptors and thus a complex network of signaling pathways.

1.2 Platelet activation and thrombus formation

As described above, blood platelets are responsible for maintaining the balance between hemostasis and thrombosis in the vascular system. The complex signaling process, which is involved in platelet activation and thrombus formation can be divided into three major steps: (1) platelet binding occurs via the interaction of platelet-receptors with exposed ECM constituents, thereby decelerating the platelets, (2) platelet activation encompasses the initiation of receptor triggered signaling cascades resulting in integrin activation and exocytosis of α- and dense granules and (3) firm adhesion and platelet aggregation is facilitated through the recruitment of further platelets into the growing thrombus and the remodeling of the platelet cytoskeleton leading to spreading on the reactive surface (Figure 1-1).
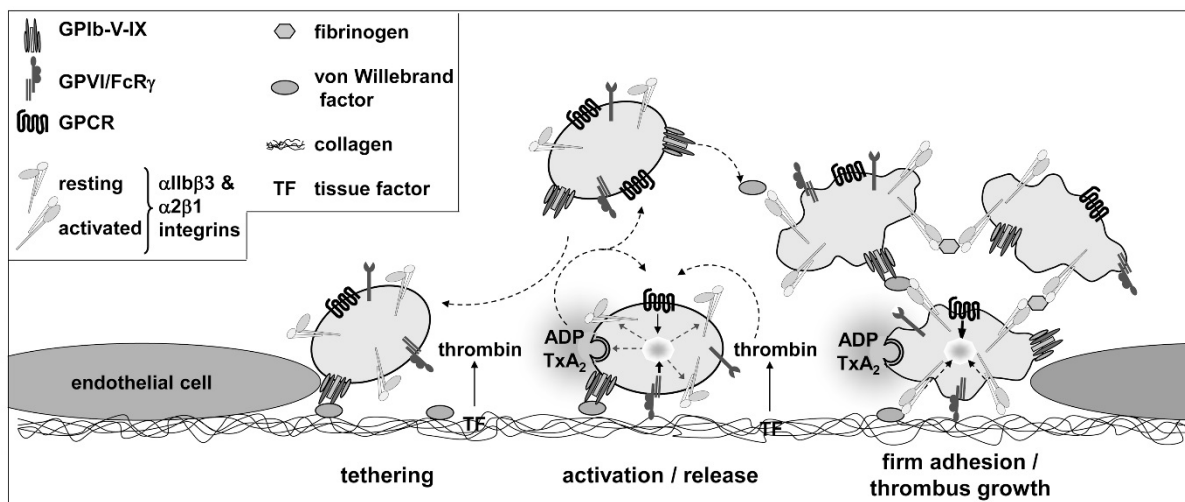
Figure 1-1: Multistep model of platelet activation and subsequent thrombus formation at sites of vascular injury. The interaction of *glycoprotein* (GP)Ibα to the exposed ECM decelerates the platelet and enables GPVI-collagen interaction. This triggers the release of soluble mediators such as *adenosine diphosphate* (ADP) and *thromboxane* (TX)A$_2$ and the shift of integrins from a low to a high affinity state. In parallel, locally released *tissue factor* (TF) induces thrombin formation enabling additional platelets to become activated and recruited into the growing thrombus. The forming thrombus is stabilized by firm platelet adhesion to the ECM via αIIbβ3-bound fibrinogen or vWF. Taken from Stegner *et al.*, 2011 [5].

In different vascular beds, different rheological conditions are present. In laminar blood flow, platelets are exposed to strong hemodynamic forces close to the vessel wall. This is due to shear forces between distinct fluid layers that are caused by different velocities of the fluid in the center and the periphery of the vessel [6]. Under high wall shear rates (>1000 s^{-1}), particularly present in arterioles or stenosed vessels, the interaction of the platelet receptor *glycoprotein* (GP)Ib and *von Willebrand Factor* (vWF), which is immobilized on exposed collagen, allows initial platelet tethering. This results in the deceleration of platelets enabling other platelet receptors to bind to the ECM [7]. Besides this function, activated GPIb can transduce signaling events leading to weak αIIbβ3 integrin activation. Although the underlying mechanisms are not fully understood proteins such as actin binding protein 14-3-3ζ, PI3K, Src

related tyrosine kinases, GTPase activating proteins and *phospholipase* (PL)D1 have been proposed to be important for GPIb dependent adhesion processes [6, 8].

Binding of the major platelet activating receptor GPVI to collagens leads to platelet activation downstream of the phosphorylation of the *immunoreceptor tyrosine-based activation motif* (ITAM)-bearing Fc *receptor* (FcR) *γ* chain [9]. Whereas the ITAM harbors two YXXL-motifs through which receptor activation is initiated, the transmembrane related *C-type lectin-like receptor* (CLEC)-2 encompasses only one YXXL-motif and is therefore a "hemITAM" receptor [10]. The Src family kinases Fyn and Lyn are involved in this phosphorylation step for ITAM signaling, while for hemITAM signaling the responsible kinases are still elusive. Subsequently, Syk kinase can bind to the phosphorylated ITAM motif and becomes autophosphorylated resulting in the phosphorylation of adaptor proteins such as *linker for activated T cells* (LAT), *growth factor receptor-bound protein* 2 (Grb2) and *Src homology 2 domain-containing leukocyte phosphoprotein of 76-kDa* (SLP-76). These events finally converge in the activation of effector molecules such as PLCγ2 or *phosphoinositide 3 kinase* (PI3K) [11, 12]. Activated PLCγ2 cleaves the membrane phospholipid *phosphatidylinositol-4,5-bisphosphate* (PIP$_2$) into *inositol-1,4,5-triphosphate* (IP$_3$) and *diacylglycerol* (DAG). IP$_3$ binds to the IP$_3$ receptor on the membrane of the intracellular *calcium* (Ca^{2+}) stores and induces the release of Ca^{2+} from the store into the cytosol. The decrease of Ca^{2+} level in the store is sensed by the sarcoplasmic membrane protein *stromal interaction molecule* (STIM) 1 via its EF hand domain. STIM1 induces, in turn, the opening of the *store operated Ca^{2+}* (SOC) channel Orai1 and results in *store operated calcium entry* (SOCE) [13]. Together with Ca^{2+}, PLCγ generated DAG binds to *protein kinase* (PK)Cs mediating a conformational change that leads to enzyme activation and thus to the phosphorylation of its substrates (Figure 1-3). The different PKC isoforms in platelets have been implicated in granule secretion, *thromboxane* A$_2$ (TX)A$_2$ synthesis and platelet spreading [14].

During platelet activation, the initial signals need to be amplified in order to recruit additional platelets into the growing thrombus. This is achieved by the accumulation of different mediators that are locally produced and released once platelet adhesion is initiated. Platelet α-granules release, besides a plethora of other molecules, the adhesive proteins vWF and fibrinogen, whereas dense granules secrete the second wave mediators *adenosine diphosphate* (ADP), *adenosine triphosphate* (ATP), Ca^{2+}, histamines and serotonin [15]. Thrombin is locally produced on the surface of activated platelets linking platelet activation to coagulation. There are two blood coagulation pathways, the extrinsic and the intrinsic pathway, both converging in thrombin formation. Upon vascular injury, exposed TF interacts with FVII, which is circulating in the blood stream, promoting the extrinsic pathway of blood coagulation. In parallel, negatively charged *phosphatidylserine* (PS) is exposed on the platelet surface in response to sustained Ca^{2+} signaling. This allows the assembly and activation of the prothrombinase and

tenase complex accelerating the clotting process [16-18]. Regarding the intrinsic pathway, negatively charged surfaces, such as polyphosphates or RNA, have been proposed as physiological initiators. This pathway includes the activation of FXII which triggers, in turn, sequential activation of FXI, FIX and FX becomes activated [19].

In murine platelets, the G-protein coupled *protease activated receptors* (PAR)-4 and PAR-3 are expressed. Platelet activation by thrombin is dependent on PAR-4, whereby PAR-3 only acts as cofactor. In contrast to this, in humans both PAR receptors, PAR-1 and PAR3, are required for proper transmembrane signaling. However, in both cases, thrombin cleaves the receptor thereby unmasking the N-terminus which serves as ligand and transduces the signal [20, 21].
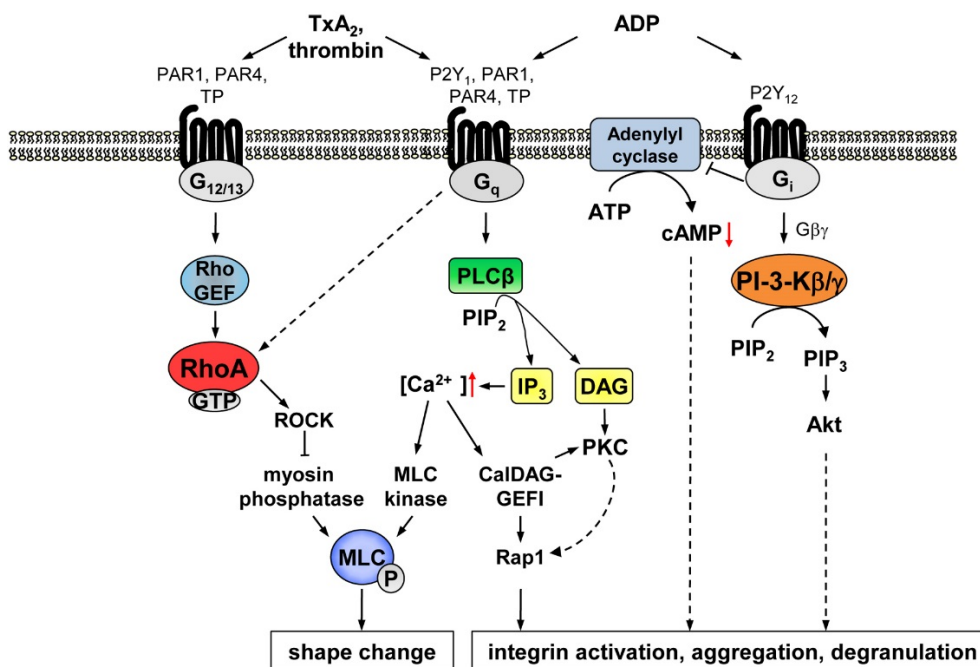
Figure 1-2: Signaling pathways induced by *G-protein coupled receptor* (GPCR) stimulation in platelets. Platelet agonists such as *adenosine diphosphate* (ADP), *thromboxane A₂* (TxA₂) and thrombin activate platelets via GPCR. The G-proteins $G_{12/13}$, G_q and G_i link receptor activation to platelet shape change, integrin activation, aggregation and degranulation. PLC, *Phospholipase C*; MLC, *myosin light chain*; DAG, *diacyl glycerol*; CalDAG-GEF, *calcium and diacyl glycerol-regulated guanine nucleotide exchange factor*; PIP₃, *phosphatidylinositol-3,4,5-trisphosphate*; PIP₂, *phosphatidylinositol-4,5-bisphosphate*; PAR, *protease-activated receptor*; TxA₂, *thromboxane A₂;* TP, *TxA₂ receptor;* RhoGEF, *Rho-specific guanine nucleotide exchange factor;* PI3K, *phosphoinositide-3-kinase*; PIP₃, *phosphatidylinositol-3,4,5-trisphosphate*; ROCK, *RhoA kinase;* ATP, *adenosine triphosphate,* cAMP, *cyclic adenosine monophosphate.* Based on Offermanns *et al.* [22]. Figure kindly provided by Ina Hagedorn.

The aforementioned diffusible mediators and the locally produced thrombin have in common that they act on platelets through binding to receptors coupled to heterotrimeric G-proteins. The PAR receptors couple to the G-proteins $G_{12/13}$, G_i and G_q, whereas the ADP receptors $P2Y_{12}$ and $P2Y_1$ signal through G_q and G_i proteins, respectively, and the *TxA₂ receptor* (TP) via G_q and $G_{12/13}$ activation. Upon stimulation of the different heterotrimeric G-proteins, specific

signaling cascades are triggered [22]. Stimulation of $G_{12/13}$ coupled receptors leads to increased phosphorylation of *myosin light chain* (MLC) via *RhoA kinase* (ROCK) and *myosin light chain phosphatase* (MLCP) finally resulting in actomyosin contraction and shape change [23]. G_q signaling is crucial for the activation of PLCβ contributing to platelet aggregation and degranulation via PKC activation. Furthermore, G_q can also stimulate cytoskeletal changes by activating RhoA [24]. Upon activation of G_i type proteins, βγ complexes, which can regulate a variety of enzymes, most notably *adenylyl cyclase* (AC) and PI3K, are released [25, 26] (Figure 1-2).
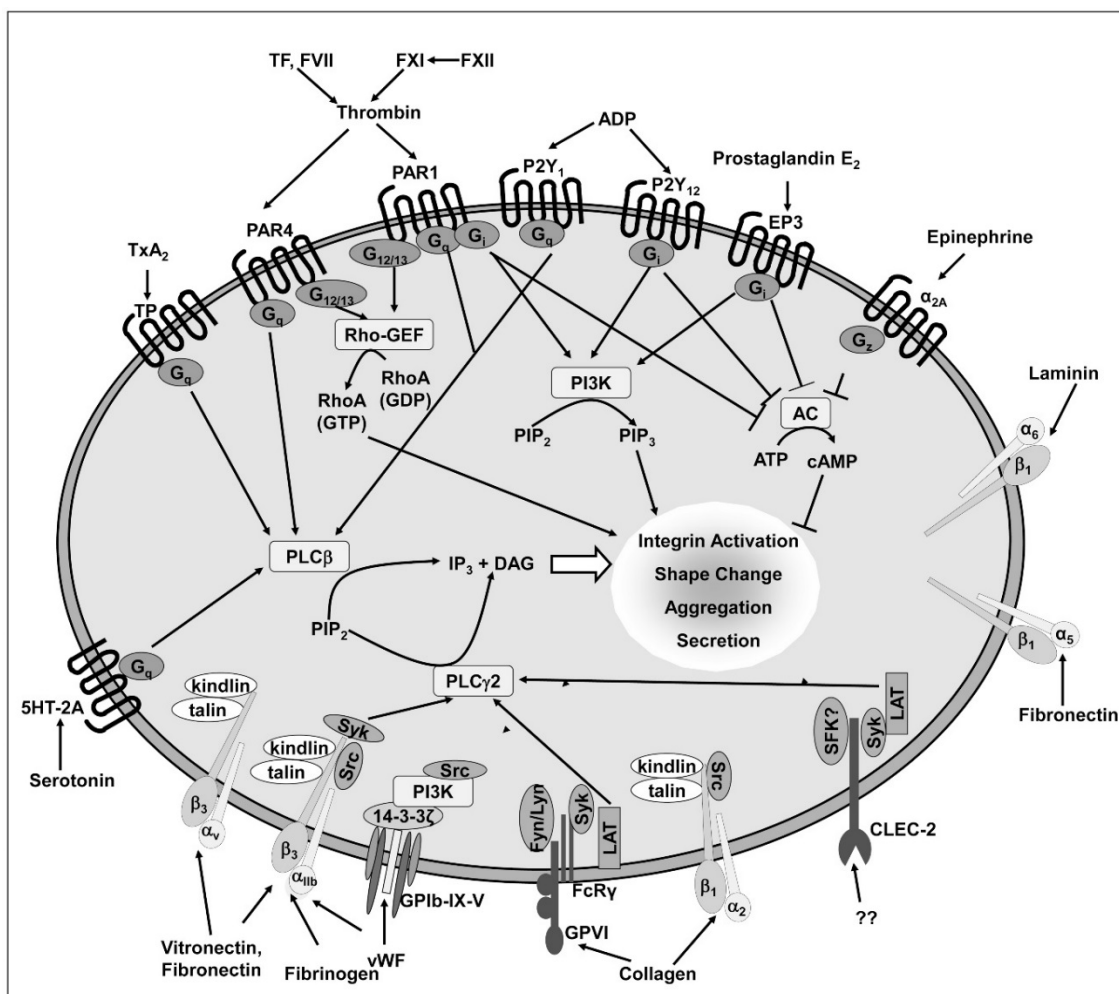
Figure 1-3: Signaling mechanisms during platelet activation. Different signaling pathways are induced upon platelet receptor stimulation. *G-protein coupled receptors* (GPCRs) transduce signals through different G-proteins. $G_{12/13}$ activation triggers RhoA/Rho kinase dependent pathways and G_q activates *phospholipase* (PL)Cβ, while $G_{i/z}$ inhibits *adenylyl cyclase* (AC). (hem)ITAM signaling is induced by the activation of *glycoprotein* (GP)VI or *C-type lectin-like receptor* (CLEC-2) receptor initiating a complex tyrosine phosphorylation cascade resulting in the activation of PLCγ2. Active PLCs generate *inositol-1,4,5-triphosphate* (IP3) and *diacylglycerol* (DAG) increasing the cytosolic Ca^{2+} concentration and activating PKCs. Altogether these events lead to the activation of integrins resulting in platelet aggregation, secretion and shape change. PIP2, *phosphatidylinositol-4,5-bisphosphate*; PAR *protease-activated receptor*; TxA2*, thromboxane A2;* TP*, TxA2 receptor*; RhoGEF, *Rho-specific guanine nucleotide exchange factor*; PI3K, *phosphoinositide-3-kinase*; PIP3, *phosphatidylinositol-3,4,5-trisphosphate*. Taken from Stegner *et al.*, 2010 [5].

Signaling events downstream of GPIb, ITAM or GPCRs result in the activation and subsequent accumulation of platelets into a hemostatic plug. This process is termed platelet aggregation and is mediated by binding of the activated (high affinity conformation) αIIbβ3 integrin to the ECM protein fibronectin, plasma fibrinogen or collagen-bound vWF. In resting platelets the inactive αIIbβ3 integrin has low affinity to its ligands. The intracellular signaling pathways during platelet activation lead to the functional upregulation of αIIbβ3 integrins. The shift from the low affinity to a high affinity state is called inside-out signaling. Other integrin-ligand interactions, such as α2β1 integrin - collagen, α5β1 integrin - fibronectin, α6β1 integrin - laminin as well as the αvβ3 integrin binding to several ECM proteins are also important to allow firm platelet adhesion to the ECM. Ligand-occupied integrins regulate cytoskeletal dynamics leading to platelet spreading and clot retraction (outside-in signaling). Although the exact mechanisms linking platelet stimulation to the activation of the main platelet integrin αIIbβ3 are incompletely understood, Ca^{2+}-*dependent diacylglycerol regulated guanine nucleotide exchange factor I* (CalDAG-GEF1) and PKC activation have been described to be involved in the activation of the small GTPase Rap1. Subsequently, the effector molecule *Rap1-GTP-interacting adapter protein* (RIAM) and its binding partner talin1 are recruited to the plasma membrane enabling talin1 to bind to the β3 integrin tail. Together with the binding of kindlin to the cytoplasmic tail of the β integrins, talin1 facilitates αIIbβ3 integrin activation [27] (Figure 1-3).

1.3 Phospholipase D

1.3.1 Structure and function

PLD is an enzyme that is commonly found in bacteria, fungi, plants and animals. As a phosphodiesterase, it catalyzes the hydrolysis of the phospholipid *phosphatidylcholine* (PC) to choline and *phosphatidic acid* (PA) [28, 29]. PA can, in turn, be converted into important lipid effectors, namely DAG, catalyzed by lipid phosphate phosphohydrolase and lyso-PA catalyzed by PLA. Next to phosphatidylcholine, both *phosphatidylethanolamine* (PE) and *phosphatidylinositol* (PI) can serve as substrates for PLD [30, 31]. Water, normally essential for the hydrolytic reaction, can be substituted by primary alcohols, such as 1-butanol or ethanol, generating *phosphatidylethanol* (PtdEtOH) or *phosphatidylbutanol* (PtdButOH), respectively, at the expense of PA. This reaction, termed transphosphatidylation, is unique for PLD and can be used to measure the activity of the enzyme [32] (Figure 1-4).

There are two classical mammalian PLD isoforms which are ubiquitously expressed and share a homology of more than 50%: PLD1 (120 kDa) and PLD2 (106 kDa) [33, 34] (Figure 1-5). PLD1 exists as two splice variants, whereas PLD2 exists as four splice variants [34, 35].

Together with classical plant, yeast and bacterial PLD, as well as with a *Yersinia* murine toxin, a topoisomerase-DNA hydrolase, two poxvirus envelope proteins, a cardiolipin synthase, a phosphatidylserine synthase, a bacterial endonuclease and a helicase like protein from *E. coli*, mammalian PLDs belong to the PLD superfamily characterized by the highly conserved *HxKx4-Dx6GSxN*-motif (HKD) [36].
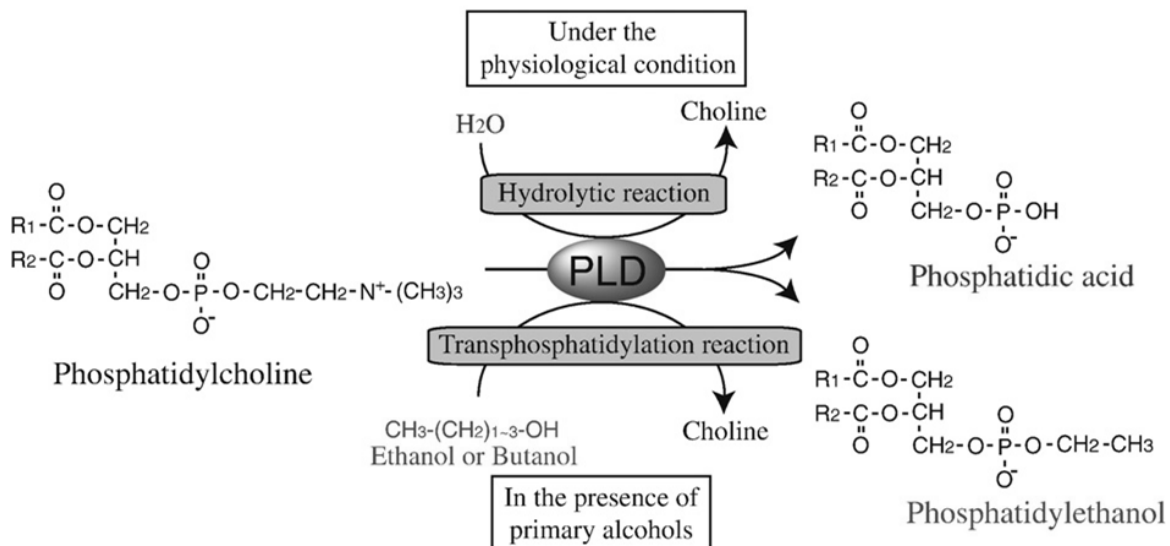
Figure 1-4: Enzymatic reaction of mammalian phospholipase D. In the presence of water *phospholipase* (PL) D catalyzes the hydrolysis of *phosphatidylcholine* (PC) to *phosphatidic acid* (PA) and choline. If a primary alcohol is present PLD generates phosphatidylethanol at the expense of PA which is a unique reaction for PLD termed transphosphatidylation. Modified from Kanaho *et al*., 2009 [37].

The mammalian PLD family also includes non-classical PLDs, such as mitoPLD (PLD6), PLD3, PLD4 and PLD5. MitoPLD encodes only one HKD site and exhibits no PX and PH domains. It is localized to the mitochondrion and hydrolyses cardiolipin to PA participating in mitochondrial fission and fusion [38]. For PLD3, PLD4 and PLD5 neither canonical activity has been detected, nor have any substrates been identified [39-41].

The two classical PLD isoforms contain several conserved regions including the *phox homology* (PX) domain, the *pleckstrin homology* (PH) domain and the conserved PLD regions I-IV (Figure 1-5). The two conserved regions II and IV harbor the HKD sites that form the catalytic site. Two histidine residues allow the formation of a phosphoenzyme intermediate and the subsequent hydrolysis of the substrate phosphodiester bond [42-44]. The conserved regions I and III are also critical for PLD activity [43]. The PH domain is responsible for the localization of the protein by binding to the phosphoinositides. Furthermore, a function of the PH domain of PLD2 as *guanine exchange factor* (GEF) for the small G-protein Rac2 has been postulated [45, 46]. The PX domain specifically interacts with PIP_3. By serving as a binding site

for several molecules, the PX domain is proposed to be involved in several enzymatic functions. This includes the regulation of the GTPase activity of dynamin, the activation of PLCγ1, the stimulation of PKCζ and the tyrosine kinase Syk, as well as the initiation of the *extracellular-signal-regulated kinase* (ERK)/MAPK pathway by binding to Grb2 [45, 47-52]. Finally, the structure of PLD1 is uniquely characterized by a loop domain of 116 amino acids which is suggested to have autoinhibitory functions explaining the low basal activity of PLD1 compared to PLD2 [53]. Other parts of the enzyme are also able to bind and regulate a vast variety of molecules. For example, the N-terminus of PLD1 has been shown to bind and activate PKCα and serves as a binding site for F-actin [54]. The C-terminus is involved in the localization of the enzyme, enables binding to small GTPases of the Rho family and stabilizes the active conformation of the catalytic site of PLD1 [55].

The classical PLD isoforms, PLD1 and PLD2, are expressed in nearly all mammalian tissues [56-58]. Concerning the subcellular localization of PLDs, several studies reported inconsistent findings. For PLD1, perinuclear expression in the ER, Golgi apparatus, late endosomes and on secretory vesicles has been reported, while PLD2 is rather located to the plasma membrane, cytosol and vesicles involved in the sorting/recycling center [59-63]. Many reports show that PLD1 has a low basal activity in its resting state which increases upon stimulation with a variety of small GTP binding proteins or PKC. In contrast, PLD2 is suggested to have a high basal activity that is less responsive to the aforementioned activators [64, 65]. However, this is still a matter of debate, since other reports also demonstrate inducible PLD2 activity e.g. by Rac2 [66]. The distinct subcellular distribution and regulation patterns suggest isoform specific functions of the PLD enzymes [66].
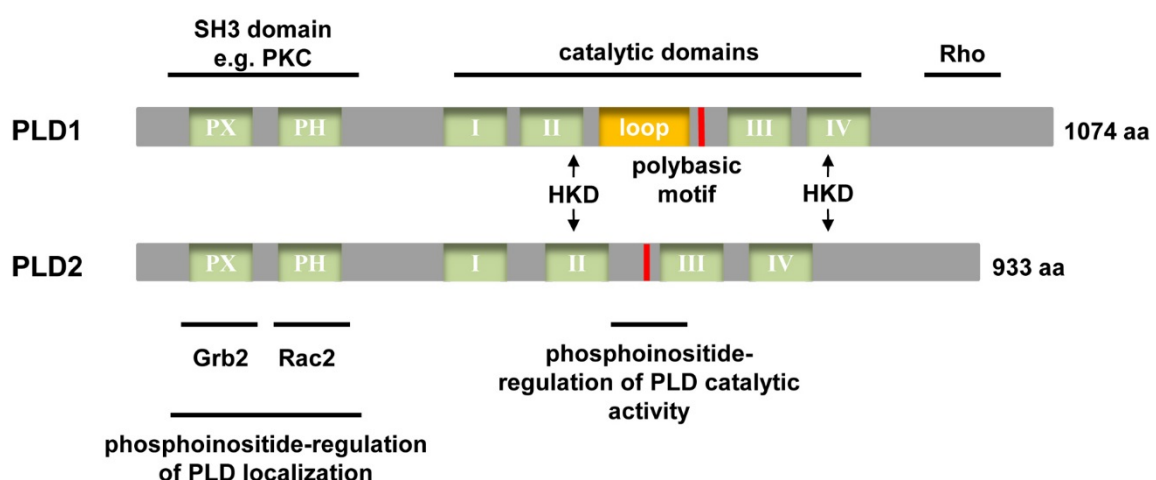
Figure 1-5: Mammalian PLD isoforms. The PLD isoforms contain highly conserved regions including the *phox homology* (PX) domain, the *pleckstrin homology* (PH) domain and the conserved PLD regions I-IV harboring the HKD motifs. The loop region in PLD1 exhibits autoinhibiting functions. aa, amino acid residues. Modified from Cockcroft, 2001 [67].

1.3.2 Regulation of PLD enzyme activity

As mentioned above, it has been shown that the different PLD isoforms are localized to distinct membrane compartments exerting specific enzymatic functions. Membranes consist of a unique lipid and protein composition that harbors distinct binding sites for molecules which can interact with PLD. For example, phosphoinositides which are enriched in specific membrane microdomains are important cofactors for PLD activity [68]. Translocation of PLD1 from the intracellular compartment to the plasma membrane upon stimulation emphasizes the importance of PLD localization for its function and constitutes one of the mechanisms regulating the proposed inducible activity of PLD1 [53].

A large variety of agonists including hormones, growth factors and antigens increase PLD activity by stimulating GPCRs or tyrosine kinase receptors. The transduction of signals by these receptors occurs via PLC activation, an intracellular Ca^{2+} increase, tyrosine phosphorylation cascades or small G-proteins. This implies tight and complex mechanisms regulating PLD activity (Figure 1-6).

1.3.2.1 Small G-proteins and PKC

The complex regulation of PLD is in part mediated by small GTPases of the Rho and Arf family. The GTPases of the Rho family regulate important cellular processes such as cytoskeletal rearrangements, cell cycle progression and gene expression. All members of the Rho family of GTPases, RhoA [69], Rac1 [70] and Cdc42 [71], have been identified as PLD1 activators. They bind to PLD1 in their active GTP bound state and they are able to lower the enzymatic activity by decreasing the Michaelis constant of PLD [72]. Additional studies revealed that the C3 exoenzyme of *clostridium botulinum*, which is an inhibitor of Rho proteins, decreases the activity of PLD [73]. A binding site for RhoA at the carboxyl terminus of PLD1 has been identified and direct RhoA interaction activates PLD [55, 74]. Others report that RhoA can also bind the PX domain of PLD enabling nucleotide exchange of RhoA [75]. However, indirect regulating mechanisms are also possible e.g. via RhoA dependent activation of *phosphatidylinositol 4-P 5-kinase* (PIP5K), that enhances, in turn, the generation of PIP_2, an important cofactor for PLD [76].

PLD activity was also demonstrated to be dependent on GTPases of the Arf family. Arf proteins are involved in membrane trafficking and cytoskeletal organization. All six Arf family members have been shown to robustly increase PLD1 activity *in vitro*, whereas the activity of PLD2 is increased only mildly [58, 77]. *In vivo,* Arf1 and Arf6 mediate the activation of PLD1, while PLD2 is activated by Arf6 but not by Arf1 [78, 79]. Comparable to the Rho GTPases, PLD1 and PLD2 activation can only be induced by the GTP-bound Arf6 protein and is dependent on its translocation to the membrane [80-82]. The N-terminal part of PLD is critical for the activation of PLD by Arf [83]. Another GTPase affecting PLD activity is RalA. However, RalA

only exerts its stimulatory effect by forming a complex with Rho and Arf proteins [84, 85]. Further, synergistic effects of Rho, Arf1 and PKCα have been reported suggesting different binding sites of these enzymes on PLD [86].

The specific PKC activator *phorbol 12-myristate 13-acetate* (PMA) is able to stimulate PLD in a large variety of different tissues and cell lines. Confirming these observations, other studies with PKC inhibitors showed full or partial inhibition of agonist-stimulated PLD activity [87]. In addition, different interactions of the two PLD enzymes with various PKC isoforms have been reported [86, 88-90]. Whether direct PKC dependent phosphorylation is involved in the activation of PLD is still discussed controversially. Many studies postulate that PKC mediated phosphorylation activates PLD [91-93]. In contrast, Min *et al.* demonstrated that *in vitro* PKCα and PKCβII dependent PLD1 phosphorylation inhibited the catalytic activity [89]. Contrary to the phosphorylation dependent mechanism, later reports showed that PKC can stimulate PLD in the absence of ATP indicating a direct phosphorylation-independent PKC-PLD interaction to be critical for PLD activation [88, 89, 94]. Also dual mechanisms including phosphorylation and protein-protein interactions were proposed [95].
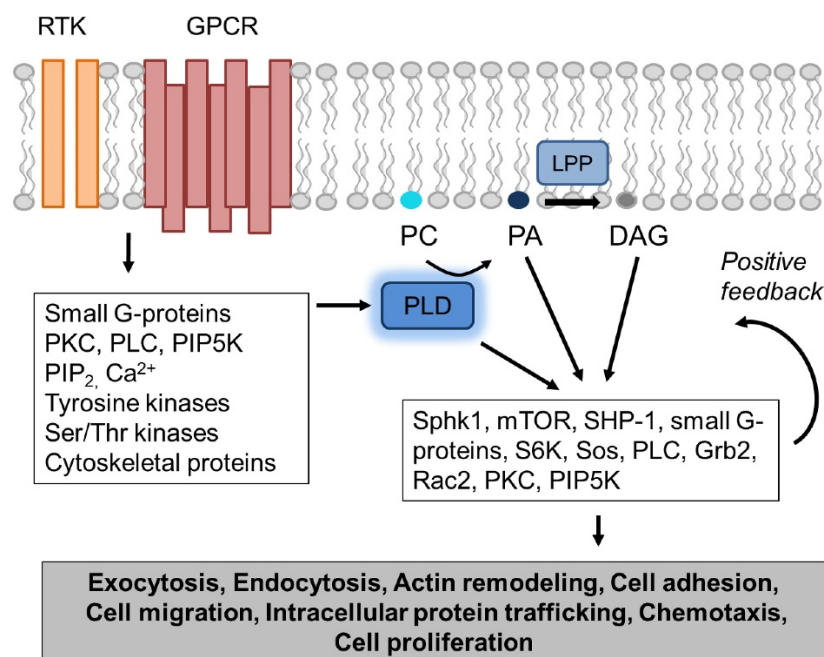
Figure 1-6: Signaling network of PLD and PA. *Phospholipase* (PL) D is activated upon stimulation of *receptor tyrosine kinases* (RTK) or *G-protein coupled receptors* (GPCR). Signals are transduced via several signaling molecules including small G-proteins, *protein kinase* (PK) C, PLC, *phosphatidylinositol 4-phosphate 5 kinase* (PIP5K) and *phosphatidyl-inositol-4,5-bisphosphate* (PIP_2). Upon PLD activation, PLD itself or its product *phosphatidic acid* (PA) transmits the stimulus by interacting with proteins such as *sphingosine kinase* (Sphk) 1, *ribosomal protein S 6 kinase* (S6K), *son of sevenless* (Sos), PLCs, *growth factor receptor bound protein* (Grb) 2, Rac-2, *mammalian target of rapamycin* (mTOR), PKCs or PIP5Ks. Signaling pathways of PLD activation are involved in secretion, chemotaxis, cell proliferation and migration.

1.3.2.2 PIP$_2$ and PIP5K

Phosphoinositides have been considered to be very important for the regulation of PLD activity. Among others, Sciorra *et al.* identified PIP$_2$ as an essential cofactor for PLD1 and PLD2 [96]. PIP$_2$ binds the PH domain and another conserved sequence between motifs II and III on PLD [45]. This interaction is important for the stimulation of PLD enzymes, probably by promoting its binding to the lipid bilayer [86]. PIP$_2$ can trigger PLD activity also indirectly, as it can be hydrolyzed to IP$_3$ and DAG promoting PKC activity and an intracellular Ca^{2+} increase [97]. Furthermore, PIP5K, the kinase catalyzing the production of PIP$_2$, is able to bind to both PLD isoforms enabling the recruitment of PIP5K to specific vesicular compartments [98]. Interestingly, integrin activation during cell adhesion has been demonstrated to be dependent on PLD derived PA via stimulation of PIP5K [99]. Furthermore, it has been shown that PIP5K promotes an increase in PLD activity by generating PIP$_2$ in Cos7 cells [98]. PIP5K is an essential effector of small G-proteins that anchor the kinase to specific membrane regions. The subsequent localized production of PIP$_2$ recruits and activates PLD which, in turn, produces PA enhancing PIP5K activity creating a stimulatory feed forward loop [100]. Taken together, distinct co-localizations and temporal activations, including feed forward activation loops, are crucial for the regulation of PLD by PIP5K and PIP$_2$.

1.3.2.3 Additional mechanisms of regulation

Besides the aforementioned regulators of PLD enzymes, a plethora of additional molecules affecting PLD activity, including kinases, phosphatases, Ca^{2+}, cytoskeletal proteins and ceramides has been proposed.

Ca^{2+} has been well defined as a cofactor for plant PLD [101], while a direct regulatory control of Ca^{2+} on mammalian PLD has not been described. However, a physiological relevant increase of Ca^{2+} is already sufficient to trigger PLD activity [102, 103]. Various studies have shown PLD activation upon treatment with ionophores, as well as PLD inhibition upon Ca^{2+} depletion by the use of *ethylene glycol tetraacetic acid* (EGTA) or *1,2-bis(o-amonophenoxy)ethane-N,N,N',N'-tetraacetic acid* (BAPTA). Whether this is due to a direct or indirect effect of Ca^{2+} on PLD is not clear, since a variety of PLD-regulating enzymes, such as PKCs or tyrosine kinases, are influenced by Ca^{2+} as well [65].

Furthermore, *tyrosine* (Tyr) as well as *serine/threonine* (Ser/Thr) residues have been demonstrated to become phosphorylated and dephosphorylated in PLD enzymes thereby regulating its activity. Concerning the phosphorylation of Tyr sites, several Tyr kinases and phosphatases such as Fyn, Fgr, *Janus kinase* (JAK)3, Src kinase, CD45 and *protein tyrosine phosphatase* (PTP)1B have been shown to be involved [104-106]. Regarding Ser/Thr kinases, the *casein kinase* (CK)II, *cyclin dependent protein kinase* (CDK)5, *ribosomal S6 kinase* (S6K)2 and *5' adenosine monophosphate-activated protein kinase* (AMPK) trigger PLD activity via

phosphorylation [41, 107-109]. In case of the observed activation of PLD by MAP kinases it is still unclear whether this is mediated via phosphorylation or protein-protein interaction [110, 111]. Besides the regulation of PLD activity, phosphorylation also enables interactions with diverse proteins that can increase its lipase activity e.g. Grb2 binding upon Tyr179 and Tyr511 phosphorylation of mammalian PLD2 [112, 113].

In addition, various cytoskeletal proteins can act as regulators of PLD activity. PLD binds to monomeric G-actin as well as to actin filaments. While G-actin has an inhibitory function on PLD in resting cells, F-actin binds to PLD upon cellular stimulation promoting the interaction with its membrane substrate [114]. Monomeric tubulin was also found in complex with PLD2 resulting in inhibition of the enzymes lipase activity [115]. Also other proteins involved in cytoskeletal organization associate with PLD upon physiological stimulation [116]. While α-actinin, synyptojanin and fodrin have been identified as negative regulators of PLD activity [117-120], phospho-cofilin has been shown to bind and recruit PLD to the plasma membrane thereby stimulating its activity [121].

1.3.3 Physiological functions of PLD enzymes

To date a plethora of studies on the physiological relevance of PLD enzymes has been published. Mostly, these studies use biochemical or pharmaceutical approaches. Potential downstream targets of PLD were identified by correlation studies linking PLD activity to simultaneously occurring cellular events. In addition, the use of siRNAs lowering the activity of PLD1 or PLD2 or the inhibition of PLD activity by pharmacological agents, have been exploited. Pharmacological inhibition of PLD might, however, lead to off-target effects that may confound the interpretation of the obtained data. As an alternative, primary alcohols have been used frequently to induce maximal transphosphatidylation thereby inhibiting PA production [122]. Yet, alcohols only partially prevent PA production even at maximal applicable concentrations. Recently, new tools such as isoform specific knockout mice and next generation small molecule inhibitors have become available, that will help to clarify some of the contradictions found in the previously published data and, in addition, give new insights into the function of the PLD enzyme. While the PLD1 knockout mouse was published before I started my thesis, the first reports on PLD2 deficient mice were published during my work [8, 123-125].

1.3.3.1 Functions of PLD enzymes

PLD activation has been associated with a wide variety of cellular events, including membrane trafficking, cell migration and cell survival (Figure 1-6).

Regarding vesicle movement, PLD has been demonstrated to localize to the Golgi apparatus where it facilitates Arf-dependent vesicular trafficking. This includes budding of Golgi vesicles, transport from ER to Golgi and secretion of nascent vesicles from the trans Golgi network

[126]. Further, PLD generated PA has been shown to be of major importance for exocytosis, in particular for the last step, the fusion of vesicles with the plasma membrane. For example, PLD mediates the translocation of glucose transporter GLUT4 containing membrane vesicles to the plasma membrane in adipocytes or the release of insulin granules by pancreatic β-cells [127, 128]. Furthermore, it has been demonstrated that asymmetric distributed phospholipids modulated by PLD augments SNARE-dependent membrane fusion [129]. In this respect, the PA dependent recruitment of specific proteins by PA such as PIP5K, that increases the local PIP_2 concentration, is relevant [61]. In addition, PLD has been shown to be involved in the endocytosis of G-protein coupled and *epidermal growth factor* (EGF) receptors [130, 131].

In case of cell migration, adhesion, spreading and membrane ruffling, PLD has been demonstrated to be of importance due to its involvement in cytoskeletal reorganization and F-actin polymerization. This has been shown in various cell types including leukocytes, epithelial cells, cancer cells, phagocytes and fibroblasts [48, 99, 132, 133]. Proteins such as Rac2 [134], S6K [135], phospho-cofilin [121] and the tyrosine kinase Fer [136] have been revealed to be involved in these processes. For example, the interaction of PLD2 with the *Wiskott Aldrich Syndrome protein* (WASP) via Grb2 enables chemotaxis and phagocytosis. Furthermore, reports show that PLD acts as *guanine exchange factor* (GEF) for Rac2 promoting actin polymerization during chemotactic cell movement [66]. In addition, cell adhesion via integrin activation is dependent on PIP_2 which is generated at the membrane upon attachment of PIP5K to the membrane via PLD derived PA [99].

In the context of cell survival, proliferation and growth, the mechanisms by which PLD contributes to these events are largely unclear. However, PLD or PA have been shown to interact with a plethora of molecules involved in these cellular processes including PIP5K [137], *sphingosine kinase* (SK)1 [138], S6K [139], *son of sevenless* (Sos) [140], Raf-1 [141], *mammalian target of rapamycin* (mTOR) [142], the protein tyrosine phosphatase SHP-1 [143], PKCs [144] and small GTP binding proteins [134, 145]. Often, different positive feedback loops with PIP5K, PKCs and GTPases have been postulated enabling rapid and sustained signal transduction in these pathways.

In addition, PLD has been proposed to generate second messengers that are crucial for mitogenic signaling. There is evidence that the conversion of PLD derived PA to DAG is essential for the sustained DAG elevation in cells upon agonist stimulation. Whether this is sufficient for PKC activation is disputed [146]. PA can also be converted into Lyso-PA by PLA. Lyso-PA is established as lipid second messenger and might therefore account for PLD dependent effects [147].

Taken together, the large number of molecules involved in the transduction of PLD signals demonstrates its involvement in a variety of different cellular processes including vesicle trafficking, cell migration, chemotaxis, proliferation and secretion (Figure 1-6).

1.3.3.2 Roles of PLD in disease

Due to the involvement of PLD in numerous cellular processes, it is important in many physiological as well as pathological situations. Transgenic mouse models, lacking PLD isoforms, specific inhibitors, siRNAs and *in vivo* disease models present excellent tools to gain new insights into the *in vivo* functions of PLD and into its contribution to different pathophysiologies. PLD has been shown to be crucial in various diseases such as cancer, neurodegenerative diseases, cardiovascular disorders, diabetes and infectious diseases. In this thesis, only some pathophysiological functions of PLD will be introduced. More details on previous advances on the involvement of PLD in diseases have been reviewed in [148-151].

Roles for PLD in cancer have been postulated and increased expression of PLD has been observed in different types of cancer [152, 153]. Recently, Chae *et al.* could confirm the involvement of PLD1 in tumor progression with an *in vivo* mouse model. *Pld1$^{-/-}$* mice showed reduced metastasis and less angiogenic signaling capacity. This was due to a decreased tumor-platelet interaction in models of melanoma as well as lung carcinoma [154]. Another process which is important for cancer cell survival as well as for metabolism and which has been linked to PLD is macroautophagy. Macroautophagy is an important process during cell starvation that enables a cell to recover energy and nutrients by the degradation of organelles. *Pld1$^{-/-}$* mice showed decreased efficiency of autophagy due to reduced numbers of autophagosome departments in the liver [123].

Besides its potential role in cancer development, PLD was also suggested to be important in neurodegenerative. In *Alzheimer's disease* (AD), the Aβ peptides, as main components of the amyloid plaques in the brains of patients, contribute to the pathogenesis of the disease. Oliviera *et al.* showed increased PLD activity levels in brains of mice in a transgenic mouse model of AD. The genetic ablation of PLD2 led to beneficial effects in this model, because of decreased Aβ peptide synaptotoxic activity [124].

The process of inflammation involves a variety of different cell types including leukocytes, macrophages and fibroblasts. During inflammation, damaged tissue releases chemokines to attract leukocytes and macrophages [155]. In response to chemokines, these cells form leading edges enabling migration. *In vitro*, it has been extensively shown that PLD is crucial for the recruitment of certain proteins, such as Rac1 and Rap1, to the leading edge of a migrating cell. Recently, Ali *et al.* confirmed the significance of PLD in phagocytosis and cell migration *in vivo*. In macrophages, isolated from PLD1 and PLD2 deficient mice they were able to demonstrate that the lack of PLD results in impaired recruitment of Rac1 and DOCK2 leading to defective F-actin organization during phagocytic cup formation [134, 156]. Further, neutrophils lacking PLD exhibited migratory defects during acute pancreatitis [157]. However, Sato *et al.* demonstrated intact neutrophil degranulation and ROS production in *Pld1$^{-/-}$* mice excluding its contribution to migration via this pathway [158]. In line with the observation of Ali

et al., TNF-α, a cytokine which induces the acute phase reaction during inflammation, has been shown to rely on PLD function in a model of peritonitis. Cytokine and chemokine production, vascular permeability, cell adhesion molecule expression, and neutrophil and monocyte infiltration into the peritoneal cavity were inhibited during peritonitis in mice where PLD1 had been knocked down using siRNA approach [159].

In accordance to its importance in inflammation, PLD was also identified to be involved in the pathogenesis of autoimmune diseases. It was demonstrated that *Pld1*^{-/-} mice were protected in a model of autoimmune central nervous system inflammation which was associated to a defective migratory capacity of the lymphocytes (Göbel *et al.*, Eur J Immunol, in revision).

Vascular disorders are another field of disease PLD has been brought into context with. Cyclic-PA, which can be generated by PLD2 dependent hydrolysis of lyso-PA, acts as antagonist of the *peroxisome proliferator-activated receptor* (PPAR)γ. PLD2 activation results in PPARγ dependent arterial wall thickening, pointing to the possibility of cyclic PA to serve as a therapeutic in hypertensive diseases [160]. Interestingly, in a genetic screen, mutations in PLD2 have been identified as hypertensive risk factors [161]. α$_1$-adrenergic receptor is important for the regulation of blood pressure through mediating smooth muscle cell contraction. Wegener *et al.*, showed that α1-adrenergic induced contractions were reduced in *Pld1*^{-/-} mice probably through PLD1s involvement in the regulation of Ca$_v$1.2 channel activity [162].

Finally, PLD activity levels were found to be modulated upon cardiac and brain ischemia and PLD1 deficiency protected mice in a model of acute ischemic stroke [8, 163, 164]. Since many cell types are involved in the thrombo-inflammatory process of infarct development, it is unclear whether PLD from hematopoietic or non-hematopoietic cells contribute to this event. However, PLD has been shown to be of importance in thrombus formation and platelet function, suggesting platelet PLD to contribute to these pathologies [8, 125]. The *in vivo* role of PLD in thrombosis and hemostasis will be introduced below.

In summary, PLD was identified to be of importance in a variety of pathological processes like different cancer types, diabetes, neurological disorders, inflammation as well as thrombosis. In the future, further studies will help to establish whether PLD inhibition might be useful as treatment in some of these diseases.

1.3.4 Phospholipase D in platelets

As already mentioned, PLD is an important regulator of cellular processes such as cytoskeletal rearrangement or secretion, which are crucial during platelet activation. Interestingly, already in 1988, PLD was found to be activated in human platelets upon stimulation with thrombin [165]. This finding was confirmed by further studies showing PLD activation upon platelet

activation with other agonists such as collagen, *collagen related peptide* (CRP) and the thromboxane mimetic U46119 [166-168]. While the platelet agonist ADP itself does not stimulate PLD, it exerts synergistic effects together with thrombin on PLD activity [166]. In contrast, synergistic effects by TxA$_2$ were excluded since aspirin was not able to reduce PLD activation [169]. Vorland *et al.* linked PLD activity to F-actin formation and lysosomal secretion in platelets [170]. In the same line, other studies demonstrated the correlation of PLD activity to PKC dependent platelet aggregation and dense granule secretion [168, 169]. However, another study proposed rather Ca^{2+} signaling than PKC dependent mechanisms to be crucial for PLD related platelet activation [171]. Yet another study showed, that the Ca^{2+} ionophore A23187 induced PLD activity, whereas, extracellular Ca^{2+} by itself was not capable of triggering PLD activation [170, 171]. Removal of extracellular Ca^{2+} reduced, but did not abolish thrombin stimulated PLD activation indicating that PLD can also be stimulated independently of extracellular Ca^{2+} [170].

By using GTPγS, a G-protein activator, G-proteins were established as upstream regulators of PLD activity [172]. GTPγS induced secretion was accompanied by PA production in permeabilized human platelets. In rabbit platelets, synergistic effects of GTPγS with Ca^{2+} and PKC were shown to induce PLD activation and subsequent secretion, whereas others also reported PKC independent mechanisms [167, 173]. In contrast to this, Coorssen *et al.* demonstrated that PLD activation occurs with slower kinetics than platelet degranulation and showed that PA on its own cannot induce secretion. Due to these findings, PLD generated PA was proposed to exert rather modulatory than essential roles for GTPγS induced secretion and PKC activation [174]. Further, protein tyrosine kinase stimulation was demonstrated to be involved in mechanisms leading to thrombin and GTPγS mediated PLD activity in human platelets [106].

Several reports also defined a LDL- or cholesterol-dependent PLD activity in human platelets. PLD was shown to be important for cholesterol-initiated PLA$_2$ activation [175-177].

Whether PLD activity in platelets is integrin αIIbβ3-independent or -dependent is contrarily discussed. While Martinson *et al.* reported unaltered PLD activity in the presence of the fibrinogen antagonist peptide RGDS, others demonstrated thrombin and *high density lipoprotein* (HDL3) stimulated PLD activity to be dependent on αIIbβ3 integrin clustering [168, 170, 178]. Activation of Rap1, a GTPase that is essential for integrin dependent platelet aggregate formation, occurs in response to PAR-1 stimulation in human platelets. In this context, PLD has been proposed to be involved in the reinforcement of Rap1 activation through a positive feedback loop involving PIP5K and PI3K sustaining DAG production [179]. In platelets, DAG can be directly generated via PLCs as a product of PIP$_2$ hydrolysis or via lipid phosphate phosphatases [180]. A biphasic production of DAG in platelets can be observed after thrombin stimulation whereby the second peak of DAG production seems to originate

from PLD [181, 182]. However, others report only a monophasic DAG production upon platelet stimulation [183]. A very recent study from our laboratory proposed a role for PLD in enhancing SOCE during platelet activation by amplifying DAG generation. By this mechanism PLD was suggested to contribute to DAG dependent Ca^{2+} entry via the canonical *transient receptor potential cation channel* (TRPC)6 [184].

Immunoblotting and immunohistochemistry assays allowed the discrimination of the two isoforms confirming the presence of both, PLD1 and PLD2, in platelets. Upon platelet stimulation, both isoforms get translocated to the plasma membrane. Under resting conditions, PLD1 and PLD2 expression was detected throughout the platelet. However, while PLD1 was rather located to distinct granule like structures, PLD2 was found to be concentrated at the plasma membrane. The thrombin mediated translocation and activation of PLD1 was shown to be inhibited upon addition of prostaglandin E_2 or forskolin potentially by mechanisms involving protein kinase A. This inhibition of translocation was not observed for PLD2 demonstrating isoform-specific regulatory mechanisms [170, 185].

The existence of a basal PLD activity in platelets and other cell types is disputed. Martinson *et al.* were only able to detect PLD activity upon platelet stimulation, whereas Vorland *et al.* report a basal PLD activity of ~30% of total PLD response to thrombin [168, 170]. The general opinion states, however, that PLD2 exerts basal activity, while PLD1 is the inducible isoform [33, 186]. Since diverse acyl specificities of PLD in other cell types have been reported, the observed contradictions might be attributed to distinct PLD activity assay protocols utilizing different fatty acid labeling techniques [187].

The absence of an appropriate model to elucidate the function of PLD1 and PLD2 *in vivo* made it difficult to interpret the above summarized, partially contradicting, data. However, in 2010 our laboratory generated mice constitutively lacking PLD1 that were viable and fertile. In a first study, PLD1 was found to be important for αIIbβ3 integrin activation and GPIb-mediated platelet adhesion under high shear. The *in vivo* analysis of these mice established PLD1 as an important modulator for thrombotic processes and ischemic infarct development but not for hemostatic functions. These findings pointed to a possible suitability of PLD inhibition as effective therapeutic strategy to prevent intra-arterial occlusive thrombus formation. Importantly, no function for PLD1 in platelet secretion, which had been postulated beforehand, could be detected [8]. However, in another recent study that used a specific PLD inhibitor at extremely high concentrations, in wildtype and *Pld1$^{-/-}$* platelets, PLD2 was suggested to be a negative regulator of platelet secretion [188]. Nevertheless, definite proof for the aforementioned contribution of PLD2 in platelets is missing and the relevance of PLD2 and a potential redundant function of both PLD isoforms for thrombosis and hemostasis remained to be elucidated.

1.3.5 Pharmacological PLD inhibition

Many potential roles for PLD in the development of different pathologies, including cancer, cardiovascular and neurodegenerative diseases have been demonstrated as summarized in 1.3.3.2. Thus, inhibition of PLD could represent a novel therapeutic approach in these pathologies. For decades, the studies on PLD relied on the use of non-selective inhibitors or n-butanol, blocking PA production. However, even though alcohols and gene silencing tools were helpful, it has now been demonstrated that these approaches often created off-target effects, making it difficult to interpret previously made conclusions using those tools [189]. Furthermore, the applied inhibitors were no suitable therapeutic options for blocking PLD activity *in vivo*. Therefore, several groups developed new potent small-molecule inhibitors and optimized their efficiencies and isoform selectivities by diversity-oriented synthesis combined with biochemical assays and mass spectrometric lipid profiling of cellular responses [190-192]. Meanwhile, the previously identified inhibitor *5-Fluoro-2-indolyl des-chlorohalopemide* (FIPI) is the best established PLD inhibitor being used in many functional studies [123, 156, 157, 189].

FIPI is a potent and reversible inhibitor of both PLD isoforms with a half-life of 5.5 hours *in vivo* and moderate bioavailability [189, 192]. Initially FIPI was identified as a PLD2 inhibitor. Su *et al.* and others have shown, however, the potency of FIPI to block both PLD isoforms with similar kinetics [189, 192]. Several studies confirmed its specificity and effectiveness through the observation of PLD-dependent phenotypes in FIPI-treated cells. For example, Nikishima *et al.* observed decreased neutrophil migration upon FIPI treatment, which was similarly seen in n-butanol treated cells [156]. Likewise, PLD-dependent cellular processes such as cell spreading and chemotaxis were found to be abolished in the presence of FIPI, validating the role of PLD in this process [189]. Furthermore, comparable defects in starvation-induced autophagy were demonstrated in FIPI treated CHO cells and *Pld1$^{-/-}$* fibroblasts [123]. In addition, studies using FIPI helped in the re-evaluation of results which were obtained with alcohols. Sato *et al.* demonstrated the dispensability of PLD for fMLP induced superoxide generation and degranulation in neutrophils which contradicted previous findings showing PLD dependent superoxide production by using alcohols to inhibit PLD [158, 193].

Moreover, FIPI has become an essential tool for studying the physiological and pathological relevance of PLD in different processes. FIPI is an analog of the psychiatric drug halopemide [192], a dopamine receptor antagonist, that has already been evaluated in five independent clinical studies [194]. FIPI is two orders of magnitude more potent than halopemide for PLD2 inhibition [192], nonetheless, halopemide is used clinically at levels that should accomplish full PLD inhibition [194], suggesting that PLD inhibition in humans can be achieved without overt toxicity. Recently, it was demonstrated that FIPI treatment prevents tumor growth and metastasis in mice to the same extent as genetic ablation of *Pld1,* again confirming the efficacy of the inhibitor [154]. In that study, mice received FIPI for up to 10 days with no apparent

toxicity. This indicates, together with the overall unaltered appearance of *Pld1$^{-/-}$/Pld2$^{-/-}$*mice, that absence or blockade of PLD activity is compatible with normal development and physiology [125, 154].

The pharmacological inhibition of PLD in the setting of cardiovascular events, such as thrombotic processes and ischemic stroke, to which PLD1 has already been linked is part of this thesis [8, 125].

1.4 Aim of the study

Given the fact that platelets exert key roles in hemostasis under physiological conditions as well as in thrombotic events under pathological conditions, progress in elucidating platelet signaling pathways is essential to identify new potential targets for antithrombotic therapy.

Therefore, one aim of this study was to determine the function of PLD2 in platelet physiology and thrombus formation using *Pld2$^{-/-}$* mice. Further, the redundancy of the two isoforms in this setting was addressed by analyzing PLD double-deficient mice.

Platelet inhibition is a major strategy to prevent acute ischemic cardiovascular and cerebrovascular events, which is, however, often associated with an increased bleeding risk. Since mice lacking PLD are protected from arterial thrombosis and ischemic stroke without affecting hemostasis, PLD may be a promising target for antithrombotic therapy. However, *in vivo* evidence in support of this concept has been lacking. Thus, another aim of this thesis was to elucidate the efficiency of pharmacological PLD inhibition as safe therapeutic strategy to prevent arterial thrombosis and ischemic stroke. The PLD inhibitor FIPI served as a prototype anti-PLD agent.

In order to generate efficient antithrombotic agents, it is of great interest to understand the signaling network of potential targets. Therefore, different knockout mouse strains, lacking potential modulators of PLD, were screened regarding PLD activity during platelet activation.

2 Material and Methods

2.1 Materials

2.1.1 Chemicals and reagents

A23187 (Calcium ionophore)	Sigma (Deisenhofen, Germany)
Acetic acid	Roth (Karlsruhe, Germany)
ADP	Sigma (Deisenhofen, Germany)
Agarose	Roth (Karlsruhe, Germany)
Ammonium peroxodisulphate (APS)	Roth (Karlsruhe, Germany)
Apyrase	Sigma (Deisenhofen, Germany)
β-mercaptoethanol	Roth (Karlsruhe, Germany)
Bovine serum albumin (BSA)	AppliChem (Darmstadt, Germany)
Calcium chloride	Roth (Karlsruhe, Germany)
Chloroform	Roth (Karlsruhe, Germany)
Chrono-Lume®	Probe & go (Osburg, Germany)
(d-luciferase/luciferinreagent and ATP reagent)	
Convulxin (CVX)	Enzo (Lörrach, Germany)
Disodiumhydrogenphosphate	Roth (Karlsruhe, Germany)
Deoxynucleotidetriphosphate (dNTP) mix	Fermentas (St. Leon-Rot, Germany)
Dylight-488™	Pierce (Rockford, IL, USA)
ECL solution	GE Healthcare (Freiburg, Germany)
Epon 812	Roth (Karlsruhe, Germany)
Ethanol	Roth (Karlsruhe, Germany)
Ethylacetate	Millipore (Schwalbach, Germany)
Ethylenediaminetetraacetic acid (EDTA)	AppliChem (Darmstadt, Germany)
Ethyleneglycoltetraaceticacid (EGTA)	Sigma (Deisenhofen, Germany)
Fat-free dry milk	AppliChem (Darmstadt, Germany)
Fentanyl	Janssen-Cilag GmbH (Neuss, Germany)
Fibrillar type I collagen (Horm)	Nycomed (Munich, Germany)
Flumazenil	Delta Select (Dreieich, Germany)
Fluoresceine-5-isothiocyanate (FITC)	Molecular Probes (Karlsruhe, Germany)
5-Fluoro-2-indolyl des-chlorohalopemide (FIPI)	Sigma (Deisenhofen, Germany)

Forene® (isoflurane)	Abott (Wiesbaden, Germany)
GeneRuler 1kb DNA Ladder	Fermentas (St. Leon-Rot, Germany)
Glucose	Roth (Karlsruhe, Germany)
Glycine	AppliChem (Darmstadt, Germany)
Glutaraldehyde	Roth (Karlsruhe, Germany)
[^{3}H] myristic acid	Perkin Elmer (Rodgau, Germany)
High molecular weight heparin	Sigma (Deisenhofen, Germany)
Horseradish peroxidase-conjugated streptavidin	Dianova (Hamburg, Germany)
Human fibrinogen	Sigma (Deisenhofen, Germany)
Igepal CA-630	Sigma (Deisenhofen, Germany)
Immobilon-P transfer membrane	Millipore (Schwalbach, Germany)
Indomethacin	Calbiochem (Bad Soden, Germany)
Iodine	Sigma (Deisenhofen, Germany)
Iron-III-chloride hexahydrate (FeCl$_3$6H$_2$O)	Roth (Karlsruhe, Germany)
Isooctan	Millipore (Schwalbach, Germany)
Isopropanol	Roth (Karlsruhe, Germany)
6x Loading Dye Solution	Fermentas (St. Leon-Rot, Germany)
L-α-phosphatidic acid	Sigma (Deisenhofen, Germany)
Medetomidine (Dormitor)	Pfizer (Karlsruhe, Germany)
Methanol	Roth (Karlsruhe, Germany)
Midazolam (Dormicum)	Roche (Grenzach-Wyhlen, Germany)
Midori Green Advance	Biozym Scientific GmbH (Hessisch Oldenburg, Germany
Naloxon	Delta Select (Dreieich, Germany)
Nonidet P-40 (NP-40)	Roche Diagnostics (Mannheim, Germany)
PageRuler Prestained Protein Ladder	Fermentas (St. Leon-Rot, Germany)
Protease activated receptor (PAR-4) activating peptide	Thermo Fisher scientific (Dreieich, Germany)
Paraformaldehyde (PFA)	Roth (Karlsruhe, Germany)
Platelet factor (PF)4 -ELISA	Ray Biotech (Norcross, GA, USA)
Phospatidic ethanol	Enzo (Lörrach, Germany)
Phenol/chloroform/isoamylalcohol	AppliChem (Darmstadt, Germany)
Propyleneoxide	Sigma (Deisenhofen, Germany)
Prostacyclin (PGI$_2$)	Sigma (Deisenhofen, Germany)
Protease-Inhibitor cocktail tabs	Roche Diagnostics (Mannheim, Germany)
Proteinase K	Fermentas (St.Leon-Rot, Germany)

Quicksafe A	Zinsser Analytic (Frankfurt, Germany)
R-phycoerythrin (PE)	EUROPA (Cambridge, UK)
Ro-318425 (PKC inhibitor)	Calbiochem (Bad Soden, Germany)
Sodium azide	Roth (Karlsruhe, Germany)
Sodium cacodylate	Roth (Karlsruhe, Germany)
Sodium chloride	AppliChem (Darmstadt, Germany)
Sodium hydroxide	AppliChem (Darmstadt, Germany)
Sodium orthovanadate	Sigma (Deisenhofen, Germany)
Taq polymerase buffer (10x)	Fermentas (St.Leon-Rot, Germany)
Taq polymerase	Fermentas (St.Leon-Rot, Germany)
Tetramethylethylendiamin (TEMED)	Roth (Karlsruhe, Germany)
3,3,5,5-tetramethylbenzidine	Becton Dickinson (Heidelberg, Germany)
Thapsigargin (TG)	Invitrogen (Karlsruhe, Germany)
Thrombin	Roche Diagnostics (Mannheim)
2,3,5-triphenyltetrazolium chloride (TTC)	Sigma (Deisenhofen, Germany)
tris(hydroxymethyl)aminomethane (Tris) ultra	Roth (Karlsruhe, Germany)
Tris/HCL	Roth (Karlsruhe, Germany)
Triton X-100	Applichem (Darmstadt, Germany)
Trizol reagent	Invitrogen (Karlsruhe, Germany)
Tween 20	Roth (Karlsruhe, Germany)
U46619 (TxA$_2$ analogue)	Alexis Biochemicals (San Diego, USA)
U-73122 (PLC Inhibitor)	Sigma (Deisenhofen, Germany)
Uranylacetate	Electron Microscopical Sciences (Hatfield, USA)
Vectashield hardset mounting medium	Vector Laboratories (Burlingame, USA)
Western Lightning Chemiluminescence	PerkinElmer LAS (Boston, USA)
X-gal	Peqlab (Erlangen, Germany)

All enzymes were obtained from Fermentas (St. Leon-Rot, Germany), Invitrogen (Karlsruhe, Germany) or New England Biolabs (NEB, Ipswich, MA, USA). Rhodocytin was a generous gift from J. Eble (University Hospital Frankfurt, Germany). Collagen related peptide (CRP) was generated as described previously [195]. Recombinant Annexin A5 was expressed, purified and fluorescently labeled in our laboratory. All other non-listed chemicals were obtained from AppliChem (Darmstadt, Germany), Sigma (Deisenhofen, Germany) or Roth (Karlsruhe, Germany).

2.1.2 Antibodies

2.1.2.1 Purchased primary and secondary antibodies

Anti-rabbit IgG–horseradish peroxidase (HRP)	Dako Cytomation (Hamburg, Germany)
HRP conjugated polyclonal anti-hvWF antibody, A0226	Dako Cytomation (Hamburg, Germany)
Polyclonal rabbit anti-hvWF, A0082	Dako Cytomation (Hamburg, Germany)
Phalloidin-atto647N	Sigma (Deisenhofen, Germany)
Rabbit anti-PLD2 (P5993)	Sigma (Deisenhofen, Germany)
Rabbit anti-tubulin (MAB1864)	Chemicon (Hofheim, Germany)
α-tubulin antibody-Alexa 488	Invitrogen (Karlsruhe, Germany)

2.1.2.2 Monoclonal antibodies

Monoclonal antibodies (mAbs) were generated and modified in our laboratory.

Antibody	Clone	Isotype	Antigen	Source/ description
p0p/A	92H12	IgG2b	GPIb	unpublished
p0p/B	57E12	IgG2b	GPIb	[196]
p0p4	15E2	IgG2b	GPIb	[197]
p0p6	56F8	IgG2b	GPIX	[197]
DOM2	89H11	IgG2a	GPV	[197]
ULF1	96H10	IgG2a	CD9	[197]
JAQ1	98A3	IgG2a	GPVI	[198]
JON6	14A3	IgG2b	αIIbβ3	unpublished
LEN1	12C6	IgG2b	α2	[199]
Anti-integrin β1 chain (CD29)	9EG7	IgG2a	β1	BD Pharmingen
INU1	11E9	IgG1	CLEC-2	[200]
JON/A	4H5	IgG2b	αIIbβ3	[201]
WUG 1.9	5C8	IgG1	P-selectin	unpublished
EDL-1	57B10	IgG2a	β3 integrin	[197]
BAR-1	25B11	IgG1	$\alpha5$ integrin	[199]

2.1.3 Buffers

Acid-citrate-dextrose buffer (ACD), pH 4.5

Trisodium citrate dehydrate	85 nM
Citric acid anhydrous	65 nM
Glucose anhydrous	110 nM

Blocking solution for immunoblotting

BSA or fat-free dry milk 5% in PBS or PBS-T

Blotting buffer A for immunoblotting

TRIS, pH 10.4	0.3 M
Methanol	20%

Blotting buffer B for immunoblotting

TRIS, pH 10.4	25 mM
Methanol	20%

Blotting buffer C for immunoblotting

ε-amino-n-caproic acid, pH 7.6	4 mM
Methanol	20%

Cacodylate buffer (electron microscopy)

Sodium cacodylate (pH 7.2)	50 mM

Chromatography eluent

Ethylacetate	130 ml
Isooctan	20 ml
Acetic acid (100%)	30 ml
Aqua bidest.	100 ml

Mix, allow phase separation and remove lower phase

Fixation buffer I (electron microscopy)

Sodium cacodylate, pH 7.2	0.1 M
Glutaraldehyde	2.5%
Formaldehyde	2%

Fixation buffer II (electron microscopy)

Sodium cacodylate, pH 7.2	50 mM
Osmium tetroxid	2%

Laemmli buffer for SDS-PAGE

TRIS	40 mM
Glycine	0.95 M
SDS	0.5%

Lysis buffer for DNA isolation

TRIS base	100 mM
EDTA	5 mM
NaCl	200 mM
SDS	0.2%
add Proteinase K (20 mg/ml)	100 µg/mL

Phosphate buffered saline (PBS), pH 7.14

NaCl	137 mM (0.9%)
KCl	2.7 mM
KH_2PO_4	1.5 mM
$Na_2HPO_4 x 2H_2O$	8 mM

Immunoprecipitation (IP) Buffer

Tris-HCl, pH 8.0	15 mM
NaCl	155 mM
EDTA	1 mM
NaN_3	0.005%

PHEM buffer

PIPES	100 mM
HEPES	5.25 mM
EGTA	10 mM
$MgCl_2$	20 mM

SDS sample buffer, 2x

β-mercaptoethanol (for reducing conditions)	10%
TRIS buffer (1.25 M), pH 6.8	10%

Glycerine	20%
SDS	4%
Bromophenolblue	0.02%

Separating gel buffer

TRIS/HCl (pH 8.8)	1.5 M
add H_2O	

Stacking gel buffer

TRIS/HCl (pH 6.8)	0.5 M

50x TAE

TRIS base	0.2 M
Acetic acid	5.7%
EDTA (0.5 M, pH 8)	10%

TE buffer, pH 8

TRIS base	10 mM
EDTA	1 mM

Tris-buffered saline (TBS), pH 7.3

NaCl	137 nM (0.9%)
Tris/HCl	20 mM

Tyrodes buffer, pH 7.3

NaCl	137 mM (0.9%)
KCl	2.7 mM
$NaHCO_3$	12 mM
NaH_2PO_4	0.43 mM
Glucose	0.1%
HEPES	5 mM
BSA	0.35%
$CaCl_2$	1 mM
$MgCl_2$	1 mM

Washing buffer for Western blot (PBS-T)

Tween 20	0.1% in PBS

2.1.4 Animals

All animal studies were approved by the district government of Lower Franconia (Bezirksregierung Unterfranken). Specific pathogen free C57BL/6J mice were purchased from JANVIER LABS (Saint Berthevin, France).

Pld1$^{-/-}$ mice were generated in our laboratory by Attila Braun [8]. In order to generate *Pld2$^{-/-}$* mice the stem cell clone from KOMP (knockout mouse project) repository AA11 was ordered carrying one targeted PLD2 allele (*Pld2$_{tm1(KOMP)Vlcg}$*), leading to a complete deletion of the *Pld2* gene. This clone was injected into mouse blastocysts and yielded chimeric mice giving heterozygous offspring [125].

Bone marrow chimeric *Stim1$^{-/-}$* and *Orai1$^{-/-}$* mice were generated in our laboratory as described before [202, 203]. Conditional knockout mice, that carried loxP-flanked genes for *Grb2* [204], *Gna13* [205], *RhoA* [206], *Rac1* [207], *Cdc42* [208], *Tln1* [209] and *n-cofilin* [210] were generated by intercrossing mice with PF4-Cre mice [211] in order to obtain platelet- and megakaryocyte-specific knockout mice which are here referred to as *Grb2$^{-/-}$*, *G$_{13}$$^{-/-}$*, *RhoA$^{-/-}$*, *Cdc42$^{-/-}$*, *Rac1$^{-/-}$* and *n-cofilin$^{-/-}$* mice, respectively. Mice carrying the Cre recombinase under the PF4 promoter were from Radek Skoda (Basel, Switzerland). Mice with floxed genes for RhoA, Rac1 and Cdc42 were obtained from Cord Brakebusch (Copenhagen, Denmark). Mice with floxed genes for Grb2 were kindly provided by Lars Nitschke (Erlangen, Germany). *Twf2a$^{-/-}$* mice were from Pekka Lappalainen (Helsinki, Finland).

P110β$^{fl/fl,PF-4\ Cre}$ mice were kindly provided by Marie-Pierre Gratacap [212]. Profilin1 mice were purchased from EUCOMM. Double-deficient mice were obtained by intercrossing the respective single knockout mice.

Prkcb$^{-/-}$ (PKCβ), *Prkcq$^{-/-}$* (PKCθ) mice were from Michael Leitges [213-215], as were the floxed *Prkci$^{-/-}$* (PKCι) [216] which were intercrossed with PF4-Cre mice.

2.1.4.1 Generation of bone marrow chimeric mice

6 week old C57BL/6 mice were lethally irradiated with 10 Gray. The femur and tibia of respective donor mice were prepared and bone marrow was flushed with a 22G needle into prewarmed DMEM with 10% FCS and 1% penicillin/streptomycin. The bone marrow cells were counted in a Neubauer chamber and 4×10^6 cells in 150 µl DMEM were intravenously injected into recipient mice. Mice were then treated with 2 g/l neomycin for the following 6 weeks.

2.2 Methods

2.2.1 Mouse genotyping

2.2.1.1 Isolation of genomic DNA

A small part of a mouse ear was lysed in 500 µl DNA lysis buffer overnight at 56°C under shaking conditions (1000 rpm). Upon addition of 500 µl phenol/chloroform, samples were mixed and thereafter centrifuged at 11,000 rpm for 10 min at room temperature (RT). The supernatant was transferred into a new tube and 400 µl isopropanol were added. Samples were shaken vigorously and centrifuged at 14,000 rpm for 10 min at 4°C. After washing the resulting pellet with 1 ml 70% ethanol, the samples were centrifuged again at 14,000 rpm for 10 min. Finally, the pellet was left to dry and then resuspended in 50-100 µl TE buffer.

2.2.1.2 Genotyping of *Pld1*$^{-/-}$ and *Pld2*$^{-/-}$ mice

Pipeting scheme:

	1 µl	DNA
	2.5 µl	10x Taq buffer
	2.5 µl	25 mM MgCl$_2$
	1 µl	10 mM dNTP
	1 µl	10 µM fwd primer
	1 µl	10 µM rev primer
	0.25 µl	Taq polymerase
	15.75 µl	H$_2$O

Primer:

Pld1 WT allele:

T$_A$: 66°C

Fwd: 5' - TGT GCA AGT GCG TGT GGG CA - 3'

Rev: 5' - ACA GGG CAC CCA CAG GAG CA - 3'

Product size: 283 bp

Pld1 KO allele:

T$_A$: 51.4°C

Fwd: 5' - TTA TCG ATG AGC GTG GTG GTT ATG C - 3´

Rev: 5' - GCG CGT ACA TCG GGC AAA TAA TAT - 3´

Product size: 650 bp

Pld2 WT allele:

T$_A$: 59°C

Fwd: 5' - AAG CAA CAC CAC ACA TTC CA - 3'

Rev: 5' - CTT CCC GAC TCA CAG CTT TC - 3'

Product size: 445 bp

Pld2 KO allele:

T$_A$: 55°C

Fwd: 5' - TCA TTC TCA GTA TTG TTT TGC C - 3'

Rev: 5' - GGA GGA AGA GTG AGA TGA AG - 3'

Product size: 408 bp

<u>PCR program:</u>

95°C	5:00 min
95°C	0:30 min
T$_A$	0:30 min
72°C	0:30-1:00 min (depending on product size)
72°C	5:00 min
20°C	∞

95°C, T$_A$, 72°C steps repeated 35x

2.2.1.3 Agarose gel electrophoresis

To analyze the PCR products, 1.5% agarose gels were used. The respective amount of agarose was dissolved in 1x TAE buffer and boiled using a microwave. After cooling 5 µl Midori Green per 100 ml of agarose gel were added and the solution was poured into a tray containing a comb and was allowed to congeal. The tray was placed into an electrophoresis chamber already containing 1x TAE buffer. 20 µl of each PCR sample, diluted in 4x loading buffer, was loaded onto the gel, which was run at 120 V. DNA ladder was used to determine the size of the PCR products that were visualized by UV light.

2.2.2 Molecular biology and biochemistry

2.2.2.1 RNA isolation and RT PCR

Isolated platelets of 3 mice were pooled, washed with PBS/EDTA and centrifuged. The resulting pellet was lysed in 250 µl IP buffer with 1% NP-40. The samples were vortexed and incubated on ice for 5-10 min. After addition of 1 ml TRIZOL reagent the samples were mixed again and incubated for another 5-10 min. Next, 250 µl chloroform were added, the samples were vortexed and centrifuged at 10,000 rpm for 10 min at 4°C. Subsequently, the supernatant was transferred to a new tube containing 1 ml isopropanol. The samples were shaken vigorously and incubated on ice for 30 min. In order to obtain a RNA pellet, the samples were

centrifuged at 14,000 rpm for 10 min at 4°C. Then, the pellet was washed with 70% ethanol. Finally, the supernatant was discarded, the pellet was left to dry and resolved in ~20 µl RNase free water. The RNA concentration was determined by absorbance readings at 260 nm, whereas the ratios of absorbances at 260/280 and 260/230 were used to assess purity. Samples with 260/280 ratios of >1.8 and 260/230 ratios of >1.9 were used to generate cDNA.

In order to synthesize cDNA, 1 µg RNA was incubated with 1 µl oligo(dT)$_{12-18}$ in a total volume of 11.9 µl for 10 min at 70°C. Samples were placed on ice while adding 2 µl DTT (0.1 M), 1 µl dNTPs (10 mM), 0.1 µl RNasin, 4 µl 5x first strand buffer and 1 µl Super Script Reverse Transcriptase. The total volume was adjusted to 40 µl with RNase free water. After incubating the samples at 42°C for 1 h, the reaction was stopped by incubation at 70°C for 10 min.

Primer:

Pld1 transcript

Fwd: 5′ - A CAC AGG ATA CCA GGT GTG A - 3′

Rev: 5′ - T AGA CTC TAC TGA TGC TGC C - 3′

Pld2 transcript

Fwd: 5' - GTG CCA CTG TGC AGG TCT TGA GG - 3'

Rev: 5' - GCA GAA TAG CCT GGA TGG AG - 3'

Actin transcript

Fwd: 5' - GTG GGC CGC TCT AGG CAC CAA - 3'

Rev: 5' - CTC TTT GAT GTC ACG CAC GAT TTC - 3'

2.2.2.2 Preparation of tissue/platelet lysates

50 µg of the respective tissue were homogenized in 1 ml ice cold IP buffer, containing 1% NP-40 and protease inhibitors, by using a Miccra D1 homogenizing drive (ART Labortechnik, Mülheim, Germany). In order to obtain platelet lysates, isolated platelets were lysed with IP buffer containing 1% NP-40 and protease inhibitors at a concentration of ~0.5 x 10^6 *platelets*(Plt)/µl. Following an incubation at 4°C on a rotor for 1 h or 20 min on ice for tissue or platelet lysates, respectively, the samples were centrifuged at 14,000 rpm for 30 min at 4°C. Supernatants were transferred into a new tube and frozen at -80°C. For Western blot analysis, reducing or non-reducing sample buffer was added and samples were boiled for 5 min at 95°C.

2.2.2.3 Western blot

In order to separate the proteins, 20 µl of the samples were loaded per lane of a 10% polyacrylamide gel. The gel was run at 25 mA for 1.5 h. After separation, the proteins were transferred onto a polyvinylidene difluoride (PVDF) membrane by semidry immunoblotting at a current of 65 mA per gel. Afterwards, the membrane was incubated in blocking buffer in order to avoid unspecific binding of the primary antibody. Subsequently, the membrane was

incubated with the required primary antibody overnight at 4°C. To remove the unbound antibody, the membrane was washed three times for 10 min with TBS-T. Then, membranes were incubated with the respective HRP-coupled secondary antibodies for 1 h at RT. Following three washing steps, the proteins were visualized by ECL.

2.2.3 *In vitro* analysis of platelet function

2.2.3.1 Platelet isolation and counting

700 µl blood, taken from the retroorbital plexus of anesthetized mice (isofluorane) were transferred in a 1.5 ml reaction tube containing either 300 µl heparin in TBS (20 U/ml, pH 7.3) or 300 µl acid citrate dextrose (ACD). Next, the blood was centrifuged at 800 rpm (Eppendorf Centrifuge 5415C) for 5 min at RT. The supernatant and buffy coat were collected and again centrifuged at 800 rpm for 5 min. The resulting platelet rich plasma was transferred into a new tube and the platelets were pelleted at 2,800 rpm for 5 min. The pellet was washed twice with Ca^{2+}-free Tyrode's buffer containing 1.0 µg/ml PGI_2 and 0.02 U/ml apyrase. The platelet concentration of each sample was determined by measuring a 1:1 dilution of the platelet suspension in PBS in a Sysmex counter (KX-21N, Sysmex Corp., Kobe, Japan). The pellet was resuspended in Tyrode's buffer at the desired platelet concentration. For determination of platelet count and size, 50 µl blood was drawn from the retroorbital plexus of anesthetized mice using heparinized microcapillaries, diluted 1:20 in PBS and analyzed in a Sysmex cell counter.

2.2.3.2 Plasma preparation

700 µl blood was taken from the retroorbital plexus of an anesthetized mouse and transferred in a tube containing 300 µl heparin. The blood was centrifuged at 2,800 rpm for 5 min and the upper phase was transferred into a new tube. After another centrifugation at 10,000 rpm for 5 min, the supernatant was collected. The plasma was either used directly or stored at -20°C.

2.2.3.3 Flow cytometric analysis

In order to determine basal glycoprotein expression levels, washed platelets (1 x 10^6) were stained for 15 min at RT with saturating amounts of fluorophore-conjugated antibodies. For activation studies, the platelets were activated with different agonists in the presence of saturating amounts of *phycoerythrin* (PE)-coupled JON/A and *fluorescein isothiocyanate* (FITC)-coupled α-P-selectin antibodies. Samples were incubated for 7 min at 37°C and additional 7 min at RT. The reaction was stopped by addition of 500 µl PBS. The samples were analyzed directly on a FACSCalibur (BD, Heidelberg, Germany). For a two-color staining, the following settings were used.

Detectors/Amps:

Parameter	Detector	Voltage
P1	FSC	E01
P2	SSC	380
P3	FL1	650
P4	FL2	580
P5	FL3	150

Threshold:

Value	Parameter
253	FSC-H
52	SSC-H
52	FL1-H
52	FL2-H
52	FL3-H

Compensation:

Parameter	Value
FL1	2.4% of FL2
FL2	7.0% of FL1
FL3	0% of FL3
FL4	0% of FL2

2.2.3.4 Aggregation studies

Washed platelets were adjusted to a concentration of 0.3×10^6 platelets/µl. 50 µl platelets or heparinized PRP (used for ADP-induced aggregation measurements) were transferred into a cuvette containing 110 µl Tyrode's buffer with 2 mM Ca^{2+}. For all measurements with washed platelets (except when activating platelets with thrombin) Tyrode's buffer with 100 µg/ml human fibrinogen was used. To induce aggregation, agonists or reagents (100-fold concentrated) were added and light transmission was recorded over 10 min on an Apact-4-channel optical aggregation system (APACT, Hamburg, Germany). For calibration before each measurement, Tyrode's buffer was set as 100% and the washed platelet suspension or PRP was set as 0% aggregation.

2.2.3.5 ATP release

For determination of ATP release, platelets were adjusted to a concentration of 0.5×10^6 plts/ml with Tyrode's buffer. Then, 80 µl platelets were added to 160 µl Tyrode's with 2 mM Ca^{2+} and incubated for 2 min at 37°C under stirring conditions with 25 µl Chrono-Lume reagent. Subsequently, 2.6 µl of the respective agonists (50-fold working solution) were added and the ATP release and light transmission were measured with a Chrono-Log 4 channel aggregation system (Probe & go, Osburg, Germany). Calibrations were performed as mentioned above (section 2.2.3.4) and an ATP standard was used to calculate the agonist-induced ATP release.

2.2.3.6 vWF secretion

Platelets were adjusted to a concentration of 0.5×10^6 plts/µl and 120 µl were activated with the indicated agonists for 15 min at 37°C. The samples were centrifuged at 2,800 rpm for 5 min, the supernatant was transferred into a new reaction tube and centrifuged at 14,000 rpm for another 5 min. 100 µl of the supernatant were given into the first lane of an ELISA plate which had been coated with a rabbit anti-human vWF antibody (diluted 1:600 in 50 mM $NaHCO_3$, pH 9.0, 50 µl per well) overnight at 4°C, subsequently blocked with 200 µl 5% BSA in ddH_2O per well and washed 3 times with PBS 0.1% Tween. 12 1:1 dilutions in PBS were prepared per sample on the ELISA plate. Platelet lysate was used as positive control. The plate was incubated for 2 h at 37°C. After washing the plate 3 times with PBS 0.1% Tween, the samples were incubated with rabbit anti-human vWF-HRP (diluted 1:3000 in PBS 0.1% Tween and 1% BSA, 50 µl per well) for 2 h at 37°C. After washing the plate, it was developed by incubating with 50 µl 3,3,5,5-tetramethylbenzidine (TMB-one substrate). The reaction was stopped by adding 50 µl 0.5 M H_2SO_4. Absorbance was measured at 650 nm using a Multiscan device (Thermo Scientific).

2.2.3.7 PF4 secretion

The samples were prepared as in section 2.2.3.6 and the assay was performed according to the manufacturers' protocol (PF-4 ELISA Kit, RayBio).

2.2.3.8 Determination of platelet filamentous (F)-actin content

Platelets were washed and adjusted to a concentration of 15×10^5 plts/µl and diluted 1:10 in Tyrode's buffer with Ca^{2+} to a final volume of 50 µl per sample. The samples were incubated for 3 min at 37°C with 5 µl of Dylight 649-conjugated anti-GPIX derivative and stimulated with 1 U/ml thrombin for 2 min at 37°C under shaking conditions (400 rpm). Next, the platelets were fixed by adding 0.55% volume 10% PFA in PBS and subsequently centrifuged for 5 min at 2800 rpm. The pellets were resuspended in 55 µl Tyrode's with Ca^{2+} and transferred into FACS tubes containing 10 µM phalloidin-FITC. After incubation for 30 min at RT in the dark, the reaction was stopped by adding 500 µl PBS. The samples were kept on ice and analyzed with a FACSCalibur.

2.2.3.9 Clot retraction

For clot retraction, 700 µl blood was collected with non-heparinized capillaries in a tube containing 70 µl sodium citrate. During platelet washing, platelet poor plasma (PPP) was collected and the resulting platelet pellet was adjusted to a concentration of 3×10^5 plts/µl with PPP. To 250 µl of this suspension 1.5 µl red blood cells and 5 µl 1 M $CaCl_2$ were added. To induce clot retraction the samples were incubated at 37°C with 3 U/ml thrombin. Images were taken every 15 min. After 4 h the residual fluid in the tube was measured.

2.2.3.10 Static adhesion on ECM proteins

2.2.3.10.1 Static adhesion on fibrinogen

Rectangular glass coverslips (Roth, Karlsruhe, Germany) were coated with 100 µg/ml human fibrinogen at 4°C overnight in a humid chamber. The slides were blocked with 200 µl 3% BSA in PBS. Platelets were washed and adjusted to a concentration of 3×10^5 plts/µl. The platelets were diluted with Tyrode's with Ca^{2+} and stimulated with 0.01 U/ml thrombin. Immediately afterwards, the samples were transferred to a fibrinogen-coated coverslip, which had previously been washed with Tyrode's with Ca^{2+}. At the respective time points, spread platelets were fixed by adding 300 µl of 4% PFA/PBS. The slides were analyzed by microscopy (Axiovert 200M, Zeiss, Göttingen, Germany) at 100x magnification and representative *differential interference contrast* (DIC) images were taken. For evaluation, the numbers of platelets at different spreading stages were determined.

2.2.3.10.2 Static adhesion on vWF

Rectangular glass coverslips were coated with 200 µl/slide polyclonal rabbit-α-human vWF-antibody (1:500 in 50 mM carbonate-bicarbonate, pH 9.6) overnight at 4°C in a humidity chamber. To rinse of unbound antibody, the slides were rinsed 3 times with PBS and blocked for 1 h in 3% BSA. Meanwhile, plasma was prepared according to section 2.2.3.2. After rinsing the slides thoroughly, they were incubated with 100 µl plasma for 1 h at 37°C and rinsed again thereafter. 30 µl (5 min) or 50 µl (15 and 30 min) platelets at a concentration of 3×10^5 plts/µl, were incubated with Tyrode's with Ca^{2+} in the presence of 40 µg/ml integrillin for 10 min at 37°C under stirring conditions. Subsequently the GPIb clustering was induced by addition of 2.5 U/ml botrocetin. Immediately afterwards, the platelets were allowed to spread on a vWF-coated slide and were fixed at the respective timepoints with 4% PFA in PBS. The slides were analyzed by microscopy (Axiovert 200M, Zeiss, Göttingen, Germany) at 100x magnification and representative images were taken. For evaluation, the platelets were sorted into different categories according to the number of filopodia they formed.

2.2.3.10.3 Staining of spread platelets for confocal microscopy

Fully spread platelets were fixed and permeabilized in PHEM buffer supplemented with 4% PFA and 1% NP40 for 20 min at 4°C and thereafter blocked with 5% BSA in PBS for 2 h at 37°C. The samples were washed and stained with anti-α-tubulin Alexa F488 (clone B-5-1-2, Invitrogen) or phalloidin-Atto647N (Fluka) in the dark for 1 h at 37°C. Subsequently, the samples were mounted with Fluoroshield (Sigma-Aldrich) and left to dry at 4°C. All used fluorophore-conjugated secondary antibodies were purchased from Invitrogen. Samples were analyzed using a Leica TCS SP5 confocal microscope (Leica Microsystems). This experiment was performed by Simon Stritt from our laboratory.

2.2.3.11 Adhesion under flow conditions

2.2.3.11.1 Flow adhesion assay on collagen

Rectangular glass coverslips were coated with 100 µl 200 µg/ml fibrilar type I collagen (Horm) overnight at 37°C. On the next day, the coverslips were blocked with 300 µl 3% BSA in PBS. The slides were put into a transparent flow chamber with a slit depth of 50 µm. Unwanted bubbles were removed by perfusing the chamber with prewarmed Tyrode's buffer. Meanwhile, 700 µl blood from a mouse was collected in heparin (20 U/ml). The platelets were labeled with a Dylight-488 conjugated anti-GPIX derivative (0.2 µg/ml) for 5 min at 37°C. Subsequently the blood was diluted 2:1 in Tyrode's buffer with Ca^{2+} and taken up into a 1 ml syringe, which was connected to the flow chamber and placed in the pulse-free pump. Perfusion was performed for 10 min (150 s^{-1}) or 4 min under high or low shear stress equivalent to wall shear rates of 150, 1,000 and 1,700 s^{-1}. Platelet adhesion and thrombus growth on collagen was monitored using a Zeiss Axiovert 200 inverted microscope (40x objective). Images were taken every second using a CoolSNAP-EZ camera. After the indicated times, Tyrode's buffer was perfused at the same shear rate for half of the time used for the perfusion. Subsequently, phase-contrast and fluorescent images were taken from at least 6 different visual fields. Analysis of the images was performed using Metamorph® software (Visitron, Munich, Germany). Thrombus formation was determined as the mean percentage of total area covered by platelets/thrombi and thrombus volume was expressed as mean integrated intensity per mm^2.

2.2.3.11.2 Flow adhesion assay on vWF

Coverslips were prepared as in section 2.2.3.10.2 and perfusion of blood over vWF-coated slides was performed at wall shear rates of 1,000 s^{-1} and 1,700 s^{-1} as described in section 2.2.3.11.1.. The representative images were analyzed by counting adherent platelets per visual field.

2.2.3.11.3 Procoagulant activity measurements

Flow adhesion assays were grossly performed as described above in 2.2.3.11.1. The blood was supplemented with 5 U/ml heparin and, after perfusion, adherent platelets were washed with Tyrode's buffer containing 250 ng/ml Fluorophore-Annexin V. Next, the samples were washed with Tyrode's buffer to remove the residual antibody. Subsequently, phase contrast and fluorescent images were taken from 10 different visual fields.

2.2.3.12 Phospholipase D activity assay

Platelets, at a concentration of 3 x 10^5 plts/µl, were labeled with 50 µCi/ml ^{3}H-myristic acid in Ca^{2+}-free Tyrode's buffer for 90 min at 37°C under shaking condition (300 rpm). For this purpose, the ethanol in which ^{3}H-myristic acid was diluted, was vaporized under an air current

using a Pierce Reacti-Vap III evaporation unit (1.5 psi, Thermo Scientific, Schwerte, Germany). Subsequently, the ^{3}H-myristic acid was resuspended with the platelet suspension. After incubation, the samples were centrifuged at 2,800 rpm for 5 min at RT. The supernatant was discarded and the pellet was resuspended in Tyrode's buffer. Next, the samples were aliquoted into 2 ml reaction tubes (80 µl platelet suspension/reaction). The samples were incubated with 0.5% ethanol for 10 min at 37°C before the respective agonist/inhibitor/agent was added. The reaction was stopped by adding 500 µl of ice-cold methanol, vortexed briefly and put on ice immediately. After adding 350 µl of ddH$_2$0 and 500 µl of chloroform, the samples were vortexed and subsequently centrifuged at 2,600 g for 12 min at RT to ensure phase separation. The upper phase and interphase were removed with a vacuum pump and 300 µl of the lower phase were transferred into a new 1.5 ml reaction tube. Next, the samples were vaporized for ~ 10 min using the Pierce Reacti-Vap III evaporation unit. The samples were resuspended in 40 µl of a Marker Mix, containing 0.125 mg/ml PtdEtOH and 0.125 mg/ml L-α-PA in chloroform. The samples were then transferred onto TLC silica gel 60 (Millipore, Schwalbach, Germany) plates. For lipid separation the plates were put into a chromatography chamber containing eluent buffer. Afterwards, the silica plates were dried and transferred to an iodine-containing chamber to stain the phospholipids as well as the markers PtdEtOH and PA. For each sample, the silica plate was scratched at the heights of stained PtdEtOH and total phospholipids. The samples were transferred into 6 ml miniature Pony Vials (Perkin Elmer, Rodgau, Germany) and 2 ml of Zinsser Analytic Quicksafe A was added. To determine the decays per minute, a Tri-Carb 2910 liquid Scintillation Analyzer (Perkin Elmer) was used applying a preset quench curve.

2.2.4 *In vivo* murine models

2.2.4.1 Determination of platelet life span

Mice were injected intravenously with 3.5 µg of a Dylight-488 conjugated anti-GPIX Ig derivative. Before injection and at the indicated time points 50 µl blood was collected and the percentage of positive platelets were determined by flow cytometric analysis.

2.2.4.2 Triple anesthesia

Mice were anesthetized intraperitoneally with a combination of midazolam/ medetomidine/fentanyl (5/0.5/0.05 mg/kg body weight).

2.2.4.3 FeCl$_3$-induced thrombus formation in small mesenteric arterioles

Four week old mice were injected with 1.5 µg of a Dylight-488 conjugated anti-GPIX Ig derivative, anesthetized with 450 µg/g body weight 2,2,2-tribromoethanol and the mesentery was exteriorized through a midline abdominal incision [217]. Arterioles were visualized with a Zeiss Axiovert 200 inverted microscope (10x/0.3 NA objective, Carl Zeiss) equipped with a

100-W HBO fluorescent lamp source, and a CoolSNAP-EZ camera (Visitron, Munich, Germany). Digital images were recorded once a second and analyzed off-line using Metavue software. Injury was induced by topical application of a 3-mm² filter paper saturated with $FeCl_3$ (20%). Adhesion and aggregation of fluorescently labeled platelets (Dylight-488–conjugated anti-GPIX Ig derivative) in arterioles were monitored for 40 min or until occurrence of complete occlusion which was reached when blood flow ceased for >1 min.

2.2.4.4 $FeCl_3$-induced thrombus formation in the carotid artery

6 to 8 weeks old mice were anesthetized and the right carotid artery was exposed through a vertical midline incision in the neck. An ultrasonic flow probe (0.5PSB699; Transonic System, New York, USA) was placed around the vessel and thrombosis was induced by topical application of a 0.5 mm by 1 mm filter paper saturated with 10-15% $FeCl_3$ for 90 s. Blood flow was monitored for 30 min or until full occlusion of the vessel.

2.2.4.5 Mechanical injury of the abdominal aorta

A longitudinal incision was used to open the abdominal cavity and expose the abdominal aorta of 8-12 weeks old anesthetized mice. An ultrasonic flow probe (0.5PSB699; Transonic System, New York, USA) was placed around the vessel and thrombosis was induced by a single firm compression with forceps. Blood flow was monitored for 30 min.

2.2.4.6 Bleeding time assay

Mice were anesthetized by intraperitoneal injection with triple anesthesia and a 2 mm segment of the tail tip was removed with a scalpel. Tail bleeding was monitored by gently absorbing blood using filter papers at 20 s intervals without making contact with the wound site. As soon as no blood could be observed on the paper, bleeding was determined to have ceased. Experiments were stopped after 20 min.

2.2.4.7 Transient occlusion model of the middle cerebral artery

Transient middle cerebral artery occlusion (tMCAO) model experiments were performed by Peter Kraft, a member of the research group of Prof. Guido Stoll (Department of Neurology, University of Würzburg). 8-10 weeks-old mice were conducted to the experiment according to previously published recommendations for research in mechanism-driven basic stroke studies [218]. tMCAO was induced under inhalation anesthesia (isoflurane in a 70% N_2/30% O_2 mixture) using the intraluminal filament (Doccol Company) technique [219]. Briefly, the filament was inserted into the right common carotid artery and advanced via the internal carotid artery in order to occlude the basis of the *middle cerebral artery* (MCA). After 60 min, the filament was withdrawn to allow reperfusion. For measurements of ischemic brain volume, animals were sacrificed 24 h after induction of tMCAO, and brain sections were stained with 2% 2,3,5-

TTC. Brain infarct volumes were calculated and corrected for edema [219]. Neurological function and motor function were assessed by two independent and blinded investigators 24 h after tMCAO, as previously described [219]. The experiments were conducted according to the recommendations for research in experimental stroke studies [218] and the current ARRIVE guidelines (http://www.nc3rs.org/ARRIVE). Magnetic resonance imaging (MRI) was performed 24 hours after transient ischemia on a 1.5 T unit (Vision; Siemens) under inhalation anesthesia. A custom-made dual-channel surface coil was used for all measurements (A063HACG; Rapid Biomedical). The MR protocol included a coronal T2-weighted sequence (slice thickness, 2 mm) and a coronal T2-weighted gradient-echo *constructed interference in steady state* (CISS) sequence (slice thickness, 1 mm). MR images were transferred to an external workstation (Leonardo; Siemens) for data processing. The visual analysis of infarct morphology and the search for eventual intracerebral hemorrhage were performed in a blinded manner. Infarct volumes were calculated by planimetry of hyperintense areas on high-resolution CISS images.

2.2.5 Transmission electron microscopy (TEM) of platelets

Platelets were adjusted to a concentration of 3×10^8 plts/µl in Tyrode's buffer. Resting or activated platelets were fixed with the equal volume of 2.5% glutaraldehyde in 0.1 M cacodylate buffer (pH 7.2) containing 2% sucrose and incubated for 1 h at RT. Samples were stored at 4°C. For further processing, 1 ml cacodylate buffer was added to the sample and centrifuged for 5 min at 1,000 g. This washing process was repeated twice. Next, the platelets were resuspended in 1 ml agarose solution (2% low melting agarose in cacodylate buffer prewarmed to 45°C) and centrifuged again at 14,000 rpm for 5 min at 37°C. The upper agarose solution was discarded except residual 100 µl which were incubated directly on ice for 10 min. The agarose platelet pellets were taken out of the tube and cut into 1 mm^3 cubes and were further stored in cacodylate buffer. For sample fixation, cacodylate buffer containing 1% OsO_4 was added and the samples were incubated for 45 min at RT. Subsequently, the samples were washed three times with ddH_2O, dehydrated in 70% (4 x 5 min), 95% (3 x 15 min) and 100% (3 x 15 min) ethanol and finally incubated with a 1:1 mixture of propylenoxyde and epon for 1 h under rotation. Samples were again incubated with epon at RT overnight and afterwards additional 2-3 h. Next, samples were embedded in gelatine capsules and left to dry for 48 h at 60°C. With a Leica Ultracut microtom UCT (Leica Microsystems, Wetzlar, Germany) 50 nm thin sections were cut. The sections were contrasted. Finally, samples were analyzed at 120 kV under a CN12ß BioTWIN transmission electron (FEI). Images were taken with a Megaview camera (Olympus SIS). This method was performed by Sebastian Dütting from our laboratory.

2.2.6 Statistical data analysis

Most results are presented as means ± SD or scatter blots. Differences between two groups were assessed by the Welch's test or if applicable with the Mann Whitney U test. For the stroke model, infarct volumes and functional data were tested for Gaussian distribution with the D'Agostino and Pearson omnibus normality test and then analyzed using the two-tailed Student's t test. For statistical analysis, SPSS statistics 20 and Microsoft Excel were used. Differences between more than two groups were analyzed by one-way analysis of variance (ANOVA) with Dunnetts T3 as post-hoc test. $P < 0.05$ was considered as statistically significant.

3 Results

3.1 Phospholipase D2 is dispensable for platelet activation and thrombus formation

Both mammalian PLD isoforms, PLD1 and PLD2, are expressed in platelets [36, 186]. In order to elucidate the physiological role of PLD in platelets *in vivo*, PLD deficient mice were generated. Previously, *Pld1*^{-/-} mice were analyzed by Margitta Elvers and David Stegner from our laboratory demonstrating that PLD1 is important for GPIb dependent integrin activation and thrombus formation *in vivo* [8]. To reveal the significance of PLD2 in thrombosis and hemostasis, *Pld2*^{-/-} mice were generated and analyzed together with David Stegner [125].

3.1.1 Abolished PLD2 expression and decreased PLD activity in PLD2 deficient mice

Mice deficient for PLD2 were born in an expected mendelian ratio, developed and grew normally and were fertile. These findings were in line with a previous report describing *Pld2*^{-/-} mice for the first time [124]. RT-PCR (Figure 3-1A) and Western blot analysis (Figure 3-1B) confirmed the absence of PLD2 in platelets and other tissues. Furthermore, RT-PCR demonstrated that neither *Pld1* mRNA levels in *Pld2*^{-/-} platelets nor *Pld2* mRNA levels in *Pld1*^{-/-} platelets were altered (Figure 3-1A), proving the absence of a compensatory mechanism upregulating the respective other PLD isoform on transcriptional level. In addition, PLD activity in platelets, assessed by detection of PtdEtOH, a non-degradable product of PLD, was significantly reduced in *Pld2*^{-/-} mice (Figure 3-1C). Contradicting to previous reports on PLD activity in resting platelets, only minimal basal PLD activity levels were detected [170]. While common platelet agonists, such as *collagen-related peptide* (CRP) and thrombin induced PLD activation in platelets prominently, induction of PLD activity in *Pld2*^{-/-} mice was reduced. These findings demonstrate a contribution of PLD2 to the tightly regulated basal and inducible PLD activity in platelets. However, when stimulating platelets with the indicated agonists for a longer time period, PLD activity levels of wildtype and PLD2 deficient mice were indistinguishable suggesting a more important role for PLD1.
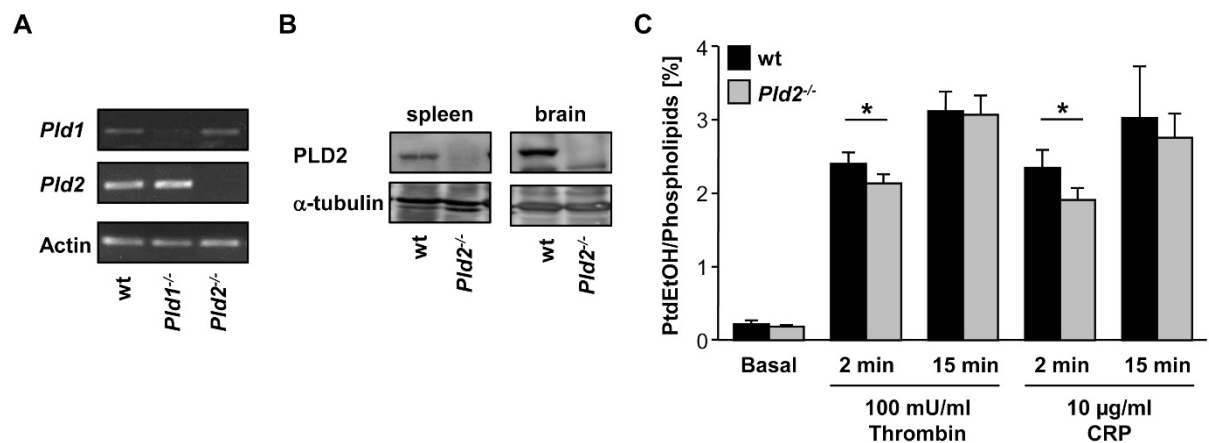
Figure 3-1: PLD2 expression and activity in *Pld2⁻ᐟ⁻* platelets and tissues. (A) Analyses of *Pld1* and *Pld2* mRNA in platelets of the indicated mice by RT-PCR. *Actin*-mRNA served as control. (B) Western blot of spleen and brain lysates of mice with the indicated genotypes. Expression of α-tubulin was used as loading control. (C) Platelets were labeled with [^{3}H]-myristic acid and stimulated with the indicated agonists. PLD activity is depicted as percentage of *phosphatidylethanol* (PtdEtOH) of total [^{3}H]-labeled phospholipids. Data are mean ± SD of 4 mice per group. *$P<0.05$. (Thielmann*, Stegner* *et al.*, J Thromb Haemost, 2012)

In order to analyze whether the PLD2 deficiency has an effect on the hematopoietic system, blood cell counts were measured with a Sysmex counter. All measured blood parameters from *Pld2⁻ᐟ⁻* mice were unaltered when compared to wildtype samples suggesting that PLD2 is not required for blood cell production.
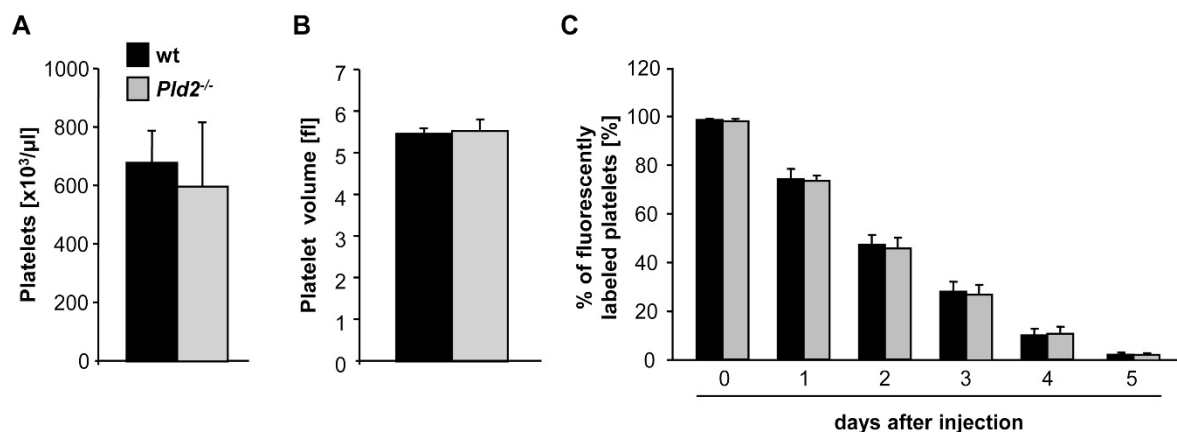

Figure 3-2: Platelet count, volume and life span are unaltered in *Pld2⁻ᐟ⁻* mice. (A) Platelet counts (platelets x 10^3/μl) and (B) platelet volumes (femtoliters) were determined by a hematologic analyzer (Sysmex). (C) Platelet life span was determined by injecting DyLight 488-conjugated anti-GPIX Ig derivative into wildtype and *Pld2⁻ᐟ⁻* mice. The percentages of fluorescently labeled platelets are depicted. Values are mean ± SD of ≥5 mice per group.

	wt		$Pld2^{-/-}$		P-values
Red blood cells [x 10^6/µl]	6.8	± 1.3	5.9	± 1.2	0.16
White blood cells [x 10^3/µl]	8.3	± 1.9	7.1	± 1.5	0.15
HCT [%]	36.5	± 7.0	32.1	± 7.2	0.21
α-GPIb [MFI]	433.0	± 37.0	390.0	± 14.3	0.06
α-GPV [MFI]	317.0	± 30.6	325.2	± 33.2	0.59
α-GPIX [MFI]	558.5	± 16.4	548.3	± 9.2	0.27
α-GPVI [MFI]	52.3	± 2.7	52.8	± 4.5	0.89
α-CLEC-2 [MFI]	142.8	± 8.4	141.0	± 10.2	0.69
α-α2 [MFI]	65.1	± 3.2	64.5	± 2.3	0.69
α-α5 [MFI]	32.1	± 1.9	33.5	± 3.1	0.28
α-β1 [MFI]	173.2	± 18.1	178.0	± 2.7	0.45
α-β3 [MFI]	68.9	± 3.9	71.5	± 3.0	0.14
α-αIIbβ3 [MFI]	707.7	± 25.6	729.3	± 27.9	0.11
α-CD9 [MFI]	1340.5	± 39.7	1360.3	± 39.8	0.32

Table 3-1: Absence of PLD2 does not affect platelet glycoprotein expression. Expression of glycoproteins on the platelet surface of wildtype and $Pld2^{-/-}$ mice was determined by flow cytometry. Diluted whole blood was labeled with FITC-conjugated antibodies for 15 min at RT and analyzed directly on a FACSCalibur. Results are presented as mean fluorescence intensity ± SD of ≥5 mice per group. Mean platelet size was determined by forward scatter characteristics. Abbreviations: HCT, hematocrit. (Thielmann*, Stegner* *et al.*, J Thromb Haemost, 2012)

To assess whether lack of PLD2 affects megakaryopoiesis and platelet formation, platelet count, mean platelet volume, expression of prominent platelet surface glycoproteins and platelet life span was analyzed. Expression of prominent glycoproteins on the platelet surface of $Pld2^{-/-}$ and wildtype platelets was comparable (Table 3-1). Platelet count and size in PLD2 deficient mice were unaltered (Figure 3-2A, B; wt: 680.8 ± 110.0 x 10^3/µl, $Pld2^{-/-}$: 599.0 ± 219.9 x 10^3/µl; wt: 5.5 ± 0.1 fl, $Pld2^{-/-}$: 5.5 ± 0.3 fl). Furthermore, analysis of platelet life span, as described in section 2.2.4.1., revealed that wildtype and PLD2 deficient platelets have similar platelet turnover rates (Figure 3-2C). Together, these results indicate that megakaryopoiesis and platelet formation occur independently of PLD2.

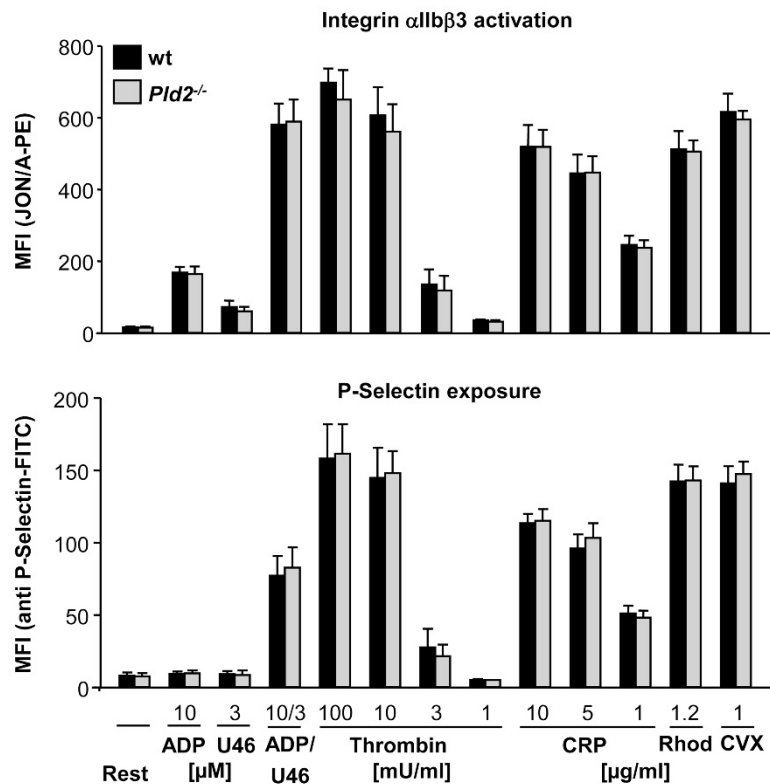## 3.1.2 Platelet activation and degranulation is unaltered in PLD2 deficient mice

Figure 3-3: Absence of PLD2 has no effect on platelet activation *in vitro*. Flow cytometric analyses of (A) αIIbβ3 integrin activation (JON/A-PE) and (B) degranulation dependent P-selectin exposure in response to indicated agonists. Results are mean fluorescence intensities (MFI) ± SD of 6 mice per group. Abbreviations: Rest, resting; U46, U46619; CVX, convulxin; Rhod, rhodocytin; CRP, collagen related peptide. (Thielmann*, Stegner* *et al.*, J Thromb Haemost, 2012)

Since PLD was suggested to be important for platelet secretion (reviewed in [170]), we investigated whether the reduced PLD activity in *Pld2*⁻⁄⁻ mice affects platelet activation. To that end, α-degranulation dependent P-selectin exposure on the platelet surface and activation of the major integrin αIIbβ3 was measured. Upon stimulation of ITAM- and GPCR-coupled receptors, P-selectin exposure and αIIbβ3 integrin activation in wildtype and PLD2 deficient platelets were indistinguishable (Figure 3-3). In order to have a second measurement for α-granule secretion during platelet activation, the secretion of vWF, another α-granular protein, was determined. VWF secretion in *Pld2*⁻⁄⁻ platelets was unaltered, confirming that PLD2 has no role in α-granule secretion (Figure 3-4B). To rule out that PLD2 has an effect on dense granule secretion, ATP release was assessed and found to be comparable in wildtype and PLD2 deficient platelets (Figure 3-4A). Platelet aggregation is highly dependent on second wave mediator stimulation. Some of these second wave mediators are secreted during platelet degranulation [220]. In line with the unaltered degranulation, platelet aggregation upon

stimulation with the indicated agonists of wildtype and $Pld2^{-/-}$ platelets was unaltered (Figure 3-4C). Altogether, these results indicate that PLD2 is dispensable for initial platelet activation.
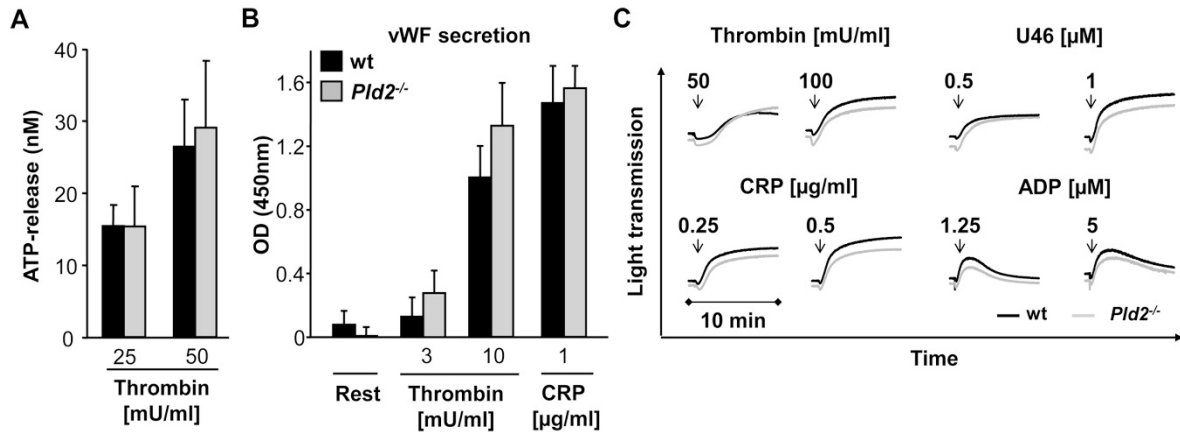

Figure 3-4: $Pld2^{-/-}$ platelets display unaltered platelet granule secretion and aggregation. (A) ATP secretion after platelet stimulation with the indicated thrombin concentrations was measured on a Chronolog aggregometer. Results are mean of ATP (nM) ± SD of 4 mice per group. (B) Measurement of secreted vWF in the supernatant of resting or activated wildtype and $Pld2^{-/-}$ platelets. Data are presented as $OD_{450 nm}$ ± SD of 4 mice per group. (C) Washed platelets were stimulated with the indicated agonists and light transmission was recorded on a Born aggregometer. Representative aggregation traces of 3 individual experiments are depicted. Abbreviations: Rest, resting; U46, U46619; CRP, collagen related peptide. (Thielmann*, Stegner* *et al.*, J Thromb Haemost, 2012)

3.1.3 $Pld2^{-/-}$ mice show normal platelet adhesion under flow

Our study on $Pld1^{-/-}$ platelets revealed a role for this enzyme downstream of the platelet receptor GPIb, which is difficult to assess under static conditions [8]. Therefore, flow adhesion assays in an *ex vivo* flow chamber system were performed by perfusing whole blood over a collagen- or vWF-coated surface at different shear rates (1,000 s^{-1}, 1,700 s^{-1} and 3,400 s^{-1}). Wildtype and $Pld2^{-/-}$ platelets rapidly bound to the collagen coated surface and formed three-dimensional stable aggregates to the same extent and with the same kinetics (Figure 3-5A). Evaluation of the platelet covered surface and thrombus volume did not reveal a statistically significant difference between wildtype and $Pld2^{-/-}$ samples. These findings indicate that PLD2 is not involved in the growth and stabilization of platelet-rich thrombi. Likewise, rolling and firm adhesion of single wildtype or $Pld2^{-/-}$ platelets on vWF, the physiological ligand of GPIb, were indistinguishable (Figure 3-5B). This suggests that, in contrast to PLD1, PLD2 has no impact on GPIb-dependent integrin activation.
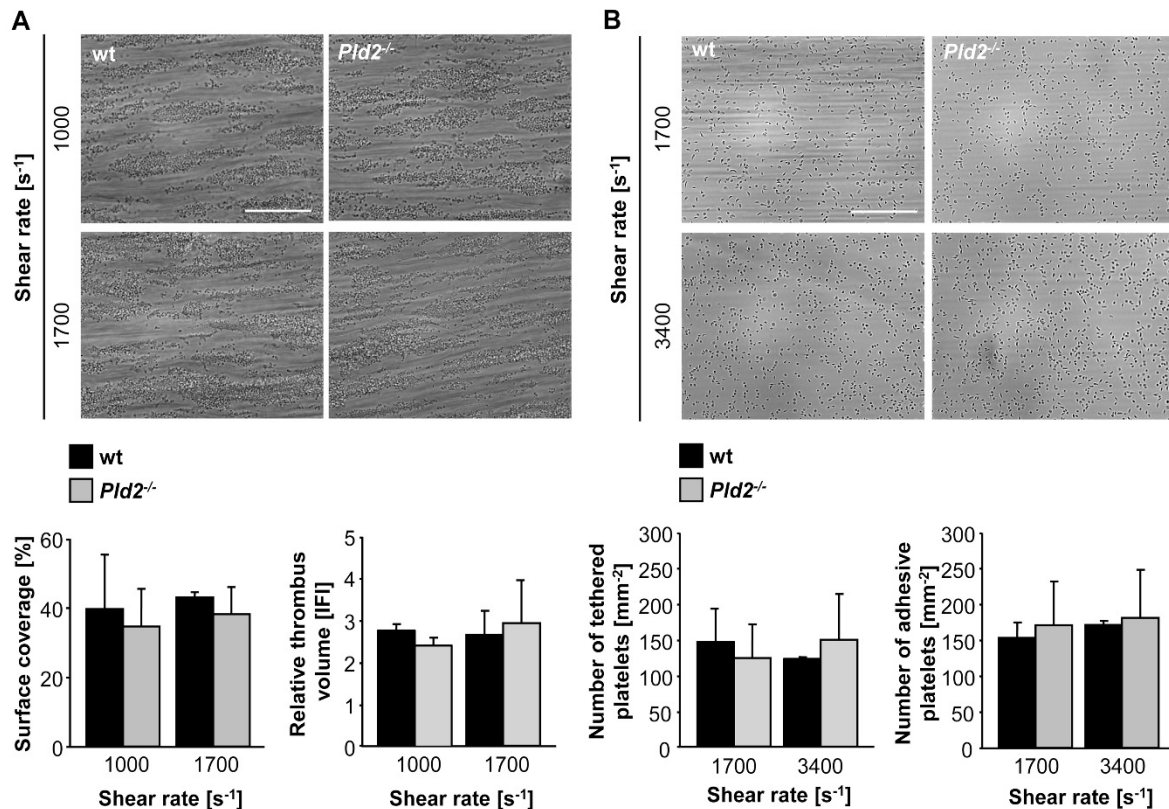
Figure 3-5: Lack of PLD2 neither influences thrombus formation on collagen nor platelet adhesion on vWF. (A) Whole blood was perfused over a collagen-coated (0.2 mg/ml) surface. Representative images are depicted (top). Blood was perfused at the indicated perfusion rates for 4 min and washing with Tyrode's buffer was performed for half of the period of the perfusion time. Platelet surface coverage (bottom, left) and relative thrombus volume as measured by the *integrated fluorescence intensity* (IFI) per square millimeter (bottom, right) ± SD of 5 mice per group were measured. Bar: 50 µm. (B) Whole blood was perfused at the indicated perfusion rates over a vWF-coated surface and then washed with Tyrode's buffer for half of the period of the perfusion time. Representative images are depicted (top). Tethered platelets were counted after 100 s of blood perfusion (bottom, left). The number of firmly adherent platelets were counted at the end of the washing step (bottom, right). Bar graphs depict mean values ± SD of ≥ 4 mice per group. (Thielmann*, Stegner* *et al.*, J Thromb Haemost, 2012)

3.1.4 Spreading, clot retraction and F-actin polymerization of *Pld2-/-* platelets is unaltered

In the literature PLD is discussed as an important mediator of cytoskeletal rearrangements [64, 221]. Platelet integrin αIIbβ3 outside-in signaling leads to the reorganization of the cytoskeleton and thereby induces the formation of filopodia and lamellipodia. However, upon prestimulation with thrombin, PLD2 deficient platelets were able to spread on fibrinogen to the same extent and with similar kinetics as wildtype platelets (Figure 3-6). Another process underlying outside-in signaling and cytoskeletal rearrangements is the αIIbβ3-mediated clot retraction. During this process the clot decreases in size due to forces being generated by platelets on the clot fibrin mesh [222]. Clot retraction in wildtype and PLD2 deficient platelet rich plasma in the presence of Ca^{2+} started at approximately 30 min upon pre-stimulation with thrombin and showed similar

kinetics over a time period of 2 hours. The excess fluid extruded during clot retraction was comparable in wildtype and PLD2 deficient platelet rich plasma (wt: 49.6 ± 10.4 %, $Pld2^{-/-}$: 60 ± 4.6 % of initial PRP volume; Figure 3-7A).
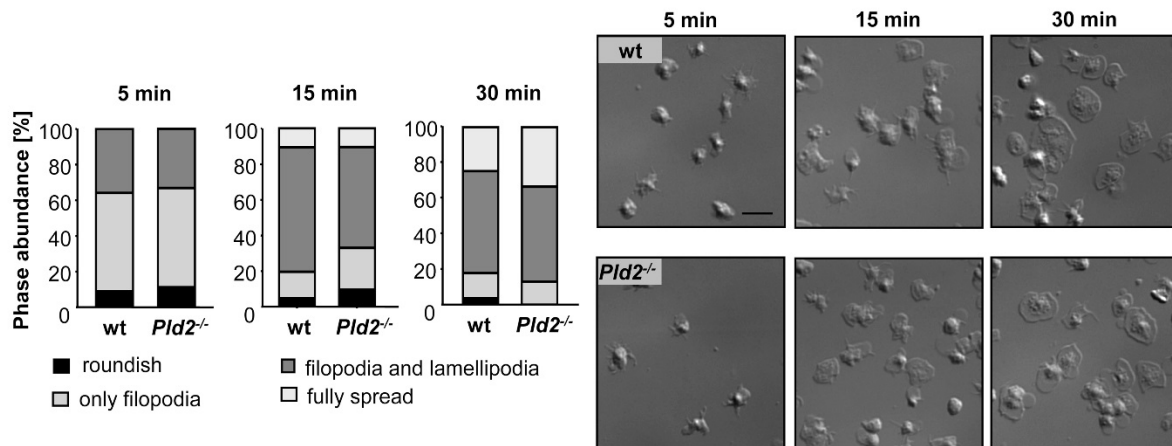

Figure 3-6: Platelet spreading is not affected by the lack of PLD2. Washed platelets were stimulated with 0.01 U/ml thrombin and allowed to spread on fibrinogen (100 µg/ml). Representative DIC images of 3 individual experiments (right) and statistical evaluation of the percentage of spread platelets at different spreading stages (left). Bar 5 µm. (Thielmann*, Stegner* *et al.*, J Thromb Haemost, 2012)
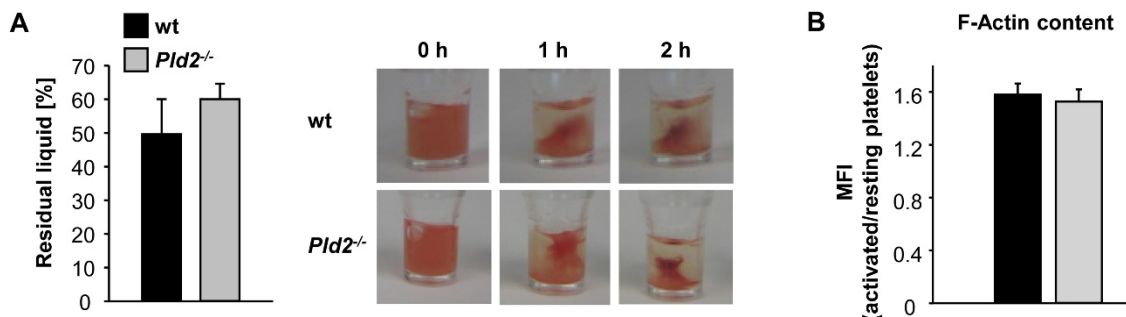

Figure 3-7: Actin polymerization and dynamics in platelets are functional despite the lack of PLD2. (A) Clot retraction of PRP upon activation with 3.5 U/ml thrombin in the presence of 20 mM $CaCl_2$ at the indicated time points. Representative images of two different experiments are depicted (left). Residual liquid is depicted as % of starting volume ± SD of 5 mice per group (left). (B) F-actin content measured by flow cytometry after incubating the platelets with phalloidin-FITC. MFI ± SD of 4 mice per group are depicted.

Moreover, F-actin levels were measured in thrombin-activated and resting platelets by using a flow cytometric approach. The ratio of the F-actin content in activated and resting platelets was unaltered in PLD2 deficient platelets (1.6 ± 0.1 vs. 1.5 ± 0.1; Figure 3-7B). Taken together, these results argue against a role of PLD2 in platelet outside-in signaling and the reorganization of the actin cytoskeleton, which is known to facilitate platelet spreading and clot retraction.

3.1.5 Normal *in vivo* thrombus formation and hemostasis in PLD2 deficient mice

Next, we analyzed the functional relevance of PLD2 deficiency in hemostasis and thrombosis *in vivo*. Thrombus formation was induced by application of 20% $FeCl_3$ on the exteriorized mesenteric arterioles of wildtype and *Pld2*$^{-/-}$ mice. This resulted in fast platelet adhesion and the appearance of first thrombi >10 μm after 8.4 ± 1.3 min in wildtype and after 7.1 ± 1.6 min in *Pld2*$^{-/-}$ mice (data not shown). Irreversible vessel occlusion in PLD2 deficient mice occurred after 14.2 ± 4.1 min, which was comparable to the thrombus formation observed in wildtype animals (13.8 ± 3.4 min; Figure 3-8).
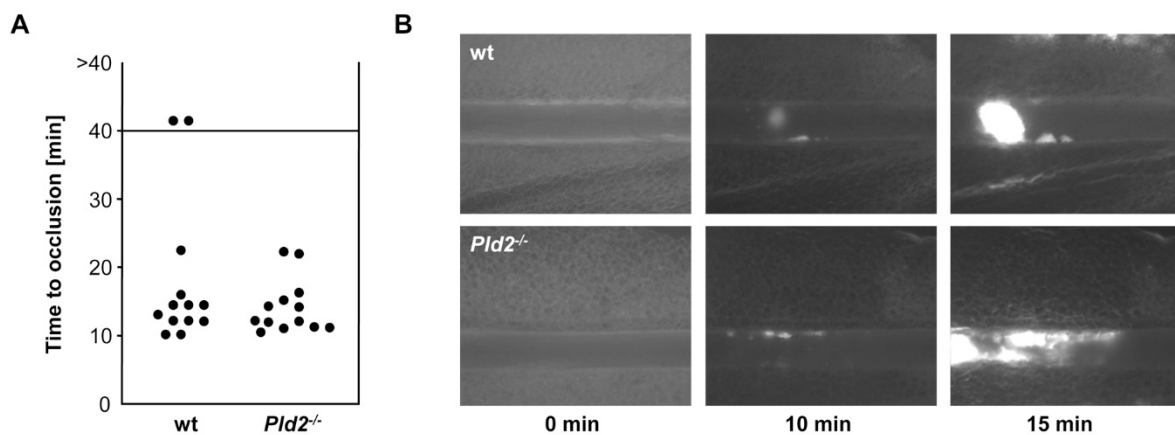

Figure 3-8: Lack of PLD2 has no influence on thrombus formation *in vivo*. Thrombus formation in small mesenteric arterioles was induced by topical application of 20% $FeCl_3$. In order to monitor thrombus formation by intravital microscopy, platelets were labeled fluorescently. Time to stable occlusion (A) and representative images (B) are shown. Each symbol represents one individual. (Thielmann*, Stegner* *et al.*, J Thromb Haemost, 2012)

To verify these results, a second model for thrombosis was utilized. Here the abdominal aorta was injured by firm compression with forceps and the blood flow was monitored with an ultrasonic perivascular Doppler flowmeter. Previously, our laboratory had shown that *Pld1*$^{-/-}$ mice were protected in this model [8]. However, vessel occlusion in *Pld2*$^{-/-}$ mice occurred after 193.6 ± 128.7 s, which was comparable to the mean time of vessel occlusion of wildtype mice (164.1 ± 45.7 s; Figure 3-9A, B). These findings indicate that PLD2 is dispensable for *in vivo* thrombus formation in microvascular and macrovascular settings. In order to assess whether PLD2 has an impact on hemostasis, mice were analyzed in a tail bleeding time model. Bleeding times upon amputation of a small piece of the tail tip were comparable in wildtype and *Pld2*$^{-/-}$ mice (wt: 335.0 ± 242.3 s, *Pld2*$^{-/-}$: 398.5 ± 282.2 s; Figure 3-9C), indicating that PLD2 is not an important regulator of hemostasis.
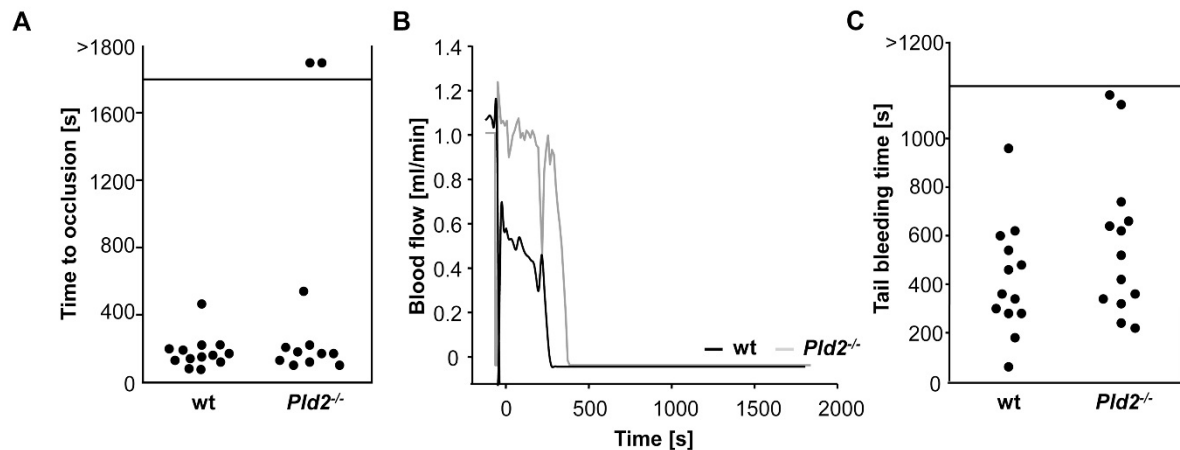
Figure 3-9: PLD2 is dispensable for hemostasis and for thrombus formation *in vivo*. (A) By tight compression with forceps, a mechanical injury of the abdominal aorta was induced and the blood flow was monitored for 30 min. Time to stable occlusion (A) and representative blood flow charts (B) are presented. Each symbol represents one individual. (B) Tail bleeding times of wildtype and *Pld2-/-* mice. Each symbol represents one individual. (Thielmann*, Stegner* *et al.*, J Thromb Haemost, 2012)

The development of focal cerebral infarction, which is described as a thrombo-inflammatory process, depends on platelets as well as on immune cells [223, 224]. Since PLD2 is not only expressed in platelets but also in immune cells [225-227], we wanted to study whether PLD2 deficiency has an impact on the development of neuronal damage following *transient middle cerebral artery occlusion* (tMCAO). Therefore, a thread was advanced into the MCA in order to reduce cerebral blood flow and induce cerebral ischemia. To allow reperfusion, the thread was removed 1 h later. Infarct volumes and neurological scores were analyzed 24h after reperfusion. *Pld2-/-* mice developed infarcts comparable in size to those of wildtype mice (wt: 99.4 ± 34.4 mm^3, *Pld2-/-*: 100.1 ± 34.0 mm^3; Figure 3-10A). Neurological deficits, as determined with the Bederson score, and the overall motor function and coordination, assessed by the grip test, were comparable in wildtype and *Pld2-/-* mice (Figure 3-10B,C).

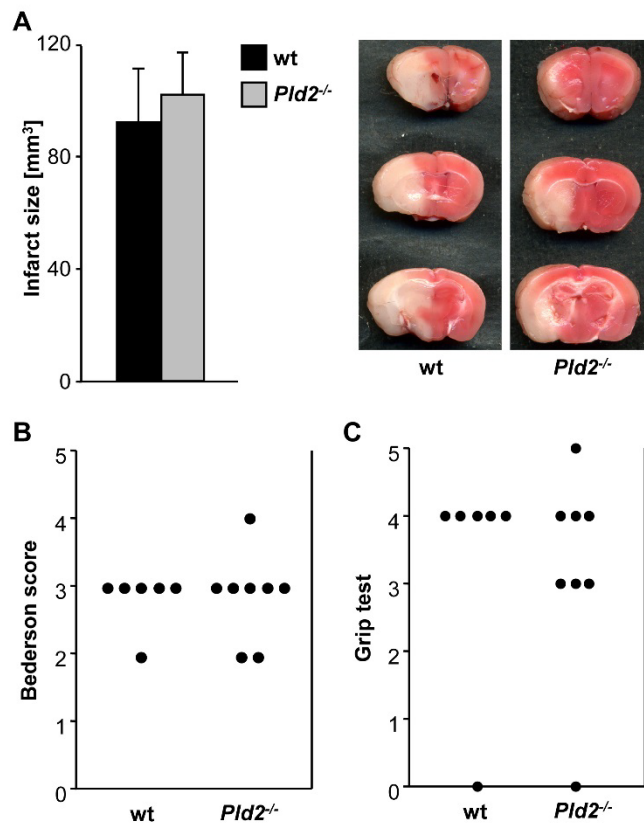These results demonstrated that infarct development and progression upon tMCAO occurs independently of PLD2.

Figure 3-10: Infarct development after tMCAO in *Pld2^-/-* mice is comparable to wildtype mice. (A) Brain infarct volumes of wildtype and Pld2^-/- mice which were subjected to the transient middle cerebral artery model (60 min occlusion time, 24 h after reperfusion). Data are mean ± SD of 10 mice per group. Neurological and motor function was determined with Bederson score (B) and Grip test (C), respectively. Each symbol represents one individual. (Thielmann*, Stegner* *et al.*, J Thromb Haemost, 2012)

3.2 Redundant functions of PLD1 and PLD2 in α-granule release and their relevance in models of pathological thrombus formation

The two PLD isoforms, PLD1 and PLD2, share a sequence homology of 50% [186] and both generate PA. Therefore, it is possible that the two isoforms have redundant functions in platelet signaling. In order to address this question, *Pld2^-/-* mice were intercrossed with the previously published *Pld1^-/-* mice. Even though, PLD had been predicted to be of importance in embryonic development [228, 229], *Pld1^-/-/Pld2^-/-* mice were viable and developed normally. The animals appeared healthy and did not show spontaneous bleeding. With regard to their behavior and appearance they were indistinguishable from wildtype animals. The analysis of *Pld1^-/-/Pld2^-/-* mice was performed in collaboration with David Stegner from our laboratory [125].

3.2.1 Abolished PLD activity in *Pld1^-/-/Pld2^-/-* mice

Lack of PLD did not have an impact on peripheral blood cell counts. In addition, mean platelet volume, platelet count and the expression of prominent surface glycoprotein receptors (Table 3-2) were grossly normal despite the abrogated PLD activity of PLD deficient platelets (Figure 3-11). Only β1 integrin levels on the platelet surface were slightly altered.

	wt	Pld1$^{-/-}$/Pld2$^{-/-}$	P-values
Red blood cells [x 10^6/µl]	7.7 ± 1.0	7.23 ± 1.0	0.27
White blood cells [x 10^3/µl]	5.8 ± 0.7	6.9 ± 0.6	<0.05
HCT [%]	33.7 ± 2.6	34.0 ± 19.5	0.97
α-GPIb [MFI]	364.0 ± 16.7	358.3 ± 21.0	0.62
α-GPV [MFI]	293.8 ± 11.6	294.0 ± 12.0	0.98
α-GPIX [MFI]	414.2 ± 14.4	413.8 ± 18.3	0.97
α-GPVI [MFI]	27.0 ± 1.6	26.3 ± 1.0	0.40
α-CLEC-2 [MFI]	143.6 ± 9.9	143.17± 6.1	0.92
α-α2 [MFI]	51.5 ± 3.7	55.3 ± 1.5	0.05
α-α5 [MFI]	28.8 ± 5.0	33.8 ± 1.9	0.06
α-β1 [MFI]	120.3 ± 12.2	136.2 ± 7.2	<0.05
α-β3 [MFI]	285.8 ± 37.0	265.2 ± 11.2	0.24
α- αIIbβ3 [MFI]	592.7 ± 60.2	566.8 ± 51.1	0.44
α-CD9 [MFI]	1090.0± 57.7	1098.3± 37.4	0.77

Table 3-2: Lack of PLD1 and PLD2 has no effect on platelet glycoprotein expression. Expression of glycoproteins on the platelet surface of wildtype and Pld$^{-/-}$/Pld2$^{-/-}$ mice was determined by flow cytometric measurements. Diluted whole blood was labeled with FITC-conjugated antibodies for 15 min at RT and analyzed directly on a FACSCalibur. Results are presented as mean fluorescence intensity (MFI) ± SD of ≥ 5 mice per group. Mean platelet size was determined by forward scatter characteristics. Abbreviations: MPV, mean platelet volume; HCT, hematocrit. (Thielmann*, Stegner* et al., J Thromb Haemost, 2012)

To analyze platelet turnover, life span experiments were performed. These revealed a slightly, but significantly decreased life span of Pld1$^{-/-}$/Pld2$^{-/-}$ platelets (Figure 3-12A) that was also observed in Pld1$^{-/-}$ mice [8]. In order to see whether this defect was still apparent under conditions of thrombocytopenia, mice were intravenously injected with an anti-GPIbα antibody which depletes mice of platelets by an Fc-independent mechanism [197, 230]. Five days after anti-GPIbα injection, platelet count started to recover and was normal within 4 days. This process occurred with comparable kinetics in wildtype and Pld2$^{-/-}$ mice (Figure 3-12B) indicating that PLD is dispensable for platelet formation. Furthermore, analysis of hematologic parameters (Table 3-2) did not show any significant differences between wildtype and Pld1$^{-/-}$/Pld2$^{-/-}$ mice apart from slightly elevated white blood cell counts. These findings suggest that PLD does not contribute to platelet or other blood cell formation.
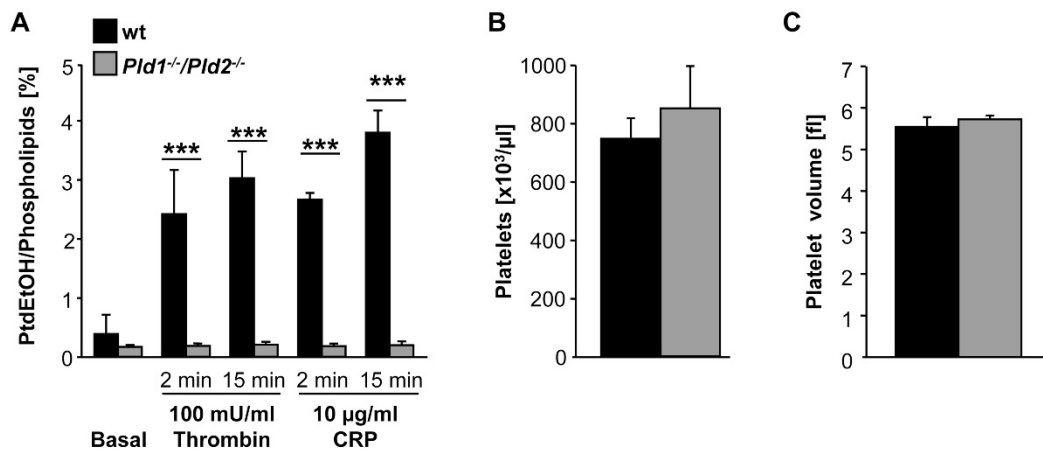
Figure 3-11: Normal platelet counts and volume in *Pld1⁻/⁻/Pld2⁻/⁻* mice despite abolished PLD activity (A) Platelets were labeled with [^{3}H]-myristic acid and stimulated with the indicated agonists. PLD activity is depicted as percentage of *phosphatidylethanol* (PtdEtOH) of total [^{3}H]-labeled phospholipids. Data are mean ± SD of 4 mice per group. *$P<0.05$; **$P<0.01$, ***$P<0.005$. (B,C) Platelet counts (platelets x 10^3/µl) (B) and platelet volumes (femtoliters) (C) were determined by a hematologic analyzer (Sysmex). Values are mean ± SD of 8 mice per group. (Thielmann*, Stegner* *et al.*, J Thromb Haemost, 2012)
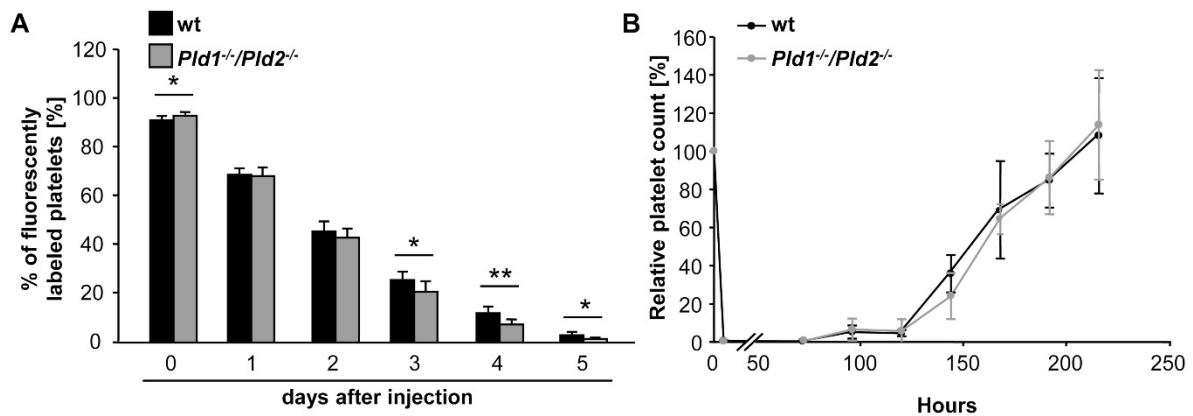
Figure 3-12: Normal platelet production in *Pld1⁻/⁻/Pld2⁻/⁻* mice. (A) Platelet life span was determined by injecting DyLight 488-conjugated anti-GPIX Ig derivative into wildtype and *Pld1⁻/⁻/Pld2⁻/⁻* mice. The percentages of fluorescently labeled platelets are depicted. Values are mean ± SD of 5 mice per group. (B) Platelet depletion of wildtype and double deficient mice was induced by injection of anti-GPIb antibody and the platelet count was monitored at the indicated time points. Values are relative platelet counts in % of 5 mice per group ± SD. *$P<0.05$; **$P<0.01$.

3.2.2 Impaired integrin activation and α-granule release in *Pld1⁻/⁻/Pld2⁻/⁻* mice

Previously, PLD had been proposed to modulate secretion of α-granules and lysosomes [67, 170]. Therefore, it was tested whether PLD is involved in agonist-induced platelet degranulation. Since the deficiency of PLD1 already resulted in mild defects in platelet integrin activation [8], the analyses were performed with wildtype, *Pld1⁻/⁻* and *Pld1⁻/⁻/Pld2⁻/⁻* platelets, to allow direct comparison of single and double-deficient platelets. In addition, the present study exclusively used mice backcrossed to C57BL/6 background. Platelet degranulation upon platelet stimulation with CRP or ADP/U46619 was unaltered in *Pld1⁻/⁻* and *Pld1⁻/⁻/Pld2⁻/⁻* mice. However, degranulation upon stimulation with intermediate concentrations of thrombin was significantly decreased in *Pld1⁻/⁻/Pld2⁻/⁻* platelets, whereas *Pld1⁻/⁻* mice showed similar P-selectin exposure as wildtype mice (Figure 3-13A). Since thrombin does not only bind and cleave the PAR-4 receptor, but also interacts with other glycoproteins such as GPV or GPIb, platelet activation studies were repeated with a specific PAR-4 activating peptide [231]. Comparable to the defects observed upon thrombin stimulation, degranulation of *Pld1⁻/⁻/Pld2⁻/⁻* platelets was defective when triggering platelet activation with intermediate concentrations of PAR-4 (Figure 3-13A). This data indicates that PLD is indeed mediating thrombin-triggered signaling events downstream of PAR-4. The secretion of other α-granular proteins, such as PF4 and vWF, was also decreased in *Pld1⁻/⁻/Pld2⁻/⁻* platelets (Figure 3-13B,C), while *Pld1⁻/⁻* platelets did not show significantly altered vWF secretion (Figure 3-13D). To analyze whether this degranulation defect is specific for α-granules, the secretion of ATP from dense granules was measured. No differences in ATP-release of wildtype and double deficient platelets was observed when stimulating with thrombin (Figure 3-13E), suggesting that PLD is not involved in dense granule secretion. In this assay higher thrombin concentrations than previously used were applied, since it was not possible to detect ATP release at lower concentrations of thrombin (data not shown). These data reveal redundant functions of PLD1 and PLD2 in platelet α-granule release.

Defective α-granule release could be caused by defective α-granule biogenesis or localization. Therefore, transmission electron microscopy was performed in resting and activated platelets of wildtype, PLD1 single and double deficient mice. Upon stimulation with low concentration of thrombin, platelets from all genotypes started forming protrusions (Figure 3-14). Comparing α-granule morphology and localization of all tested genotypes revealed no differences indicating that α-granule formation is not altered in PLD deficient platelets.
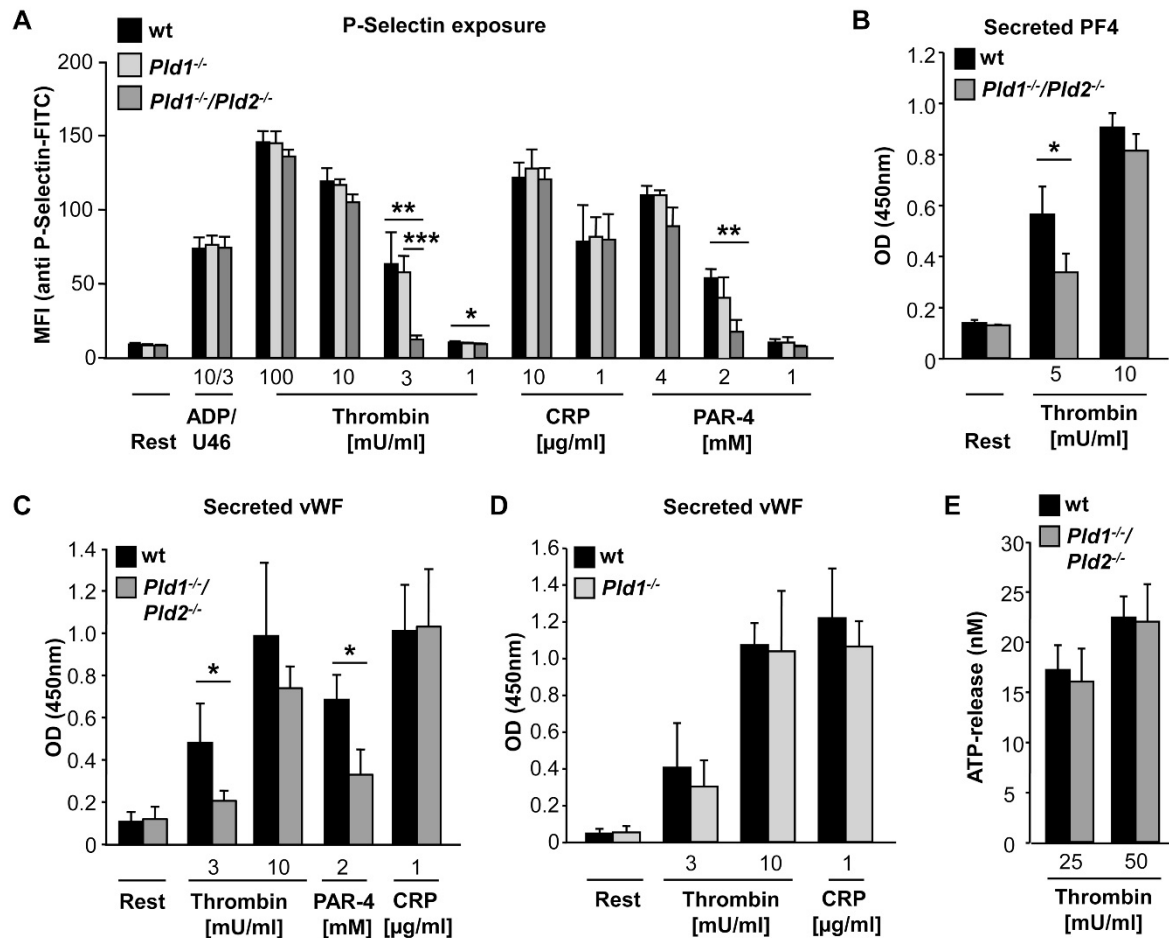
Figure 3-13: *Pld1^-/-^/Pld2^-/-* platelets show defective α-granule release upon PAR-4 receptor stimulation. (A) Flow cytometric analyses of degranulation-dependent P-selectin exposure of wildtype, *Pld1^-/-^* and *Pld1^-/-^/Pld2^-/-* platelets in response to indicated agonists. Results are mean fluorescence intensities (MFI) ± SD of 6 mice per group. (B) Detection of secreted PF4 in the supernatant of resting or activated wildtype and *Pld1^-/-^/Pld2^-/-* platelets. Data are presented as OD$_{450 nm}$ ± SD of 4 mice per group. (C, D) Measurement of secreted vWF in the supernatant of resting or activated wildtype, *Pld1^-/-^* and *Pld1^-/-^/Pld2^-/-* platelets. Data are presented as OD$_{450 nm}$ ± SD of 4 mice per group. (E) ATP secretion after stimulation of wildtype and *Pld1^-/-^/Pld2^-/-* platelets with the indicated thrombin concentration was measured on a Chronolog aggregometer. Results are mean of ATP (nM) ± SD of 4 mice per group. Abbreviations: U46, U46619; CVX, convulxin; Rhod, rhodocytin; Rest, resting; CRP, collagen related peptide. *P<0.05; **P<0.01, ***P<0.005. (Thielmann*, Stegner* *et al.*, J Thromb Haemost, 2012)

As previously published in the report on *Pld1^-/-^* mice with mixed background, also C57/BL6 *Pld1^-/-^* platelets exhibited decreased αIIbβ3 activation upon stimulation with low and intermediate thrombin concentrations independently of the genetic background (Figure 3-15A) [8]. *Pld1^-/-^/Pld2^-/-* platelets exhibited an even more pronounced integrin defect. Again, αIIbβ3 integrin activation was not altered when stimulating the platelets with other common platelet agonists. Since a subpopulation of integrins are recruited onto the platelet surface during platelet activation, the defective degranulation might be the reason for the reduction of active integrins on the surface of stimulated *Pld1^-/-^/Pld2^-/-* platelets. In order to assess this, the abundance of total αIIbβ3 integrins on the surface of resting and activated platelets was

determined by flow cytometry. During stimulation of wildtype and $Pld1^{-/-}$ platelets significantly more αIIbβ3 integrins were translocated to the platelet surface than in $Pld1^{-/-}/Pld2^{-/-}$ platelets (Figure 3-15B). These findings suggest that the additional integrin defect of $Pld1^{-/-}/Pld2^{-/-}$ platelets is, at least in part, due to decreased degranulation which results in reduced integrin translocation to the plasma membrane.

However, similar to the findings in $Pld1^{-/-}$ platelets, the defects in integrin activation and degranulation did not lead to differences in the aggregation ability of $Pld1^{-/-}/Pld2^{-/-}$ platelets (Figure 3-15C). This is in line with reports showing that normal aggregation can occur under conditions of sub-optimal integrin activation [9, 232].
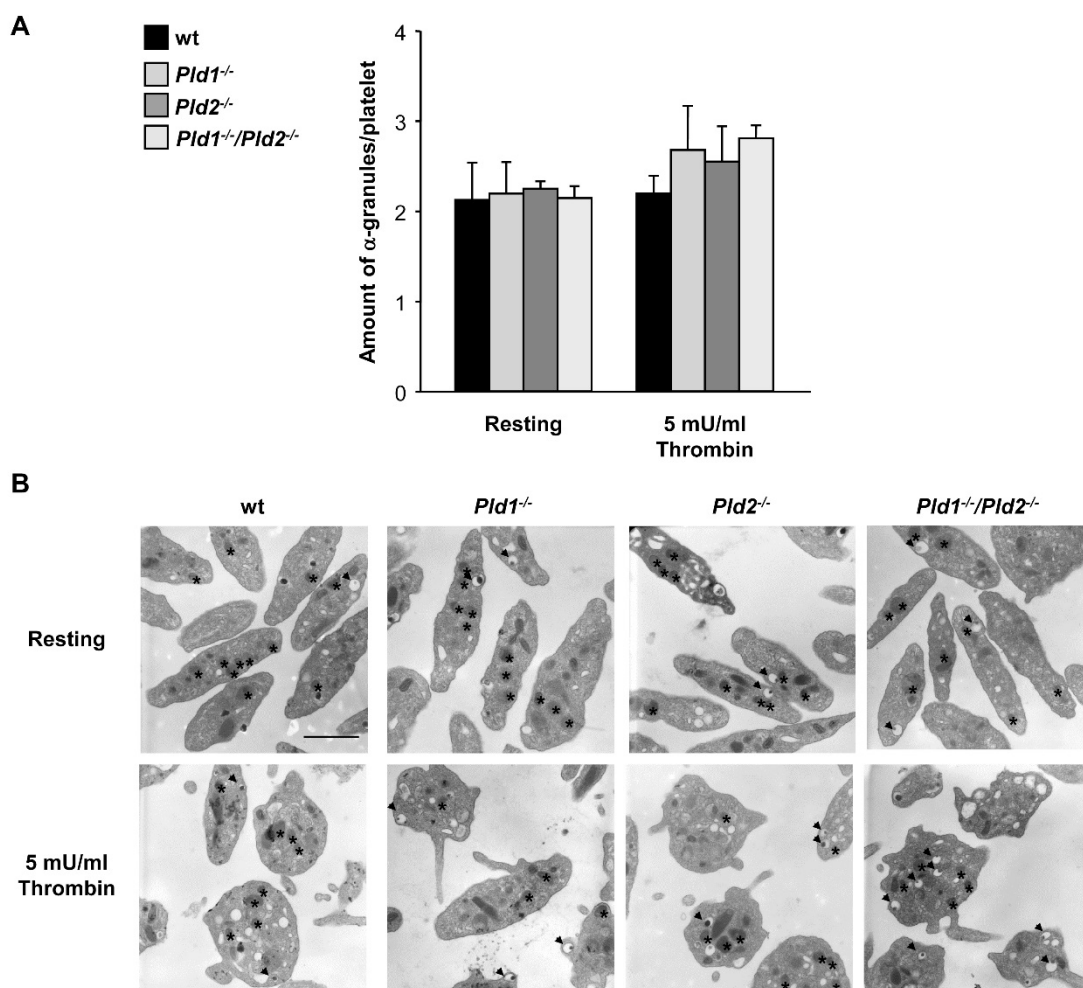
Figure 3-14: α-granule localization and abundance is unchanged in PLD deficient platelets.
(A) Platelets were activated with low amounts of thrombin, electron microscopic images were taken and the number of α-granules was determined. Data is presented as mean ± SD of 4 mice per group. (B) Representative TEM images of wildtype or PLD-deficient platelets. Asterisks indicate α-granules, arrowheads indicate dense granules, bar 1 μM. (Thielmann*, Stegner* *et al.*, J Thromb Haemost, 2012)
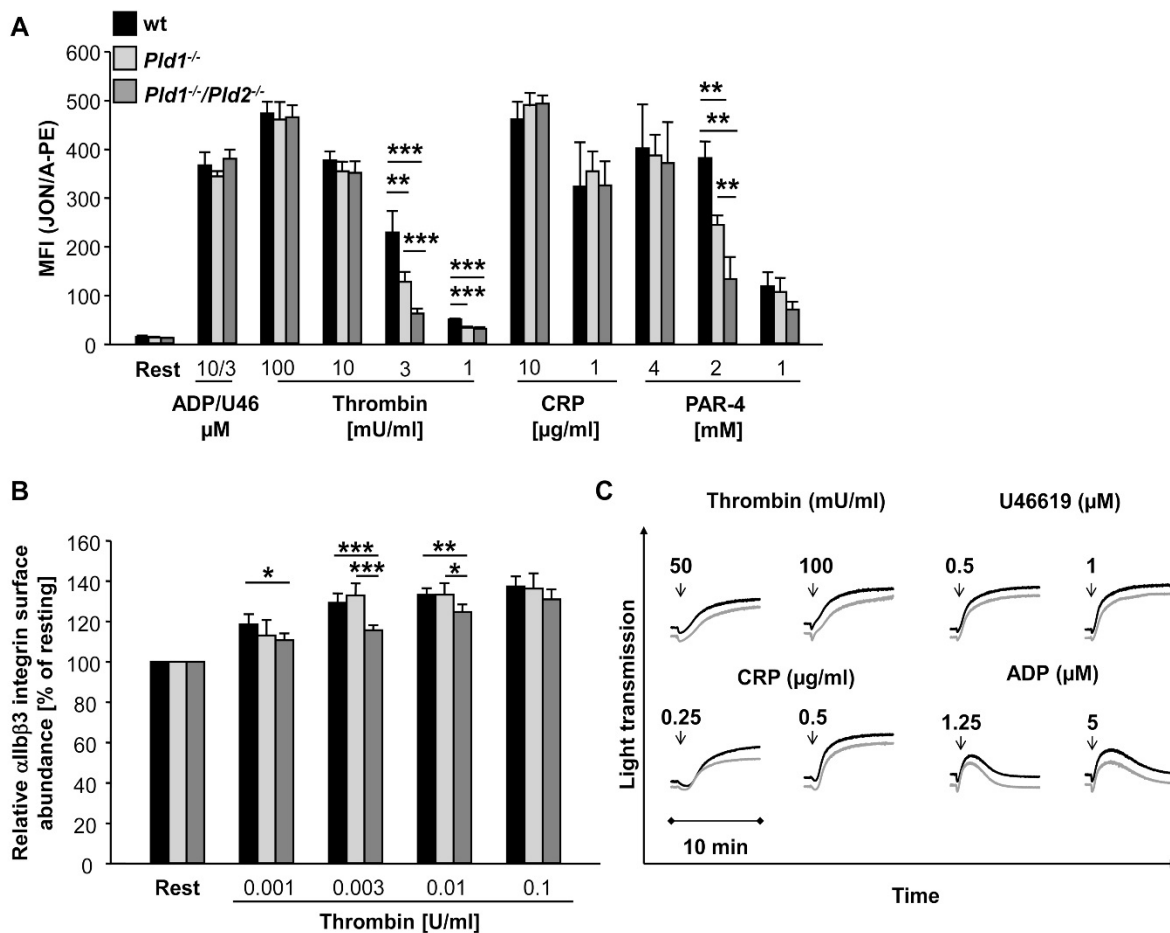
Figure 3-15: Deficiency of PLD1 and PLD2 results in decreased integrin activation and mobilization without affecting platelet aggregation. (A) Flow cytometric analyses of αIIbβ3 integrin activation (JON/A-PE) in response to indicated agonists. Results are mean fluorescence intensities (MFI) ± SD of 6 mice per group. (B) Relative αIIbβ3 integrin abundance (14A3) on the platelet surface in response to thrombin. Results are given as relative amount of integrin surface abundance of resting platelets ± SD of 6 mice per group. (C) Washed platelets were stimulated with the indicated agonists and light transmission was recorded on a Born aggregometer. Representative aggregation traces of 3 individual experiments are depicted. Abbreviations: U46, U46619; CVX, convulxin; Rest, resting; CRP, collagen related peptide. *$P<0.05$, **$P<0.01$, ***$P<0.001$. (Thielmann*, Stegner* *et al.*, J Thromb Haemost, 2012)

3.2.3 Combined loss of PLD1 and PLD2 has a minor impact on platelet spreading on fibrinogen, whereas spreading on vWF, clot retraction and F-actin polymerization are unaltered

To test the ability of *Pld1^-/-^/Pld2^-/-^* platelets to perform shape change and to rearrange the actin cytoskeleton, a process mediated by integrin outside-in signaling during platelet activation, spreading analysis were conducted. Platelets were allowed to spread on a fibrinogen coated surface in the presence of thrombin. The abundance of lamellipodia and filopodia was analyzed after 5, 15 and 30 min. After 5 min, wildtype and *Pld1^-/-^/Pld2^-/-^* platelets started forming filopodia and lamellipodia to the same extent. However, after 15 min *Pld1^-/-^/Pld2^-/-^* platelets formed

significantly more lamellipodia than wildtype platelets indicating enhanced integrin outside-in signaling (wt: 17.1 ± 0.4; *Pld1^-/-^/Pld2^-/-^*: 42.3 ± 7.2 % of platelets in stage 4). Surprisingly, this effect was no longer observable after 30 min, where the proportion of fully spread platelets was comparable between the two groups. Furthermore, the morphology of formed lamellipodia and filopodia was indistinguishable between wildtype and *Pld1^-/-^/Pld2^-/-^* platelets (Figure 3-16). For a more detailed analysis of actin and tubulin distribution during platelet spreading, immunofluorescence stainings of fully spread platelets on fibrinogen were performed. There was no difference in the centrally localized actin fibers and the widely distributed tubulin coils detectable (Figure 3-16, right panel). These findings suggest that PLD has a minor function in promoting cytoskeletal organization especially during early phases of platelet spreading.
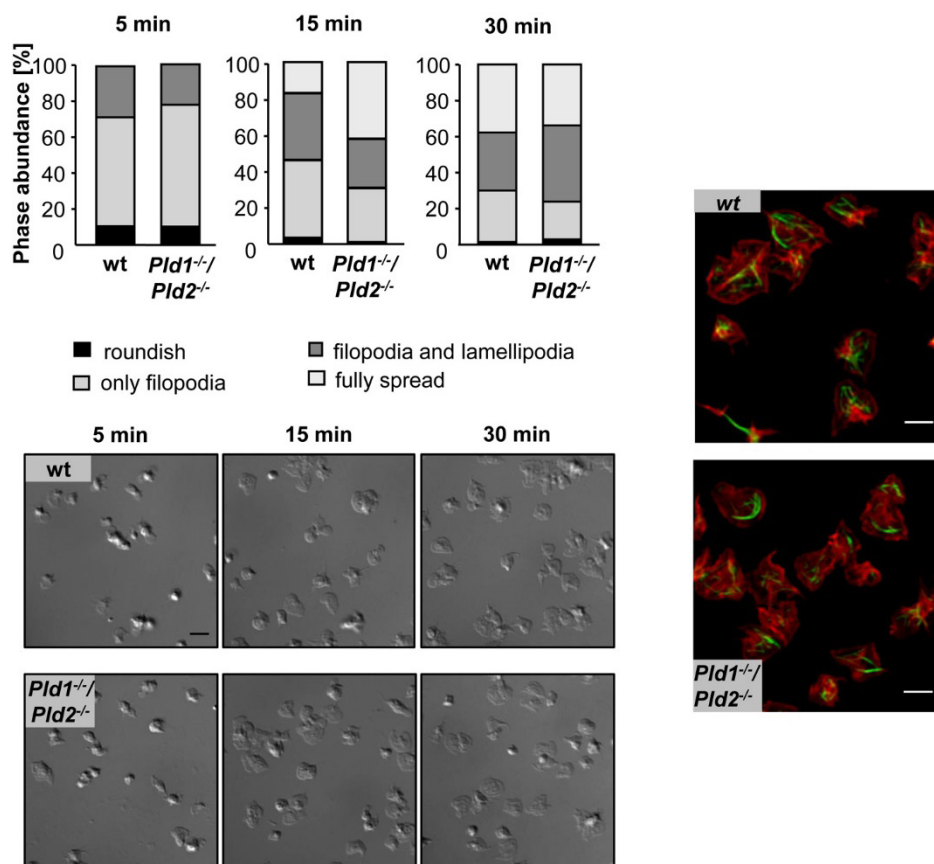
Figure 3-16: PLD has a minor impact on platelet spreading on fibrinogen. Washed platelets were stimulated with 0.01 U/ml thrombin and allowed to spread on fibrinogen (200 µg/ml). Representative DIC images of 3 individual experiments (bottom) and statistical evaluation of the percentage of spread platelets at different spreading stages (top). Bar 5 µm. Spread platelets were stained with Phalloidin-atto647N (red) and α-tubulin antibody-Alexa 488 (green) and analyzed by confocal microscopy. Representative images taken 30 min after spreading are depicted (right). Bar 2 µm.

Clot retraction is also a process relying on integrin outside-in signaling. To analyse whether this was altered, clot formation was induced in PRP of wildtype and *Pld1^-/-^/Pld2^-/-^* mice and clot retraction was monitored. The clot size decreased to the same extent and with similar kinetics in both groups. Furthermore, the amount of residual fluid retracted from the clot was similar

(Figure 3-17A). Since reorganization of actin facilitates shape change and retraction of platelets, the F-actin assembly ability of wildtype and *Pld1⁻/⁻/Pld2⁻/⁻* platelets was measured. However, there were no significant differences (Figure 3-17B).
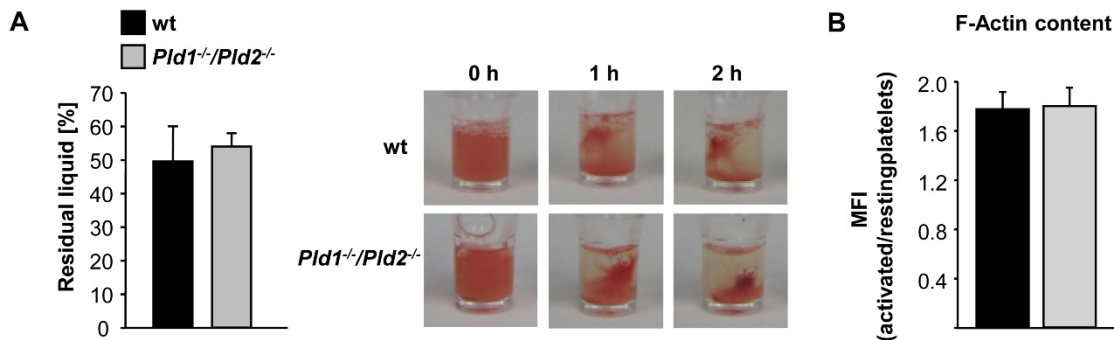
Figure 3-17: Actin polymerization and dynamics are normal in PLD deficient platelets. (A) Clot retraction of PRP upon activation with 3.5 U/ml thrombin in the presence of 20 mM $CaCl_2$ at the indicated time points. Representative images of two different experiments are depicted (right). Residual liquid is depicted as relative amount of starting volume ± SD of 5 mice per group (left). (B) F-actin content measured by flow cytometry after incubating the platelets with phalloidin-FITC. The ratio of mean fluorescence intensity (MFI) from activated and resting platelets ± SD of 4 mice per group is depicted.
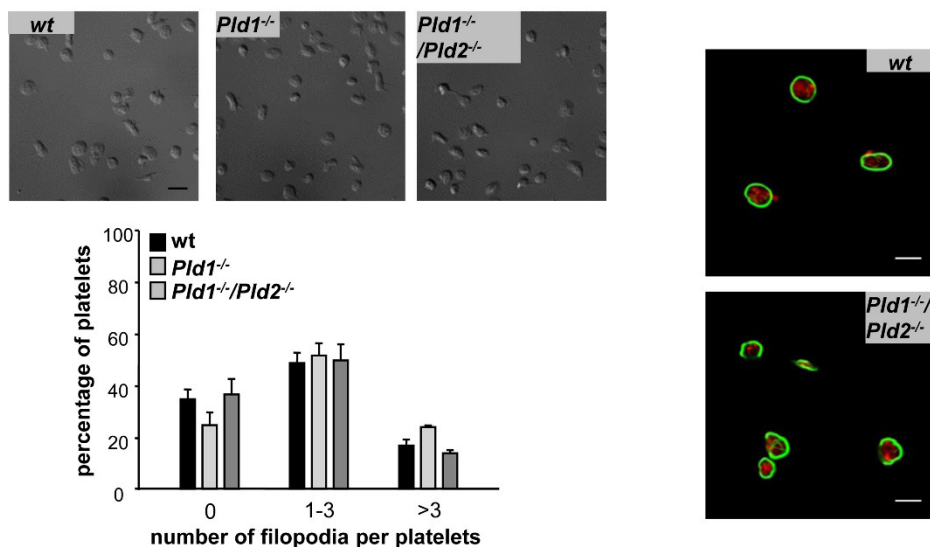
Figure 3-18: PLD is not required for spreading of platelets on vWF. Wildtype, *Pld1⁻/⁻* and *Pld1⁻/⁻/Pld2⁻/⁻* platelets were allowed to spread on vWF for 20 min. Representative DIC images are shown (top). Bar 10 µm. Lower panel shows statistical evaluation of filopodia formation according to the number of extensions per platelet (0, 1-3, >3) in 7 different fields. The results are mean values ± SD (n=5 per group). Spread platelets were stained with Phalloidin-atto647N (red) and α-tubulin antibody-Alexa 488 (green) and analyzed with confocal microscopy. Representative images taken after 30 min of spreading are depicted (right). Bar 3 µm.

While spreading on fibrinogen triggers the signaling of αIIbβ3 integrins, spreading on vWF is caused by GPIb-triggered signaling. Previous studies have shown that GPIb-dependent

integrin activation is dependent on PLD1 under shear stress [8]. To test whether this is also the case under static conditions and whether PLD1 and PLD2 have redundant functions in GPIb signaling, spreading studies on immobilized vWF in the presence of the αIIbβ3 integrin blocking agent integrillin were performed with wildtype, $Pld1^{-/-}$ and $Pld1^{-/-}/Pld2^{-/-}$ platelets. Spreading of platelets on vWF is limited to cell contraction and filopodia formation. Wildtype, $Pld1^{-/-}$ and $Pld1^{-/-}/Pld2^{-/-}$ platelets efficiently extended filopodia (~60% of the platelets formed 1-3 filopodia, Figure 3-18) which were morphologically indistinguishable. Also actin and tubulin distribution during spreading on vWF, which was analyzed by immunofluorescence stainings, did not show any differences. Taken together, these results revealed grossly normal formation and structure of filopodia and lamellipodia as well as unaltered actin and tubulin organization during spreading of $Pld1^{-/-}$ and $Pld1^{-/-}/Pld2^{-/-}$ platelets on different immobilized substrates.

3.2.4 No difference in procoagulant responses between wildtype and $Pld1^{-/-}/Pld2^{-/-}$ platelets

Upon strong platelet stimulation, the intracellular Ca^{2+} concentration increases and leads to the exposure of phosphatidylserine on the platelet surface. This process induces platelet procoagulant activity and promotes blood coagulation. αIIbβ3 integrins are supposed to contribute to the procoagulant response of platelets [233, 234]. In a previous study, using $Pld1^{-/-}$ mice with mixed background, it had already been shown that PLD1 contributes to procoagulant activity. This was attributed to the defective integrin activation of $Pld1^{-/-}$ platelets [8]. In order to test whether this defect is also evident in C57BL/6 $Pld1^{-/-}$ platelets, heparinized whole blood of wildtype and $Pld1^{-/-}$ mice was perfused over a collagen-coated surface. Procoagulant platelets were stained with Annexin A5 which specifically binds to phosphatidylserine [235]. However, in contrast to the decreased procoagulant activity observed in $Pld1^{-/-}$ mice with mixed background, collagen-induced platelet adhesion and procoagulant activity was not altered in platelets of $Pld1^{-/-}$ C57BL/6 mice (data not shown). This discrepancy might be explained by the absence of the defect in GPVI triggered integrin activation of $Pld1^{-/-}$ C57BL/6 platelets (Figure 3-15A). Next, it was tested whether the lack of both PLD isoforms alters platelet procoagulant activity. Notably, the collagen-induced procoagulant activity of wildtype and $Pld1^{-/-}/Pld2^{-/-}$ platelets was indistinguishable indicating that PLD1 and PLD2 do not contribute to induction of procoagulant activity in platelets (wt: 0.8 ± 0.2%; $Pld1^{-/-}/Pld2^{-/-}$: 0.9 ± 0.1% Annexin V labeled platelets, Figure 3-19).
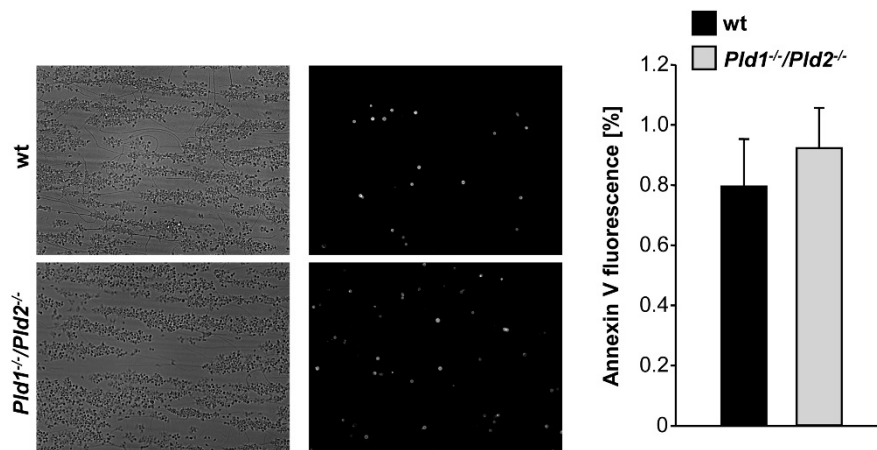
Figure 3-19: PLD deficiency does not alter platelet procoagulant activity. Whole blood was perfused over a collagen-coated (0.2 mg/ml) surface at a shear rate of 1,700 s^{-1} for 4 min. Adherent platelets were stained with Alexa488–annexin V (0.25 mg/ml). Representative phase contrast, fluorescence images and mean relative amount of annexin V positive platelets ± SD of >5 mice per group is shown.

3.2.5 Absence of both PLD isoforms protects mice from pathological thrombus formation and stroke without affecting tail bleeding times

In vivo, platelet activation and thrombus formation occurs in flowing blood, where locally produced soluble mediators are rapidly diluted. Under these conditions, subtle defects in integrin activation may translate into reduced thrombus formation. It was previously shown that *Pld1*$^{-/-}$ mice were protected from arterial thrombosis in larger vessels, namely in the models of chemical injury of the carotid artery and mechanical injury of the abdominal aorta, whereas thrombus formation in smaller vessels, such as mesenteric arterioles, was normal [8]. Therefore, *Pld1*$^{-/-}$/*Pld2*$^{-/-}$ mice were subjected to this thrombosis model to assess a potential redundant role of the two PLD isoforms. Upon vessel injury by topical application of FeCl$_3$, fast platelet adhesion occurred and first thrombi, which were bigger than 10 µm, appeared in vessels of *Pld1*$^{-/-}$ mice at a similar time point as in wildtype vessels (data not shown). Irreversible vessel occlusion occurred after 19.4 ± 4.1 min in *Pld1*$^{-/-}$ mice and after 20.8 ± 3.5 min in wildtype vessels (Figure 3-20A,B), indicating that PLD1 deficiency does not affect thrombus formation *in vivo*.

However, when both PLD isoforms were lacking, initial platelet adhesion and appearance of first thrombi was similar in wildtype and *Pld1*$^{-/-}$/*Pld2*$^{-/-}$ mice (wt: 7.5 ± 2.9 min, *Pld1*$^{-/-}$/*Pld2*$^{-/-}$: 7.7 ± 2.9 min, data not shown), but the time to occlusive thrombus formation was more variable. Time to full vessel occlusion was significantly prolonged in double-deficient mice (wt: 15.5 ± 3.9 min, *Pld1*$^{-/-}$/*Pld2*$^{-/-}$: 19.8 ± 7.7 min, Figure 3-20C,D). Further, the incidence of full vessel occlusion was significantly lower in *Pld1*$^{-/-}$/*Pld2*$^{-/-}$ mice than in wildtype mice. While in double-deficient mice only 12 out of 34 vessels occluded within the observation period of 40 min, in

34 out of 38 wildtype vessels occlusive thrombus formation occurred. These findings indicate that in this model of vascular injury PLD1 and PLD2 have partially redundant functions.
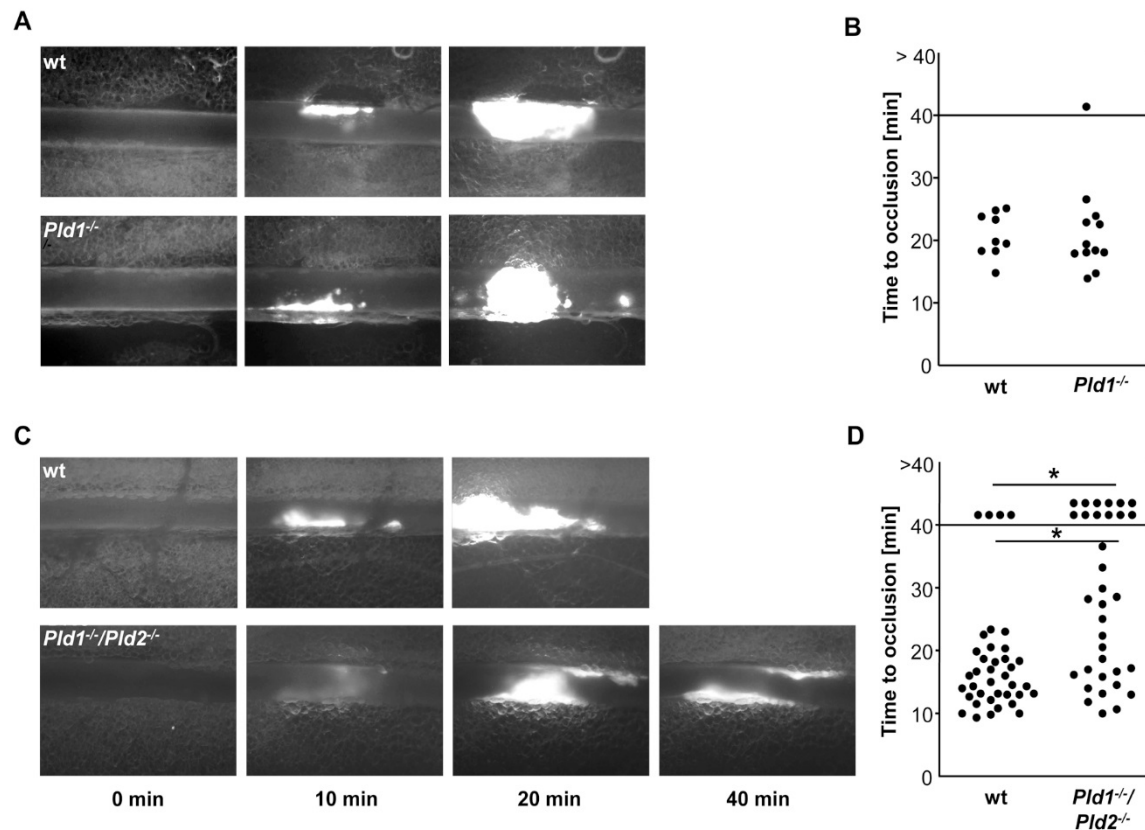
Figure 3-20: Mice lacking both PLD isoforms display defective thrombus formation *in vivo*. Thrombus formation in small mesenteric arterioles was induced by topical application of 20% $FeCl_3$. In order to monitor thrombus formation by intravital microscopy platelets were labeled fluorescently. Representative images and time to stable occlusion of vessels from wildtype and *Pld1*-/- mice (A, B) and representative images and time to stable occlusion (C, D) of vessels from wildtype and *Pld1*-/-/*Pld2*-/- mice are shown. Each symbol represents one individual. *$P<0.05$. (Thielmann*, Stegner* *et al.*, J Thromb Haemost, 2012)

To confirm these findings, mice were subjected to another thrombosis model. Thrombus formation was induced by applying $FeCl_3$ to the carotid artery. In contrast to the mesenterial arterioles the carotid artery represents a macrovascular bed. 7 out of 9 vessels of *Pld1*-/-/*Pld2*-/- mice did not occlude, while all wildtype vessels showed occlusive thrombus formation within the observation period of 30 min (Figure 3-21A,B). Given the fact that PLD1 single deficient mice are protected in this model [8] this finding does not provide any further information on the redundant functions of PLD1 and PLD2.
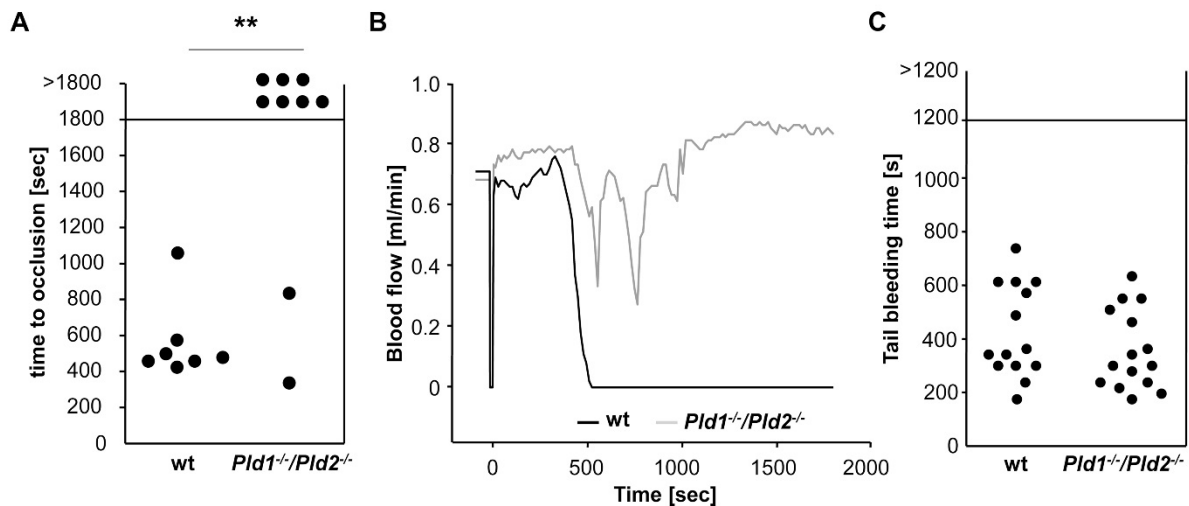
Figure 3-21: *Pld1⁻/⁻/Pld2⁻/⁻* **mice show defective thrombus formation** *in vivo* **but unaltered hemostasis.** (A) The carotid artery was injured by topical application of 15 % FeCl₃ for 1.5 min and blood flow was monitored for 30 min. Time to stable occlusion (A) and representative blood flow charts (B) are presented. Each symbol represents one individual. (B) Tail bleeding times of wildtype and *Pld1⁻/⁻/Pld2⁻/⁻* mice. Each symbol represents one individual. **P<0.01. (Thielmann*, Stegner* *et al.*, J Thromb Haemost, 2012)

To analyze whether the combined deficiency of both PLD isoforms has an impact on infarct development upon MCAO, wildtype and *Pld1⁻/⁻/Pld2⁻/⁻* mice were subjected to the tMCAO model. *2,3,5-triphenyltetrazolium chloride* (TTC) staining of the brains was performed 24 hours after reperfusion, in order to differentiate between metabolically active and inactive tissues. Infarct volumes of *Pld1⁻/⁻/Pld2⁻/⁻* mice were reduced (wt: 87.0 ± 24.8 mm³, *Pld1⁻/⁻/Pld2⁻/⁻*: 51.5 ± 31.0 mm³, Figure 3-22A) leading to a better neurological outcome as assessed by the Bederson score (Figure 3-22B). Motoric function and coordination of infarcted mice was determined by the grip test demonstrating a better outcome in double-deficient mice (data not shown). However, this difference did not reach statistical significance. This model was also repeated with PLD1 deficient mice with C57BL/6 background confirming the previously published protection of PLD1 deficient mice with mixed background (Figure 3-22C, D) [8]. All in all, these findings show that PLD1 is the major isoform contributing to infarct development in cerebral ischemia since PLD2 deficiency did not elicit protection and *Pld1⁻/⁻/Pld2⁻/⁻* mice were not better protected than *Pld1⁻/⁻* mice in this model (Figure 3-10).

The observed deficiencies in thrombus formation of *Pld1⁻/⁻/Pld2⁻/⁻* mice *in vivo* might lead to defective hemostasis. In order to test this, tail bleeding times were assessed. Notably, bleeding times of wildtype (422.9 ± 166.4 sec) and double-deficient mice (354.4 ± 150.4 sec; Figure 3-21C) were comparable indicating that both isoforms are dispensable for normal hemostasis.
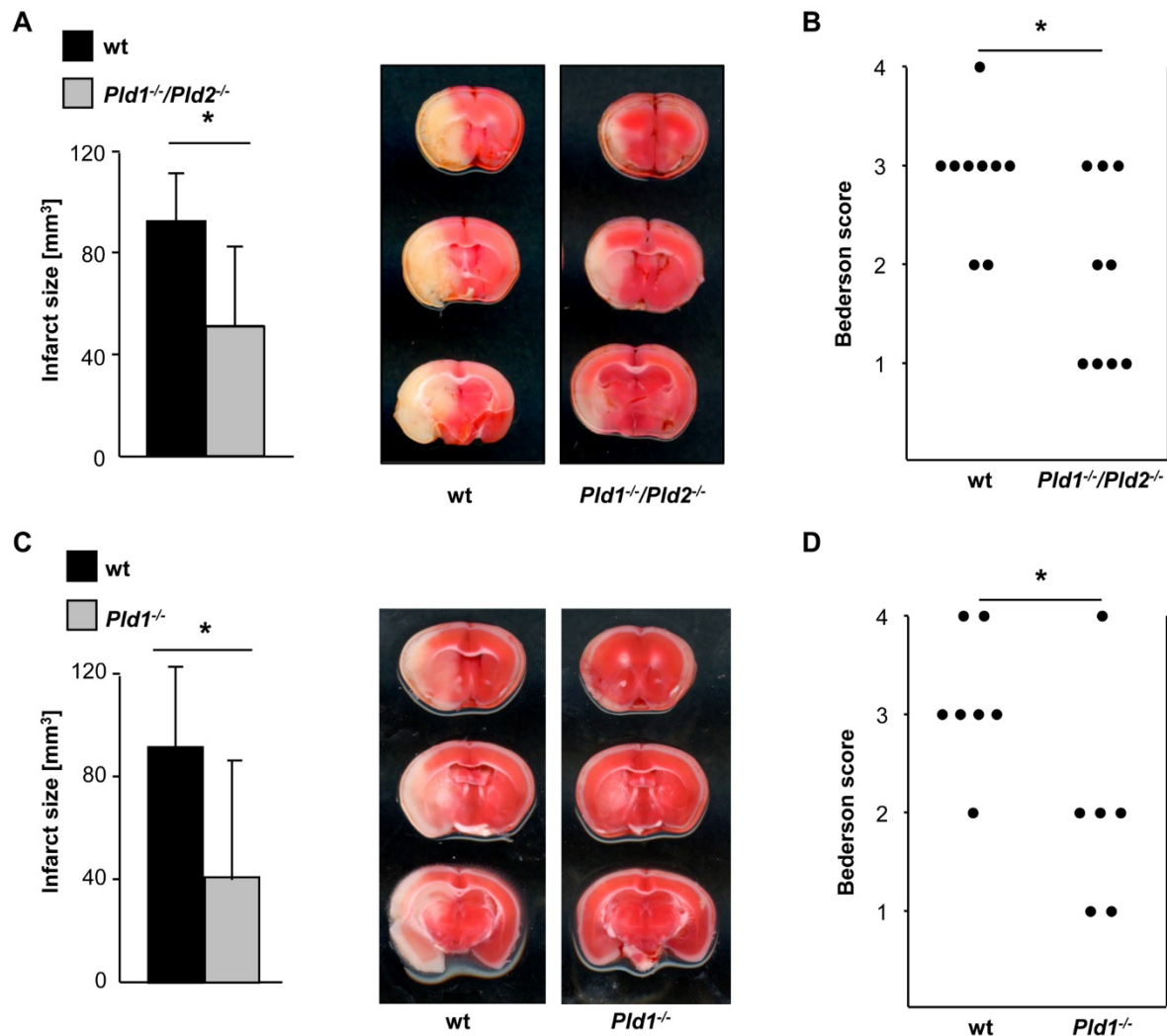
Figure 3-22: PLD-double deficient mice are protected from ischemic stroke. (A, D) Representative images of three corresponding coronal sections and brain infarct volumes of wildtype and *Pld1⁻/⁻/Pld2⁻/⁻* or C57BL/6 *Pld1⁻/⁻* mice which were subjected to the transient middle cerebral artery occlusion model. Data are mean ± SD of 10 mice per group. (B, D) Neurological Bederson score assessed 24 h after tMCAO. *$P<0.05$. (Thielmann*, Stegner* *et al.*, J Thromb Haemost, 2012)

3.2.6 Comparable to constitutive *Pld1⁻/⁻/Pld2⁻/⁻* mice, *Pld1⁻/⁻/Pld2⁻/⁻* bone marrow chimeric mice show impaired thrombus formation *in vivo*

Since both PLD isoforms are lacking systemically in *Pld1⁻/⁻/Pld2⁻/⁻* mice, it is important to address distinct functions of blood-borne and vessel wall PLD in thrombus formation *in vivo*. For this purpose, bone marrow chimeric mice were generated by reconstituting lethally irradiated wildtype mice with wildtype or *Pld1⁻/⁻/Pld2⁻/⁻* bone marrow. These mice were subjected to two different thrombosis models, namely the carotid artery injury model, as a macrovascular thrombosis model, and the mesenteric arteriole injury model, as a microvascular thrombosis model. In both models thrombus formation was induced by injury of the vessel with FeCl₃. Upon injury of the carotid artery, all vessels of animals that were

transplanted with wildtype bone marrow occluded, while in 4 out of 6 vessels of mice reconstituted with bone marrow derived from $Pld1^{-/-}/Pld2^{-/-}$ mice no occlusive thrombus formation occurred (Figure 3-23A). Similarly, only 9 out of 16 vessels of bone marrow chimeric double-deficient mice occluded in the mesenteric arteriole injury model. Additionally, a prolonged time to vessel occlusion (25.4 ± 8.4 min) was evident in those animals when compared to animals reconstituted with wildtype bone marrow (18.4 ± 3.5 min, Figure 3-23B). In summary, bone marrow chimeric and constitutive knockout mice were protected from pathological thrombus formation to similar extents. Thus, blood-borne PLD is the major modulator of *in vivo* thrombus formation (Figure 3-23).
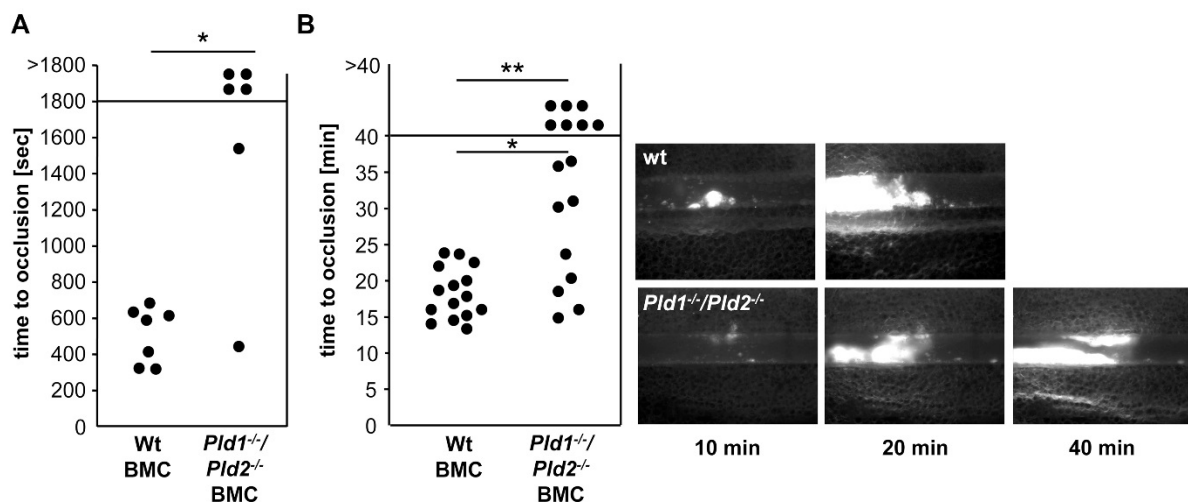
Figure 3-23: Mice lacking both PLD isoforms exclusively in the blood system display defective thrombus formation *in vivo*. *Bone marrow chimeric* (BMC) $Pld1^{-/-}/Pld2^{-/-}$ mice were generated and thrombus formation *in vivo* was analyzed. (A) Thrombus formation in the carotid artery was induced by topical application of 20% $FeCl_3$. Blood flow was monitored with an ultrasonic Doppler flow probe. Time to stable occlusion in mice reconstituted with bone marrow derived from wildtype or $Pld1^{-/-}/Pld2^{-/-}$ mice is depicted. Each symbol represents one individual. (B) Mesenteric arterioles were injured by applying $FeCl_3$ and platelets were labeled fluorescently in order to monitor thrombus formation by intravital microscopy. Representative images and time to stable occlusion are shown. Each symbol represents one individual. *$P<0.05$, **$P<0.01$.

3.3 Pharmacological inhibition of PLD protects mice from thrombus formation and stroke without impairing hemostasis

Since the aforementioned data demonstrates that deficiency of PLD1 and PLD2 protects from arterial thrombosis and ischemic stroke without affecting hemostasis, PLD was suggested as potential target for antithrombotic therapy [125]. However, *in vivo* evidence in support of this concept has been lacking. The activity of both PLD isoforms can be blocked by using small molecule inhibitors [236]. FIPI was identified as a potent and reversible inhibitor of both PLD isoforms, with a half-life of 5.5 hours *in vivo* and moderate bioavailability [158, 189]. To investigate whether FIPI injected mice show a similar phenotype as $Pld1^{-/-}/Pld2^{-/-}$ mice with

regard to thrombosis and hemostasis, FIPI treated platelets and mice were analyzed in different *in vitro* an *in vivo* platelet assays [237].

Other groups have already observed PLD-dependent phenotypes in FIPI treated cells and animals confirming its specificity and effectiveness [123, 149, 156, 157]. Long-term (10 days) *in vivo* treatment of mice did not show any overt toxicity [154].

3.3.1 FIPI treatment abolishes PLD activity and leads to defective integrin activation and α-granule release
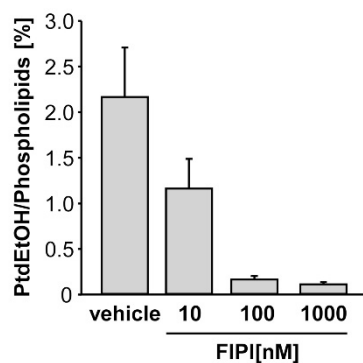
Figure 3-24: *In vitro* **FIPI treatment abolishes PLD activity.** Platelets were incubated with indicated concentrations of FIPI for 5 min at 37°C, stimulated with 0.1 U/ml thrombin for 5 min and PLD activity was measured. PLD activity is depicted as percentage of *phosphatidylethanol* (PtdEtOH) of total [³H]-labeled phospholipids. Data are mean ± SD of 4 mice per group. *P<0.05, ***P<0.001. (Stegner*, Thielmann* *et al.*, Arterioscler Thromb Vasc Biol., 2013)

In order to test whether the pharmacological PLD inhibition leads to similar platelet phenotypes as observed in *Pld1⁻ᐟ⁻/Pld2⁻ᐟ⁻* mice, initial experiments on FIPI treated platelets were conducted. To assess the lowest concentration abolishing PLD activity, a dose-response experiment by measuring PLD activity using an assay, detecting PLD dependent PtdEtOH production, in the presence of different FIPI concentrations was performed. In line with previous reports, the lowest FIPI concentration leading to maximal PLD inhibition was 100 nM (Figure 3-24) [189]. Thus, the dose of 100 nM FIPI was chosen for further experiments. To test whether glycoprotein expression on the platelet surface and platelet activation were affected by treatment with 100 nM FIPI, flow cytometric analyses were conducted. Glycoprotein expression of FIPI treated platelets was indistinguishable from vehicle treated platelets (Table 3-3). Interestingly, upon platelet stimulation with an intermediate concentration of thrombin FIPI treated wildtype platelets exhibited similar defects in integrin activation and P-selectin exposure as observed in *Pld1⁻ᐟ⁻/Pld2⁻ᐟ⁻* platelets (Figure 3-25). To exclude potential off-target effects by FIPI, flow cytometric assays were also performed with FIPI treated *Pld1⁻ᐟ⁻/Pld2⁻ᐟ⁻* platelets showing no additional effects of the FIPI treatment compared to *Pld1⁻ᐟ⁻/Pld2⁻ᐟ⁻* platelets or FIPI treated wildtype platelets. As a second readout for α-granule release, vWF secretion was measured in vehicle and FIPI treated platelets. In line with the impaired P-selectin exposure, vWF secretion was reduced in FIPI treated platelets upon thrombin stimulation whereas CRP triggered vWF secretion was unaltered (Figure 3-25).

	vehicle	FIPI	P-values
α-GPIb	330.4 ± 36.8	363.8 ±17.6	0.12
α-GPV	253.4 ± 16.9	282.6 ±25.2	0.07
α-GPIX	372.8 ± 22.8	395.4 ± 8.4	0.09
α-GPVI	49.8 ± 4.0	48.2 ± 2.5	0.48
α-CLEC-2	118.2 ± 11.8	138.2 ±16.1	0.06
α-α2	69.8 ± 4.0	69 ± 2.1	0.7
α-α5	16.0 ± 2.2	18.2 ± 0.8	0.09
α-β1	101.8 ± 8.4	108.6 ± 5.1	0.17
α-β3	148.8 ± 21.5	162.0 ± 7.9	0.25
α-αIIbβ3	463.4 ± 50.8	477.2 ±23.7	0.6
CD9	1173.2±102.2	1253.2±41.1	0.16

Table 3-3: FIPI treatment has no effect on platelet glycoprotein expression. Platelets were incubated with 100 nM FIPI for 5 min at 37°C and expression of glycoproteins on the platelet surface of vehicle and FIPI treated mice was determined by flow cytometric measurements. Diluted whole blood was labeled with FITC-coupled antibodies for 15 min at RT and analyzed directly on a FACSCalibur. Results are presented as mean fluorescence intensity ± SD of ≥ 5 mice per group.

Taken together, these observations proved the efficiency and specificity of FIPI in platelets. Nevertheless, the aforementioned assays were performed administering FIPI *in vitro*. In order to test the efficiency of FIPI *in vivo*, animals were treated with 3 mg/kg FIPI. The dose of 3 mg/kg (7.2 μM) was chosen with consideration of the half-life of 5.5 hours and 18.5% bioavailability when administered orally, in order to establish a conservative protocol keeping plasma levels above the lowest required inhibiting concentration of 100 nM, with twice-daily administration [154]. If the bioavailability of intraperitoneal delivery is higher than 18.5%, as expected, the trough levels of FIPI would be even higher than the required 100 nM, reaching plasma concentrations of up to 500 nM. Thus, ELISA and flow cytometric assays were repeated using 500 nM. No off-target effects were observed indicating the suitability of this FIPI-regiment for *in vivo* PLD inhibition (data not shown). As reported previously by Chen *et al.*, mice receiving 3 mg/kg FIPI did not show any obvious side-effects and behaved normally indicating the good tolerance of FIPI treatment [154]. Together with this study, these calculations and findings implicate that 3 mg/kg should be sufficient to fully inhibit PLD without exerting obvious side-effects.

A

B
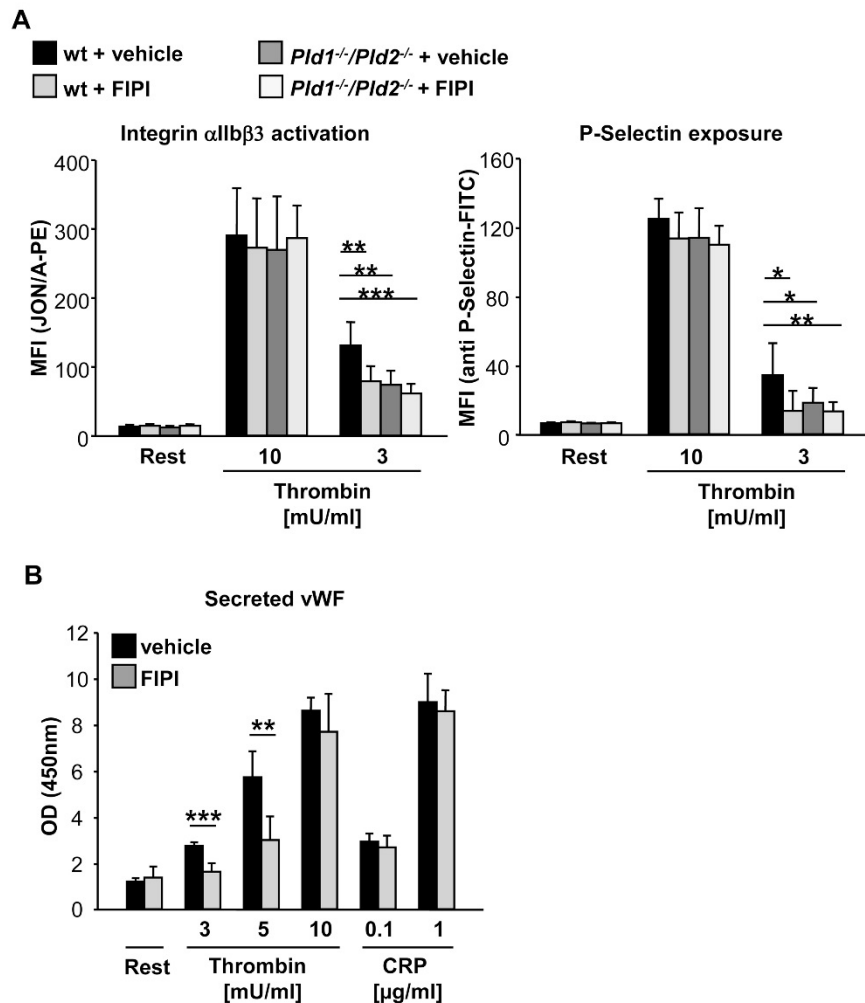
Figure 3-25: *In vitro* **FIPI treatment of platelets results in specific integrin activation and α-granule release defects.** Platelets were incubated with FIPI for 5 min at 37°C. (A) Flow cytometric analyses of αIIbβ3 integrin activation (JON/A-PE) and degranulation dependent P-selectin exposure in response to thrombin of vehicle and FIPI treated platelets. Results are mean fluorescence intensities (MFI) ± SD of 4 mice per group. (B) Measurement of secreted vWF in the supernatant of vehicle and FIPI treated platelets. Data are presented as OD_{450nm} ± SD of 4 mice per group. *P<0.05; **P<0.01, ***P<0.005. (Stegner*, Thielmann* *et al.*, Arterioscler Thromb Vasc Biol., 2013)

The efficiency of FIPI *in vivo* treatment was tested by measuring PLD activity of platelets isolated from FIPI treated mice. Surprisingly, PLD activity of isolated platelets was only slightly reduced (data not shown) and did not show ablation of PLD activity as observed after *in vitro* FIPI treatment. To analyze whether this discrepancy can be explained by the fact that FIPI is a reversible inhibitor and therefore its activity might recover during platelet washing, platelets were treated with FIPI *in vitro* before and after platelet washing and PLD activity was determined upon thrombin stimulation. Indeed, platelets treated with FIPI before platelet washing showed normal thrombin-triggered PLD activity, whereas PLD activity was abolished when platelets were treated after washing (Figure 3-26) demonstrating that platelet washing abolishes the effect of FIPI treatment. Therefore, it was only possible to perform the respective *in vitro* platelet assays with *in vitro* treated platelets.
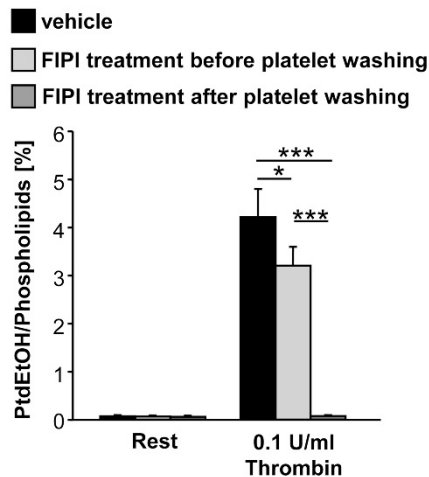
Figure 3-26: *In vitro* **FIPI treatment is reversible.** Platelets were incubated with FIPI for 5 min at 37°C and PLD activity was measured. PLD activity is depicted as percentage of *phosphatidylethanol* (PtdEtOH) of total [^{3}H]-labeled phospholipids. Data are mean ± SD of 4 mice per group. *P<0.05, ***P<0.001.

Since aggregation assays can be performed with PRP, at least one *in vitro* assay was suitable to test *in vivo* treated platelets. Therefore, platelet aggregation studies of heparinized platelet-rich plasma of vehicle- and FIPI-treated mice were performed. For this purpose, PAR-4 peptide had to be used to stimulate platelets instead of thrombin since heparin was still present. Platelets of FIPI treated mice aggregated to the same extent and with similar kinetics as platelets from vehicle treated mice (Figure 3-27). Since it has already been shown that *Pld1*$^{-/-}$ and *Pld1*$^{-/-}$/*Pld2*$^{-/-}$ platelets aggregate normally, these findings support once more the notion that the treatment with 3 mg/kg FIPI does not exert obvious off-target effect [8, 125]. However, they do not provide evidence for the *in vivo* efficacy of FIPI treatment.
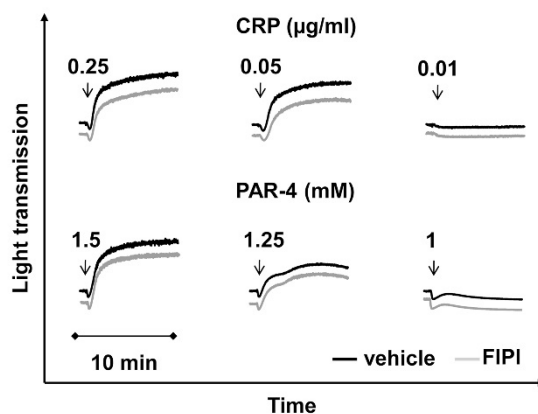
Figure 3-27: FIPI treatment does not affect platelet aggregation. Platelet rich plasma of vehicle and FIPI treated mice was stimulated with the indicated agonists and light transmission was recorded on a Born aggregometer. Representative aggregation traces of 3 individual experiments are depicted. (Stegner*, Thielmann* *et al.*, Arterioscler Thromb Vasc Biol, 2013)

3.3.2 FIPI treatment results in impaired thrombus formation *in vivo* without exerting obvious off-target effects

So far, the aforementioned tests did not reveal whether the *in vivo* administration of FIPI inhibits PLD specific effects. In order to test this, mice were injected with 3 mg/kg FIPI and *in vivo* thrombus formation was analyzed by subjecting these mice to two well-established thrombosis models.
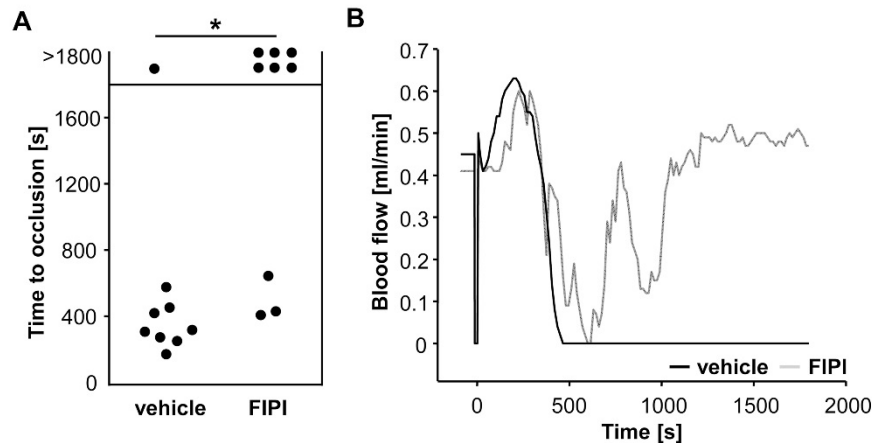
Figure 3-28: FIPI treatment results in impaired thrombus formation *in vivo.* PLD activity in platelets was blocked by intraperitoneal injection of 3 mg/kg FIPI 13 and 1 h before the experiment. Carotid arteries were topically injured with a filter paper saturated with 15% FeCl₃ for 1.5 min and blood flow was measured. Time to stable occlusion (A) and a representative blood flow chart (B) are depicted. *$P<0.05$. (Stegner*, Thielmann* *et al.*, Arterioscler Thromb Vasc Biol, 2013)

First, the carotid artery was injured and blood flow was monitored using an ultrasonic flow probe. Similar to the prominent phenotypes of *Pld1$^{-/-}$* and *Pld1$^{-/-}$/Pld2$^{-/-}$* mice in this model, only 3 out of 9 vessels of FIPI treated mice occluded upon injury by topical application of FeCl₃, while in control mice vessel occlusion occurred in all, but one, vessel (Figure 3-28). In a second model, where thrombus formation was induced in mesenteric arterioles, FIPI treatment also showed a protective effect. Although the time to first appearance of thrombi >10 μm was unaltered (vehicle: 11.5 ± 3.1 min, FIPI: 11.4 ± 3.0 min; Figure 3-29A), the time to vessel occlusion was significantly prolonged in FIPI treated mice (vehicle: 20.7 ± 3.9 min, FIPI: 25.1 ± 7.7 min; Figure 3-29B). These findings demonstrate that the antithrombotic effect of FIPI treatment is not limited to larger vessels, which is consistent with the observations in *Pld1$^{-/-}$/Pld2$^{-/-}$* mice.

In order to test whether the phenotype is due to FIPI-induced PLD inhibition, vehicle- and FIPI-treated wildtype and *Pld1$^{-/-}$/Pld2$^{-/-}$* mice were analyzed in the mesenteric arteriole model. Thrombi bigger than 10 μm appeared in similar time frames in all groups (Figure 3-29C). In line with the previous data, all vehicle treated vessels of wildtype mice occluded after 14.2 ± 3.8 min, whereas 4 out of 13 vessels of vehicle-treated double-deficient mice showed no occlusion (Figure 3-29D). In cases where vessel occlusion occurred, the time to vessel occlusion of vehicle-treated *Pld1$^{-/-}$/Pld2$^{-/-}$* mice was significantly prolonged (19.8 ± 6.4 min, Figure 3-29D). Further, FIPI-treated *Pld1$^{-/-}$/Pld2$^{-/-}$* mice exhibited occlusion times (22.2 ± 7.7 min, Figure 3-29D) indistinguishable from vehicle-treated *Pld1$^{-/-}$/Pld2$^{-/-}$* mice. These results are similar to the findings in FIPI treated wildtype mice demonstrating no additional effect of FIPI treatment in double-deficient mice. Together, these results show that FIPI is effective *in vivo* without exerting off-target effects.
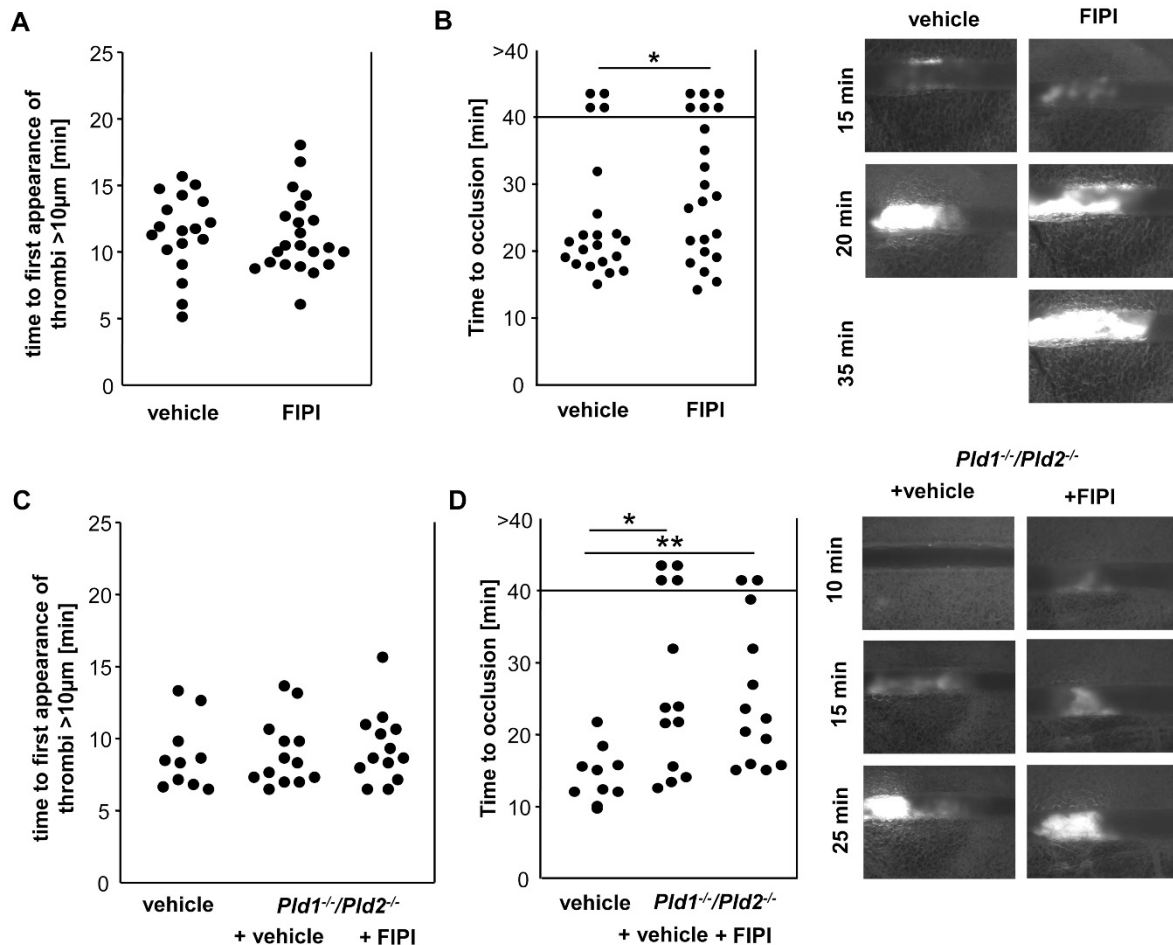
Figure 3-29: FIPI treatment results in impaired thrombus formation *in vivo* without exerting obvious off-target effects. PLD activity in platelets was blocked by intraperitoneal injection of 3 mg/kg FIPI 13 and 1 h before the experiment. Thrombus formation in small mesenteric arterioles of vehicle and FIPI treated wildtype and *Pld1-/-/Pld2-/-* mice was induced by topical application of 20% FeCl$_3$. First appearance of thrombi >10 µm (A, C) and time to occlusion (B, D) was assessed. Representative images are shown. Each symbol represents one individual. *P<0.05, **P<0.01. (Stegner*, Thielmann* *et al.*, Arterioscler Thromb Vasc Biol, 2013)

3.3.3 FIPI treatment protects from ischemic stroke without impairing hemostasis

Since the combined deficiency of PLD1 and PLD2 leads to protection from infarct progression in a model of ischemic stroke we analyzed the effect of FIPI treatment on the outcome of thrombo-inflammatory brain infarction. Mice received 3 mg/kg FIPI prior induction of middle cerebral artery occlusion. The infarct volumes, which were determined 24 hours after infarction by 2,3,5-TTC staining, were significantly reduced (vehicle: 108.7 ± 35.4 mm^3, FIPI: 65.5 ± 19.5 mm^3, Figure 3-30A). Accordingly, these mice showed better motor function and coordination as assessed by the grip test (Figure 3-30B) and showed less neurological deficits determined by the Bederson score (Figure 3-30C).
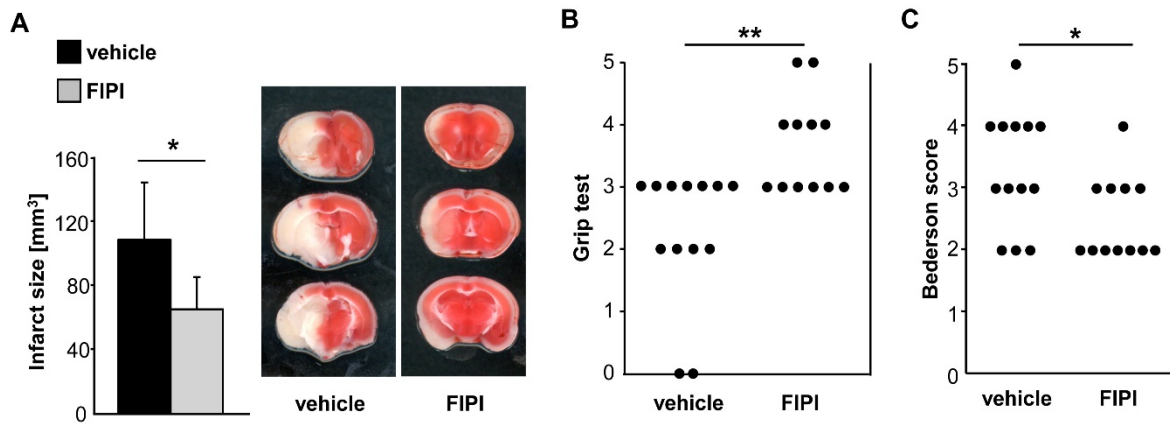
Figure 3-30: FIPI treatment protects mice from ischemic stroke. (A) Brain infarct volumes and representative images of three corresponding coronal sections of vehicle and FIPI-treated mice subjected to the transient middle cerebral artery model. Data are mean ± SD of 7 mice per group. (B,C) Grip test (B) and neurological Bederson score (C) assessed 24 h after tMCAO. *P<0.05, **P<0.01. (Stegner*, Thielmann* *et al.*, Arterioscler Thromb Vasc Biol, 2013)

Antithrombotic treatment can be accompanied by increased intracerebral hemorrhages [219, 238, 239]. In order to test whether this is the case upon FIPI-treatment, infarct morphology was visualized by *magnetic resonance imaging* (MRI). Infarct volumes determined on FIPI treated mice were significantly smaller compared to vehicle treated animals (vehicle: 151.4 ± 20.0 mm^3, FIPI: 90.6 ± 21.8 mm^3). Remarkably, there were no intracerebral hemorrhages, which would have been detectable as hyper-intense regions in the brain (Figure 3-31A). This indicates that FIPI does not affect the maintenance of intracerebral hemostasis. In line with this observation, tail bleeding times of FIPI treated mice were unaltered as well. In this experiment one set of mice also received 6 mg/kg FIPI to see whether a higher inhibitor concentration would exert any off-target effects influencing tail bleeding time. Due to the limited solubility of FIPI and a maximal tolerable concentration of the solvent DMSO, 6 mg/kg was the highest dose that could be delivered intraperitoneally [240]. In theory, application of 6 mg/kg (14.4 µM) FIPI should result in plasma concentration levels well above 1 µM, taking the presented half-life and bioavailability into account [154]. This is 10-fold above the 100 nM concentration required to completely abrogate platelet PLD activity *in vitro* (Figure 3-24). However, even a concentration as high as this did not influence tail bleeding times (Figure 3-31B). There is no clear correlation between bleeding time and risk of clinical hemorrhages [241]. Nevertheless, our data argues for the suitability of pharmacological PLD inhibition as a safe and effective treatment for inhibition of thrombotic activity and prevention of ischemic stroke.
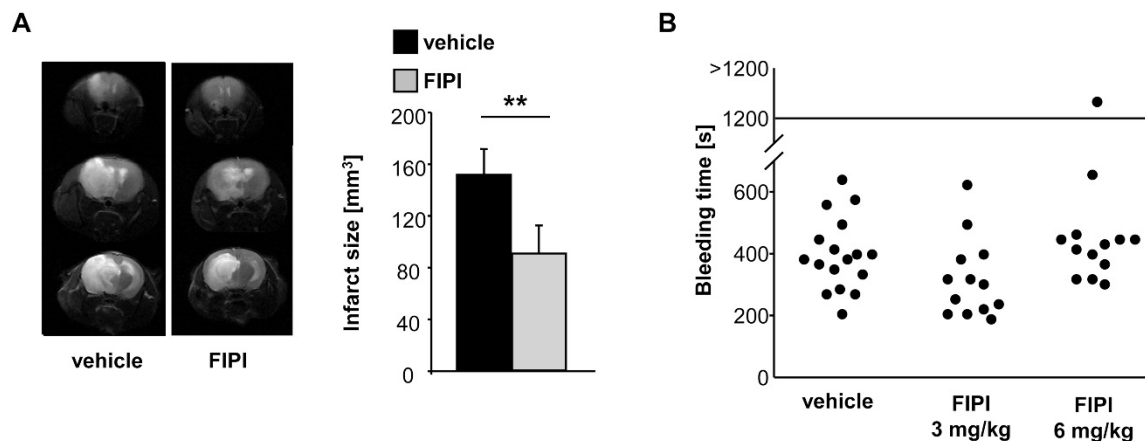
Figure 3-31: FIPI treatment protects from ischemic stroke without impairing hemostasis.
(A) Representative magnetic resonance (MR) T2-weighted gradient echo images of cerebral infarcts at three coronal planes and corresponding brain infarct volumes at day 1 after tMCAO in control and FIPI-treated mice. Data are mean ± SD of 4 mice per group. (B) Tail bleeding times of vehicle and FIPI treated mice. *P<0.05, **P<0.01. (Stegner*, Thielmann* *et al.*, Arterioscler Thromb Vasc Biol, 2013)

3.3.4 Therapeutic FIPI treatment might exert protective effects on mice suffering from ischemic stroke

There is a strong demand to develop effective and safe treatments for acute stroke since conventional therapies for the prevention of ischemic stroke and thromboembolism using platelet aggregation inhibitors are associated with an increased bleeding risk [219, 238, 239, 241]. FIPI might be suitable for the prevention of ischemic stroke without affecting hemostasis. However, as most patients suffering from stroke arrive in the clinics upon neurological deficits, it is of great importance to develop treatments that can be used therapeutically after cerebral vessel occlusion.

In order to test whether FIPI also exerts therapeutic benefits in the setting of acute stroke, mice were treated with 3 or 6 mg/kg FIPI directly and 8 hours after tMCAO. Infarct volumes of control mice were 116.5 ± 26.2 mm^3 which was comparable to sizes detected in brains of mice receiving 3 mg/kg FIPI (120.0 ± 24.6 mm^3; Figure 3-32A). Mice injected with 6 mg/kg FIPI showed slightly reduced infarct sizes (86.9 ± 45.0 mm^3), which did not reach statistical significance (Figure 3-32A). In line with this, the motorical and global neurological appearance of vehicle and 3 mg/kg FIPI treated mice were unaltered, while mice treated with 6 mg/kg had slightly better Bederson score values (Figure 3-32B,C). Taken together, these data indicate that therapeutic treatment with high dose FIPI might be suitable to protect from ischemic stroke. However, for the clinical application further optimization of drug delivery, potency and bioavailability is required.
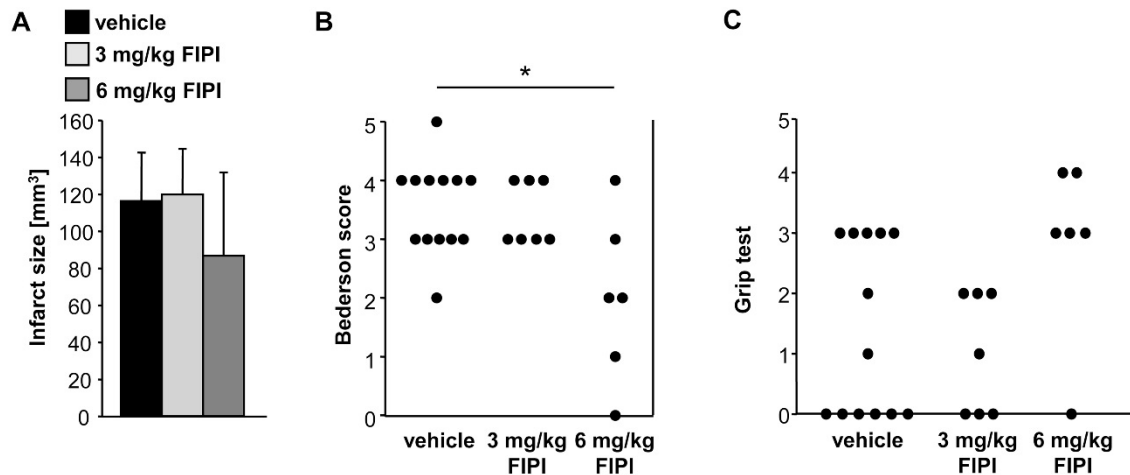
Figure 3-32: Therapeutic FIPI treatment might exert protective effects in mice suffering from ischemic stroke. Mice were treated with 3 or 6 mg/kg FIPI after middle cerebral artery occlusion and 8 hours later. (A) Brain infarct volumes of control and FIPI-treated mice subjected to the transient middle cerebral artery model. Data are mean ± SD of 7 mice per group. (B,C) Neurological Bederson score (B) and grip test (C) assessed 24 h after tMCAO. (Stegner*, Thielmann* *et al.*, Arterioscler Thromb Vasc Biol, 2013)

3.4 PLD activity and regulation in blood platelets

The above described data revealed an important role for PLD in platelet α-granule secretion and integrin activation, indicating that PLD might be important for pathological thrombus formation and ischemic stroke development (chapter 3.1 and 3.2). Therefore, it is of great interest to elucidate the mechanisms underlying the regulation of PLD activity in platelets. It has already been shown that PLD is activated in response to stimulation of platelets with common platelet agonists [165, 167-169] and PLD has been postulated to be regulated by many signaling molecules which are also crucial for platelet activation [66, 97, 242]. However, previous studies on the regulation of PLD were conducted mainly in cell culture using inhibitors which might exert off-target effects [62, 243, 244]. Often, contradicting conclusions have been drawn from those studies, which emphasizes the need for clarification [168, 170]. Thus, analyzing PLD activity in different knockout mouse strains lacking potential modulators of the enzyme presents a unique strategy to gain firm evidence of the complex regulation of PLDs. There are several methods for the detection of PLD activity available. The transphosphatidylation assay takes advantage of the fact that PLD generates PtdEtOH instead of PA in the presence of EtOH. PtdEtOH, which is, in contrast to PA, a stable metabolite, can be detected by radioactive labeling. This widely accepted PLD activity assay was established in our laboratory. To check the suitability and specificity of this assay, PA and PtdEtOH levels were determined in resting and activated platelets in the presence and absence of EtOH. In thrombin activated platelets PtdEtOH levels were only detectable if EtOH was present (data not shown). Under these conditions, PA was only produced to a minor extent indicating the

high efficiency of the transphosphatidylation reaction in this setting. As already shown in Figure 3-11A and 3-24, no PtdEtOH can be detected in PLD deficient or FIPI treated platelets confirming that the PtdEtOH production can be solely ascribed to PLD activity. In order to analyze which platelet agonists trigger PLD activity in our hands, platelets were stimulated with common platelet agonists and PLD activity was measured. In line with previous publications [165, 167-169], platelet activation with the common platelet agonists thrombin, CRP and U46619 increased PLD activation, whereas ADP had no such effect (Figure 3-33).
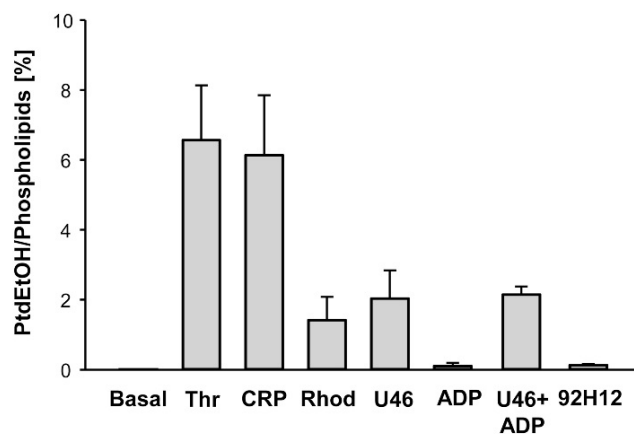
Figure 3-33: PLD activity in platelets is stimulated by various agonists. Wildtype platelets were labeled with [^{3}H]-myristic acid and stimulated with the indicated agonists for 15 min. PLD activity is depicted as percentage of *phosphatidylethanol* (PtdEtOH) of total [^{3}H]-labeled phospholipids. Data are mean ± SD of 4 mice per group. Abbreviations: Thr, thrombin; U46, U46619; Rhod, Rhodocytin. Concentrations: 0.1 U/ml thrombin, 10 µg/ml CRP, 0.12 µg/ml Rhodocytin, 3 µM U46619, 10 µM ADP, 50 µg/ml 92H12.

Weaker platelet agonists such as U46619 induced lower PLD activity as compared to strong platelet activation with CRP or thrombin (Figure 3-34). Furthermore, the level of PLD activity decreased with the duration of platelet stimulation (Figure 3-33). These findings confirmed that the assay is of sufficient sensitivity to discriminate between different PLD activity levels. Of note, the CLEC-2 activating snake venom toxin rhodocytin stimulated PLD activity to a lower extent than the GPVI agonist CRP (Figure 3-33) pointing to differential PLD regulation downstream the two (hem)ITAM receptors. Furthermore, in ADP stimulated platelets only basal PLD activity levels were detected. However, ADP is an important secondary mediator being released during platelet stimulation thereby maintaining sustained platelet activation. Therefore, ADP might exert synergistic effects with other agonists. This was analyzed by triggering PLD activity with different agonists in the presence of the ADP scavenger apyrase. For this approach and for subsequent measurements the following conditions were chosen: Platelet stimulation with CRP or thrombin were conducted for 2 and 15 min in order to monitor initial and sustained PLD activation upon stimulation with strong agonists while stimulation with U46619 was carried out for 15 min in order to have a setting with weak agonist stimulation. Independent of the used agonist, apyrase treated wildtype platelets showed slightly reduced PLD activity demonstrating the importance of second wave mediators to sustain platelet activation and therefore PLD stimulation in this setting (Figure 3-34).

Considering that the previous reports from our laboratory suggested the platelet receptor GPIb to signal upstream of PLD, PLD activity in response to GPIb signaling was analyzed. Crosslinking of GPIb to vWF is commonly induced by the snake venom toxin botrocetin [8, 245, 246]. However, the interaction of GPIb to vWF is species-specific and since murine recombinant vWF is commercially not available, experiments need to be performed in PRP [247]. Unfortunately, the PLD assay cannot be performed in PRP due to excess of phospholipids disturbing the thin layer chromatography. Therefore, the GPIb crosslinking antibody 92H12 was used. 92H12 was generated in our laboratory (Nieswandt *et al.*, unpublished) and triggers GPIb-dependent agglutination and thus, presumably induces the GPIb-signaling cascade. Nevertheless, crosslinking of GPIb did not induce PLD activity (Figure 3-33) indicating that GPIb activation itself under static conditions is not sufficient to activate PLD enzymatic activity (Figure 3-33).

Taken together, these data confirm the involvement of PLD in several platelet signaling pathways and propose that the enzyme is tightly regulated during platelet activation. Therefore, the aim of the study was to gain insights into these regulatory mechanisms by analyzing PLD activity in different knockout mouse strains.
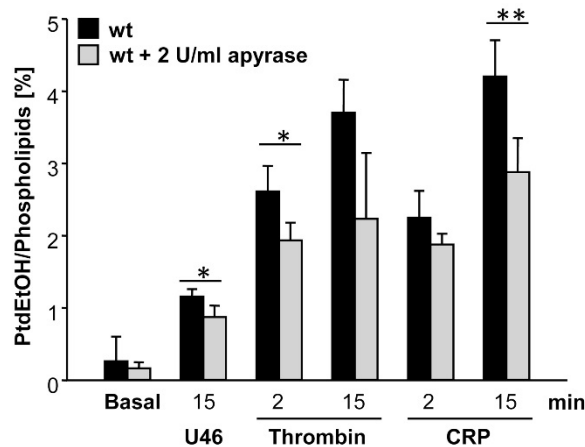
Figure 3-34: Blocking reinforcement of platelet activation diminishes PLD activity. Platelets were labeled with [³H]-myristic acid and stimulated with the indicated agonists in the presence or absence of 2 U/ml apyrase. PLD activity is depicted as percentage of *phosphatidylethanol* (PtdEtOH) of total [³H]-labeled phospholipids. Data are mean ± SD of 4 mice per group. Abbreviations: U46, U46619; CRP, collagen related peptide. Concentrations: 0.1 U/ml thrombin, 10 µg/ml CRP, 3 µM U46619. *P<0.05, **P<0.01, ***P<0.001.

3.4.1 The adapter molecule Grb2 as well as PI3Kβ are crucial regulators in GPVI-mediated PLD activation

The adaptor protein Grb2 is a part of the LAT signalosome and is involved in the tyrosine kinase signaling cascade contributing significantly to PLCγ activation in platelets [242]. There are several possibilities how Grb2 might influence PLD activity. One option would be indirectly through tyrosine kinase modulation since receptor tyrosine kinase stimulation is believed to activate PLD and several tyrosine kinases have been shown to interact and phosphorylate PLD [67]. Another possibility could be the modulation of PLD enzyme activity by direct interaction with Grb2 at specific phosphorylated sites as proposed previously [52]. In order to

investigate whether Grb2 influences PLD activity in platelets, PLD activity in wildtype and *Grb2⁻ᐟ⁻* platelets was determined. PLD activity in *Grb2⁻ᐟ⁻* platelets was normal upon stimulation with agonists triggering GPCR pathways, such as thrombin and U46619. In line with the reduced functionality of ITAM signaling in *Grb2⁻ᐟ⁻* mice, PLD activity was severely reduced in these platelets when being activated with CRP (Figure 3-35A). These data indicate that Grb2 contributes to PLD activity downstream of GPVI, but not downstream of GPCRs.
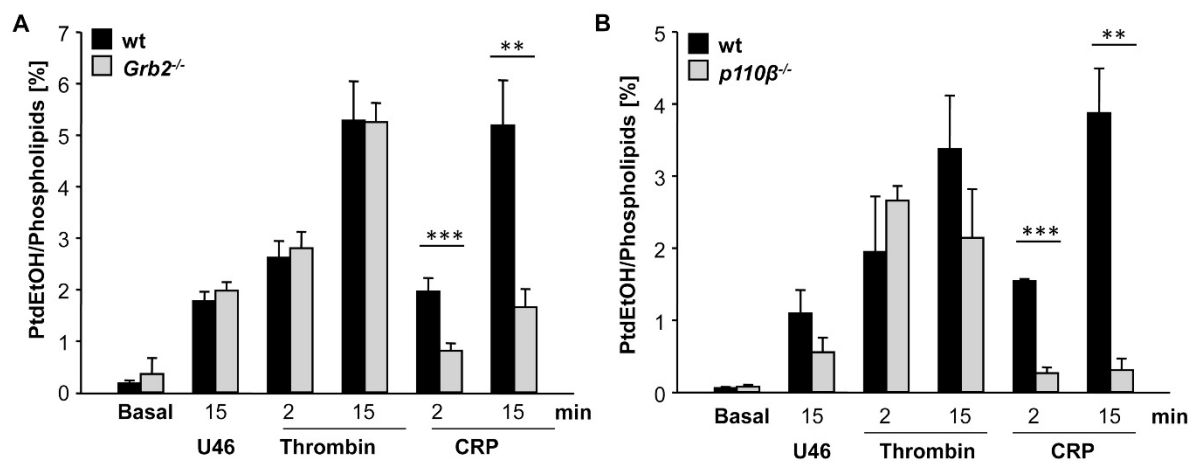
Figure 3-35: Grb2 and PI3Kβ are important mediators of ITAM-triggered PLD activity. Platelets were labeled with [³H]-myristic acid and stimulated with the indicated agonists. PLD activity is depicted as percentage of *phosphatidylethanol* (PtdEtOH) of total [³H]-labeled phospholipids. Data are mean ± SD of 4 mice per group. PLD activity of resting and activated wildtype and *Grb2⁻ᐟ⁻* (A) or *p110β⁻ᐟ⁻* (B) platelets. Abbreviations: U46, U46619; CRP, collagen related peptide. Concentrations: 0.1 U/ml thrombin, 10 µg/ml CRP, 3 µM U46619. *P<0.05, **P<0.01, ***P<0.001.

PI3Kβ is important for PIP, PIP_2 and PIP_3 production and PKB/Akt activation downstream of GPCR and ITAM signaling. Furthermore, PI3Kβ is critically involved in regulating the formation and stability of integrin αIIbβ3 bonds in platelets [248, 249]. Mice with defective PI3Kβ do not have functional platelet responses and are therefore protected from pathological thrombus formation [212]. To reveal whether the lack of PI3Kβ and resulting differences in the phosphorylation status of phosphatidylinositol affects PLD activity, the PLD assay was performed with wildtype and *p110β^{fl/fl,PF-4 Cre}* platelets. Deficiency of PI3Kβ resulted in defective PLD activation upon stimulation of the collagen receptor GPVI with CRP, whereas PLD activation downstream of GPCRs was normal (Figure 3-35B). These findings show that PI3Kβ is crucial for GPVI dependent PLD activation.

3.4.2 GPCR-triggered PLD activity is presumably mainly mediated via G_q

During thrombus growth, second wave mediators such as ADP, TxA_2 and thrombin are required for the recruitment of additional platelets into the growing thrombus. These mediators signal through GPCRs which activate the G-proteins G_q, G_{13} and G_i/G_z. RhoA is involved in the signaling cascade downstream of G_{13} and G_q proteins regulating MLC phosphorylation and

thereby enabling platelet shape change. Furthermore, the activation of the proposed PLD activator PKC is prominent downstream of G_q stimulation [22, 250].
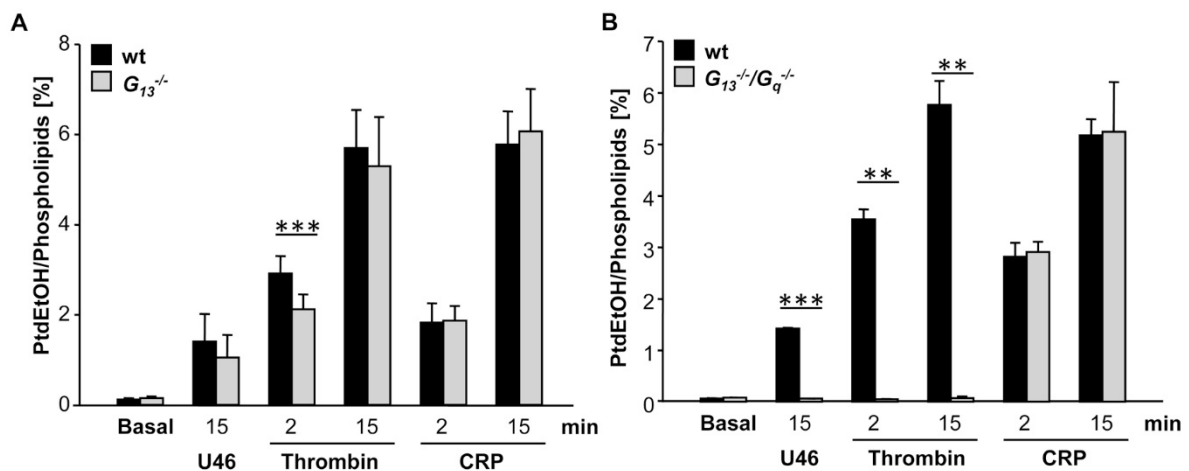
Figure 3-36: Different G-proteins are involved in the regulation of PLD activity. Platelets were labeled with [³H]-myristic acid and stimulated with the indicated agonists. PLD activity is depicted as percentage of *phosphatidylethanol* (PtdEtOH) of total [³H]-labeled phospholipids. Data are mean ± SD of 4 mice per group. PLD activity of resting and activated wildtype and $G_{13}^{-/-}$ (A) or $G_{13}^{-/-}/G_q^{-/-}$ platelets (B). Abbreviations: U46, U46619; CRP, collagen related peptide. Concentrations: 0.1 U/ml thrombin, 10 µg/ml CRP, 3 µM U46619. *P<0.05, **P<0.01, ***P<0.001.

Since PLD becomes activated by platelet stimulation with the GPCR agonists thrombin and U46619 it was analyzed which GPCR signaling pathway contributes most to PLD regulation. $G_{13}^{-/-}$ platelets revealed grossly normal PLD activation downstream of all tested agonists except slightly reduced thrombin dependent PLD activation following 2 min of stimulation. However, this difference was not evident upon 15 min of stimulation indicating only a weak contribution of G_{13}-coupled receptor signaling to PLD activation (Figure 3-36A). To clarify the impact of G_q stimulation on PLD activity the G_q single knockout mice would be the appropriate model to study. However, at the time when the experiments were conducted, only mice with combined deficiency of G_{13} and G_q were available from collaboration partners. In contrast to the effects observed in G_{13} knockout platelets, the combined deficiency of G_{13} and G_q proteins led to abolished PLD activation upon stimulation with U46619 or thrombin, indicating that G_q proteins are essential to generate signals leading to PLD activation (Figure 3-36B). However, due to lack of measurements of $G_q^{-/-}$ platelets, redundant roles of G_{13} and G_q cannot be excluded and need to be resolved in the future.

3.4.3 Rho GTPases contribute to the regulation of PLD activity

Following stimulation of GPCRs several small GTPases become activated [22] and GTPases of the Arf and Rho family have been proposed to play major roles in PLD activation [67]. Therefore, it was assessed whether Rho GTPases contribute to the regulation of PLD activity in platelets. Rac1, a member of the Rho GTPase family, becomes activated through ITAM-, but also through G_q-coupled receptor stimulation in platelets [251]. It has been shown to be essential for ITAM-dependent PLCγ2 activation in platelets which is critical for thrombus formation *in vivo* [251]. Rac1 deficiency resulted in decreased PLD activation upon stimulation with the GPCR agonist U46619 and upon stimulation of GPVI indicating that ITAM and G_q signaling utilize Rac1 to promote PLD activation. However, thrombin triggered PLD activation was unaltered in Rac1 deficient mice suggesting that other molecules mediate PLD activation in this pathway (Figure 3-37A). Next, the impact of RhoA on PLD activity was investigated. Lack of RhoA, which is active in response to G_{13}-coupled receptor signaling, led to reduced PLD activation upon platelet stimulation with the GPCR agonists thrombin and U46619, whereas PLD activity was normal upon GPVI activation with CRP (Figure 3-37B). PLD activity upon stimulation with U46619 was largely reduced identifying RhoA as a key player in this pathway. Cdc42 also belongs to the Rho family and has diverse functions in platelet activation [252]. Similar to RhoA and Rac1, Cdc42 has been identified as activator of PLD1 [71]. However, in platelets Cdc42 was established as a negative regulator of platelet secretion and aggregation [252]. The PLD assay of *Cdc42$^{-/-}$* platelets revealed a tendency towards increased PLD activity independently of the applied agonist (Figure 3-37C). Together with the finding that PLD activity is to some extent dependent on second wave reinforcement of platelet activation (Figure 3-34), the enhanced platelet degranulation and increased ADP/ATP content of *Cdc42$^{-/-}$* platelets might account for the slightly elevated PLD response of *Cdc42$^{-/-}$* platelets [252].

To analyze potential redundant functions of the GTPases, PLD activity of double deficient mice was measured. Surprisingly, the analysis of *Cdc42$^{-/-}$/RhoA$^{-/-}$* platelets revealed similar PLD activity levels as observed in Cdc42 deficient platelets. Notably, also PLD activation upon stimulation of GPCRs, which was diminished in *RhoA$^{-/-}$* platelets, was unaltered (Figure 3-38A). This suggests, that Cdc42 exerts a role as negative regulator of PLD activity.
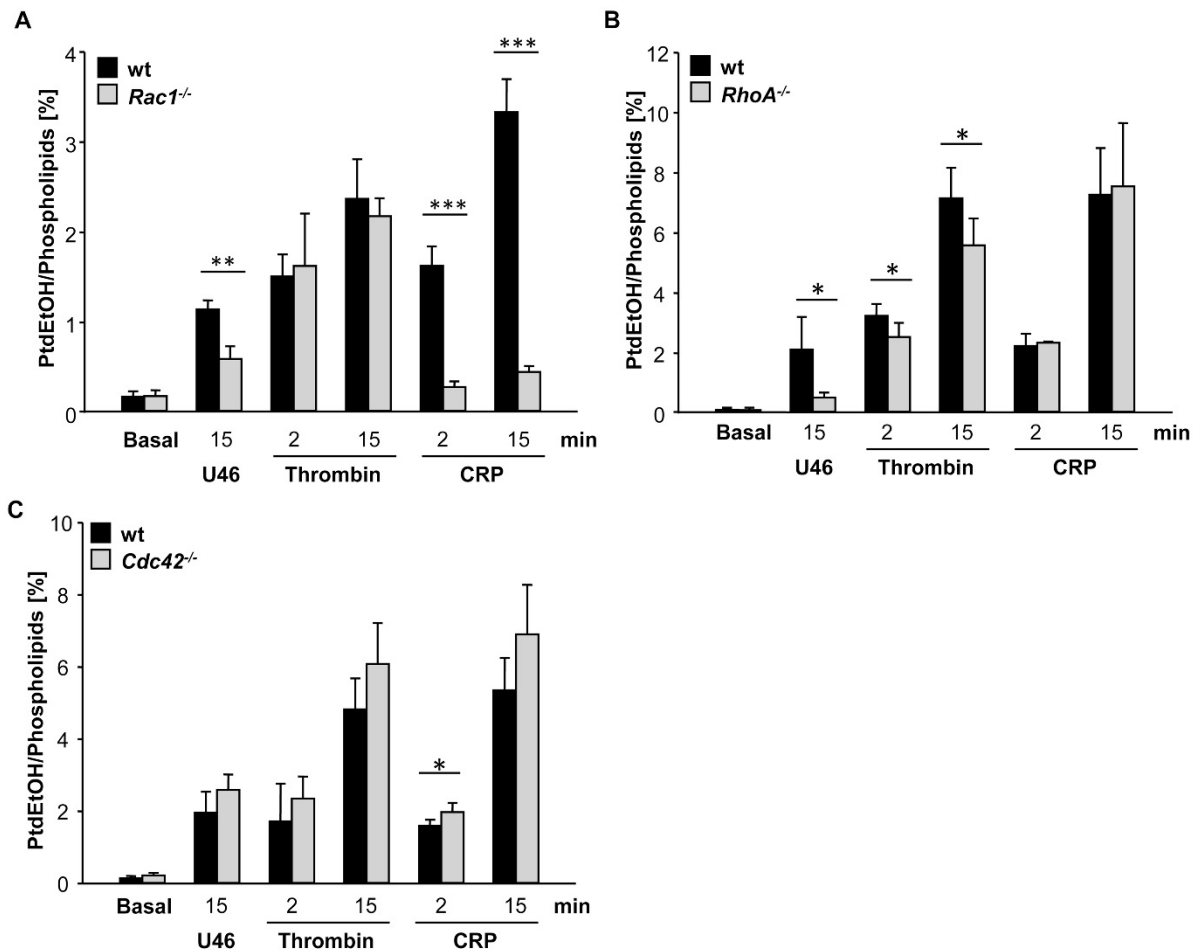
Figure 3-37: Rac1 and RhoA are activators of PLD while Cdc42 might serve as negative regulator of PLD regulator. Platelets were labeled with [^{3}H]-myristic acid and stimulated with the indicated agonists. PLD activity is depicted as percentage of *phosphatidylethanol* (PtdEtOH) of total [^{3}H]-labeled phospholipids. Data are mean ± SD of 4 mice per group. PLD activity of resting and activated wildtype and *Rac1*$^{-/-}$ (A), *RhoA*$^{-/-}$ (B) or *Cdc42*$^{-/-}$ (C) platelets. Abbreviations: U46, U46619; CRP, collagen related peptide. Concentrations: 0.1 U/ml thrombin, 10 µg/ml CRP, 3 µM U46619. *P<0.05, **P<0.01, ***P<0.001.

In *Rac1*$^{-/-}$*RhoA*$^{-/-}$ platelets, GPVI-induced PLD activity was similarly decreased as in *Rac1*$^{-/-}$ platelets whereas thrombin-induced PLD activity was reduced to a greater extent when compared to *RhoA*$^{-/-}$ platelets (Figure 3-38B). These findings suggest redundant functions of the two GTPases Rac1 and RhoA in mediating PLD activation downstream of thrombin stimulation.

Taken together, the findings imply that distinct as well as redundant functions of GTPases strongly contribute to PLD activation.
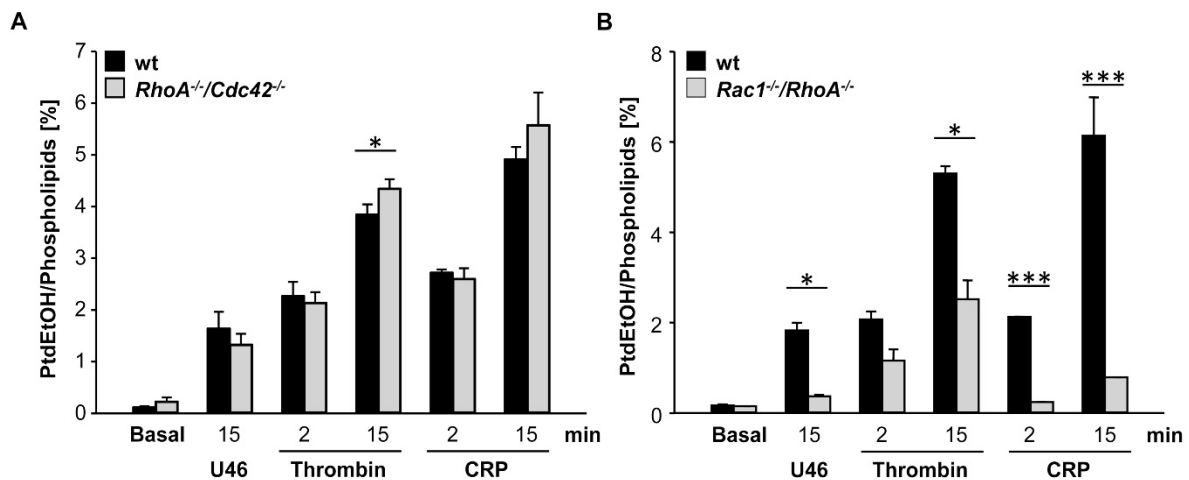
Figure 3-38: The GTPases have redundant as well as distinct functions in the regulation of PLD activity. Platelets were labeled with [³H]-myristic acid and stimulated with the indicated agonists. PLD activity is depicted as percentage of *phosphatidylethanol* (PtdEtOH) of total [³H]-labeled phospholipids. Data are mean ± SD of 4 mice per group. PLD activity of resting and activated wildtype and *RhoA⁻/⁻ /Cdc42⁻/⁻* (A) or *Rac1⁻/⁻/RhoA⁻/⁻* (B) platelets. Abbreviations: U46, U46619; CRP, collagen related peptide. Concentrations: 0.1 U/ml thrombin, 10 µg/ml CRP, 3 µM U46619. *P<0.05, **P<0.01, ***P<0.001.

3.4.4 Proteins involved in actin dynamics do not influence the activity of PLD

Previous reports suggested that integrin αIIbβ3 outside-in signaling is important for the activation of PLD in platelets [178, 185]. Platelet activation shifts integrins from a low affinity to a high affinity state enabling the binding of ligands. For this process, as well as for integrin outside-in signaling, talin1 is indispensable [209]. Outside-in signaling of αIIbβ3 integrins triggers various cellular processes such as spreading. This requires the rearrangement of the cytoskeleton, which includes a change in platelet shape from discoid to spheric [253]. Several proteins such as profilin1, twinfillin2 and cofilin are involved in actin remodeling and contribute to outside-in signaling [253-256]. Furthermore, it has been demonstrated that actin filaments bind to PLD and are supposed to exert bidirectional modulation of PLD activity [114]. With knockout animals harboring deficiencies in αIIbβ3 integrin activation or actin remodeling the impact of outside-in signaling on PLD activity in platelets can be assessed. Remarkably, *n-cofilin⁻/⁻*, *Pfn1⁻/⁻* and *Twf2a⁻/⁻* mice showed normal PLD activation following platelet activation independent of the stimulating agonist demonstrating that impaired actin dynamics do not influence PLD activity (Figure 3-39). Since integrin activation is still functional in *n-cofilin⁻/⁻*, *Pfn⁻/⁻* and *Twf2a⁻/⁻* mice, PLD activity of mice deficient in talin1, a direct αIIbβ3 integrin regulator, was measured. However, also in *Tln1⁻/⁻* platelets PLD activity was triggered to the same extent as in wildtype platelets clearly excluding integrin αIIbβ3 as important regulator of PLD activation (Figure 3-39D).
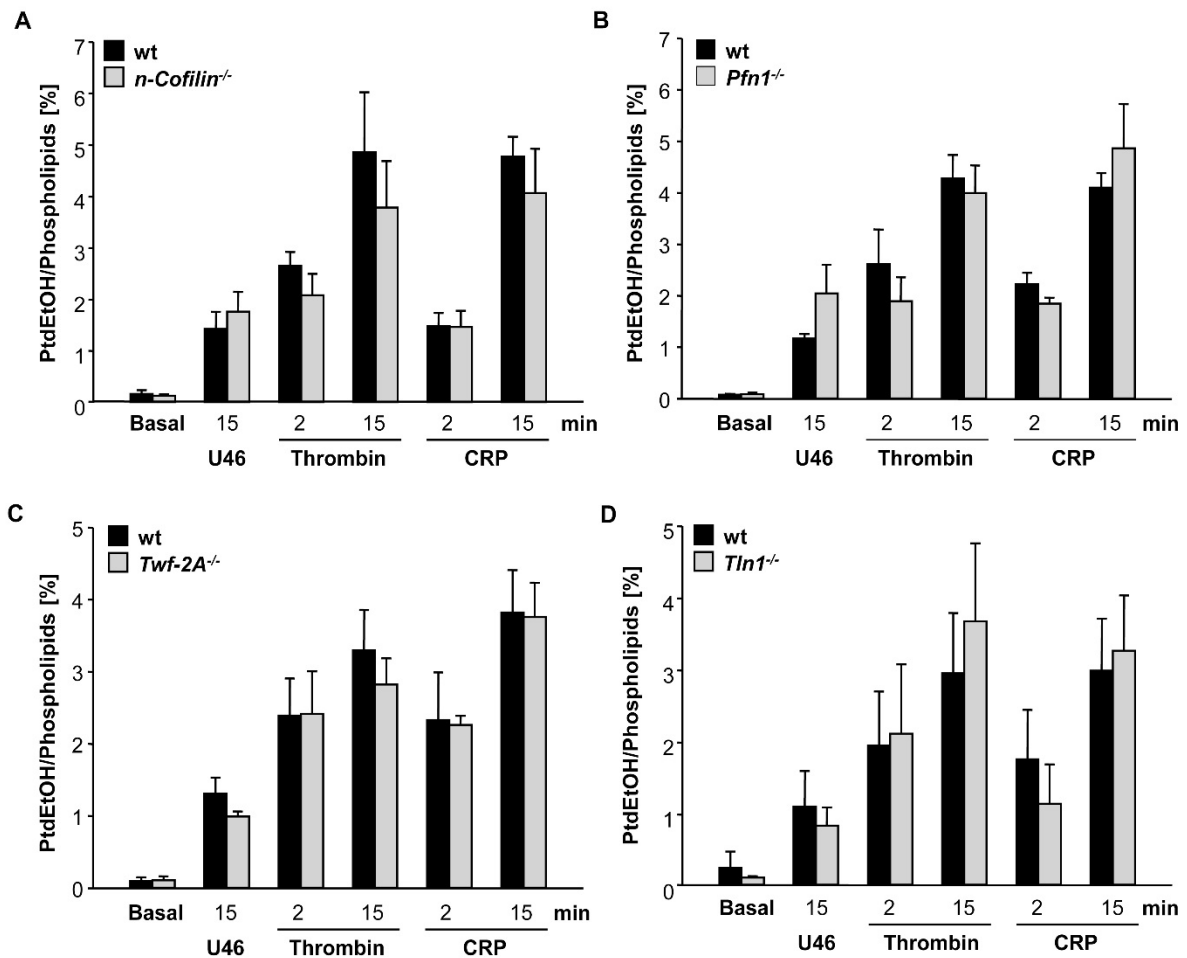
Figure 3-39: Proteins involved in platelet outside-in signaling or actin remodeling do not influence the activity of PLD. Platelets were labeled with [3H]-myristic acid and stimulated with the indicated agonists. PLD activity is depicted as percentage of *phosphatidylethanol* (PtdEtOH) of total [3H]-labeled phospholipids. Data are mean ± SD of 4 mice per group. PLD activity of resting and activated wildtype and *n-cofilin*^{-/-} (A), *Pfn*^{-/-} (B), *Twf2a*^{-/-} (C) or *Tln1*^{-/-} (D) platelets. Abbreviations: U46, U46619. Concentrations: 0.1 U/ml thrombin, 10 µg/ml CRP, 3 µM U46619. *P<0.05, **P<0.01, ***P<0.001.

3.4.5 PKCs regulate PLD activity in platelets

The data presented in this thesis demonstrates the upregulation of PLD activity in various platelet signaling pathways. Most of these pathways converge in the activation of PLCs leading to an increase in intracellular Ca^{2+} levels and DAG, an activator of PKC [257]. Platelet function has been shown to be distinctly regulated by the different PKC isoforms [258, 259]. It has already been shown that the phorbol ester PMA, a direct PKC activator, is capable of activating PLD and that the different PKC isoforms can bind PLD, thereby modulating its activity [67, 95]. Therefore, it is of great interest to elucidate the impact of PLC and the different PKC isoforms on PLD activity. Since not all required knockout mice were available also inhibitors had to be used. Notably, off-target effects of these inhibitors cannot be excluded. However, the here utilized inhibitors are established and were applied at recommended concentrations thereby

reducing non-specific effects [260]. First of all, platelets were treated with the PLC inhibitor U-73122 and PLD activity was measured. In accordance with the general notion that PLCs are of relevance for the regulation of PLDs, PLD activity of U-73122 treated platelets was strongly decreased in all tested pathways (Figure 3-40A). However, residual PLD activity was detected in thrombin stimulated platelets.
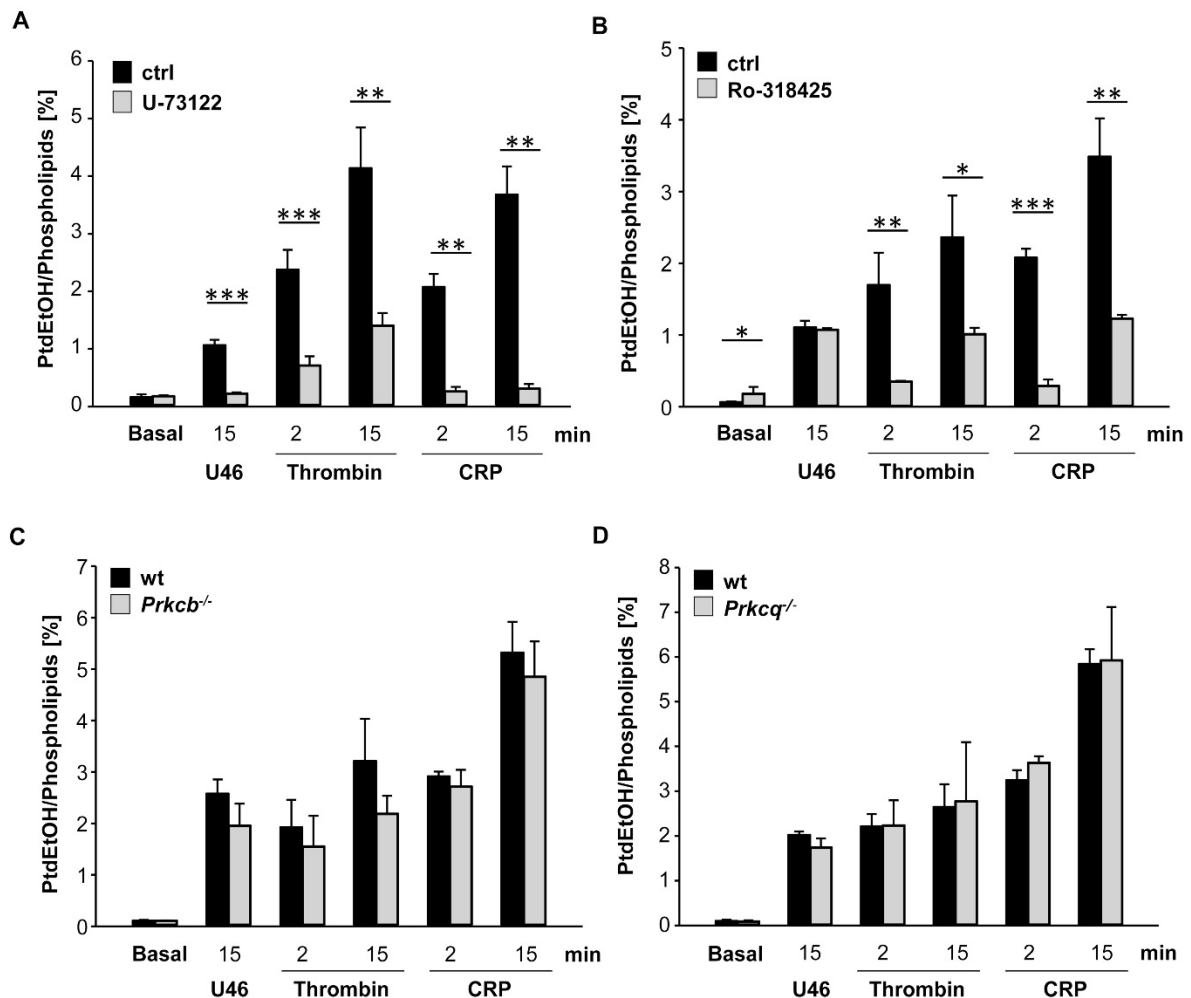
Figure 3-40: PLCs regulate PLD activity in platelets. Platelets were labeled with [³H]-myristic acid and stimulated with the indicated agonists. PLD activity is depicted as percentage of *phosphatidylethanol* (PtdEtOH) of total [³H]-labeled phospholipids. PLD activity of resting and activated vehicle and PLC Inhibitor U-73122 (5 μM) treated platelets (A), vehicle and Ro-318425 (10 μM) treated platelets (B), platelets from wildtype mice and mice lacking PKCβ (*Prkcb$^{-/-}$*) (C) or platelets from wildtype mice and mice lacking PKCθ (*Prkcq$^{-/-}$*) (D). Data are mean ± SD of 4 mice per group. Abbreviations: U46, U46619; CRP, collagen related peptide. Concentrations: 0.1 U/ml thrombin, 10 μg/ml CRP, 3 μM U46619. *P<0.05, **P<0.01, ***P<0.001.

To analyze whether this defect can be ascribed to insufficient PKC activation, the effect of platelet treatment with the non-selective PKC inhibitor Ro-318425 on PLD activity was analyzed. Under these conditions, PMA induced PLD activity was totally abolished proving the efficacy of the inhibitor treatment (data not shown). Interestingly, U46619 triggered PLD activity of inhibitor treated platelets was indistinguishable from control platelets demonstrating PKC

independent pathways in this setting. Furthermore, in the presence of Ro-318425, early PLD activation upon stimulation with thrombin or CRP was reduced to basal levels whereas sustained platelet stimulation with these agonists triggered PLD activity to a small extent (Figure 3-40B). These results demonstrated a major role for PKCs in regulating PLD activity, but also suggested alternative PKC independent pathways to exist. To elucidate which PKC isoforms are responsible for the observed effects, PLD activation in mice deficient in specific PKC isoforms in platelets were analyzed. Platelets of $Prkcb^{-/-}$ and $Prkcq^{-/-}$ mice showed similar levels of PLD activity as compared to wildtype platelets excluding these isoforms as major regulators for PLD activity (Figure 3-40C,D). Ro-318425 treatment most prominently inhibits PKC isoforms α and β and PKCα has been shown to be the most important PKC isoform in respect to platelet functions. Together with the presented results, this indicates that the inhibitor mediated reduction of PLD activity might be PKCα dependent. Other PLC triggered processes such as Ca^{2+} influx might account for the residual levels of PLD activity in Ro-318425 treated platelets. Taken together, these findings are in line with previous publications and demonstrate an important, but not exclusive, role for PLCs and PKCs in the regulation of PLD.

3.4.6 Ca^{2+} is required for proper PLD activation

Activation of PLC isoforms does not only generate DAG, triggering PKC activation, but also results in the production of IP_3 leading to the release of Ca^{2+} from its intracellular stores. Declining Ca^{2+} levels in the stores, in turn, result in sustained influx of extracellular Ca^{2+} through Orai channels, a process called *store operated calcium entry* (SOCE) [203, 261]. Since platelet stimulation induces Ca^{2+} release and PLD became activated upon stimulation with most common platelet agonists, Ca^{2+} might be a major regulator of PLD activity. To address the relevance of Ca^{2+} in PLD regulation, platelets were treated with different Ca^{2+} modulating agents and platelets of knockout mice with defects in the SOCE machinery were analyzed. Initially, platelets were incubated with the Ca^{2+} chelator EGTA and stimulated with common platelet agonists. EGTA mediated chelation of extracellular Ca^{2+} resulted in significantly decreased PLD activity upon stimulation with all used agonists demonstrating that Ca^{2+} is of importance for PLD activation (Figure 3-41A). However, minor PLD activity could still be detected in the absence of extracellular Ca^{2+} upon strong platelet stimulation. To exclude unspecific effects by EGTA, PLD activity measurements were also performed in the presence of EGTA and high levels of Ca^{2+}. In this case, PLD activity between EGTA treated and control platelets was indistinguishable confirming the Ca^{2+} specific effect of EGTA (data not shown). To analyze the contribution of Ca^{2+} on PLD activity in a more direct approach, the PLD activity of platelets treated with Ca^{2+} mobilizing agents was determined. *Thapsigargin* (TG) increases the cytosolic Ca^{2+} concentration by inhibiting the *sarco/endoplasmic reticulum Ca^{2+}-ATPase* (SERCA) pump leading to the release of Ca^{2+} from the intracellular stores [1, 262]. In line with

previous publications, TG induces PLD activation to a small extent (basal: 0.06 ± 0.0; TG: 2.3 ± 0.6 % PtdEtOH of total phospholipids; Figure 3-41B). A23187, an ionophore highly selective for Ca^{2+}, that can also increase cytosolic Ca^{2+} concentrations, confirmed that the release of intracellular Ca^{2+} was able to trigger PLD activity (basal: 0.2 ± 0.1; A23187: 1.9 ± 0.4 % PtdEtOH of total phospholipids; Figure 3-41B). However, in both cases Ca^{2+} immobilization increased PLD activity only slightly when compared to PLD activity triggered by strong platelet agonists, suggesting that an additional trigger is required for proper PLD activation.
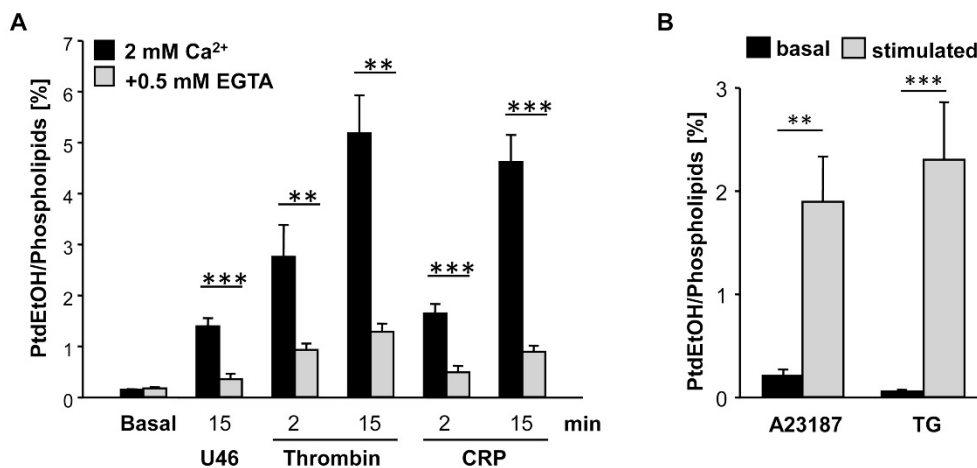
Figure 3-41: Extracellular Ca^{2+} is required for proper PLD activation. Platelets were labeled with [³H]-myristic acid and stimulated with the indicated agonists. PLD activity is depicted as percentage of *phosphatidylethanol* (PtdEtOH) of total [³H]-labeled phospholipids. Data are mean ± SD of 4 mice per group. (A) PLD activity of resting and activated platelets in the absence or presence of extracellular Ca^{2+}. (B) PLD activity in wildtype platelets upon treatment with the indicated ionophores for 10 min. Abbreviations: U46, U46619; TG, thapsigargin; CRP, collagen related peptide. Concentrations: 0.1 U/ml thrombin, 10 µg/ml CRP, 3 µM U46619, 5 µM TG, 10µM A23187. *P<0.05, **P<0.01, ***P<0.001.

The influence on PLD activity on extracellular Ca^{2+} influx can also be analyzed using *Orai1⁻ᐟ⁻* and *Stim1⁻ᐟ⁻* mice, which have strongly reduced *store operated calcium entry* (SOCE) presenting a less artificial system than EGTA treatment. Remarkably, PLD activity upon platelet stimulation of *Orai1⁻ᐟ⁻* and *Stim1⁻ᐟ⁻* platelets was comparable to PLD activity in wildtype platelets except when stimulating shortly with thrombin upon which PLD activity was slightly reduced in *Stim1⁻ᐟ⁻* platelets (Figure 3-42A,B). These data show that PLD can still be activated despite the severe reduction of extracellular Ca^{2+} influx indicating that the contribution of intracellular Ca^{2+} might be more important. These findings appear to contradict the data obtained using EGTA. This might, however, be explained by an imbalance in the distribution of Ca^{2+} after treatment with EGTA indirectly affecting intracellular Ca^{2+} levels and pathways.

Taken together, these findings demonstrate that the increase of intracellular Ca^{2+} levels is of relevance for PLD activation.
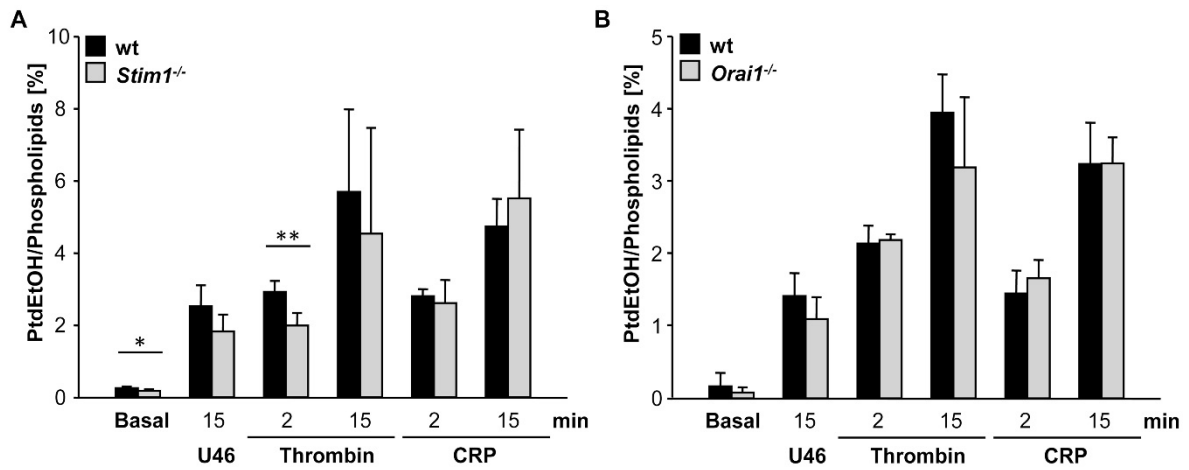
Figure 3-42: Only weak Ca^{2+} influx is required for proper PLD activation. Platelets were labeled with [^{3}H]-myristic acid and stimulated with the indicated agonists. PLD activity is depicted as percentage of *phosphatidylethanol* (PtdEtOH) of total [^{3}H]-labeled phospholipids. Data are mean ± SD of 4 mice per group. PLD activity of resting and activated wildtype and *Stim1$^{-/-}$* (A) or *Orai1$^{-/-}$* (B) platelets. Abbreviations: U46, U46619; CRP, collagen related peptide. Concentrations: 0.1 U/ml thrombin, 10 µg/ml CRP, 3 µM U46619. *P<0.05, **P<0.01, ***P<0.001.

4 Discussion

Platelet plug formation is essential to limit excessive blood loss at sites of vascular injury. On the one hand, the control of bleeding requires a dynamic interplay of coagulation pathways, platelet function and fibrinolysis. Dysregulation of one of these processes can lead to severe bleeding disorders that can often be attributed to specific gene defects such as in Glanzmann's thrombasthenia or Bernard-Soulier syndrome [263]. On the other hand, uncontrolled thrombus formation has to be prevented since this can lead to full vessel occlusion resulting in myocardial infarction or ischemic stroke, which are both leading causes of death worldwide [4, 264, 265]. After ischemic stroke, therapeutic thrombolysis is currently the only approved treatment. This does, however, not assure a recovery of the tissue. So-called reperfusion injuries that occur frequently can lead to secondary infarction events. To avoid this, agents infering with platelet aggregation, such as clopidogrel or aspirin, are used on a regular basis, although its applicability is often limited due to increased risk of intracranial hemorrhages [239]. Recent studies proposed that the initial platelet adhesion and activation process by the platelet receptors GPIb or GPVI contribute to the pathomechanism in acute cerebral ischemia. Blocking these receptors protected mice in the tMCAO model without inducing intracerebral hemorrhages [219, 266]. However, further analysis of the tight signaling network, that underlies platelet activation as well as coagulation, is required to identify potentially druggable molecules that are critical for pathological thrombus formation and infarct development without affecting vascular homeostasis.

This thesis shows that the redundant functions of PLD1 and PLD2 in platelet α-granule release contribute to pathological thrombus formation (Figure 4-1). By using genetic and pharmacological approaches, PLD blockade as strategy for antithrombotic therapy was shown to be effective. The PLD inhibitor FIPI was established as potential lead-structure for the development of antithrombotic agents. As the findings indicated a crucial role for PLD in thrombo-inflammatory processes, the underlying regulatory network of PLD activity was also analyzed and demonstrated complex regulation mechanisms of PLD enzymes during initial platelet activation.

4.1 PLD2 is dispensable for platelet function in thrombosis and hemostasis

The results presented in this thesis show for the first time that PLD2, in contrast to PLD1, is not required for appropriate platelet function, at least in the assays tested. PLD2 deficient animals were able to form occlusive thrombi in response to different types of injuries and

developed normal infarcts in a stroke model. These findings suggest that PLD2 is not a fundamental mediator of arterial thrombosis and thrombo-inflammatory disease (Figure 4-1).

Similar to PLD1, PLD2 has been implicated in many elementary cellular processes such as cytoskeletal reorganization, secretion, cell migration and chemotaxis (Figure 1-6) [67]. Due to the supposed involvement of PLD in essential cellular processes, PLD was hypothesized to be of major importance during development as well. This, of course, could become overt in constitutive knockout mice. Our laboratory has already demonstrated that constitutive genetic PLD1 deficiency had no impact on the viability, health and fertility of these mice. In line with other studies [124], also PLD2 deficient mice did not display any obvious developmental defects, which led to the assumption that the lack of one isoform can be functionally compensated by the other isoform [124, 125]. In addition, it has to be considered that many experiments suggesting PLD as an indispensable molecule were performed using inhibitors, mostly primary alcohols, which clearly have off-target effects. This might have led to an over-estimation of the significance of PLD. Thus, former results obtained with inhibitors should be carefully re-evaluated making use of knockout mice.

This study and a previous publication on *Pld1*$^{-/-}$ mice from our laboratory confirmed the presence of both PLD isoforms in platelets and their increased activity upon platelet activation (Figure 3-1) [8]. Previous studies on the functions of PLD in platelets were often performed by linking PLD activity to simultaneously occurring cellular events. Commonly, PLD activity is measured by lipid labeling of PtdEtOH with radioactive fatty acids, as PtdEtOH is produced by PLD in the presence of ethanol at the expense of PA. However, there are also other approaches to quantify PLD activity by using choline production as read-out or using different non-radioactive techniques to label products of PLD [32]. However, it is not possible to discriminate between the contributions of one single PLD isoform to the overall PLD activity. By quantifying PLD activity in isoform-specific knockout mice, this study revealed that PLD2 only weakly contributes to the total PLD activity in platelets. This identifies PLD1 as the major PLD isoform in platelets which is in line with previous reports (Figure 3-1) [8, 170]. However, since the PLD activity assay only measures the lipase activity, scaffold functions or other lipase-independent functions of the enzymes cannot be excluded. For example, it was shown that PLD can activate RhoA in a lipase independent manner by enabling nucleotide exchange [75]. A similar mechanism was proposed by Mahankali *et al*. identifying PLD2 as GEF for Rac2 [267].

The increase of PLD activity upon platelet stimulation in *Pld2*$^{-/-}$ platelets was attenuated compared to wildtype platelets demonstrating that PLD2 is inducible upon platelet stimulation (Figure 3-1). This contradicted previous reports which suggested PLD1 to be the only inducible PLD isoform. Due to its structure and high basal activity *in vitro*, PLD2 has been postulated to exhibit constitutive PLD activity [33, 65, 268]. Notably, the herein presented data shows that

the basal PLD activity in resting platelets is only very low and PLD2 deficiency does not decrease this basal activity, excluding this isoform as mediator of constitutive PLD activity. In contrast, Vorland *et al.* showed a basal PLD activity of 30% of thrombin response [170]. Although the authors also used PtdEtOH production as read-out, they used arachidonic acid instead of myristic acid for labeling PLD substrates which might have caused platelet activation via the thromboxane receptor triggering PLD activity [168]. Further, the diviating results might also be attributed to different acyl specificities of PLD which has been demonstrated similarly for PLA_2 and PLC and might become apparent by labeling different fatty acids [269]. In addition, a report on PLD1 deficiency in platelets from Elvers *et al.* also showed a high basal PLD activity measuring choline release as read-out for PLD activity [8]. Nevertheless, others report a negligible constitutive PLD activity in platelets as it is shown in this thesis [168]. In general, it is not possible to compare the different results that were obtained with different assays under distinct settings directly. However, the transphosphatidylation assay used in this study is the most established assay. The primary advantage is the underlying PLD specific transphosphatidylation reaction which traps the metabolically labile PLD specific products as phosphatidylalcohols. In addition, the labeling with suitable radioactive tracers enables the measurement of PLD products in intact cells [32].

Despite reduction in PLD activity, platelet function of $Pld2^{-/-}$ mice was normal. Similar to $Pld1^{-/-}$ platelets, PLD2 deficient mice displayed unaltered platelet production, assessed by platelet size, count and life span. In contrast to the observed αIIbβ3 integrin defect in $Pld1^{-/-}$ mice, $Pld2^{-/-}$ platelets showed intact integrin activation. Since PLDs have been proposed as regulators of endocytosis, exocytosis and vesicle trafficking, it was speculated that PLD might be essential for platelet degranulation. In addition, several studies linked PLD activity to platelet aggregation and secretion without being able to discriminate between the contributions of the two isoforms. As PLD1 deficiency had no impact on platelet aggregation and secretion, it was postulated that PLD2 is required for these processes [8]. This notion was supported by various studies showing that the two PLD isoforms are distinctly regulated and localized [65, 87]. However, neither aggregation nor α- and dense-granule release was affected by the absence of PLD2 (Figure 3-4). This observation stands in stark contrast to a recent publication by Elvers *et al.* suggesting PLD2 to be a negative regulator of platelet degranulation. The authors found enhanced aggregation and degranulation of wildtype and $Pld1^{-/-}$ platelets upon FIPI treatment proposing a PLD2 mediated inhibition [188]. However, in that study, the authors used a very high concentration of FIPI which not only blocks both PLD isoforms, but probably also has additional off-target effects. This is critical in that particular case since the FIPI concentration was titrated until effects on platelet degranulation (not on PLD activity) could be observed. Consequently, the inhibitor concentration used by Elvers *et al.* was 100-times higher than that necessary to abrogate PLD activity [189], suggesting that this may not have been the optimal

approach to study PLD function. In addition, they suggest a completely opposite function for PLD than previously proposed by using ethanol to abrogate PLD activity. Even though data obtained using ethanol need to be carefully re-evaluated it is quite unlikely to identify opposing functions using FIPI. For example, a report by Su *et al.* showed comprehensively that several biological processes blocked by alcohol were not affected by FIPI treatment and suggested additional inhibitory side-effects of ethanol. However, other processes, such as cell spreading and chemotaxis which had been suggested to be PLD mediated, were blocked by FIPI and ethanol treatment similarly [158, 189].

Comparable to the results obtained in *Pld1*^{-/-} platelets and in contrast to previous suggestions proposing PLD as mediator in outside-in signaling, integrin signaling dependent spreading and clot retraction was not affected by the lack of PLD2. PLD2 mediated cytoskeletal reorganization in cell spreading, cell migration or phagocytosis has been demonstrated amongst others in Cos-7 and CHO cell *in vitro* and in neutrophils *in vivo* [157, 189]. Again, these discrepancies might be ascribed to differences in functional compensation of PLD2 deficiency by PLD1 or other PA-generating enzymes in different cell types. In addition, differences in expression, regulation and localization of PLD in different cellular settings are very likely.

Ex vivo blood perfusion assays showed that PLD2 is neither essential for stable thrombus formation on collagen nor for firm platelet adhesion on vWF (Figure 3-5). Previously, our laboratory demonstrated that PLD1 is of importance for integrin activation downstream of GPIb-vWF interaction at high shear rates [8]. This defect was accompanied by defective phosphatidylserine exposure during collagen induced thrombus formation [8]. Neither GPIb mediated integrin activation, nor procoagulant activity was hampered in *Pld2*^{-/-} platelets, establishing PLD1 as the dominant isoform in this respect (Figure 3-5 and data not shown).

Since protein functions might only become obvious in analyses under *in vivo* conditions, that might also involve additional cell types or specific niches, mice constitutively lacking PLD2 were subjected to several experimental *in vivo* models of thrombosis and hemostasis. *In vivo* thrombus formation and tail bleeding times were unaltered in *Pld2*^{-/-} mice demonstrating the dispensability of PLD2 in these processes (Figure 3-8, 3-9). Taking into account that *Pld2*^{-/-} platelets exhibited no defects in the standard *in vitro* assays and that arterial thrombi in these settings are mainly composed of platelets, these results were not surprising. The development of stroke, however, has recently been proposed to be a thrombo-inflammatory pathology involving the thrombotic activity of platelets and a strong immune cell response. Platelet adhesion receptors, such as GPVI and GPIb, have been proposed to mediate these events, but the exact mechanisms remain elusive [270]. It has been postulated that the receptors link thrombotic activity to inflammation e.g. by inducing secretion of immune modulators from platelets or by facilitating platelet-immune cell interactions [271-273]. It is tempting to speculate that PLD2 might play a role in these mechanisms. Furthermore, PLD2 is broadly expressed in

immune cells, but the role of the enzyme in the thrombo-inflammatory process of ischemic stroke has been unclear. However, the results in *Pld2$^{-/-}$* mice in an experimental model of ischemic stroke provide evidence that neither platelet nor immune cell PLD2 is involved in the development of infarct after focal cerebral ischemia (Figure 3-10).

Taken together, our results show that PLD2 was of minor relevance for platelet function and *in vivo* thrombus formation, at least under the experimental conditions used in this study. It is conceivable that the lack of PLD2 might fully be compensated by PLD1. In order to investigate redundant functions of the two PLD isoforms, *Pld1$^{-/-}$/Pld2$^{-/-}$* mice were generated. Data obtained with these mice are discussed in section 4.2.

Even though PLD2 was dispensable for platelet function in our experimental settings it is absolutely possible that the presence of PLD2 in platelets becomes crucial under specific physiological or pathophysiological conditions involving additional cell types. These could, however, not be established with the tools used in this thesis and remain to be elucidated.

4.2 Functional redundancy of PLD1 and PLD2 in α-granule release and pathological thrombus formation

The herein presented data demonstrates that the combined deficiency of PLD1 and PLD2 resulted in a selective defect in α-granule secretion in response to submaximal thrombin stimulation and thus protection in a model of arterial thrombosis which makes PLDs attractive targets for safe antithrombotic therapy (Figure 4-1).

The double deficient PLD mice provided a valuable tool for the identification of redundant roles of the PLD enzymes. The viability of the PLD single deficient mice and the fact that PLD had been associated with elementary developmental functions led to the assumption that the absence of one PLD isoform can be compensated by the other (as discussed in section 4.1) [8, 28, 151]. However, this study, which is the first report on mice lacking both PLD isoforms, shows that these animals do not display any obvious defects demonstrating that PLD is not required for normal development [125]. Nevertheless, it is conceivable that the PLD derived lipid messenger PA might be generated by other mechanisms. This notion is strengthened by a report of Pettitt *et al.* demonstrating that butanol mediated inhibition of PLD did not alter the overall amount and molecular species composition of PA [274]. PA production can occur through different pathways. While PLD can hydrolyse phospholipids and DAG kinase phosphorylates DAG, *de novo* formation of PA is facilitated by the acylation of glycerol 3-phosphate or dihydroxyacetone phosphate [275, 276]. The distinctly generated PAs harbor different fatty acid compositions and are, thus, suggested to exert distinct functions. PA derived from DAG kinase or PLD are thought to be relevant for signaling, while the *de novo* generated

PAs are supposed to be crucial as intermediates for membrane lipid synthesis. Their specific contribution, is, however, still under investigation [276]. Despite the different functions of the specific PA species, redundancies of PA generating enzymes is possible and might account for the surprising observation on the viability of $Pld1^{-/-}/Pld2^{-/-}$ mice.

Analyses of platelet function in $Pld1^{-/-}/Pld2^{-/-}$ mice revealed a defect in α-granule release downstream of sub-maximal stimulation with thrombin, which was not observed in either single knockout platelet population (Figure 3-4, 3-13). Previous correlation studies already linked PLD activity to secretion and secretory vesicles in different cell types, including platelets [28, 106, 170]. These did, however, propose PLD to regulate lysosomal and dense granule secretion. Our measurements of ATP secretion from platelet dense granules excluded a critical role of PLD in this process (Figure 3-13). Furthermore, the observation of reduced secretion in PLD-deficient platelets contradicts a recently proposed model, which suggested that PLD2 is a negative regulator of platelet degranulation [188]. As discussed in section 4.1 this might be due to the use of too high inhibitor concentrations exerting off-target effects.

The finding of the specific α-granule secretion defect in $Pld1^{-/-}/Pld2^{-/-}$ platelets downstream of PAR-4 receptor stimulation might have complex reasons. In general, granule secretion and biogenesis is highly dependent on PKC [14] and PLD and PKC regulate each other via a positive feedback loop [277]. Mice lacking PKCα show defective α-granule release, while dense granules are absent [258] demonstrating that one PKC isoform has differential effects on the biogenesis and release of the major granule subtypes. Thus, one could speculate that the selective α-granule defect observed in platelets lacking PLD results from differential regulation of PKC isoforms. Concerning the regulatory mechanism how PLD drives granule release, one possible model might be that PLD, or its product PA, regulates α-granule cargo proteins and thereby the final steps of vesicle membrane fusion. It has been demonstrated that the *N-ethylmaleimide-sensitive fusion protein attachment protein receptors* (SNARE) syntaxin 4 and VAMP-8 are crucial for α-granule secretion [278, 279]. *In vitro* studies with syntaxin 4 vesicles demonstrated that addition of PA enhances the rate of fusion [129]. Via this mechanism PLD might promote the secretion of platelet α-granules. The idea that PLD is rather involved in the secretion process but not in granule formation or localization is supported by the unaltered granule morphology and abundance in $Pld1^{-/-}/Pld2^{-/-}$ platelets as demonstrated by TEM analysis (Figure 3-14).

Despite the fact that PLD activity was detected upon stimulation of GPCR and ITAM coupled receptors (Figure 3-1, 3-11), the degranulation defect was only observed upon platelet stimulation with intermediate concentrations of PAR-4 receptor triggering agonists. Platelet stimulation commonly converges in the activation of PLCs, namely PLCβ or γ, which are acting downstream of GPCRs or ITAM-receptors, respectively. These two isoforms have the same function: The hydrolysis of PIP_2 to IP_3 and DAG (Figure 1-3). However, there is a growing body

of evidence suggesting slight differences downstream of the two PLC isoforms which might explain the observed thrombin-specific degranulation defect of $Pld1^{-/-}/Pld2^{-/-}$ platelets. First, DAG production via PLCs and PLDs might have distinct kinetic patterns upon the stimulation with the different agonists. DAG formation plays an important role for sustained $\alpha IIb\beta 3$ activation and platelet degranulation. Holinstat *et al.* proposed a model suggesting that PLD activity contributes to sustained DAG production via the generation of PA. This is supposed to be facilitated by the initial PLC mediated DAG production which leads to an increase in PIP_2, a cofactor of PLD and to the activation of PKC [280]. Until now, this biphasic DAG production was only shown upon thrombin stimulation [181, 182]. Together with the finding that delayed DAG accumulation happens faster upon thrombin stimulation than upon collagen stimulation, this data supports the hypothesis that PAR-4 and ITAM signaling lead to a differential regulation of DAG production [281]. Thus, PAR-4 signaling might be more dependent on PLD mediated DAG production than ITAM signaling. Secondly, PLCβ induces a rapid and short Ca^{2+} release, whereas PLCγ activation was shown to lead to a later and sustained Ca^{2+} influx [282]. Therefore, the different Ca^{2+} kinetics might also influence the dependency of both signaling pathways on PLD. Nevertheless, stimulation with other agonists or higher thrombin doses resulted in degranulation of $Pld1^{-/-}/Pld2^{-/-}$ platelets comparable to that observed in wildtype platelets (Figure 3-13), demonstrating that PLD is not strictly required for platelet secretion. Further studies will be required to reveal the exact mechanism how PLD contributes to platelet degranulation.

In the initial report on $Pld1^{-/-}$ mice [8] we observed a slight defect in integrin activation upon submaximal platelet activation with thrombin/PAR4-activating peptide or CRP. It was hypothesized that PLD1 might be required for talin-binding to the β-unit of $\alpha IIb\beta 3$-integrins thereby facilitating its activation. This mechanism had been previously proposed by Powner *et al.* in neutrophils where PLD1 was involved in the activation of the integrin MAC-1. The authors demonstrated that PLD derived PA is essential for PIP5K mediated PIP_2 production that enhances the recruitment of talin to β1 and β2 integrins and thus, their activation [283].

In the present study, we directly compared the $\alpha IIb\beta 3$-integrin inside-out signaling of wildtype, $Pld1^{-/-}$ and $Pld1^{-/-}/Pld2^{-/-}$ mice and did not detect any reduction in CRP-responses (Figure 3-15), while the defect downstream of thrombin persisted. Of note, in contrast to the initial report, for which we used mice of mixed background (Sv/129 x C57BL/6), for this study mice of a pure background (C57BL/6) were used. The different genetic background of the mice might affect GPVI responses to CRP, e.g. by slight alterations of GPVI surface expression levels. Previously, it has been demonstrated that especially CRP-responses depend to a great extent on GPVI expression levels [284], providing a possible explanation for this discrepancy between this study and our previous report [8]. Alternatively, GPVI signaling could be influenced by modifier genes which differ between the two mouse strains. Such a strong impact of modifiers

was reported to be the reason for variable *in vivo* results of *Gp6$^{-/-}$* mice [285]. The procoagulant activity of platelets is highly dependent on αIIbβ3 and GPIb activation [286]. Since integrin responses in *Pld1$^{-/-}$* platelets on mixed background were found to be more affected than in *Pld1$^{-/-}$/Pld2$^{-/-}$* on pure background platelets, the different background might also account for the defects observed in the procoagulant activities (Figure 3-19) [8]. Nevertheless, the adhesive defects of *Pld1$^{-/-}$* platelets to vWF, which was assessed by perfusion assays, were also found in PLD double deficient mice (data not shown) [8]. In both cases, platelets were able to form initial adhesion on vWF but stable adhesion or incorporation of platelets in the upper layers of thrombi on collagen was defective. This was seen especially at high shear rates, where platelet-platelet interactions are no longer dependent on integrin inside-out but rather on shear induced biomechanical signaling cascades stabilizing αIIbβ3 integrin adhesion contacts [8, 287]. Shear specific enhancement of platelet adhesion can occur via two distinct pathways: One pathway is initiated by GPIb-vWF interactions and leads to the upregulation of the binding affinity of αIIbβ3 integrins [288]. The exact underlying mechanism is still elusive, but responses such as activation of PI3K or elevation of Ca^{2+} have been proposed to be involved [289]. The other pathway involves the biomechanical adhesive function of αIIbβ3 integrins that increases the lifetime of platelet-platelet interactions at high shear. A recent publication by Hughan *et al.* identified a role of Dok-2 in regulating these shear induced adhesive functions [290]. The signaling modulator *adhesion- and degranulation-promoting adapter protein* (ADAP) was identified as a positive regulator of biomechanical outside-in signaling of αIIbβ3 integrins [291]. Besides the decreased adhesive capacity of αIIbβ3 integrins downstream of the GPIb-vWF interaction, *Pld1$^{-/-}$* and *Pld1$^{-/-}$/Pld2$^{-/-}$* platelets might also have defects in the shear induced adhesion of αIIbβ3 integrins. However, this remains to be elucidated.

The combined defects of *Pld1$^{-/-}$/Pld2$^{-/-}$* mice in GPIb mediated integrin activation and α-degranulation resulted in the protection from experimentally induced thrombosis and stroke. The α-degranulation defect of *Pld1$^{-/-}$/Pld2$^{-/-}$* mice did not lead to further decrease in infarct sizes in the tMCAO model indicating that Pld1 dependent GPIb signaling and integrin activation are of higher relevance in this pathological setting (Figure 3-22). However, *Pld1$^{-/-}$/Pld2$^{-/-}$* mice showed decreased thrombus formation in experimentally induced thrombosis in micro- and macrovascular beds, whereas *Pld1$^{-/-}$* deficiency only protected from thrombosis in larger vessels (Figure 3-20, 3-21). These findings indicate that the secretion defect, and not the GPIb dependent integrin activation defect, is the major reason for the antithrombotic effects observed in double deficient mice upon chemical injury of mesenteric arterioles. *In vivo* models used in this study were performed in distinct vascular beds and by inducing different types of injury with variable severity. All models converged, however, in the formation of platelet-rich occlusive thrombi. The models vary in their dependence on different cellular and molecular interactions during thrombus initiation and propagation. For example, under high shear, which

is present in the microvasculature such as mesenteric arterioles, the surface intensities of vWF and fibrinogen at the thrombogenic site are important in propagating stable aggregate formation. In addition, the requirement of the adhesive property of GPIb increases with the shear rate [287]. Thus, it appears likely that the reduced vWF secretion, combined with decreased GPIb signaling, at high shear rates might be the reason for the selective protection of *Pld1⁻ᐟ⁻/Pld2⁻ᐟ⁻* mice in microvascular thrombosis.

Together with the previously published data on *Pld1⁻ᐟ⁻* mice, the observation that mice lacking both PLD isoforms display reduced pathological thrombosis but no obvious hemostatic defects indicates that PLD may represent a novel target molecule for antithrombotic therapy. In accordance with these findings, the blockade of the GPIbα-vWF interaction, which had been shown to be upstream of PLD1, was also efficient in diminishing lesion progression after experimentally induced stroke without provoking intracranial bleedings [219, 292]. Furthermore, it has been proposed recently by our laboratory, that interfering with platelet granule release might also be effective, yet safe, in preventing and limiting infarct progression in acute ischemic stroke [293, 294]. Besides these findings, the overall normal appearance of the double deficient mice make PLD interesting as target for antithrombotic therapy. Blockade of such "safe" target molecules would be of particular advantage since the risk of intracranial hemorrhages is the major limitation of current antithrombotic treatment.
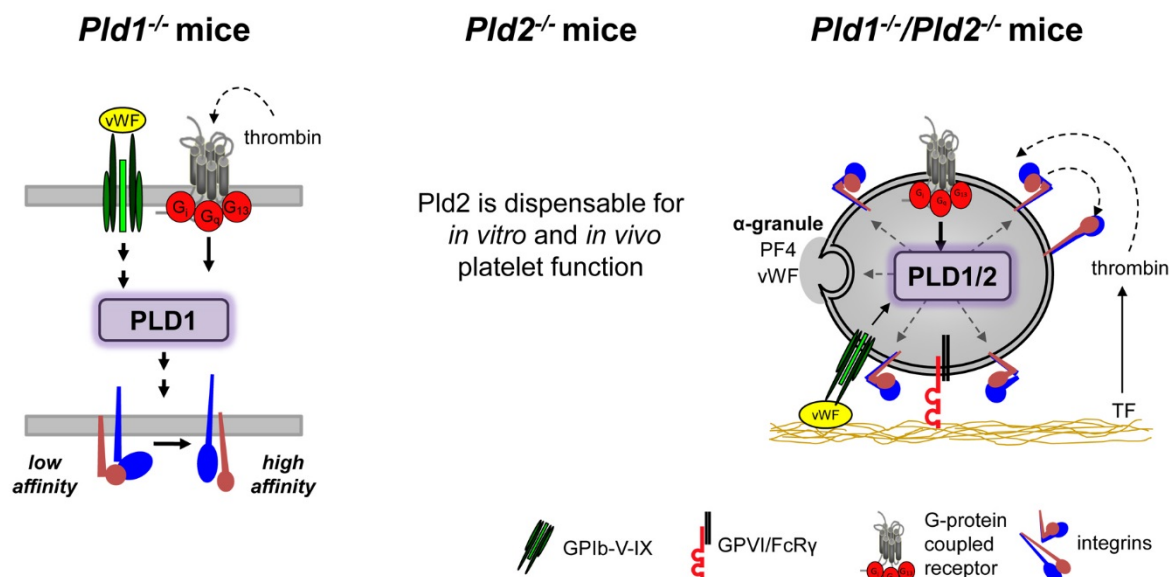
Figure 4-1: Functions of *Phospholipase* (PL)D1 and PLD2 in murine platelets. PLD1 mediates αIIbβ3 integrin activation upon stimulation of *glycoprotein* (GP)Ib by interaction with *von-Willebrand Factor* (vWF) or downstream of thrombin triggered GPCR stimulation. While *Pld2⁻ᐟ⁻* mice demonstrated no function of PLD2 in *in vitro* and *in vivo* standard platelet assays, analyses of PLD double deficient mice revealed redundant functions of PLD1 and PLD2 in platelet α-degranulation. Among other proteins α-granules contain vWF and *platelet factor* (PF)4. TF indicates *tissue factor*.

In conclusion, the data shows that PLD1 and PLD2 have a redundant function in platelet α-granule secretion downstream of protease-activated receptors. Considering that current PLD inhibitors are isoform-selective at best, but definitively not specific, the observation that mice lacking both PLD isoforms display no obvious hemostatic defect is of significant interest. Thus, modulating with PLD activity and thereby dampening GPIb-triggered integrin activation [8] and platelet degranulation might be a promising and safe strategy for antithrombotic therapy (Figure 4-1).

4.3 Pharmacological inhibition of PLD protects mice from thrombus formation and stroke without impairing hemostasis

The findings on *Pld1$^{-/-}$/Pld2$^{-/-}$* mice suggested that PLD might serve as novel potential target for antithrombotic therapy. In order to analyze whether pharmacological PLD blockade is suitable as a treatment strategy, the characterization of an *in vivo* applicable PLD inhibitor with regard to its antithrombotic potential is of importance. However, up to date *in vivo* evidence in support of this concept has been lacking. Therefore, the efficiency of the well-established PLD inhibitor FIPI in blocking PLD function *in vivo* and its influence on thrombosis, hemostasis and thrombo-inflammatory events were analyzed.

FIPI protected mice from thrombotic events and ischemic stroke without any detectable side effects on hemostasis (section 3.3). These findings are in agreement with the data that was obtained in *Pld1$^{-/-}$/Pld2$^{-/-}$* mice [8, 125] and with a previous report showing that pharmacological PLD inhibition *in vivo* phenocopies genetic *Pld1* ablation in a mouse cancer model. These results suggest potential employment of FIPI as a cancer therapeutic [154]. Our *in vitro* analyses demonstrated that FIPI treatment specifically inhibits PLD-mediated integrin activation and α-granule release without affecting platelet surface glycoprotein abundance or aggregation ability (Figure 3-25, 3-27; Table 3-3). In addition, *in vivo* analysis of FIPI treated mice revealed a comparable protective effect in the experimental thrombosis and stroke models as observed in PLD double deficient mice, but did not show additive effects of FIPI treatment in mice lacking both PLD isoforms (Figure 3-29, 3-30). This finding strongly suggests a very high specificity of the inhibitor (section 3.3) and is in line with reports from several other groups using FIPI in different settings that also describe the absence of any off-target effects [154, 157, 158, 189, 295].

Comparable to the observations in *Pld1$^{-/-}$/Pld2$^{-/-}$* mice, the antithrombotic effect upon FIPI treatment was evident upon chemical injury of mesenteric arterioles. This implies that the inhibitor sufficiently blocks both PLD isoforms since single knockout mice were not protected in this model (Figure 3-20) [8]. Again, in these settings the secretion defect, rather than the GPIb dependent integrin activation defect seemed to be causative for the antithrombotic effect

of FIPI-treatment (Figure 3-29). However, this was not limited to smaller vessels since the protective antithrombotic effect was also observed upon injury of carotid arteries (Figure 3-28). This is in line with the reports on *Pld1*^{-/-} [8] and *Pld1*^{-/-}*/Pld2*^{-/-} mice (section 3.2) [125].

Furthermore, these findings demonstrate that prophylactic FIPI treatment markedly protects mice from infarct progression in the setting of acute stroke. As discussed in section 4.2, the development of effective and safe treatments for acute stroke and secondary stroke prevention is of particular interest since conventional therapies with platelet aggregation inhibitors are associated with an increased bleeding risk. For example, platelet inhibition, e.g. by blocking GPIIb/IIIa, protects from arterial thrombosis but also leads to increased intracerebral hemorrhages in the setting of acute stroke [219, 238, 239]. The paucity of effective therapy makes stroke one of the leading causes of death and disability worldwide [3, 4]. Notably, FIPI treatment had no obvious effect on intracranial hemostasis proposing PLD inhibition as a promising strategy to inhibit thrombotic activity and to prevent secondary infarction [219, 265]. This is in line with previous findings of our group implying GPIb blockade or inhibition of platelet degranulation as effective and safe approaches to diminish lesion progression in ischemic brain tissue [219, 293, 294].

However, therapeutic treatment with FIPI, even at high doses, resulted only in a moderate protection in ischemic stroke. One may speculate that this was due to limited bioavailability of FIPI and, potentially, an insufficient rate of drug delivery from the i.p injection site. Further studies with optimized PLD inhibitors or improved drug delivery methods are required to finally determine the efficacy of PLD inhibition in the setting of acute stroke. Analogs of FIPI, that are also PLD1/PLD2 dual inhibitors, are currently being developed and may eventually provide more effective options for PLD inhibition *in vivo* [296]. A particular challenge concerning this is the ubiquitous expression of PLD within the body. Delivery strategies targeting specific cell types, e.g. by addition of targeting tags or lipid moieties, would therefore be useful. Nevertheless, prophylactic blockade of PLD activity may help to decrease the risk of vessel re-occlusion after thrombolytic therapy in secondary stroke prevention.

In summary, our study provides a proof-of-principle that blockade of PLD1 or both isoforms by using small molecule inhibitors constitutes a potent and safe antithrombotic approach and suggests that FIPI could serve as a good lead structure for drug optimization.

4.4 Antithrombotic targets

The above discussed parts of this thesis demonstrate that PLD may serve as a potential antithrombotic target as the genetic and pharmacological blockade of the enzyme reduces pathological thrombus formation without affecting hemostasis. This is underscored by the fact that PLD deficiency only led to a subtle phenotype in the standard platelet and thrombosis

assays. Further, genetic ablation and long term pharmacological blockade of the enzyme showed no obvious side-effects demonstrating that the enzyme does not play a crucial role in development and normal physiology. Thus, PLD is not as important in physiological settings as it had been postulated previously, which is, however, advantageous in regard to its use as safe antithrombotic target. Our group investigates the complex signaling network controlling platelet function in order to identify novel targets for antithrombotic therapy. This includes proteins involved in distinct steps of thrombus formation such as platelet -adhesion, -signaling, and -granule release as well as coagulation pathways (Figure 4-2). In addition to the profound study on the role of PLD in thrombus formation, my work during the thesis also included the *in vivo* analysis of pharmacologically treated or genetically modified mice lacking proteins which are important for these processes.

Regarding platelet granule release NBEAL2 deficient mice were investigated. The *Gray platelet syndrome* (GPS) is a rare inherited bleeding disorder that is accompanied by lack of platelet α-granules and that has been linked to mutations in the *neurobeachin-like* (*Nbeal)2* gene. Mice deficient for NBEAL2 displayed the characteristics of human GPS. Subjecting these mice to our *in vivo* thrombosis models demonstrated the critical contribution of α-granule components in the setting of pathological thrombosis. However, NBEAL2 deficiency also led to indefinite bleeding of mice in the tail bleeding time model, excluding this protein as antithrombotic target [293].

Furthermore, I was involved in studies on mice with genetic deficiencies in platelet signaling molecules. (hem)ITAM signaling is one of two major pathways leading to platelet activation and aggregation. Its significance in *in vivo* thrombus formation has been demonstrated by several groups, including ours. Our studies and other on mice deficient in GPVI and CLEC-2 revealed unexpected functional redundancy of both (hem)ITAM receptors not only in thrombosis, but also in hemostasis, which needs to be taken into account when considering GPVI blockade as antithrombotic strategy [297, 298]. In addition, we were able to demonstrate the involvement of the tyrosine kinase Syk, as an effector of the (hem)ITAM receptors, in *in vitro* and *in vivo* platelet function (van Eeuwijk *et al.*, unpublished) [299]. Other studies comprised the importance of the receptor-operated Ca^{2+} channel TRPC6 in *in vivo* thrombus formation and hemostasis. These analyses excluded TRPC6 as antithrombotic target as it did not contribute to thrombus development [300]. Analysis of *Orai$^{-/-}$/Trpc6$^{-/-}$* mice also excluded redundant functions of the two Ca^{2+} channels in this aspect [184].

With regard to coagulation pathways, the contribution of the extrinsic coagulation pathway modulator *Factor VII activating protease* (FSAP) to pathological thrombus formation was demonstrated by analyzing *Fsap$^{-/-}$* mice in collaboration with the group of Prof. Dr. Kanse Sandip (Subramaniam *et al.*, submitted for publication)*.
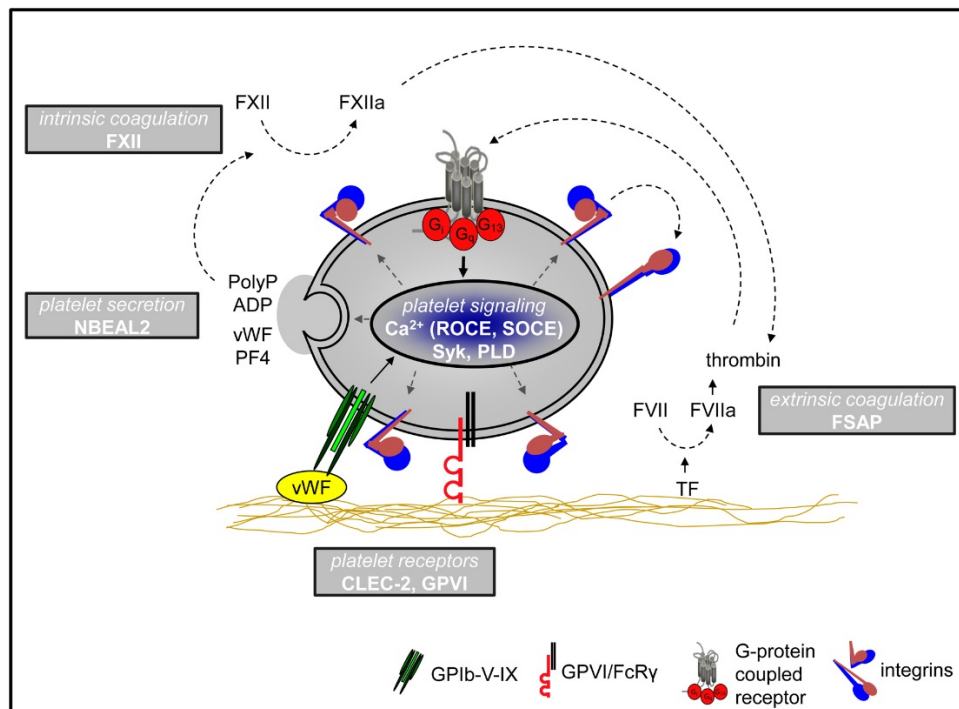
Figure 4-2: Molecules involved in platelet function and blood coagulation: potential antithrombotic targets. Platelet signaling via the platelet receptors *glycoprotein* (GP)VI and *C-type lectin-like receptor* (CLEC)2 involves the activation of Syk and *phospholipase* (PL)D as well as the increase of *intracellular calcium* (Ca^{2+}) via *store operated Ca^{2+} entry* (SOCE) and *receptor operated Ca^{2+} entry* (ROCE). Platelet activation involves secretion of dense and α-granules. For the biogenesis of the latter *Neurobeachin like* (NBEAL)2 is of importance. Strong platelet activation also leads to the activation of the coagulation cascade which is comprised of two pathways. These are the intrinsic pathway which is initiated by the activation of the *coagulation factor* (F)XII and the extrinsic pathway triggered by *tissue factor* (TF). FSAP, *factor seven activating protease*; vWF, *von Willebrand factor*; PF, *platelet factor*.

The abovementioned findings demonstrate that experimental mouse models give defined answers to questions concerning the *in vivo* role of a specific molecule in thrombus formation. Thus, studies on mice are indispensable tools in order to advance the development of clinically relevant antithrombotic treatment strategies. The blockade of the initiator of the extrinsic coagulation pathway FXII, for example, has already been shown to be beneficial in terms of pathological thrombus formation without exerting bleeding tendencies and, thus, its pharmacological inhibition has been proposed as antithrombotic strategy [301-303]. In collaboration with CSL Behring we screened the potency of recombinant human FXII blocking antibodies to dampen *in vivo* thrombus formation (unpublished data). One of these antibodies has recently been shown to be effective in reducing thrombotic activity in extracorporeal circulation without increasing bleeding risk underscoring, that mouse model based conclusions are the basis for the development of safe anticoagulation for clinical application [304].

The obtained findings demonstrate that, besides PLD, diverse molecules are distinctly regulated during different steps of thrombus growth. Certain molecules are more important for the regulation of thrombosis than for hemostasis or vice versa suggesting that these processes

are not necessarily linked. In addition, the findings clearly demonstrate the importance of murine models in cardiovascular research for the elucidation of the regulation of key steps of thrombosis. Among mammalian models mice are most amenable to genetic engineering, they are fertile, have a short life cycle and are easy to keep. Since several *in vivo* thrombosis models and experimental models of ischemic stroke are established in mice, the mouse provides an excellent tool to study thrombosis, hemostasis and thrombo-inflammatory events, as well as the underlying complex signaling pathways. However, it has to be considered that there are differences in the metabolism and physiology of the different mammalian species. Therefore, data obtained in murine disease models cannot be extrapolated directly to human patients. However, analyses in mice are a crucial first step for the identification of new and safe antithrombotic targets in humans.

4.5 PLD activity and regulation in blood platelets

Our findings on the role of PLD in thrombus formation indicated that PLD inhibition might be a feasible therapeutic strategy. Thus, understanding how PLD activity is regulated might reveal novel pharmacological targets. The regulation of PLD activity has been addressed in a number of reports (see 1.3.2) [87]. However, these studies used overexpression of PLD, potentially unspecific inhibitors or *in vitro* correlation studies. Thus, genetically modified mice lacking potential modulators of PLD activity provide a valuable tool to address this question.

The herein presented data suggests that PLD activity is tightly controlled, most probably by PLC enzymes, during initial platelet activation, while integrin outside-in signaling does not affect the enzyme activity.

PLD activity in platelets in response to classical agonist

PLD activation was found in response to common platelet agonists such as CRP, thrombin and U46619, while ADP did not interfere with PLD activity (Figure 3-33). In contrast, lipase activity was diminished in the presence of the ADP scavenger apyrase suggesting that secreted ADP amplifies agonist induced PLD activation (Figure 3-34). Most probably this is an indirect effect through enhancement of the general platelet response including an upregulation of PLD activators. Figure 3-33 revealed that stimulation of platelets with the CLEC-2 stimulating toxin rhodocytin induces PLD activity, albeit to a smaller extent than observed in CRP treated platelets. This discrepancy might be attributed to different Src family kinase members active in response to stimulation of CLEC-2 and GPVI [12]. These might, in turn, also influence the phosphorylation and activation of PLD, as tyrosine kinases have been demonstrated to modulate PLD activity [104-106].

Taken together, the prominent PLD activity downstream of the common platelet agonists is in accordance with previous reports and demonstrates the regulation of PLD within various platelet signaling pathways [166, 168, 170].

Even though PLD has been shown to regulate integrin activation downstream of GPIb, only a minor increase in PLD activity of platelets treated with the GPIb clustering antibody 92H12 was detected (Figure 3-33). However, the PLD assay does not provide suitable conditions for the analysis of GPIb signaling. Incubation of platelets with the 92H12 antibody led to agglutination, but it is well established that GPIb activation can only occur properly under shear stress, which cannot be applied during PLD activity measurements [247]. Further, it has not been studied, whether 92H12 mediated agglutination is dependent on GPIb signaling.

PLD activity in platelet ITAM signaling

In platelets lacking proteins involved in ITAM signaling, such as Grb2, PI3Kβ or Rac1, the reduced platelet reactivity upon stimulation of ITAM signaling, correlated with a decrease in PLD activity (Figure 3-35, 3-37A). Grb2 and PI3Kβ deficient platelets show reduced PLCγ activation, while lack of Rac1 results in abolished PLCγ activity. Thus, the observed defects are probably due to the decreased activity of PLCγ2 in these knockout mice, leading to defective activation of the PLD regulators PKC and Ca^{2+}. This hypothesis is strengthened by our findings on mice treated with the PLC-inhibitor U-73122, which show ablated PLD activity in response to ITAM stimulation (Figure 3-40).

Of note, PLD activity downstream of GPCRs was not affected by the lack of Grb2 or PI3Kβ. Therefore, previously proposed regulations by interactions of PLD with Grb2 and PIP_3, the product of PI3K, if present in platelets at all, are probably not essential for general PLD activity [47, 305]. Nevertheless, these interactions might be important in lipase-independent functions of the enzyme.

Taken together, our PLD activity measurements in mice lacking molecules involved in ITAM signaling pathways indicate that PLCγ2 is an important regulator of the enzyme activity.

G-protein mediated PLD activity

For GPCR mediated PLD activity, knockout mice lacking molecules of G-protein mediated signaling have been analysed (Figure 4-3). Regarding G_i mediated signaling, it was demonstrated that PLD mediates the activation of mTOR in the PI3K/Akt pathway [142, 306]. Lack of PI3Kβ did, however, not influence GPCR triggered PLD activity demonstrating that PLD activity is independent of G_i signaling (Figure 3-35B). This is in line with the absence of PLD activity in response to ADP in wildtype platelets and to GPCR agonists in $G_{13}^{-/-}/G_q^{-/-}$ platelets (Figure 3-36, 3-33). However, addressing the effect of G_i ablation on PLD activity using knockout mice is required to prove this hypothesis.

In contrast to G_i, G_{13} and G_q signaling pathways are involved in PLD regulation. While the combined deficiency of G_{13} and G_q coupled signaling led to abolished PLD activity in response to thrombin and U46619, G_{13} single knockout platelets exhibited only slightly reduced PLD activity levels upon stimulation with thrombin. This finding indicates that mainly G_q mediated signaling contributes to PLD activation in thrombin triggered pathways (Figure 3-36A). G_{13} specifically signals via RhoA, while G_q additionally transmits signals through activation of PKC [22]. Thus, PLD responses might be compensated for by G_q signaling in G_{13} deficient platelets. However, to gain insights into possible redundant or non-redundant functions of the G-proteins, platelets of G_q single knockout mice need to be analyzed.
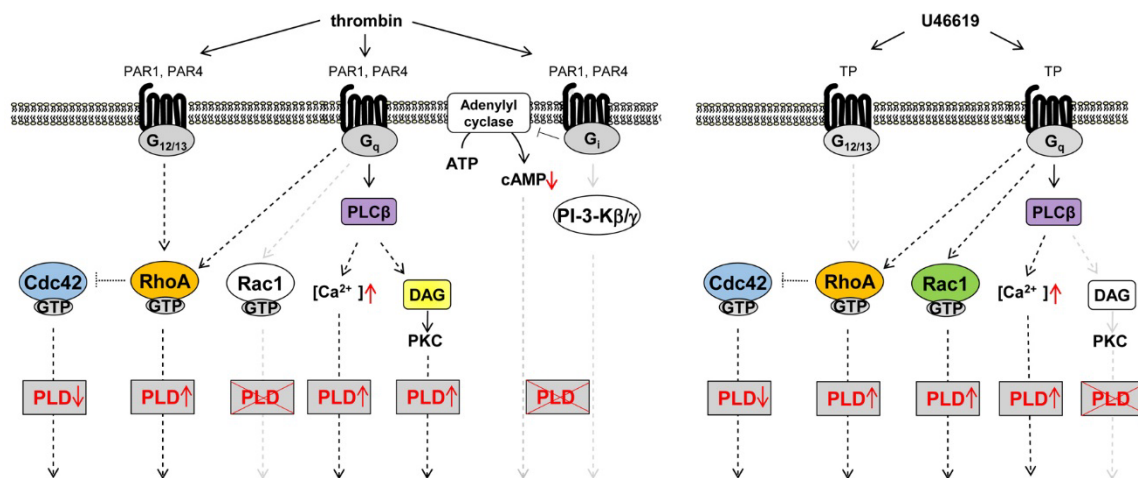
Figure 4-3: PLD activation induced by G-protein coupled receptor (GPCR) stimulation in platelets. Upon platelet stimulation with the GPCR stimulating agonists thrombin and U46619 phospholipase (PL)D is distinctly regulated. DAG, *diacyl glycerol*; PAR, *protease-activated receptor*; TP*, TxA₂ receptor*; ATP*, adenosine triphosphate;* cAMP*, cyclic adenosine monophosphate;* PI3K*, phosphoinositide-3-kinase.*

Role of GTPases in the regulation of PLD activity

Platelets lacking specific GTPases that are relevant for transducing signals from G-proteins to PLD, helped to elucidate GPCR mediated PLD regulation. Considering that RhoA can be activated via G_{13}, a similar reduction in PLD activity would be expected in G_{13} and RhoA deficient platelets. However, PLD activity levels were more strongly reduced in RhoA deficient platelets than in $G_{13}^{-/-}$ platelets upon stimulation with thrombin as well as U46619 which indicates the relevance of G_q mediated RhoA activation under these conditions. Interestingly, U46619 triggered PLD activity was almost abolished in $RhoA^{-/-}$ platelets, whereas it was normal in G_{13} knockout platelets suggesting U46619 to induce PLD activation mainly via G_q and RhoA (Figure 3-36, 3-37B, 4-3). Since PKC inhibitor treated platelets show normal PLD activity in response to U46619, the G_q-RhoA-PLD pathway appears to be independent of PKC (Figure 3-40B). Interestingly, U46619 mediated PLD activity was completely abolished in platelets treated with a PLC inhibitor (Figure 3-40A). Based on these findings one might hypothesize

that a PKC independent pathway involving RhoA and PLC exists downstream of G_q. This hypothesis is strengthened by reports demonstrating direct activation of PLCε and δ by RhoA [307, 308]. Nevertheless, it always has to be considered that the roles of PLCs and PKCs on PLD activity have been analyzed using inhibitors which might exert off-target effects.

Rac1, another GTPase downstream of G_q proteins, is not as important as RhoA in GPCR mediated PLD activation, as the isolated loss of Rac1 only led to a PLD activity decrease of ~50% after stimulation with U46619 (Figure 3-37A), whereas thrombin triggered PLD activity was unaffected. This might be explained by the fact that RhoA becomes activated downstream of G_{13} and G_q, while Rac1 is only proposed to be activated downstream of G_q in the GPCR signaling pathways (Figure 4-3) (Dütting *et al.*, unpublished) [22, 309]. However, the data on *RhoA$^{-/-}$/Rac1$^{-/-}$* platelets imply redundant functions of the two GTPases upon platelet stimulation with thrombin. Under these conditions, PLD activity is stronger reduced than in the respective single deficient platelets (Figure 3-38A).

Besides RhoA and Rac1, Cdc42 has been proposed as an activator of PLD [71, 87]. Determination of PLD activity, showed, however, a slightly increased activity in *Cdc42$^{-/-}$* platelets, establishing this molecule rather as an inhibiting modulator (Figure 3-37). This inhibiting effect might not be direct, as an increased degranulation and ADP/ATP content of *Cdc42$^{-/-}$* platelets might indirectly act on PLD activity [252]. The combined deficiency in RhoA and Cdc42 reversed the defective PLD activation observed in *RhoA$^{-/-}$* platelets indicating counteracting functions of RhoA on Cdc42 (Figure 3-38A). In the absence of RhoA, Cdc42 would not be inhibited and can, therefore, block PLD activity. Thus, PLD becomes activated if both molecules are missing. This hypothesis is strengthened by a report of Cox *et al.* proposing several cross-talk interactions between Rac1, RhoA and Cdc42 during integrin mediated cell migration [310].

Taken together, RhoA and Rac1 are activators of PLD activity, as expected, whereas for Cdc42 this could not be confirmed.

Role of PLCs in PLD enzyme regulation

Again, PLD activity strongly correlates with platelet reactivity levels and treatment of platelets with a PLC-inhibitor ablated PLD activity. Therefore, it is conceivable that, again, rather the reduction of PLCβ activity, than the previously proposed protein-protein interactions between GTPases and PLD account for the observed defects.

In summary, our data point to a role of PLCs in PLD enzyme regulation. PLC activation leads to Ca^{2+} influx and PKC activation (Figure 1-3). Concerning the involvement of PKC in PLD regulation, our data excludes essential roles for PKCβ and PKCθ (Figure 3-40C,D). Nevertheless, treatment with the broad spectrum PKC inhibitor Ro-318425 led to a strong reduction of PLD activity (Figure 3-40A). As PKCα has been demonstrated to be the most

crucial isoform during platelet stimulation, one may speculate that inhibition of this isoform accounts for the reduced PLD activity in the presence of the PKC inhibitor [14]. However, to exclude off-target effects of the inhibitor and to shed light on potential redundant functions of the different isoforms, PLD activity measurements in platelets from mice lacking PKCα or two PKC isoforms are required.

Furthermore, Ca^{2+} can act synergistically in response to common platelet agonists and an isolated Ca^{2+} increase can activate PLD by itself (Figure 3-41). These findings are in line with the above discussed data implying PLCs as main regulators of PLD activity. PLC inhibition led to a more pronounced reduction of PLD activity upon stimulation with U46619 or CRP than the treatment of platelets with the PKC inhibitor (Figure 3-40). This is probably due to the fact that SOCE is still normal in the presence of the PKC inhibitor, while PLC inhibition diminishes Ca^{2+} influx and blocks PKC activation. Of note, platelets of $Stim1^{-/-}$ and $Orai1^{-/-}$ mice, both exhibiting defective SOCE, displayed normal PLD activity upon stimulation of ITAM and G-protein coupled receptors, while the chelation of extracellular Ca^{2+} by EGTA led to a strong reduction of PLD activity levels (Figure 3-41A, 3-42) [203, 217]. However, $Orai1^{-/-}$ as well as $Stim1^{-/-}$ mice display residual SOCE that might be sufficient to activate PLD [202, 203]. Furthermore, this data fits into the current model in which PLD is tightly regulated during store release and SOCE [184].

In U-73122 treated platelets, residual PLD activity was detectable upon stimulation with thrombin, whereas PLD activity was blocked in the other tested pathways upon PLC inhibition (Figure 3-40). This is conceivable as thrombin triggered PLD activation involves also PLC independent mechanisms e.g. via G_{13} (Figure 4-3). Further, this finding indicates that CRP induced activation of PLD is strongly dependent on PLC and subsequent PKC activation and Ca^{2+} influx. This is in line with the fact that SOCE is more important for CRP triggered induction of platelet signaling pathways, than for thrombin mediated platelet stimulation [202, 203].

The contribution of platelet integrin outside-in signaling to PLD activity is still a matter of debate. While some groups postulated that integrin signaling leads to PLD activation, others reported no effects on the PLD activation status when blocking integrins [168, 185]. In support of the latter, PLD activity levels were normal in platelets with abolished αIIbβ3 integrin activation and signaling. This was demonstrated by using platelets lacking talin1. Loss of talin1 in platelets abrogates integrin activation and outside-in signaling, while other cellular responses such as degranulation and shape change are not affected [209]. In addition, our PLD activity measurements of platelets with defective integrin signaling such as in n-$cofilin^{-/-}$, $Pfn1^{-/-}$ and $Twf2a^{-/-}$ platelets revealed unaltered PLD activation [209, 254] (Stritt et $al.$, unpublished data). These data rule out any regulatory functions of integrin inside-out and outside-in signaling on PLD activation in platelets. Furthermore, neither actin remodeling defects, which are evident

in *n-cofilin*^{-/-}, *Pfn1*^{-/-} and *Twf2a*^{-/-} platelets, nor the proposed interaction of PLD and phosphorylated n-cofilin are of relevance in the regulation of PLD activity.

In summary, the above discussed findings indicate that PLD is tightly regulated during initial platelet activation by PLCs. The exact mechanism involves, however, various molecules in distinct platelet signaling pathways and cannot be defined by our assay. Further, previously proposed regulatory effects of G_i mediated signaling and integrin outside-in signaling seem not to be required for PLD regulation. In addition, direct protein-protein interactions appear to be of minor importance in the analyzed pathways. Some of these conclusions have already been proposed by others and are, thus, not entirely unexpected, but definite evidence has been lacking [65, 87].

The application of the PLD activity assay yields a linear readout that only allows the analysis of upstream modulators of PLD lipase activity. Complex mechanisms including stimulatory or inhibiting feedback loops as well as lipase-independent functions of PLD cannot be addressed by this approach. However, to date, the systematic screening of genetically modified mice as an approach to elucidate aspects of PLD regulation has not been performed and will help to clarify the controversial discussions on the regulatory network underlying PLD activity.

4.6 Concluding remarks and future plans

The herein presented results provide new insights into the contribution of the intracellular signaling enzyme PLD to the complex mechanisms underlying thrombus formation. The current strategy to prevent ischemic cardio- and cerebrovascular diseases includes platelet inhibition, which is, however, often accompanied by increased bleeding risks. Therefore, it is of high interest to identify target proteins that drive pathological thrombus formation without affecting hemostasis. The analysis of genetically modified mice in experimental models of arterial thrombosis and thrombo-inflammatory diseases represents a powerful approach to identify new target structures. Notably, the data discussed here clearly showed that blocking phospolipase D *in vivo* is efficient and safe to prevent pathological thrombosis and might be a suitable approach for future antithrombotic therapy. This is especially based on the functional characterization of the PLD inhibitor FIPI which appears to be an appropriate lead structure for further drug optimization. Finally, the understanding of the complex regulatory network acting on PLD, as well as the PLD mediated processes contributing to thrombus formation are of great value concerning the development of new antithrombotic drugs. For future studies new anti-PLD drugs with improved bioavailability, efficiency and dosage need to be developed and characterized. Regarding the regulation of PLD, further assays with additional knockout mouse strains will be crucial to test conclusions that were drawn from experiments in which inhibitors were used and to elucidate other PLD regulating molecules.
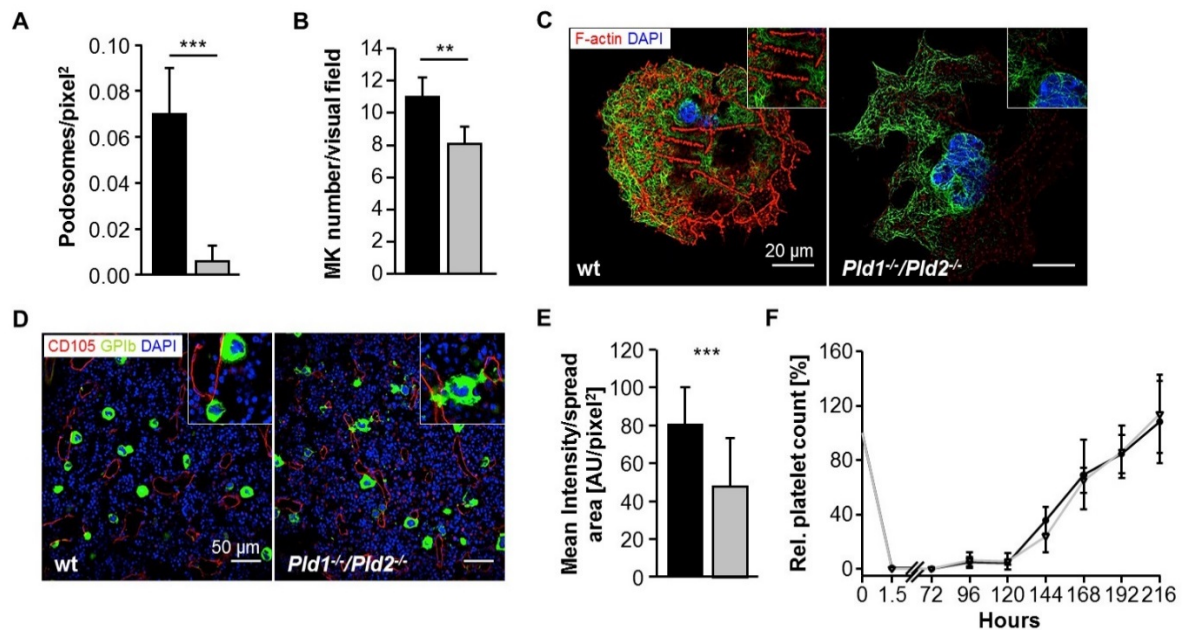
Figure 4-4: Impaired podosome formation and reduced F-actin content in PLD double deficient bone marrow megakaryocytes spread on a collagen I matrix. (A,B,C) Wildtype and *Pld1⁻ᐟ⁻/Pld2⁻ᐟ⁻ bone marrow* (BM) *megakaryocytes* (MKs) were allowed to spread for 180 min on a collagen I-coated (50 µg/ml) surface and number of podosomes (A) and the mean intensity of the F-actin staining (B) of spread wildtype (black bars) and *Pld1⁻ᐟ⁻/Pld2⁻ᐟ⁻* (grey bars) MKs was quantified with the help of ImageJ (NIH) software. Representative images acquired with a TCS SP5 confocal microscope (Leica Microsystems) are shown (C). (D) 7 µm cryo sections of whole femora were probed with anti-CD105 (Alexa647-labeled; red), anti-GPIb (Alexa488-conjugated; green) antibodies and counterstained with DAPI (blue). (E) Quantification of BM MKs per visual field (294 x 221 µm) in histological sections. (F) Platelet recovery in mice monitored for 7 days post platelet depletion with an anti-GPIb antibody. Data are presented as mean ± SD of at least 100 vs. 100 MKs. *P<0.05, **P<0.01, ***P<0.001.

Another aspect, which is currently investigated in collaboration with Simon Stritt in our laboratory, is the role of PLD in megakaryo- and thrombocytopoiesis. Recently, Ali *et al.* have shown that macrophages from PLD1 or PLD2 deficient mice display abnormalities in actin dynamics leading to irregularly shaped podosomes and deficiencies in phagocytic capacities [157]. Besides macrophages, podosomes have also been shown to be crucial for the adhesion of megakaryocytes to the extracellular matrix of the bone marrow during maturation and migration to the vascular niche [311]. MKs in the bone marrow are in close contact with various extracellular matrix proteins, such as collagen I and fibronectin in the osteoblastic niche during maturation or collagen IV, laminin and fibrinogen in the vascular niche when forming pro-platelets [311]. However, to date nothing is known on the functional role of PLD in MK podosome formation. Initial experiments showed that PLD deficient MKs spread normally on collagen I but displayed defective podosome formation and a severely reduced abundance of actin filaments (Figure 4-2A, B, C). Further studies displayed aberrant MK morphology in the bone marrow of *Pld1⁻ᐟ⁻/Pld2⁻ᐟ⁻* mice with a slightly reduced abundance of MKs in the bone marrow (Figure 4-2D, 4-2E). Most interestingly, despite PLDs' contribution to collagen I

mediated podosome formation, platelet production upon antibody-induced thrombocytopenia was normal in PLD deficient mice (Figure 4-2F). In order to understand these observations and to analyze how these defects are compensated during platelet production, additional studies will be required.

5 References

1   Italiano JE, Jr., Patel-Hett S, Hartwig JH. Mechanics of proplatelet elaboration. *J Thromb Haemost*. 2007; 5 Suppl 1: 18-23. 10.1111/j.1538-7836.2007.02487.x.

2   Ruggeri ZM. Platelets in atherothrombosis. *Nat Med*. 2002; 8: 1227-34. 10.1038/nm1102-1227.

3   Caro JJ, Huybrechts KF, Duchesne I. Management patterns and costs of acute ischemic stroke : an international study. For the Stroke Economic Analysis Group. *Stroke*. 2000; 31: 582-90.

4   Lopez AD, Mathers CD, Ezzati M, Jamison DT, Murray CJ. Global and regional burden of disease and risk factors, 2001: systematic analysis of population health data. *Lancet*. 2006; 367: 1747-57. 10.1016/S0140-6736(06)68770-9.

5   Stegner D, Nieswandt B. Platelet receptor signaling in thrombus formation. *Journal of molecular medicine*. 2011; 89: 109-21. 10.1007/s00109-010-0691-5.

6   Turitto VT, Baumgartner HR. Effect of temperature on platelet interaction with subendothelium exposed to flowing blood. *Haemostasis*. 1974; 3: 224-36.

7   Savage B, Saldivar E, Ruggeri ZM. Initiation of platelet adhesion by arrest onto fibrinogen or translocation on von Willebrand factor. *Cell*. 1996; 84: 289-97.

8   Elvers M, Stegner D, Hagedorn I, Kleinschnitz C, Braun A, Kuijpers ME, Boesl M, Chen Q, Heemskerk JW, Stoll G, Frohman MA, Nieswandt B. Impaired alpha(IIb)beta(3) integrin activation and shear-dependent thrombus formation in mice lacking phospholipase D1. *SciSignal*. 2010; 3: ra1.

9   Nieswandt B, Watson SP. Platelet-collagen interaction: is GPVI the central receptor? *Blood*. 2003; 102: 449-61. 10.1182/blood-2002-12-3882.

10   Fuller GL, Williams JA, Tomlinson MG, Eble JA, Hanna SL, Pohlmann S, Suzuki-Inoue K, Ozaki Y, Watson SP, Pearce AC. The C-type lectin receptors CLEC-2 and Dectin-1, but not DC-SIGN, signal via a novel YXXL-dependent signaling cascade. *J Biol Chem*. 2007; 282: 12397-409. 10.1074/jbc.M609558200.

11   Watson SP, Auger JM, McCarty OJ, Pearce AC. GPVI and integrin alphaIIb beta3 signaling in platelets. *J Thromb Haemost*. 2005; 3: 1752-62. 10.1111/j.1538-7836.2005.01429.x.

12   Watson SP, Herbert JM, Pollitt AY. GPVI and CLEC-2 in hemostasis and vascular integrity. *J Thromb Haemost*. 2010; 8: 1456-67. 10.1111/j.1538-7836.2010.03875.x.

13   Varga-Szabo D, Braun A, Nieswandt B. Calcium signaling in platelets. *J Thromb Haemost*. 2009; 7: 1057-66. 10.1111/j.1538-7836.2009.03455.x.

14   Harper MT, Poole AW. Diverse functions of protein kinase C isoforms in platelet activation and thrombus formation. *J Thromb Haemost*. 2010; 8: 454-62. 10.1111/j.1538-7836.2009.03722.x.

15   Ren Q, Ye S, Whiteheart SW. The platelet release reaction: just when you thought platelet secretion was simple. *Current opinion in hematology*. 2008; 15: 537-41. 10.1097/MOH.0b013e328309ec74.

16   Krishnaswamy S, Nesheim ME, Pryzdial EL, Mann KG. Assembly of prothrombinase complex. *Methods in enzymology*. 1993; 222: 260-80.

17   Fay PJ. Activation of factor VIII and mechanisms of cofactor action. *Blood reviews*. 2004; 18: 1-15.

18   Lentz BR. Exposure of platelet membrane phosphatidylserine regulates blood coagulation. *Progress in lipid research*. 2003; 42: 423-38.

19   Maas C, Oschatz C, Renne T. The plasma contact system 2.0. *Seminars in thrombosis and hemostasis*. 2011; 37: 375-81. 10.1055/s-0031-1276586.

20   Coughlin SR. Thrombin signalling and protease-activated receptors. *Nature*. 2000; 407: 258-64. 10.1038/35025229.

21   Sambrano GR, Weiss EJ, Zheng YW, Huang W, Coughlin SR. Role of thrombin signalling in platelets in haemostasis and thrombosis. *Nature*. 2001; 413: 74-8. 10.1038/35092573.

22   Offermanns S. Activation of platelet function through G protein-coupled receptors. *Circulation research*. 2006; 99: 1293-304. 10.1161/01.RES.0000251742.71301.16.

23   Wettschureck N, Offermanns S. Rho/Rho-kinase mediated signaling in physiology and pathophysiology. *Journal of molecular medicine*. 2002; 80: 629-38. 10.1007/s00109-002-0370-2.

24   Offermanns S, Toombs CF, Hu YH, Simon MI. Defective platelet activation in G alpha(q)-deficient mice. *Nature*. 1997; 389: 183-6. 10.1038/38284.

25   Clapham DE, Neer EJ. G protein beta gamma subunits. *Annual review of pharmacology and toxicology*. 1997; 37: 167-203. 10.1146/annurev.pharmtox.37.1.167.

26   Cantley LC. The phosphoinositide 3-kinase pathway. *Science*. 2002; 296: 1655-7. 10.1126/science.296.5573.1655.

27   Shattil SJ, Kim C, Ginsberg MH. The final steps of integrin activation: the end game. *Nature reviews Molecular cell biology*. 2010; 11: 288-300. 10.1038/nrm2871.

28   McDermott M, Wakelam MJ, Morris AJ. Phospholipase D. *Biochemistry and cell biology = Biochimie et biologie cellulaire*. 2004; 82: 225-53. 10.1139/o03-079.

29   Oblozinsky M, Bezakova L, Mansfeld J, Ulbrich-Hofmann R. The transphosphatidylation potential of a membrane-bound phospholipase D from poppy seedlings. *Phytochemistry*. 2011; 72: 160-5. 10.1016/j.phytochem.2010.11.020.

30   Huang C, Wykle RL, Daniel LW, Cabot MC. Identification of phosphatidylcholine-selective and phosphatidylinositol-selective phospholipases D in Madin-Darby canine kidney cells. *J Biol Chem*. 1992; 267: 16859-65.

31   Mukherjee JJ, Chung T, Ways DK, Kiss Z. Protein kinase Calpha is a major mediator of the stimulatory effect of phorbol ester on phospholipase D-mediated hydrolysis of phosphatidylethanolamine. *J Biol Chem*. 1996; 271: 28912-7.

32   Morris AJ, Frohman MA, Engebrecht J. Measurement of phospholipase D activity. *Analytical biochemistry*. 1997; 252: 1-9. 10.1006/abio.1997.2299.

33   Colley WC, Altshuller YM, Sue-Ling CK, Copeland NG, Gilbert DJ, Jenkins NA, Branch KD, Tsirka SE, Bollag RJ, Bollag WB, Frohman MA. Cloning and expression analysis of murine phospholipase D1. *The Biochemical journal*. 1997; 326 (Pt 3): 745-53.

34   Hammond SM, Jenco JM, Nakashima S, Cadwallader K, Gu Q, Cook S, Nozawa Y, Prestwich GD, Frohman MA, Morris AJ. Characterization of two alternately spliced forms of phospholipase D1. Activation of the purified enzymes by phosphatidylinositol 4,5-bisphosphate, ADP-ribosylation factor, and Rho family monomeric GTP-binding proteins and protein kinase C-alpha. *J Biol Chem*. 1997; 272: 3860-8.

35   Redina OE, Frohman MA. Organization and alternative splicing of the murine phospholipase D2 gene. *The Biochemical journal*. 1998; 331 (Pt 3): 845-51.

36   Hammond SM, Altshuller YM, Sung TC, Rudge SA, Rose K, Engebrecht J, Morris AJ, Frohman MA. Human ADP-ribosylation factor-activated phosphatidylcholine-specific phospholipase D defines a new and highly conserved gene family. *J Biol Chem*. 1995; 270: 29640-3.

37   Kanaho Y, Funakoshi Y, Hasegawa H. Phospholipase D signalling and its involvement in neurite outgrowth. *Biochim Biophys Acta*. 2009; 1791: 898-904. 10.1016/j.bbalip.2009.03.010.

38   Choi SY, Huang P, Jenkins GM, Chan DC, Schiller J, Frohman MA. A common lipid links Mfn-mediated mitochondrial fusion and SNARE-regulated exocytosis. *Nature cell biology*. 2006; 8: 1255-62. 10.1038/ncb1487.

39   Pedersen KM, Finsen B, Celis JE, Jensen NA. Expression of a novel murine phospholipase D homolog coincides with late neuronal development in the forebrain. *J Biol Chem*. 1998; 273: 31494-504.

40   Yoshikawa F, Banno Y, Otani Y, Yamaguchi Y, Nagakura-Takagi Y, Morita N, Sato Y, Saruta C, Nishibe H, Sadakata T, Shinoda Y, Hayashi K, Mishima Y, Baba H, Furuichi T. Phospholipase D family member 4, a transmembrane glycoprotein with no phospholipase D activity, expression in spleen and early postnatal microglia. *PLoS One*. 2010; 5: e13932. 10.1371/journal.pone.0013932.

41   Anney R, Klei L, Pinto D, Regan R, Conroy J, Magalhaes TR, Correia C, Abrahams BS, Sykes N, Pagnamenta AT et al. A genome-wide scan for common alleles affecting risk for autism. *Hum Mol Genet*. 2010; 19: 4072-82. 10.1093/hmg/ddq307.

42   Rudolph AE, Stuckey JA, Zhao Y, Matthews HR, Patton WA, Moss J, Dixon JE. Expression, characterization, and mutagenesis of the Yersinia pestis murine toxin, a phospholipase D superfamily member. *J Biol Chem*. 1999; 274: 11824-31.

43   Sung TC, Roper RL, Zhang Y, Rudge SA, Temel R, Hammond SM, Morris AJ, Moss B, Engebrecht J, Frohman MA. Mutagenesis of phospholipase D defines a superfamily including a trans-Golgi viral protein required for poxvirus pathogenicity. *Embo J*. 1997; 16: 4519-30. 10.1093/emboj/16.15.4519.

44   Gottlin EB, Rudolph AE, Zhao Y, Matthews HR, Dixon JE. Catalytic mechanism of the phospholipase D superfamily proceeds via a covalent phosphohistidine intermediate. *Proc Natl Acad Sci U S A*. 1998; 95: 9202-7.

45   Hodgkin MN, Masson MR, Powner D, Saqib KM, Ponting CP, Wakelam MJ. Phospholipase D regulation and localisation is dependent upon a phosphatidylinositol 4,5-biphosphate-specific PH domain. *Current biology : CB*. 2000; 10: 43-6.

46   Peng HJ, Henkels KM, Mahankali M, Marchal C, Bubulya P, Dinauer MC, Gomez-Cambronero J. The dual effect of Rac2 on phospholipase D2 regulation that explains both the onset and termination of chemotaxis. *Mol Cell Biol*. 2011; 31: 2227-40. 10.1128/MCB.01348-10.

47   Lee JS, Kim JH, Jang IH, Kim HS, Han JM, Kazlauskas A, Yagisawa H, Suh PG, Ryu SH. Phosphatidylinositol (3,4,5)-trisphosphate specifically interacts with the phox homology domain of phospholipase D1 and stimulates its activity. *J Cell Sci*. 2005; 118: 4405-13. 10.1242/jcs.02564.

48   Lee CS, Kim IS, Park JB, Lee MN, Lee HY, Suh PG, Ryu SH. The phox homology domain of phospholipase D activates dynamin GTPase activity and accelerates EGFR endocytosis. *Nature cell biology*. 2006; 8: 477-84. 10.1038/ncb1401.

49   Stahelin RV, Ananthanarayanan B, Blatner NR, Singh S, Bruzik KS, Murray D, Cho W. Mechanism of membrane binding of the phospholipase D1 PX domain. *J Biol Chem*. 2004; 279: 54918-26. 10.1074/jbc.M407798200.

50   Jang IH, Lee S, Park JB, Kim JH, Lee CS, Hur EM, Kim IS, Kim KT, Yagisawa H, Suh PG, Ryu SH. The direct interaction of phospholipase C-gamma 1 with phospholipase D2 is important for epidermal growth factor signaling. *J Biol Chem*. 2003; 278: 18184-90. 10.1074/jbc.M208438200.

51   Lee JH, Kim YM, Kim NW, Kim JW, Her E, Kim BK, Kim JH, Ryu SH, Park JW, Seo DW, Han JW, Beaven MA, Choi WS. Phospholipase D2 acts as an essential adaptor protein in the activation of Syk in antigen-stimulated mast cells. *Blood*. 2006; 108: 956-64. 10.1182/blood-2005-10-009159.

52   Mahankali M, Peng HJ, Cox D, Gomez-Cambronero J. The mechanism of cell membrane ruffling relies on a phospholipase D2 (PLD2), Grb2 and Rac2 association. *Cellular signalling*. 2011; 23: 1291-8. 10.1016/j.cellsig.2011.03.010.

53   Sung TC, Zhang Y, Morris AJ, Frohman MA. Structural analysis of human phospholipase D1. *J Biol Chem*. 1999; 274: 3659-66.

54   Farquhar MJ, Powner DJ, Levine BA, Wright MH, Ladds G, Hodgkin MN. Interaction of PLD1b with actin in antigen-stimulated mast cells. *Cellular signalling*. 2007; 19: 349-58. 10.1016/j.cellsig.2006.07.016.

55   Yamazaki M, Zhang Y, Watanabe H, Yokozeki T, Ohno S, Kaibuchi K, Shibata H, Mukai H, Ono Y, Frohman MA, Kanaho Y. Interaction of the small G protein RhoA with the C terminus of human phospholipase D1. *J Biol Chem*. 1999; 274: 6035-8.

56   Katayama K, Kodaki T, Nagamachi Y, Yamashita S. Cloning, differential regulation and tissue distribution of alternatively spliced isoforms of ADP-ribosylation-factor-dependent phospholipase D from rat liver. *The Biochemical journal*. 1998; 329 (Pt 3): 647-52.

57   Saqib KM, Wakelam MJ. Differential expression of human phospholipase D genes. *Biochemical Society transactions*. 1997; 25: S586.

58   Lopez I, Arnold RS, Lambeth JD. Cloning and initial characterization of a human phospholipase D2 (hPLD2). ADP-ribosylation factor regulates hPLD2. *J Biol Chem*. 1998; 273: 12846-52.

59   Toda K, Nogami M, Murakami K, Kanaho Y, Nakayama K. Colocalization of phospholipase D1 and GTP-binding-defective mutant of ADP-ribosylation factor 6 to endosomes and lysosomes. *FEBS letters*. 1999; 442: 221-5.

60   Freyberg Z, Sweeney D, Siddhanta A, Bourgoin S, Frohman M, Shields D. Intracellular localization of phospholipase D1 in mammalian cells. *Mol Biol Cell*. 2001; 12: 943-55.

61   Vitale N, Caumont AS, Chasserot-Golaz S, Du G, Wu S, Sciorra VA, Morris AJ, Frohman MA, Bader MF. Phospholipase D1: a key factor for the exocytotic machinery in neuroendocrine cells. *Embo J*. 2001; 20: 2424-34. 10.1093/emboj/20.10.2424.

62   Brown FD, Thompson N, Saqib KM, Clark JM, Powner D, Thompson NT, Solari R, Wakelam MJ. Phospholipase D1 localises to secretory granules and lysosomes and is plasma-membrane translocated on cellular stimulation. *Current biology : CB*. 1998; 8: 835-8.

63   Du G, Huang P, Liang BT, Frohman MA. Phospholipase D2 localizes to the plasma membrane and regulates angiotensin II receptor endocytosis. *Mol Biol Cell*. 2004; 15: 1024-30. 10.1091/mbc.E03-09-0673.

64   Colley WC, Sung TC, Roll R, Jenco J, Hammond SM, Altshuller Y, Bar-Sagi D, Morris AJ, Frohman MA. Phospholipase D2, a distinct phospholipase D isoform with novel regulatory properties that provokes cytoskeletal reorganization. *Current biology : CB*. 1997; 7: 191-201.

65   Exton JH. Phospholipase D: enzymology, mechanisms of regulation, and function. *Physiological reviews*. 1997; 77: 303-20.

66   Gomez-Cambronero J. The exquisite regulation of PLD2 by a wealth of interacting proteins: S6K, Grb2, Sos, WASp and Rac2 (and a surprise discovery: PLD2 is a GEF). *Cellular signalling*. 2011; 23: 1885-95. 10.1016/j.cellsig.2011.06.017.

67   Cockcroft S. Signalling roles of mammalian phospholipase D1 and D2. *Cellular and molecular life sciences : CMLS*. 2001; 58: 1674-87.

68   Hope HR, Pike LJ. Phosphoinositides and phosphoinositide-utilizing enzymes in detergent-insoluble lipid domains. *Mol Biol Cell*. 1996; 7: 843-51.

69   Everett PB, Senogles SE. D3 dopamine receptor signals to activation of phospholipase D through a complex with Rho. *Journal of neurochemistry*. 2010; 112: 963-71. 10.1111/j.1471-4159.2009.06508.x.

70   Momboisse F, Lonchamp E, Calco V, Ceridono M, Vitale N, Bader MF, Gasman S. betaPIX-activated Rac1 stimulates the activation of phospholipase D, which is associated with exocytosis in neuroendocrine cells. *J Cell Sci*. 2009; 122: 798-806. 10.1242/jcs.038109.

71   Yoon MS, Cho CH, Lee KS, Han JS. Binding of Cdc42 to phospholipase D1 is important in neurite outgrowth of neural stem cells. *Biochem Biophys Res Commun*. 2006; 347: 594-600. 10.1016/j.bbrc.2006.06.111.

72   Genth H, Schmidt M, Gerhard R, Aktories K, Just I. Activation of phospholipase D1 by ADP-ribosylated RhoA. *Biochem Biophys Res Commun*. 2003; 302: 127-32.

73   Gayral S, Deleris P, Laulagnier K, Laffargue M, Salles JP, Perret B, Record M, Breton-Douillon M. Selective activation of nuclear phospholipase D-1 by g protein-coupled receptor agonists in vascular smooth muscle cells. *Circulation research*. 2006; 99: 132-9. 10.1161/01.RES.0000232323.86227.8b.

74   Xie Z, Ho WT, Exton JH. Association of the N- and C-terminal domains of phospholipase D. Contribution of the conserved HKD motifs to the interaction and the requirement of the association for Ser/Thr phosphorylation of the enzyme. *J Biol Chem*. 2000; 275: 24962-9. 10.1074/jbc.M909745199.

75   Jeon H, Kwak D, Noh J, Lee MN, Lee CS, Suh PG, Ryu SH. Phospholipase D2 induces stress fiber formation through mediating nucleotide exchange for RhoA. *Cellular signalling*. 2011; 23: 1320-6. 10.1016/j.cellsig.2011.03.014.

76   Oude Weernink PA, Schulte P, Guo Y, Wetzel J, Amano M, Kaibuchi K, Haverland S, Voss M, Schmidt M, Mayr GW, Jakobs KH. Stimulation of phosphatidylinositol-4-phosphate 5-kinase by Rho-kinase. *J Biol Chem*. 2000; 275: 10168-74.

77   Brown HA, Gutowski S, Kahn RA, Sternweis PC. Partial purification and characterization of Arf-sensitive phospholipase D from porcine brain. *J Biol Chem*. 1995; 270: 14935-43.

78   Begle A, Tryoen-Toth P, de Barry J, Bader MF, Vitale N. ARF6 regulates the synthesis of fusogenic lipids for calcium-regulated exocytosis in neuroendocrine cells. *J Biol Chem*. 2009; 284: 4836-45. 10.1074/jbc.M806894200.

79   Garcia A, Zheng Y, Zhao C, Toschi A, Fan J, Shraibman N, Brown HA, Bar-Sagi D, Foster DA, Arbiser JL. Honokiol suppresses survival signals mediated by Ras-dependent phospholipase D activity in human cancer cells. *Clinical cancer research : an official journal of the American Association for Cancer Research*. 2008; 14: 4267-74. 10.1158/1078-0432.CCR-08-0102.

80   Mitchell R, Robertson DN, Holland PJ, Collins D, Lutz EM, Johnson MS. ADP-ribosylation factor-dependent phospholipase D activation by the M3 muscarinic receptor. *J Biol Chem*. 2003; 278: 33818-30. 10.1074/jbc.M305825200.

81   Ma WN, Park SY, Han JS. Role of phospholipase D1 in glucose-induced insulin secretion in pancreatic Beta cells. *Experimental & molecular medicine*. 2010; 42: 456-64. 10.3858/emm.2010.42.6.047.

82   Muralidharan-Chari V, Clancy J, Plou C, Romao M, Chavrier P, Raposo G, D'Souza-Schorey C. ARF6-regulated shedding of tumor cell-derived plasma membrane microvesicles. *Current biology : CB*. 2009; 19: 1875-85. 10.1016/j.cub.2009.09.059.

83   Zhang GF, Patton WA, Lee FJ, Liyanage M, Han JS, Rhee SG, Moss J, Vaughan M. Different ARF domains are required for the activation of cholera toxin and phospholipase D. *J Biol Chem*. 1995; 270: 21-4.

84   Xu L, Frankel P, Jackson D, Rotunda T, Boshans RL, D'Souza-Schorey C, Foster DA. Elevated phospholipase D activity in H-Ras- but not K-Ras-transformed cells by the synergistic action of RalA and ARF6. *Mol Cell Biol*. 2003; 23: 645-54.

85   Vitale N, Mawet J, Camonis J, Regazzi R, Bader MF, Chasserot-Golaz S. The Small GTPase RalA controls exocytosis of large dense core secretory granules by interacting with ARF6-dependent phospholipase D1. *J Biol Chem*. 2005; 280: 29921-8. 10.1074/jbc.M413748200.

86   Henage LG, Exton JH, Brown HA. Kinetic analysis of a mammalian phospholipase D: allosteric modulation by monomeric GTPases, protein kinase C, and polyphosphoinositides. *J Biol Chem*. 2006; 281: 3408-17. 10.1074/jbc.M508800200.

87   Cockcroft S. Phospholipase D: regulation by GTPases and protein kinase C and physiological relevance. *Progress in lipid research*. 1996; 35: 345-70.

88   Hu T, Exton JH. Protein kinase Calpha translocates to the perinuclear region to activate phospholipase D1. *J Biol Chem*. 2004; 279: 35702-8. 10.1074/jbc.M402372200.

89   Min DS, Park SK, Exton JH. Characterization of a rat brain phospholipase D isozyme. *J Biol Chem*. 1998; 273: 7044-51.

90   Chae YC, Kim KL, Ha SH, Kim J, Suh PG, Ryu SH. Protein kinase Cdelta-mediated phosphorylation of phospholipase D controls integrin-mediated cell spreading. *Mol Cell Biol*. 2010; 30: 5086-98. 10.1128/MCB.00443-10.

91   Kim Y, Han JM, Han BR, Lee KA, Kim JH, Lee BD, Jang IH, Suh PG, Ryu SH. Phospholipase D1 is phosphorylated and activated by protein kinase C in caveolin-enriched microdomains within the plasma membrane. *J Biol Chem*. 2000; 275: 13621-7.

92   Lopez I, Burns DJ, Lambeth JD. Regulation of phospholipase D by protein kinase C in human neutrophils. Conventional isoforms of protein kinase C phosphorylate a phospholipase D-related component in the plasma membrane. *J Biol Chem*. 1995; 270: 19465-72.

93   Chen JS, Exton JH. Regulation of phospholipase D2 activity by protein kinase C alpha. *J Biol Chem*. 2004; 279: 22076-83. 10.1074/jbc.M311033200.

94   Singer WD, Brown HA, Jiang X, Sternweis PC. Regulation of phospholipase D by protein kinase C is synergistic with ADP-ribosylation factor and independent of protein kinase activity. *J Biol Chem*. 1996; 271: 4504-10.

95   Oka M, Hitomi T, Okada T, Nakamura Si S, Nagai H, Ohba M, Kuroki T, Kikkawa U, Ichihashi M. Dual regulation of phospholipase D1 by protein kinase C alpha in vivo. *Biochem Biophys Res Commun*. 2002; 294: 1109-13. 10.1016/S0006-291X(02)00614-9.

96   Sciorra VA, Rudge SA, Prestwich GD, Frohman MA, Engebrecht J, Morris AJ. Identification of a phosphoinositide binding motif that mediates activation of mammalian and yeast phospholipase D isoenzymes. *Embo J*. 1999; 18: 5911-21. 10.1093/emboj/18.21.5911.

97   Oude Weernink PA, Lopez de Jesus M, Schmidt M. Phospholipase D signaling: orchestration by PIP2 and small GTPases. *Naunyn Schmiedebergs Arch Pharmacol*. 2007; 374: 399-411. 10.1007/s00210-007-0131-4.

98   Divecha N, Roefs M, Halstead JR, D'Andrea S, Fernandez-Borga M, Oomen L, Saqib KM, Wakelam MJ, D'Santos C. Interaction of the type Ialpha PIPkinase with phospholipase D: a role for the local generation of phosphatidylinositol 4, 5-bisphosphate in the regulation of PLD2 activity. *Embo J*. 2000; 19: 5440-9. 10.1093/emboj/19.20.5440.

99   Powner DJ, Payne RM, Pettitt TR, Giudici ML, Irvine RF, Wakelam MJ. Phospholipase D2 stimulates integrin-mediated adhesion via phosphatidylinositol 4-phosphate 5-kinase Igamma b. *J Cell Sci*. 2005; 118: 2975-86. 10.1242/jcs.02432.

100   Santarius M, Lee CH, Anderson RA. Supervised membrane swimming: small G-protein lifeguards regulate PIPK signalling and monitor intracellular PtdIns(4,5)P2 pools. *The Biochemical journal*. 2006; 398: 1-13. 10.1042/BJ20060565.

101   Pappan K, Zheng L, Krishnamoorthi R, Wang X. Evidence for and characterization of Ca2+ binding to the catalytic region of Arabidopsis thaliana phospholipase Dbeta. *J Biol Chem*. 2004; 279: 47833-9. 10.1074/jbc.M402789200.

102   Kessels GC, Roos D, Verhoeven AJ. fMet-Leu-Phe-induced activation of phospholipase D in human neutrophils. Dependence on changes in cytosolic free Ca2+ concentration and relation with respiratory burst activation. *J Biol Chem*. 1991; 266: 23152-6.

103   Gustavsson L, Moehren G, Torres-Marquez ME, Benistant C, Rubin R, Hoek JB. The role of cytosolic Ca2+, protein kinase C, and protein kinase A in hormonal stimulation of phospholipase D in rat hepatocytes. *J Biol Chem*. 1994; 269: 849-59.

104 Choi WS, Hiragun T, Lee JH, Kim YM, Kim HP, Chahdi A, Her E, Han JW, Beaven MA. Activation of RBL-2H3 mast cells is dependent on tyrosine phosphorylation of phospholipase D2 by Fyn and Fgr. *Mol Cell Biol*. 2004; 24: 6980-92. 10.1128/MCB.24.16.6980-6992.2004.

105 Ho WT, Xie Z, Zhao ZJ, Exton JH. Tyrosine phosphorylation of phospholipase D1 by v-Src does not per se result in activation. *Cellular signalling*. 2005; 17: 691-9. 10.1016/j.cellsig.2004.10.007.

106 Martinson EA, Scheible S, Presek P. Inhibition of phospholipase D of human platelets by protein tyrosine kinase inhibitors. *Cellular and molecular biology*. 1994; 40: 627-34.

107 Ahn BH, Min G, Bae YS, Bae YS, Min DS. Phospholipase D is activated and phosphorylated by casein kinase-II in human U87 astroglioma cells. *Experimental & molecular medicine*. 2006; 38: 55-62. 10.1038/emm.2006.7.

108 Lee HY, Jung H, Jang IH, Suh PG, Ryu SH. Cdk5 phosphorylates PLD2 to mediate EGF-dependent insulin secretion. *Cellular signalling*. 2008; 20: 1787-94. 10.1016/j.cellsig.2008.06.009.

109 Zeniou-Meyer M, Liu Y, Begle A, Olanich ME, Hanauer A, Becherer U, Rettig J, Bader MF, Vitale N. The Coffin-Lowry syndrome-associated protein RSK2 is implicated in calcium-regulated exocytosis through the regulation of PLD1. *Proc Natl Acad Sci U S A*. 2008; 105: 8434-9. 10.1073/pnas.0710676105.

110 Patel S, Djerdjouri B, Raoul-Des-Essarts Y, Dang PM, El-Benna J, Perianin A. Protein kinase B (AKT) mediates phospholipase D activation via ERK1/2 and promotes respiratory burst parameters in formylpeptide-stimulated neutrophil-like HL-60 cells. *J Biol Chem*. 2010; 285: 32055-63. 10.1074/jbc.M110.171058.

111 Wakelam MJ, McNee GS, Rudge SA. Cross-talk between phospholipase D and MAP kinases activities. *Advances in enzyme regulation*. 2010; 50: 57-61. 10.1016/j.advenzreg.2009.10.032.

112 Henkels KM, Peng HJ, Frondorf K, Gomez-Cambronero J. A comprehensive model that explains the regulation of phospholipase D2 activity by phosphorylation-dephosphorylation. *Mol Cell Biol*. 2010; 30: 2251-63. 10.1128/MCB.01239-09.

113 Henkels KM, Short S, Peng HJ, Di Fulvio M, Gomez-Cambronero J. PLD2 has both enzymatic and cell proliferation-inducing capabilities, that are differentially regulated by phosphorylation and dephosphorylation. *Biochem Biophys Res Commun*. 2009; 389: 224-8. 10.1016/j.bbrc.2009.08.109.

114 Kusner DJ, Barton JA, Wen KK, Wang X, Rubenstein PA, Iyer SS. Regulation of phospholipase D activity by actin. Actin exerts bidirectional modulation of Mammalian phospholipase D activity in a polymerization-dependent, isoform-specific manner. *J Biol Chem*. 2002; 277: 50683-92. 10.1074/jbc.M209221200.

115 Chae YC, Lee S, Lee HY, Heo K, Kim JH, Kim JH, Suh PG, Ryu SH. Inhibition of muscarinic receptor-linked phospholipase D activation by association with tubulin. *J Biol Chem*. 2005; 280: 3723-30. 10.1074/jbc.M406987200.

116 Iyer SS, Kusner DJ. Association of phospholipase D activity with the detergent-insoluble cytoskeleton of U937 promonocytic leukocytes. *J Biol Chem*. 1999; 274: 2350-9.

117 Park JB, Kim JH, Kim Y, Ha SH, Yoo JS, Du G, Frohman MA, Suh PG, Ryu SH. Cardiac phospholipase D2 localizes to sarcolemmal membranes and is inhibited by alpha-actinin in an ADP-ribosylation factor-reversible manner. *J Biol Chem*. 2000; 275: 21295-301. 10.1074/jbc.M002463200.

118 Lukowski S, Lecomte MC, Mira JP, Marin P, Gautero H, Russo-Marie F, Geny B. Inhibition of phospholipase D activity by fodrin. An active role for the cytoskeleton. *J Biol Chem*. 1996; 271: 24164-71.

119 Lukowski S, Mira JP, Zachowski A, Geny B. Fodrin inhibits phospholipases A2, C, and D by decreasing polyphosphoinositide cell content. *Biochem Biophys Res Commun*. 1998; 248: 278-84. 10.1006/bbrc.1998.8942.

120 Chung JK, Sekiya F, Kang HS, Lee C, Han JS, Kim SR, Bae YS, Morris AJ, Rhee SG. Synaptojanin inhibition of phospholipase D activity by hydrolysis of phosphatidylinositol 4,5-bisphosphate. *J Biol Chem*. 1997; 272: 15980-5.

121 Han L, Stope MB, de Jesus ML, Oude Weernink PA, Urban M, Wieland T, Rosskopf D, Mizuno K, Jakobs KH, Schmidt M. Direct stimulation of receptor-controlled phospholipase D1 by phospho-cofilin. *Embo J*. 2007; 26: 4189-202. 10.1038/sj.emboj.7601852.

122 Ella KM, Meier KE, Kumar A, Zhang Y, Meier GP. Utilization of alcohols by plant and mammalian phospholipase D. *Biochemistry and molecular biology international*. 1997; 41: 715-24.

123 Dall'Armi C, Hurtado-Lorenzo A, Tian H, Morel E, Nezu A, Chan RB, Yu WH, Robinson KS, Yeku O, Small SA, Duff K, Frohman MA, Wenk MR, Yamamoto A, Di Paolo G. The phospholipase D1 pathway modulates macroautophagy. *Nat Commun*. 2010; 1: 142. 10.1038/ncomms1144.

124 Oliveira TG, Chan RB, Tian H, Laredo M, Shui G, Staniszewski A, Zhang H, Wang L, Kim TW, Duff KE, Wenk MR, Arancio O, Di Paolo G. Phospholipase d2 ablation ameliorates Alzheimer's disease-linked synaptic dysfunction and cognitive deficits. *The Journal of neuroscience : the official journal of the Society for Neuroscience*. 2010; 30: 16419-28. 10.1523/JNEUROSCI.3317-10.2010.

125 Thielmann I, Stegner D, Kraft P, Hagedorn I, Krohne G, Kleinschnitz C, Stoll G, Nieswandt B. Redundant functions of phospholipases D1 and D2 in platelet alpha-granule release. *J Thromb Haemost*. 2012. 10.1111/j.1538-7836.2012.04924.x.

126 Riebeling C, Morris AJ, Shields D. Phospholipase D in the Golgi apparatus. *Biochim Biophys Acta*. 2009; 1791: 876-80. 10.1016/j.bbalip.2009.04.003.

127 Hughes WE, Elgundi Z, Huang P, Frohman MA, Biden TJ. Phospholipase D1 regulates secretagogue-stimulated insulin release in pancreatic beta-cells. *J Biol Chem*. 2004; 279: 27534-41. 10.1074/jbc.M403012200.

128 Huang P, Altshuller YM, Hou JC, Pessin JE, Frohman MA. Insulin-stimulated plasma membrane fusion of Glut4 glucose transporter-containing vesicles is regulated by phospholipase D1. *Mol Biol Cell*. 2005; 16: 2614-23. 10.1091/mbc.E04-12-1124.

129 Vicogne J, Vollenweider D, Smith JR, Huang P, Frohman MA, Pessin JE. Asymmetric phospholipid distribution drives in vitro reconstituted SNARE-dependent membrane fusion. *Proc Natl Acad Sci U S A*. 2006; 103: 14761-6. 10.1073/pnas.0606881103.

130 Koch T, Wu DF, Yang LQ, Brandenburg LO, Hollt V. Role of phospholipase D2 in the agonist-induced and constitutive endocytosis of G-protein coupled receptors. *Journal of neurochemistry*. 2006; 97: 365-72. 10.1111/j.1471-4159.2006.03736.x.

131 Shen Y, Xu L, Foster DA. Role for phospholipase D in receptor-mediated endocytosis. *Mol Cell Biol*. 2001; 21: 595-602. 10.1128/MCB.21.2.595-602.2001.

132 Iyer SS, Agrawal RS, Thompson CR, Thompson S, Barton JA, Kusner DJ. Phospholipase D1 regulates phagocyte adhesion. *Journal of immunology*. 2006; 176: 3686-96.

133 Shen Y, Zheng Y, Foster DA. Phospholipase D2 stimulates cell protrusion in v-Src-transformed cells. *Biochem Biophys Res Commun*. 2002; 293: 201-6. 10.1016/S0006-291X(02)00204-8.

134 Chae YC, Kim JH, Kim KL, Kim HW, Lee HY, Heo WD, Meyer T, Suh PG, Ryu SH. Phospholipase D activity regulates integrin-mediated cell spreading and migration by inducing GTP-Rac translocation to the plasma membrane. *Mol Biol Cell*. 2008; 19: 3111-23. 10.1091/mbc.E07-04-0337.

135 Knapek K, Frondorf K, Post J, Short S, Cox D, Gomez-Cambronero J. The molecular basis of phospholipase D2-induced chemotaxis: elucidation of differential pathways in macrophages and fibroblasts. *Mol Cell Biol*. 2010; 30: 4492-506. 10.1128/MCB.00229-10.

136 Itoh T, Hasegawa J, Tsujita K, Kanaho Y, Takenawa T. The tyrosine kinase Fer is a downstream target of the PLD-PA pathway that regulates cell migration. *Sci Signal*. 2009; 2: ra52. 10.1126/scisignal.2000393.

137 Jarquin-Pardo M, Fitzpatrick A, Galiano FJ, First EA, Davis JN. Phosphatidic acid regulates the affinity of the murine phosphatidylinositol 4-phosphate 5-kinase-Ibeta for phosphatidylinositol-4-phosphate. *Journal of cellular biochemistry*. 2007; 100: 112-28. 10.1002/jcb.21027.

138 Delon C, Manifava M, Wood E, Thompson D, Krugmann S, Pyne S, Ktistakis NT. Sphingosine kinase 1 is an intracellular effector of phosphatidic acid. *J Biol Chem*. 2004; 279: 44763-74. 10.1074/jbc.M405771200.

139 Lehman N, Ledford B, Di Fulvio M, Frondorf K, McPhail LC, Gomez-Cambronero J. Phospholipase D2-derived phosphatidic acid binds to and activates ribosomal p70 S6 kinase independently of mTOR. *FASEB journal : official publication of the Federation of American Societies for Experimental Biology*. 2007; 21: 1075-87. 10.1096/fj.06-6652com.

140 Zhao C, Du G, Skowronek K, Frohman MA, Bar-Sagi D. Phospholipase D2-generated phosphatidic acid couples EGFR stimulation to Ras activation by Sos. *Nature cell biology*. 2007; 9: 706-12. 10.1038/ncb1594.

141 Rizzo MA, Shome K, Watkins SC, Romero G. The recruitment of Raf-1 to membranes is mediated by direct interaction with phosphatidic acid and is independent of association with Ras. *J Biol Chem*. 2000; 275: 23911-8. 10.1074/jbc.M001553200.

142 Fang Y, Vilella-Bach M, Bachmann R, Flanigan A, Chen J. Phosphatidic acid-mediated mitogenic activation of mTOR signaling. *Science*. 2001; 294: 1942-5. 10.1126/science.1066015.

143 Frank C, Keilhack H, Opitz F, Zschornig O, Bohmer FD. Binding of phosphatidic acid to the protein-tyrosine phosphatase SHP-1 as a basis for activity modulation. *Biochemistry*. 1999; 38: 11993-2002.

144 Limatola C, Schaap D, Moolenaar WH, van Blitterswijk WJ. Phosphatidic acid activation of protein kinase C-zeta overexpressed in COS cells: comparison with other protein kinase C isotypes and other acidic lipids. *The Biochemical journal*. 1994; 304 (Pt 3): 1001-8.

145 Manifava M, Thuring JW, Lim ZY, Packman L, Holmes AB, Ktistakis NT. Differential binding of traffic-related proteins to phosphatidic acid- or phosphatidylinositol (4,5)-bisphosphate-coupled affinity reagents. *J Biol Chem*. 2001; 276: 8987-94. 10.1074/jbc.M010308200.

146 Becker KP, Hannun YA. Protein kinase C and phospholipase D: intimate interactions in intracellular signaling. *Cellular and molecular life sciences : CMLS*. 2005; 62: 1448-61. 10.1007/s00018-005-4531-7.

147 Ye X, Ishii I, Kingsbury MA, Chun J. Lysophosphatidic acid as a novel cell survival/apoptotic factor. *Biochim Biophys Acta*. 2002; 1585: 108-13.

148 Gomez-Cambronero J. Phosphatidic acid, phospholipase D and tumorigenesis. *Advances in biological regulation*. 2014; 54C: 197-206. 10.1016/j.jbior.2013.08.006.

149 Peng X, Frohman MA. Mammalian phospholipase D physiological and pathological roles. *Acta physiologica*. 2012; 204: 219-26. 10.1111/j.1748-1716.2011.02298.x.

150 Park JB, Lee CS, Jang JH, Ghim J, Kim YJ, You S, Hwang D, Suh PG, Ryu SH. Phospholipase signalling networks in cancer. *Nature reviews Cancer*. 2012; 12: 782-92. 10.1038/nrc3379.

151   Klein J. Functions and pathophysiological roles of phospholipase D in the brain. *Journal of neurochemistry*. 2005; 94: 1473-87. 10.1111/j.1471-4159.2005.03315.x.

152   Uchida N, Okamura S, Nagamachi Y, Yamashita S. Increased phospholipase D activity in human breast cancer. *Journal of cancer research and clinical oncology*. 1997; 123: 280-5.

153   Uchida N, Okamura S, Kuwano H. Phospholipase D activity in human gastric carcinoma. *Anticancer research*. 1999; 19: 671-5.

154   Chen Q, Hongu T, Sato T, Zhang Y, Ali W, Cavallo JA, van der Velden A, Tian H, Di Paolo G, Nieswandt B, Kanaho Y, Frohman MA. Key roles for the lipid signaling enzyme phospholipase d1 in the tumor microenvironment during tumor angiogenesis and metastasis. *Sci Signal*. 2012; 5: ra79. 10.1126/scisignal.2003257.

155   Medzhitov R. Origin and physiological roles of inflammation. *Nature*. 2008; 454: 428-35. 10.1038/nature07201.

156   Nishikimi A, Fukuhara H, Su W, Hongu T, Takasuga S, Mihara H, Cao Q, Sanematsu F, Kanai M, Hasegawa H, Tanaka Y, Shibasaki M, Kanaho Y, Sasaki T, Frohman MA, Fukui Y. Sequential regulation of DOCK2 dynamics by two phospholipids during neutrophil chemotaxis. *Science*. 2009; 324: 384-7. 10.1126/science.1170179.

157   Ali WH, Chen Q, Delgiorno KE, Su W, Hall JC, Hongu T, Tian H, Kanaho Y, Di Paolo G, Crawford HC, Frohman MA. Deficiencies of the lipid-signaling enzymes phospholipase D1 and D2 alter cytoskeletal organization, macrophage phagocytosis, and cytokine-stimulated neutrophil recruitment. *PLoS One*. 2013; 8: e55325. 10.1371/journal.pone.0055325.

158   Sato T, Hongu T, Sakamoto M, Funakoshi Y, Kanaho Y. Molecular mechanisms of N-formyl-methionyl-leucyl-phenylalanine-induced superoxide generation and degranulation in mouse neutrophils: phospholipase D is dispensable. *Mol Cell Biol*. 2013; 33: 136-45. 10.1128/MCB.00869-12.

159   Sethu S, Pushparaj PN, Melendez AJ. Phospholipase D1 mediates TNFalpha-induced inflammation in a murine model of TNFalpha-induced peritonitis. *PLoS One*. 2010; 5: e10506. 10.1371/journal.pone.0010506.

160   Tsukahara T, Tsukahara R, Fujiwara Y, Yue J, Cheng Y, Guo H, Bolen A, Zhang C, Balazs L, Re F, Du G, Frohman MA, Baker DL, Parrill AL, Uchiyama A, Kobayashi T, Murakami-Murofushi K, Tigyi G. Phospholipase D2-dependent inhibition of the nuclear hormone receptor PPARgamma by cyclic phosphatidic acid. *Molecular cell*. 2010; 39: 421-32. 10.1016/j.molcel.2010.07.022.

161   Hong KW, Jin HS, Lim JE, Cho YS, Go MJ, Jung J, Lee JE, Choi J, Shin C, Hwang SY, Lee SH, Park HK, Oh B. Non-synonymous single-nucleotide polymorphisms associated with blood pressure and hypertension. *Journal of human hypertension*. 2010; 24: 763-74. 10.1038/jhh.2010.9.

162   Wegener JW, Loga F, Stegner D, Nieswandt B, Hofmann F. Phospholipase D1 is involved in alpha1-adrenergic contraction of murine vascular smooth muscle. *FASEB journal : official publication of the Federation of American Societies for Experimental Biology*. 2013. 10.1096/fj.13-237925.

163   Asemu G, Dent MR, Singal T, Dhalla NS, Tappia PS. Differential changes in phospholipase D and phosphatidate phosphohydrolase activities in ischemia-reperfusion of rat heart. *Archives of biochemistry and biophysics*. 2005; 436: 136-44. 10.1016/j.abb.2005.02.002.

164   Degn M, Lambertsen KL, Petersen G, Meldgaard M, Artmann A, Clausen BH, Hansen SH, Finsen B, Hansen HS, Lund TM. Changes in brain levels of N-acylethanolamines and 2-arachidonoylglycerol in focal cerebral ischemia in mice. *Journal of neurochemistry*. 2007; 103: 1907-16. 10.1111/j.1471-4159.2007.04892.x.

165 Rubin R. Phosphatidylethanol formation in human platelets: evidence for thrombin-induced activation of phospholipase D. *Biochem Biophys Res Commun*. 1988; 156: 1090-6.

166 Martinson EA, Scheible S, Marx-Grunwitz A, Presek P. Secreted ADP plays a central role in thrombin-induced phospholipase D activation in human platelets. *Thrombosis and haemostasis*. 1998; 80: 976-81.

167 Haslam RJ, Coorssen JR. Evidence that activation of phospholipase D can mediate secretion from permeabilized platelets. *Advances in experimental medicine and biology*. 1993; 344: 149-64.

168 Martinson EA, Scheible S, Greinacher A, Presek P. Platelet phospholipase D is activated by protein kinase C via an integrin alpha IIb beta 3-independent mechanism. *The Biochemical journal*. 1995; 310 (Pt 2): 623-8.

169 Chiang TM. Activation of phospholipase D in human platelets by collagen and thrombin and its relationship to platelet aggregation. *Biochim Biophys Acta*. 1994; 1224: 147-55.

170 Vorland M, Holmsen H. Phospholipase D in human platelets: presence of isoenzymes and participation of autocrine stimulation during thrombin activation. *Platelets*. 2008; 19: 211-24. 10.1080/09537100701777329.

171 Huang R, Kucera GL, Rittenhouse SE. Elevated cytosolic Ca2+ activates phospholipase D in human platelets. *J Biol Chem*. 1991; 266: 1652-5.

172 Coorssen JR, Haslam RJ. GTP gamma S and phorbol ester act synergistically to stimulate both Ca(2+)-independent secretion and phospholipase D activity in permeabilized human platelets. Inhibition by BAPTA and analogues. *FEBS letters*. 1993; 316: 170-4.

173 Van der Meulen J, Haslam RJ. Phorbol ester treatment of intact rabbit platelets greatly enhances both the basal and guanosine 5'-[gamma-thio]triphosphate-stimulated phospholipase D activities of isolated platelet membranes. Physiological activation of phospholipase D may be secondary to activation of phospholipase C. *The Biochemical journal*. 1990; 271: 693-700.

174 Coorssen JR. Phospholipase activation and secretion: evidence that PLA2, PLC, and PLD are not essential to exocytosis. *The American journal of physiology*. 1996; 270: C1153-63.

175 Kaul D, Kochhar N, Singh J. Lipoprotein receptor 'CK'--dependent signalling in human platelets. *Molecular and cellular biochemistry*. 1995; 151: 173-6.

176 Kochhar N, Kaul D. Initiator-promoter coupling of phospholipases D and A2 in platelets upon cholesterol incorporation. *FEBS letters*. 1992; 314: 17-9.

177 Hashizume T, Taniguchi M, Sato T, Fujii T. Arachidonic acid liberation induced by phosphatidic acid endogenously generated from membrane phospholipids in rabbit platelets. *Biochim Biophys Acta*. 1994; 1221: 179-84.

178 Nofer JR, Walter M, Kehrel B, Seedorf U, Assmann G. HDL3 activates phospholipase D in normal but not in glycoprotein IIb/IIIa-deficient platelets. *Biochem Biophys Res Commun*. 1995; 207: 148-54. 10.1006/bbrc.1995.1165.

179 Holinstat M, Voss B, Bilodeau ML, Hamm HE. Protease-activated receptors differentially regulate human platelet activation through a phosphatidic acid-dependent pathway. *Mol Pharmacol*. 2007; 71: 686-94. 10.1124/mol.106.029371.

180 Call FL, 2nd, Williams WJ. Phosphatidate phosphatase in human platelets. *The Journal of laboratory and clinical medicine*. 1973; 82: 663-73.

181 Fukami MH, Holmsen H. Diacylglycerol elevations in control platelets are unaccompanied by pleckstrin phosphorylation. Implications for the role of diacylglycerol in platelet activation. *European journal of biochemistry / FEBS*. 1995; 228: 579-86.

182   Nakashima S, Suganuma A, Matsui A, Nozawa Y. Thrombin induces a biphasic 1,2-diacylglycerol production in human platelets. *The Biochemical journal*. 1991; 275 (Pt 2): 355-61.

183   Preiss J, Loomis CR, Bishop WR, Stein R, Niedel JE, Bell RM. Quantitative measurement of sn-1,2-diacylglycerols present in platelets, hepatocytes, and ras- and sis-transformed normal rat kidney cells. *J Biol Chem*. 1986; 261: 8597-600.

184   Chen W, Thielmann I, Gupta S, Subramanian H, Stegner D, van Kruchten R, Dietrich A, Gambaryan S, Heemskerk J, Hermanns H, Nieswandt B, Braun A. Orai1-induced store-operated calcium entry enhances phospholipase activity and modulates TRPC6 function in murine platelets. *Journal of Thrombosis and Haemostasis*. 2013.

185   Vorland M, Holmsen H. Phospholipase D activity in human platelets is inhibited by protein kinase A, involving inhibition of phospholipase D1 translocation. *Platelets*. 2008; 19: 300-7. 10.1080/09537100801910838.

186   Kodaki T, Yamashita S. Cloning, expression, and characterization of a novel phospholipase D complementary DNA from rat brain. *J Biol Chem*. 1997; 272: 11408-13.

187   Heung YM, Postle AD. The molecular selectivity of phospholipase D in HL60 granulocytes. *FEBS letters*. 1995; 364: 250-4.

188   Elvers M, Grenegard M, Khoshjabinzadeh H, Munzer P, Borst O, Tian H, Di Paolo G, Lang F, Gawaz M, Lindahl TL, Falker K. A novel role for phospholipase D as an endogenous negative regulator of platelet sensitivity. *Cellular signalling*. 2012; 24: 1743-52. 10.1016/j.cellsig.2012.04.018.

189   Su W, Yeku O, Olepu S, Genna A, Park JS, Ren H, Du G, Gelb MH, Morris AJ, Frohman MA. 5-Fluoro-2-indolyl des-chlorohalopemide (FIPI), a phospholipase D pharmacological inhibitor that alters cell spreading and inhibits chemotaxis. *Molecular Pharmacology*. 2009; 75: 437-46.

190   Scott SA, Selvy PE, Buck JR, Cho HP, Criswell TL, Thomas AL, Armstrong MD, Arteaga CL, Lindsley CW, Brown HA. Design of isoform-selective phospholipase D inhibitors that modulate cancer cell invasiveness. *Nature chemical biology*. 2009; 5: 108-17. 10.1038/nchembio.140.

191   Lewis JA, Scott SA, Lavieri R, Buck JR, Selvy PE, Stoops SL, Armstrong MD, Brown HA, Lindsley CW. Design and synthesis of isoform-selective phospholipase D (PLD) inhibitors. Part I: Impact of alternative halogenated privileged structures for PLD1 specificity. *Bioorganic & medicinal chemistry letters*. 2009; 19: 1916-20. 10.1016/j.bmcl.2009.02.057.

192   Monovich L, Mugrage B, Quadros E, Toscano K, Tommasi R, LaVoie S, Liu E, Du Z, LaSala D, Boyar W, Steed P. Optimization of halopemide for phospholipase D2 inhibition. *Bioorganic & medicinal chemistry letters*. 2007; 17: 2310-1. 10.1016/j.bmcl.2007.01.059.

193   Bonser RW, Thompson NT, Randall RW, Garland LG. Phospholipase D activation is functionally linked to superoxide generation in the human neutrophil. *The Biochemical journal*. 1989; 264: 617-20.

194   Loonen AJ, Soudijn W. Halopemide, a new psychotropic agent. Cerebral distribution and receptor interactions. *Pharmaceutisch weekblad Scientific edition*. 1985; 7: 1-9.

195   Knight CG, Morton LF, Onley DJ, Peachey AR, Ichinohe T, Okuma M, Farndale RW, Barnes MJ. Collagen-platelet interaction: Gly-Pro-Hyp is uniquely specific for platelet Gp VI and mediates platelet activation by collagen. *Cardiovasc Res*. 1999; 41: 450-7. S0008-6363(98)00306-X [pii].

196   Massberg S, Gawaz M, Gruner S, Schulte V, Konrad I, Zohlnhofer D, Heinzmann U, Nieswandt B. A crucial role of glycoprotein VI for platelet recruitment to the injured arterial wall in vivo. *J Exp Med*. 2003; 197: 41-9.

197   Nieswandt B, Bergmeier W, Rackebrandt K, Gessner JE, Zirngibl H. Identification of critical antigen-specific mechanisms in the development of immune thrombocytopenic purpura in mice. *Blood*. 2000; 96: 2520-7.

198   Nieswandt B, Schulte V, Bergmeier W, Mokhtari-Nejad R, Rackebrandt K, Cazenave JP, Ohlmann P, Gachet C, Zirngibl H. Long-term antithrombotic protection by in vivo depletion of platelet glycoprotein VI in mice. *J Exp Med*. 2001; 193: 459-69.

199   Gruner S, Prostredna M, Schulte V, Krieg T, Eckes B, Brakebusch C, Nieswandt B. Multiple integrin-ligand interactions synergize in shear-resistant platelet adhesion at sites of arterial injury in vivo. *Blood*. 2003; 102: 4021-7. 10.1182/blood-2003-05-1391.

200   May F, Hagedorn I, Pleines I, Bender M, Vogtle T, Eble J, Elvers M, Nieswandt B. CLEC-2 is an essential platelet-activating receptor in hemostasis and thrombosis. *Blood*. 2009; 114: 3464-72. 10.1182/blood-2009-05-222273.

201   Bergmeier W, Schulte V, Brockhoff G, Bier U, Zirngibl H, Nieswandt B. Flow cytometric detection of activated mouse integrin alphaIIbbeta3 with a novel monoclonal antibody. *Cytometry*. 2002; 48: 80-6. 10.1002/cyto.10114.

202   Varga-Szabo D, Braun A, Kleinschnitz C, Bender M, Pleines I, Pham M, Renne T, Stoll G, Nieswandt B. The calcium sensor STIM1 is an essential mediator of arterial thrombosis and ischemic brain infarction. *J Exp Med*. 2008; 205: 1583-91. 10.1084/jem.20080302.

203   Braun A, Varga-Szabo D, Kleinschnitz C, Pleines I, Bender M, Austinat M, Bosl M, Stoll G, Nieswandt B. Orai1 (CRACM1) is the platelet SOC channel and essential for pathological thrombus formation. *Blood*. 2009; 113: 2056-63. 10.1182/blood-2008-07-171611.

204   Ackermann JA, Radtke D, Maurberger A, Winkler TH, Nitschke L. Grb2 regulates B-cell maturation, B-cell memory responses and inhibits B-cell Ca2+ signalling. *Embo J*. 2011; 30: 1621-33. 10.1038/emboj.2011.74.

205   Moers A, Nieswandt B, Massberg S, Wettschureck N, Gruner S, Konrad I, Schulte V, Aktas B, Gratacap MP, Simon MI, Gawaz M, Offermanns S. G13 is an essential mediator of platelet activation in hemostasis and thrombosis. *Nat Med*. 2003; 9: 1418-22. 10.1038/nm943.

206   Jackson B, Peyrollier K, Pedersen E, Basse A, Karlsson R, Wang Z, Lefever T, Ochsenbein AM, Schmidt G, Aktories K, Stanley A, Quondamatteo F, Ladwein M, Rottner K, van Hengel J, Brakebusch C. RhoA is dispensable for skin development, but crucial for contraction and directed migration of keratinocytes. *Mol Biol Cell*. 2011; 22: 593-605. 10.1091/mbc.E09-10-0859.

207   Chrostek A, Wu X, Quondamatteo F, Hu R, Sanecka A, Niemann C, Langbein L, Haase I, Brakebusch C. Rac1 is crucial for hair follicle integrity but is not essential for maintenance of the epidermis. *Mol Cell Biol*. 2006; 26: 6957-70. 10.1128/MCB.00075-06.

208   Wu X, Quondamatteo F, Lefever T, Czuchra A, Meyer H, Chrostek A, Paus R, Langbein L, Brakebusch C. Cdc42 controls progenitor cell differentiation and beta-catenin turnover in skin. *Genes Dev*. 2006; 20: 571-85. 10.1101/gad.361406.

209   Nieswandt B, Moser M, Pleines I, Varga-Szabo D, Monkley S, Critchley D, Fassler R. Loss of talin1 in platelets abrogates integrin activation, platelet aggregation, and thrombus formation in vitro and in vivo. *J Exp Med*. 2007; 204: 3113-8. 10.1084/jem.20071827.

210   Gurniak CB, Perlas E, Witke W. The actin depolymerizing factor n-cofilin is essential for neural tube morphogenesis and neural crest cell migration. *Dev Biol*. 2005; 278: 231-41. 10.1016/j.ydbio.2004.11.010.

211   Tiedt R, Schomber T, Hao-Shen H, Skoda RC. Pf4-Cre transgenic mice allow the generation of lineage-restricted gene knockouts for studying megakaryocyte and platelet function in vivo. *Blood*. 2007; 109: 1503-6. 10.1182/blood-2006-04-020362.

212   Martin V, Guillermet-Guibert J, Chicanne G, Cabou C, Jandrot-Perrus M, Plantavid M, Vanhaesebroeck B, Payrastre B, Gratacap MP. Deletion of the p110beta isoform of phosphoinositide 3-kinase in platelets reveals its central role in Akt activation and thrombus formation in vitro and in vivo. *Blood*. 2010; 115: 2008-13. 10.1182/blood-2009-04-217224.

213   Pfeifhofer C, Kofler K, Gruber T, Tabrizi NG, Lutz C, Maly K, Leitges M, Baier G. Protein kinase C theta affects Ca2+ mobilization and NFAT cell activation in primary mouse T cells. *J Exp Med*. 2003; 197: 1525-35. 10.1084/jem.20020234.

214   Pfeifhofer C, Gruber T, Letschka T, Thuille N, Lutz-Nicoladoni C, Hermann-Kleiter N, Braun U, Leitges M, Baier G. Defective IgG2a/2b class switching in PKC alpha-/- mice. *Journal of immunology*. 2006; 176: 6004-11.

215   Leitges M, Schmedt C, Guinamard R, Davoust J, Schaal S, Stabel S, Tarakhovsky A. Immunodeficiency in protein kinase cbeta-deficient mice. *Science*. 1996; 273: 788-91.

216   Bandyopadhyay G, Standaert ML, Sajan MP, Kanoh Y, Miura A, Braun U, Kruse F, Leitges M, Farese RV. Protein kinase C-lambda knockout in embryonic stem cells and adipocytes impairs insulin-stimulated glucose transport. *Molecular endocrinology*. 2004; 18: 373-83. 10.1210/me.2003-0087.

217   Grosse J, Braun A, Varga-Szabo D, Beyersdorf N, Schneider B, Zeitlmann L, Hanke P, Schropp P, Muhlstedt S, Zorn C, Huber M, Schmittwolf C, Jagla W, Yu P, Kerkau T, Schulze H, Nehls M, Nieswandt B. An EF hand mutation in Stim1 causes premature platelet activation and bleeding in mice. *JClinInvest*. 2007; 117: 3540-50.

218   Dirnagl U. Bench to bedside: the quest for quality in experimental stroke research. *Journal of cerebral blood flow and metabolism : official journal of the International Society of Cerebral Blood Flow and Metabolism*. 2006; 26: 1465-78. 10.1038/sj.jcbfm.9600298.

219   Kleinschnitz C, Pozgajova M, Pham M, Bendszus M, Nieswandt B, Stoll G. Targeting platelets in acute experimental stroke: impact of glycoprotein Ib, VI, and IIb/IIIa blockade on infarct size, functional outcome, and intracranial bleeding. *Circulation*. 2007; 115: 2323-30.

220   Charo IF, Feinman RD, Detwiler TC, Smith JB, Ingerman CM, Silver MJ. Prostaglandin endoperoxides and thromboxane A2 can induce platelet aggregation in the absence of secretion. *Nature*. 1977; 269: 66-9.

221   Rudge SA, Wakelam MJ. Inter-regulatory dynamics of phospholipase D and the actin cytoskeleton. *Biochim Biophys Acta*. 2009; 1791: 856-61. S1388-1981(09)00106-1 [pii]10.1016/j.bbalip.2009.04.008.

222   Tucker KL, Sage T, Gibbins JM. Clot retraction. *Methods in molecular biology*. 2012; 788: 101-7. 10.1007/978-1-61779-307-3_8.

223   Nieswandt B, Kleinschnitz C, Stoll G. Ischaemic stroke: a thrombo-inflammatory disease? *J Physiol*. 2011; 589: 4115-23. 10.1113/jphysiol.2011.212886.

224   Stoll G, Kleinschnitz C, Nieswandt B. Combating innate inflammation: a new paradigm for acute treatment of stroke? *Annals of the New York Academy of Sciences*. 2010; 1207: 149-54. 10.1111/j.1749-6632.2010.05730.x.

225   Norton LJ, Zhang Q, Saqib KM, Schrewe H, Macura K, Anderson KE, Lindsley CW, Brown HA, Rudge SA, Wakelam MJ. PLD1 rather than PLD2 regulates phorbol-ester-, adhesion-dependent and Fc{gamma}-receptor-stimulated ROS production in neutrophils. *J Cell Sci*. 2011; 124: 1973-83. 10.1242/jcs.082008.

226   Di Fulvio M, Gomez-Cambronero J. Phospholipase D (PLD) gene expression in human neutrophils and HL-60 differentiation. *J Leukoc Biol*. 2005; 77: 999-1007. 10.1189/jlb.1104684.

227   Mor A, Wynne JP, Ahearn IM, Dustin ML, Du G, Philips MR. Phospholipase D1 regulates lymphocyte adhesion via upregulation of Rap1 at the plasma membrane. *Mol Cell Biol*. 2009; 29: 3297-306. 10.1128/MCB.00366-09.

228 Fujita Y, Hiroyama M, Sanbe A, Yamauchi J, Murase S, Tanoue A. ETOH inhibits embryonic neural stem/precursor cell proliferation via PLD signaling. *Biochem Biophys Res Commun*. 2008; 370: 169-73. 10.1016/j.bbrc.2008.03.060.

229 Kim M, Moon C, Kim H, Shin MK, Min do S, Shin T. Developmental levels of phospholipase D isozymes in the brain of developing rats. *Acta histochemica*. 2010; 112: 81-91. 10.1016/j.acthis.2008.09.004.

230 Cadroy Y, Hanson SR, Kelly AB, Marzec UM, Evatt BL, Kunicki TJ, Montgomery RR, Harker LA. Relative antithrombotic effects of monoclonal antibodies targeting different platelet glycoprotein-adhesive molecule interactions in nonhuman primates. *Blood*. 1994; 83: 3218-24.

231 De Candia E. Mechanisms of platelet activation by thrombin: a short history. *Thrombosis research*. 2012; 129: 250-6. 10.1016/j.thromres.2011.11.001.

232 Kauffenstein G, Bergmeier W, Eckly A, Ohlmann P, Leon C, Cazenave JP, Nieswandt B, Gachet C. The P2Y(12) receptor induces platelet aggregation through weak activation of the alpha(IIb)beta(3) integrin--a phosphoinositide 3-kinase-dependent mechanism. *FEBS letters*. 2001; 505: 281-90.

233 Heemskerk JW, Vuist WM, Feijge MA, Reutelingsperger CP, Lindhout T. Collagen but not fibrinogen surfaces induce bleb formation, exposure of phosphatidylserine, and procoagulant activity of adherent platelets: evidence for regulation by protein tyrosine kinase-dependent Ca2+ responses. *Blood*. 1997; 90: 2615-25.

234 Reverter JC, Beguin S, Kessels H, Kumar R, Hemker HC, Coller BS. Inhibition of platelet-mediated, tissue factor-induced thrombin generation by the mouse/human chimeric 7E3 antibody. Potential implications for the effect of c7E3 Fab treatment on acute thrombosis and "clinical restenosis". *J Clin Invest*. 1996; 98: 863-74. 10.1172/JCI118859.

235 Heemskerk JW, Bevers EM, Lindhout T. Platelet activation and blood coagulation. *Thrombosis and haemostasis*. 2002; 88: 186-93.

236 Su W, Chen Q, Frohman MA. Targeting phospholipase D with small-molecule inhibitors as a potential therapeutic approach for cancer metastasis. *Future Oncol*. 2009; 5: 1477-86. 10.2217/fon.09.110.

237 Stegner D, Thielmann I, Kraft P, Frohman MA, Stoll G, Nieswandt B. Pharmacological inhibition of phospholipase D protects mice from occlusive thrombus formation and ischemic stroke--brief report. *Arterioscler Thromb Vasc Biol*. 2013; 33: 2212-7. 10.1161/ATVBAHA.113.302030.

238 Kellert L, Hametner C, Rohde S, Bendszus M, Hacke W, Ringleb P, Stampfl S. Endovascular stroke therapy: tirofiban is associated with risk of fatal intracerebral hemorrhage and poor outcome. *Stroke*. 2013; 44: 1453-5. 10.1161/STROKEAHA.111.000502.

239 Adams HP, Jr., Effron MB, Torner J, Davalos A, Frayne J, Teal P, Leclerc J, Oemar B, Padgett L, Barnathan ES, Hacke W. Emergency administration of abciximab for treatment of patients with acute ischemic stroke: results of an international phase III trial: Abciximab in Emergency Treatment of Stroke Trial (AbESTT-II). *Stroke*. 2008; 39: 87-99. 10.1161/STROKEAHA.106.476648.

240 Montaguti P, Melloni E, Cavalletti E. Acute intravenous toxicity of dimethyl sulfoxide, polyethylene glycol 400, dimethylformamide, absolute ethanol, and benzyl alcohol in inbred mouse strains. *Arzneimittel-Forschung*. 1994; 44: 566-70.

241 Rodgers RP, Levin J. A critical reappraisal of the bleeding time. *Seminars in thrombosis and hemostasis*. 1990; 16: 1-20. 10.1055/s-2007-1002658.

242 Dutting S, Vogtle T, Morowski M, Schiessl S, Schafer CM, Watson SK, Hughes CE, Ackermann JA, Radtke D, Hermanns HM, Watson S, Nitschke L, Nieswandt B. Grb2 Contributes to (hem)ITAM-Mediated Signaling in Platelets. *Circulation research*. 2013. 10.1161/CIRCRESAHA.114.302670.

243 Siddiqi AR, Smith JL, Ross AH, Qiu RG, Symons M, Exton JH. Regulation of phospholipase D in HL60 cells. Evidence for a cytosolic phospholipase D. *J Biol Chem*. 1995; 270: 8466-73.

244 Pertile P, Liscovitch M, Chalifa V, Cantley LC. Phosphatidylinositol 4,5-bisphosphate synthesis is required for activation of phospholipase D in U937 cells. *J Biol Chem*. 1995; 270: 5130-5.

245 Andrews RK, Booth WJ, Gorman JJ, Castaldi PA, Berndt MC. Purification of botrocetin from Bothrops jararaca venom. Analysis of the botrocetin-mediated interaction between von Willebrand factor and the human platelet membrane glycoprotein Ib-IX complex. *Biochemistry*. 1989; 28: 8317-26.

246 De Luca M, Facey DA, Favaloro EJ, Hertzberg MS, Whisstock JC, McNally T, Andrews RK, Berndt MC. Structure and function of the von Willebrand factor A1 domain: analysis with monoclonal antibodies reveals distinct binding sites involved in recognition of the platelet membrane glycoprotein Ib-IX-V complex and ristocetin-dependent activation. *Blood*. 2000; 95: 164-72.

247 Clemetson KJ, Clemetson JM. Platelet GPIb complex as a target for anti-thrombotic drug development. *Thrombosis and haemostasis*. 2008; 99: 473-9. 10.1160/TH07-12-0718.

248 Lian L, Wang Y, Draznin J, Eslin D, Bennett JS, Poncz M, Wu D, Abrams CS. The relative role of PLCbeta and PI3Kgamma in platelet activation. *Blood*. 2005; 106: 110-7. 10.1182/blood-2004-05-2005.

249 Morello F, Perino A, Hirsch E. Phosphoinositide 3-kinase signalling in the vascular system. *Cardiovasc Res*. 2009; 82: 261-71. 10.1093/cvr/cvn325.

250 Pleines I, Hagedorn I, Gupta S, May F, Chakarova L, van Hengel J, Offermanns S, Krohne G, Kleinschnitz C, Brakebusch C, Nieswandt B. Megakaryocyte-specific RhoA deficiency causes macrothrombocytopenia and defective platelet activation in hemostasis and thrombosis. *Blood*. 2012; 119: 1054-63. 10.1182/blood-2011-08-372193.

251 Pleines I, Elvers M, Strehl A, Pozgajova M, Varga-Szabo D, May F, Chrostek-Grashoff A, Brakebusch C, Nieswandt B. Rac1 is essential for phospholipase C-gamma2 activation in platelets. *Pflugers Archiv : European journal of physiology*. 2009; 457: 1173-85. 10.1007/s00424-008-0573-7.

252 Pleines I, Eckly A, Elvers M, Hagedorn I, Eliautou S, Bender M, Wu X, Lanza F, Gachet C, Brakebusch C, Nieswandt B. Multiple alterations of platelet functions dominated by increased secretion in mice lacking Cdc42 in platelets. *Blood*. 2010; 115: 3364-73. 10.1182/blood-2009-09-242271.

253 Prasad KS, Andre P, He M, Bao M, Manganello J, Phillips DR. Soluble CD40 ligand induces beta3 integrin tyrosine phosphorylation and triggers platelet activation by outside-in signaling. *Proc Natl Acad Sci U S A*. 2003; 100: 12367-71. 10.1073/pnas.2032886100.

254 Bender M, Eckly A, Hartwig JH, Elvers M, Pleines I, Gupta S, Krohne G, Jeanclos E, Gohla A, Gurniak C, Gachet C, Witke W, Nieswandt B. ADF/n-cofilin-dependent actin turnover determines platelet formation and sizing. *Blood*. 2010; 116: 1767-75. 10.1182/blood-2010-03-274340.

255 Neidt EM, Scott BJ, Kovar DR. Formin differentially utilizes profilin isoforms to rapidly assemble actin filaments. *The Journal of biological chemistry*. 2009; 284: 673-84. 10.1074/jbc.M804201200.

256 Moseley JB, Okada K, Balcer HI, Kovar DR, Pollard TD, Goode BL. Twinfilin is an actin-filament-severing protein and promotes rapid turnover of actin structures in vivo. *J Cell Sci*. 2006; 119: 1547-57. 10.1242/jcs.02860.

257 Varga-Szabo D, Pleines I, Nieswandt B. Cell adhesion mechanisms in platelets. *Arterioscler Thromb Vasc Biol*. 2008; 28: 403-12. 10.1161/ATVBAHA.107.150474.

258 Konopatskaya O, Gilio K, Harper MT, Zhao Y, Cosemans JM, Karim ZA, Whiteheart SW, Molkentin JD, Verkade P, Watson SP, Heemskerk JW, Poole AW. PKCalpha regulates platelet granule secretion and thrombus formation in mice. *J Clin Invest*. 2009; 119: 399-407. 10.1172/JCI34665.

259 Gilio K, Harper MT, Cosemans JM, Konopatskaya O, Munnix IC, Prinzen L, Leitges M, Liu Q, Molkentin JD, Heemskerk JW, Poole AW. Functional divergence of platelet protein kinase C (PKC) isoforms in thrombus formation on collagen. *The Journal of biological chemistry*. 2010; 285: 23410-9. 10.1074/jbc.M110.136176.

260 Heemskerk JW, Farndale RW, Sage SO. Effects of U73122 and U73343 on human platelet calcium signalling and protein tyrosine phosphorylation. *Biochim Biophys Acta*. 1997; 1355: 81-8.

261 Feske S. Calcium signalling in lymphocyte activation and disease. *Nature reviews Immunology*. 2007; 7: 690-702. 10.1038/nri2152.

262 Thastrup O, Cullen PJ, Drobak BK, Hanley MR, Dawson AP. Thapsigargin, a tumor promoter, discharges intracellular Ca2+ stores by specific inhibition of the endoplasmic reticulum Ca2(+)-ATPase. *Proc Natl Acad Sci U S A*. 1990; 87: 2466-70.

263 Brown DL. Congenital bleeding disorders. *Current problems in pediatric and adolescent health care*. 2005; 35: 38-62. 10.1016/j.cppeds.2004.12.001.

264 Feigin VL, Lawes CM, Bennett DA, Anderson CS. Stroke epidemiology: a review of population-based studies of incidence, prevalence, and case-fatality in the late 20th century. *Lancet neurology*. 2003; 2: 43-53.

265 Stoll G, Kleinschnitz C, Nieswandt B. Molecular mechanisms of thrombus formation in ischemic stroke: novel insights and targets for treatment. *Blood*. 2008; 112: 3555-62. 10.1182/blood-2008-04-144758.

266 Nieswandt B, Pleines I, Bender M. Platelet adhesion and activation mechanisms in arterial thrombosis and ischaemic stroke. *J Thromb Haemost*. 2011; 9 Suppl 1: 92-104. 10.1111/j.1538-7836.2011.04361.x.

267 Mahankali M, Henkels KM, Alter G, Gomez-Cambronero J. Identification of the catalytic site of phospholipase D2 (PLD2) newly described guanine nucleotide exchange factor activity. *J Biol Chem*. 2012; 287: 41417-31. 10.1074/jbc.M112.383596.

268 Sung TC, Altshuller YM, Morris AJ, Frohman MA. Molecular analysis of mammalian phospholipase D2. *J Biol Chem*. 1999; 274: 494-502.

269 Tsegaye Y, Daasvatn KO, Holmsen H. Acyl specificity of phospholipases A2 and C in thrombin-stimulated human platelets. *Platelets*. 2002; 13: 31-5. 10.1080/09537100120111531.

270 Nieswandt B, Kleinschnitz C, Stoll G. Ischaemic stroke: a thrombo-inflammatory disease? *J Physiol*. 2011; 589: 4115-23. 10.1113/jphysiol.2011.212886.

271 Nurden AT. Platelets, inflammation and tissue regeneration. *Thrombosis and haemostasis*. 2011; 105 Suppl 1: S13-33. 10.1160/THS10-11-0720.

272 Simon DI, Chen Z, Xu H, Li CQ, Dong J, McIntire LV, Ballantyne CM, Zhang L, Furman MI, Berndt MC, Lopez JA. Platelet glycoprotein ibalpha is a counterreceptor for the leukocyte integrin Mac-1 (CD11b/CD18). *J Exp Med*. 2000; 192: 193-204.

273 Soriano SG, Coxon A, Wang YF, Frosch MP, Lipton SA, Hickey PR, Mayadas TN. Mice deficient in Mac-1 (CD11b/CD18) are less susceptible to cerebral ischemia/reperfusion injury. *Stroke*. 1999; 30: 134-9.

274 Pettitt TR, McDermott M, Saqib KM, Shimwell N, Wakelam MJ. Phospholipase D1b and D2a generate structurally identical phosphatidic acid species in mammalian cells. *The Biochemical journal*. 2001; 360: 707-15.

275 Jenkins GM, Frohman MA. Phospholipase D: a lipid centric review. *Cellular and molecular life sciences : CMLS*. 2005; 62: 2305-16. 10.1007/s00018-005-5195-z.

276 Wang X, Devaiah SP, Zhang W, Welti R. Signaling functions of phosphatidic acid. *Progress in lipid research*. 2006; 45: 250-78. 10.1016/j.plipres.2006.01.005.

277 Jang JH, Lee CS, Hwang D, Ryu SH. Understanding of the roles of phospholipase D and phosphatidic acid through their binding partners. *Progress in lipid research*. 2012; 51: 71-81. 10.1016/j.plipres.2011.12.003.

278 Blair P, Flaumenhaft R. Platelet alpha-granules: basic biology and clinical correlates. *Blood reviews*. 2009; 23: 177-89. 10.1016/j.blre.2009.04.001.

279 Ren Q, Barber HK, Crawford GL, Karim ZA, Zhao C, Choi W, Wang CC, Hong W, Whiteheart SW. Endobrevin/VAMP-8 is the primary v-SNARE for the platelet release reaction. *Mol Biol Cell*. 2007; 18: 24-33. 10.1091/mbc.E06-09-0785.

280 Holinstat M, Preininger AM, Milne SB, Hudson WJ, Brown HA, Hamm HE. Irreversible platelet activation requires protease-activated receptor 1-mediated signaling to phosphatidylinositol phosphates. *Mol Pharmacol*. 2009; 76: 301-13. 10.1124/mol.109.056622.

281 Werner MH, Bielawska AE, Hannun YA. Quantitative analysis of diacylglycerol second messengers in human platelets: correlation with aggregation and secretion. *Mol Pharmacol*. 1992; 41: 382-6.

282 Elvers M, Pozgaj R, Pleines I, May F, Kuijpers MJ, Heemskerk JM, Yu P, Nieswandt B. Platelet hyperreactivity and a prothrombotic phenotype in mice with a gain-of-function mutation in phospholipase Cgamma2. *J Thromb Haemost*. 2010; 8: 1353-63. 10.1111/j.1538-7836.2010.03838.x.

283 Powner DJ, Pettitt TR, Anderson R, Nash GB, Wakelam MJ. Stable adhesion and migration of human neutrophils requires phospholipase D-mediated activation of the integrin CD11b/CD18. *Molecular immunology*. 2007; 44: 3211-21. 10.1016/j.molimm.2007.01.033.

284 Snell DC, Schulte V, Jarvis GE, Arase K, Sakurai D, Saito T, Watson SP, Nieswandt B. Differential effects of reduced glycoprotein VI levels on activation of murine platelets by glycoprotein VI ligands. *The Biochemical journal*. 2002; 368: 293-300. 10.1042/BJ20020335.

285 Cheli Y, Jensen D, Marchese P, Habart D, Wiltshire T, Cooke M, Fernandez JA, Ware J, Ruggeri ZM, Kunicki TJ. The Modifier of hemostasis (Mh) locus on chromosome 4 controls in vivo hemostasis of Gp6-/- mice. *Blood*. 2008; 111: 1266-73. 10.1182/blood-2007-09-111369.

286 Kuijpers MJ, Schulte V, Oury C, Lindhout T, Broers J, Hoylaerts MF, Nieswandt B, Heemskerk JW. Facilitating roles of murine platelet glycoprotein Ib and alphaIIbbeta3 in phosphatidylserine exposure during vWF-collagen-induced thrombus formation. *J Physiol*. 2004; 558: 403-15. 10.1113/jphysiol.2004.062414.

287 Maxwell MJ, Westein E, Nesbitt WS, Giuliano S, Dopheide SM, Jackson SP. Identification of a 2-stage platelet aggregation process mediating shear-dependent thrombus formation. *Blood*. 2007; 109: 566-76. 10.1182/blood-2006-07-028282.

288 Goto S, Ikeda Y, Saldivar E, Ruggeri ZM. Distinct mechanisms of platelet aggregation as a consequence of different shearing flow conditions. *J Clin Invest*. 1998; 101: 479-86. 10.1172/JCI973.

289 Berndt MC, Shen Y, Dopheide SM, Gardiner EE, Andrews RK. The vascular biology of the glycoprotein Ib-IX-V complex. *Thrombosis and haemostasis*. 2001; 86: 178-88.

290 Hughan SC, Spring CM, Schoenwaelder SM, Sturgeon S, Alwis I, Yuan Y, McFadyen JD, Westein E, Goddard D, Ono A, Yamanashi Y, Nesbitt WS, Jackson SP. Dok-2 regulates the shear-dependent adhesive function of platelet integrin alphaIIbbeta3 in mice. *J Biol Chem*. 2014. 10.1074/jbc.M113.520148.

291 Kasirer-Friede A, Ruggeri ZM, Shattil SJ. Role for ADAP in shear flow-induced platelet mechanotransduction. *Blood*. 2010; 115: 2274-82. 10.1182/blood-2009-08-238238.

292   Kleinschnitz C, De Meyer SF, Schwarz T, Austinat M, Vanhoorelbeke K, Nieswandt B, Deckmyn H, Stoll G. Deficiency of von Willebrand factor protects mice from ischemic stroke. *Blood*. 2009; 113: 3600-3. 10.1182/blood-2008-09-180695.

293   Deppermann C, Cherpokova D, Nurden P, Schulz JN, Thielmann I, Kraft P, Vogtle T, Kleinschnitz C, Dutting S, Krohne G, Eming SA, Nurden AT, Eckes B, Stoll G, Stegner D, Nieswandt B. Gray platelet syndrome and defective thrombo-inflammation in Nbeal2-deficient mice. *J Clin Invest*. 2013. 10.1172/JCI69210.

294   Stegner D, Deppermann C, Kraft P, Morowski M, Kleinschnitz C, Stoll G, Nieswandt B. Munc13-4-mediated secretion is essential for infarct progression but not intracranial hemostasis in acute stroke. *J Thromb Haemost*. 2013; 11: 1430-3. 10.1111/jth.12293.

295   Sanematsu F, Nishikimi A, Watanabe M, Hongu T, Tanaka Y, Kanaho Y, Cote JF, Fukui Y. Phosphatidic acid-dependent recruitment and function of the Rac activator DOCK1 during dorsal ruffle formation. *The Journal of biological chemistry*. 2013; 288: 8092-100. 10.1074/jbc.M112.410423.

296   O'Reilly MC, Scott SA, Brown KA, Oguin TH, 3rd, Thomas PG, Daniels JS, Morrison R, Brown HA, Lindsley CW. Development of dual PLD1/2 and PLD2 selective inhibitors from a common 1,3,8-Triazaspiro[4.5]decane Core: discovery of Ml298 and Ml299 that decrease invasive migration in U87-MG glioblastoma cells. *Journal of medicinal chemistry*. 2013; 56: 2695-9. 10.1021/jm301782e.

297   Bender M, May F, Lorenz V, Thielmann I, Hagedorn I, Finney BA, Vogtle T, Remer K, Braun A, Bosl M, Watson SP, Nieswandt B. Combined in vivo depletion of glycoprotein VI and C-type lectin-like receptor 2 severely compromises hemostasis and abrogates arterial thrombosis in mice. *Arterioscler Thromb Vasc Biol*. 2013; 33: 926-34. 10.1161/ATVBAHA.112.300672.

298   Boulaftali Y, Hess PR, Getz TM, Cholka A, Stolla M, Mackman N, Owens AP, 3rd, Ware J, Kahn ML, Bergmeier W. Platelet ITAM signaling is critical for vascular integrity in inflammation. *J Clin Invest*. 2013; 123: 908-16. 10.1172/JCI65154.

299   Konigsberger S, Prodohl J, Stegner D, Weis V, Andreas M, Stehling M, Schumacher T, Bohmer R, Thielmann I, van Eeuwijk JM, Nieswandt B, Kiefer F. Altered BCR signalling quality predisposes to autoimmune disease and a pre-diabetic state. *Embo J*. 2012; 31: 3363-74. 10.1038/emboj.2012.169.

300   Ramanathan G, Gupta S, Thielmann I, Pleines I, Varga-Szabo D, May F, Mannhalter C, Dietrich A, Nieswandt B, Braun A. Defective diacylglycerol-induced Ca2+ entry but normal agonist-induced activation responses in TRPC6-deficient mouse platelets. *J Thromb Haemost*. 2012; 10: 419-29. 10.1111/j.1538-7836.2011.04596.x.

301   Hagedorn I, Schmidbauer S, Pleines I, Kleinschnitz C, Kronthaler U, Stoll G, Dickneite G, Nieswandt B. Factor XIIa inhibitor recombinant human albumin Infestin-4 abolishes occlusive arterial thrombus formation without affecting bleeding. *Circulation*. 2010; 121: 1510-7. 10.1161/CIRCULATIONAHA.109.924761.

302   Kleinschnitz C, Stoll G, Bendszus M, Schuh K, Pauer HU, Burfeind P, Renne C, Gailani D, Nieswandt B, Renne T. Targeting coagulation factor XII provides protection from pathological thrombosis in cerebral ischemia without interfering with hemostasis. *J Exp Med*. 2006; 203: 513-8. 10.1084/jem.20052458.

303   Renne T, Pozgajova M, Gruner S, Schuh K, Pauer HU, Burfeind P, Gailani D, Nieswandt B. Defective thrombus formation in mice lacking coagulation factor XII. *J Exp Med*. 2005; 202: 271-81. 10.1084/jem.20050664.

304   Larsson M, Rayzman V, Nolte MW, Nickel KF, Bjorkqvist J, Jamsa A, Hardy MP, Fries M, Schmidbauer S, Hedenqvist P, Broome M, Pragst I, Dickneite G, Wilson MJ, Nash AD, Panousis C, Renne T. A Factor XIIa Inhibitory Antibody Provides Thromboprotection in Extracorporeal Circulation Without Increasing Bleeding Risk. *Science translational medicine*. 2014; 6: 222ra17. 10.1126/scitranslmed.3006804.

305   Horn J, Lopez I, Miller MW, Gomez-Cambronero J. The uncovering of a novel regulatory mechanism for PLD2: formation of a ternary complex with protein tyrosine phosphatase PTP1B and growth factor receptor-bound protein GRB2. *Biochem Biophys Res Commun*. 2005; 332: 58-67. 10.1016/j.bbrc.2005.04.093.

306   Toschi A, Lee E, Xu L, Garcia A, Gadir N, Foster DA. Regulation of mTORC1 and mTORC2 complex assembly by phosphatidic acid: competition with rapamycin. *Mol Cell Biol*. 2009; 29: 1411-20. 10.1128/MCB.00782-08.

307   Hodson EA, Ashley CC, Hughes AD, Lymn JS. Regulation of phospholipase C-delta by GTP-binding proteins-rhoA as an inhibitory modulator. *Biochim Biophys Acta*. 1998; 1403: 97-101.

308   Wing MR, Snyder JT, Sondek J, Harden TK. Direct activation of phospholipase C-epsilon by Rho. *J Biol Chem*. 2003; 278: 41253-8. 10.1074/jbc.M306904200.

309   Pandey D, Goyal P, Dwivedi S, Siess W. Unraveling a novel Rac1-mediated signaling pathway that regulates cofilin dephosphorylation and secretion in thrombin-stimulated platelets. *Blood*. 2009; 114: 415-24. 10.1182/blood-2008-10-183582.

310   Cox EA, Sastry SK, Huttenlocher A. Integrin-mediated adhesion regulates cell polarity and membrane protrusion through the Rho family of GTPases. *Mol Biol Cell*. 2001; 12: 265-77.

311   Schachtner H, Calaminus SD, Sinclair A, Monypenny J, Blundell MP, Leon C, Holyoake TL, Thrasher AJ, Michie AM, Vukovic M, Gachet C, Jones GE, Thomas SG, Watson SP, Machesky LM. Megakaryocytes assemble podosomes that degrade matrix and protrude through basement membrane. *Blood*. 2013; 121: 2542-52. 10.1182/blood-2012-07-443457.

6 Appendix

6.1 Abbreviations

μ	micro
aa	amino acid
AC	adenylyl cyclase
ACD	acid-citrate-dextrose buffer
AD	Alzheimer's disease
ADAP	adhesion- and degranulation-promoting adapter protein
ADP	adenosine diphosphate
AMPK	5' adenosine monophosphate-activated protein kinase
APS	ammonium peroxodisulphate
ARF	ADP ribosylation factor
ATP	adenosine triphosphate
BAPTA	1,2-bis(o-aminophenoxy)ethane-N,N,N',N'-tetraacetic acid
BM	bone marrow
BMC	bone marrow chimeras
bp	base pairs
BSA	bovine serum albumin
Ca^{2+}	calcium
CalDAG-GEF1	diacylglycerol regulated guanine nucleotide exchange factor I
CDK	cyclin dependent protein kinase
CISS	constructed interference in steady state
CK	casein kinase
CLEC-2	C-type lectin-like receptor 2
CRP	collagen-related peptide
CVX	convulxin
DAG	diacylglycerol
DIC	differential interference contrast
DMEM	Dulbecco's modified Eagle's medium
DMSO	dimethyl sulfoxide
dNTP	deoxynucleotidetriphosphate
Dok	downstream of tyrosine kinase
ECM	extracellular matrix

EDTA	ethylenediaminetetraacetic acid
EGF	epidermal growth factor
EGTA	ethylene glycol tetraacetic acid
ER	endoplasmic reticulum
ERK	extracellular-signal-regulated kinase
F	coagulation factor
f.c.	final concentration
FACS	fluorescence-activated cell sorting
FcR	Fc receptor
FCS	fetal calf serum
FIPI	fluoro-2-indolyl des-chlorohalopemide
FITC	fluorescein isothiocyanate
FSAP	Faktor VII activating protease
FSC	forward scatter
GDP	guanosine diphosphate
GEF	guanine exchange factor
GEF	guanine nucleotide exchange factor
GP	glycoprotein
GPCR	G protein-coupled receptors
GPS	Gray platelet syndrome
Grb2	growth factor receptor-bound protein 2
GTP	guanosine trisphosphate
h	hour(s)
HDL3	high density lipoprotein
HEPES	4-(2-hydroxyethyl)-1-piperazineethanesulfonic acid
HKD	HxKx4-Dx6GSxN
HRP	horseradish peroxidase
IFI	integrated fluorescent intensity
IFN	interferon
Ig	immunoglobulin
IL	interleukin
IP	immunoprecipitation
IP_3	inositol-1,4,5-trisphosphate
ITAM	immunoreceptor tyrosine-based activation motif
JAK	Janus kinase
kDa	kilo Dalton
LAT	linker for activation of T cells

M	molar
mAb	monoclonal antibody
MAP	mitogen-activated protein
MCA	middle cerebral artery
MFI	mean fluorescence intensity
min	minute(s)
MK	megakaryocyte
MLC	myosin light chain
MLCP	myosin light chain phosphatase
MMP	metalloproteinases
MPV	mean platelet volume
mTOR	mammalian target of rapamycin
NBEAL2	Neurobeachin like 2
PA	phosphatidic acid
PAR	protease-activated receptor
PC	phosphatidylcholine
PCR	polymerase chain reaction
PE	phosphatidylethanolamine
PE	phycoerythrin
PF	Platelet factor
PF4	platelet factor 4
PFA	paraformaldehyde
PGI_2	prostacyclin
PH	pleckstrin homology
PI	phosphatidylinositol
PI3K	phosphoinositide-3-kinase
PIP_2	phosphatidylinositol-4,5-bisphosphate
PIP5K	phosphatidylinositol 4-phosphate 5-kinase
PK	protein kinase
PL	phospholipase
Plt	platelets
PMA	phorbol 12-myristate 13-acetate
PPAR	peroxisome proliferator-activated receptor
PRP	platelet-rich plasma
PS	phosphatidylserine
PtdButOH	phosphatidylbutanol
PtdEtOH	phosphatidylethanol

PTP	protein tyrosine phosphatase
PVDF	polyvinylidene difluoride
PX	phox homology
RC	rhodocytin
RhoGEF	Rho-specific guanine nucleotide exchange factor
RIAM	Rap1-GTP-interacting adapter protein
ROCK	RhoA kinase
rpm	rotations per minute
RT	room temperature
s	second(s)
S6K	ribosomal S6 kinase
SD	standard deviation
SDS-PAGE	sodium dodecyl sulfate polyacrylamide gel electrophoresis
Ser	serine
SERCA	sarco/endoplasmic reticulum Ca^{2+}-ATPase
SH2	Src homology 2
SK	sphingosine kinase
SLP-76	Src homology 2 domain-containing leukocyte phosphoprotein of 76-kDa
SNARE	N-ethylmaleimide-sensitive fusion protein attachment protein receptors
SOCE	store-operated calcium entry
Sos1	son of sevenless homolog 1
Sphk	sphingosine kinase
SSC	side scatter
STIM	stromal interaction molecule
Syk	spleen tyrosine kinase
TAE	TRIS acetate EDTA
TBS-T	TRIS-buffered saline containing Tween
TEMED	tetramethylethylendiamin
TEM	transmission electron microscopy
TF	tissue factor
TG	thapsigargin
Thr	threonine
tMCAO	transient middle cerebral artery occlusion
TNF	tumor necrosis factor
TP	TxA_2 receptor

Treg	regulatory T cell
TRIS	tris(hydroxymethyl)aminomethane
TRPC	transient receptor potential channel
TTC	2,3,5-triphenyltetrazolium chloride
TxA_2	thromboxane
Tyr	tyrosine
U46	U46619
vWF	von Willebrand factor
w/o	without
WASP	Wiskott Aldrich Syndrome protein
wt	wildtype

6.2 Acknowledgments

The herein presented work was performed in the group of Prof. Bernhard Nieswandt at the Department of Experimental Biomedicine, University Hospital and Rudolf Virchow Center, University Würzburg.

During the period of my PhD work (September 2010 – April 2014) many people supported and helped me. I would like to thank the following people.

- My supervisor Prof. Bernhard Nieswandt for giving me the opportunity to accomplish by PhD thesis in his laboratory. His wide knowledge, support and enthusiasm have been of great value during my work. Further, I am very grateful that he allowed me to present my work at various international conferences, which were valuable experiences for my future career.
- Dr. Heike Hermanns and Prof. Manfred Gessler for their kind support, useful discussions and for reviewing my thesis.
- David Stegner for his continuous support, successful teamwork and his friendship. I am especially grateful for his scientific guidance, patience and encouragement during my PhD thesis and for carefully reading my thesis.
- My colleagues and friends in the laboratory for their great scientific and social encouragement contributing to the best working atmosphere one can imagine. I would like to thank especially Judith, Sarah, Deya, Michael, Simon, Timo and Carsten for proof-reading my thesis.
- All the past members of the lab for their experimental support and useful advices.
- Simon Stritt for fruitful discussion and his commitment to 'PLD in Megakaryocytes'.
- Ina Hagedorn for introducing me into the '*in vivo*' techniques.
- All the technicians for their kind help. My special thanks go to Juliana Goldmann for her excellent technical skills and assistance with my projects and to Sylvie Hengst for her help in the isotope laboratory.
- The animal caretakers for running the animal facility and taking care of the mice.
- Prof. Guido Stoll, Prof Christoph Kleinschnitz and especially Dr. Peter Kraft for great collaborative work.
- All the external collaboration partners for trustful cooperations and for giving me insights into new research fields.
- My final and most heartfelt acknowledgement goes to my parents and my friends for unconditional support in good and bad times during the time of my thesis.

6.3 Curriculum vitae

Name	Ina Thielmann
Date of birth	December 28th, 1984
Place of birth	Flensburg
Nationality	German

Education

2010 - now	PhD student in the group of Prof. Dr. Bernhard Nieswandt, Chair of Experimental Biomedicine / Vascular Medicine, University Hospital and Rudolf Virchow Center, Julius-Maximilians-Universität Würzburg
2010	Graduation, Diploma in Biology, Julius-Maximilians-Universität Würzburg
2004 - 2010	Study of Biology at the Johannes Gutenberg-Universität Mainz and Julius-Maximilians-Universität Würzburg
2004	German high school diploma (Abitur)
1991 - 2002	Primary, secondary and high school in Leck, Dohr, Culham (England) and Cochem

Würzburg, April 2014   _____

6.4 Publications

6.4.1 Original articles

1. Chen W, **Thielmann I**, Gupta S, Subramanian H, Stegner D, van Kruchten R, Dietrich A, Gambaryan S, Heemskerk J, Hermanns H, Nieswandt B, Braun A. Orai1-induced store-operated calcium entry enhances phospholipase activity and modulates TRPC6 function in murine platelets. *J Thromb Haemost*, 2014 Feb; 10

2. Kraft P, Göb E, Schuhmann MK, Göbel K, Deppermann C, **Thielmann I**, Herrmann AM, Lorenz K, Brede M, Stoll G, Meuth SG, Nieswandt B, Pfeilschifter W, Kleinschnitz C. FTY720 ameliorates acute ischemic stroke in mice by reducing thrombo-inflammation but not by direct neuroprotection. *Stroke.* 2013 Nov; 44; 3202-10.

3. Stegner D*, **Thielmann I***, Kraft P, Frohman MA, Stoll G, Nieswandt B. Pharmacological inhibition of phospholipase D protects mice from occlusive thrombus formation and ischemic stroke--brief report. *Arterioscler Thromb Vasc Biol.* 2013 Sep;33; 2212-7. * both authors contributed equally

4. Deppermann C, Cherpokova D, Nurden P, Schulz JN, **Thielmann I**, Kraft P, Vögtle T, Kleinschnitz C, Dütting S, Krohne G, Eming SA, Nurden AT, Eckes B, Stoll G, Stegner D, Nieswandt B. Gray platelet syndrome and defective thrombo-inflammation in Nbeal2-deficient mice. *J Clin Invest.* 2013 Jul 1.

5. Bender M, May F, Lorenz V, **Thielmann I**, Hagedorn I, Finney BA, Vögtle T, Remer K, Braun A, Bösl M, Watson SP, Nieswandt B. Combined in vivo depletion of glycoprotein VI and C-type lectin-like receptor 2 severely compromises hemostasis and abrogates arterial thrombosis in mice. *Arterioscler Thromb Vasc Biol*. 2013 May;33; 926-34.

6. **Thielmann I***, Stegner D*, Kraft P, Hagedorn I, Krohne G, Kleinschnitz C, Stoll G, Nieswandt B. Redundant functions of phospholipases D1 and D2 in platelet α-granule release. *J Thromb Haemost.* 2012 Nov;10; 2361-72. * both authors contributed equally

7. Königsberger S, Prodöhl J, Stegner D, Weis V, Andreas M, Stehling M, Schumacher T, Böhmer R, **Thielmann I**, van Eeuwijk JM, Nieswandt B, Kiefer F. Altered BCR signalling quality predisposes to autoimmune disease and a pre-diabetic state. EMBO J. 2012 Aug 1;31; 3363-74.

8. Ramanathan G, Gupta S, **Thielmann I**, Pleines I, Varga-Szabo D, May F, Mannhalter C, Dietrich A, Nieswandt B, Braun A. Defective diacylglycerol-induced Ca^{2+} entry but normal agonist-induced activation responses in TRPC6-deficient mouse platelets. *J Thromb Haemost.* 2012 Mar;10; 419-29.

6.4.2 Oral Presentation

56th Annual Meeting of the "Gesellschaft für Thrombose und Hämostase", St. Gallen, Switzerland, February 2012, 'Role of Phospholipase D in platelet function'.

6.4.3 Poster Presentation

- XXIV Congress of the International Society on thrombosis and hemostasis (ISTH), Amsterdam, The Netherlands, July 2013, 'Pharmacological Inhibition of Phospholipase D Protects Mice From Occlusive Thrombus Formation and Ischemic Stroke'.
- 17th International Vascular Biology Meeting (IVBM), Wiesbaden, Germany, June 2012 'Redundant functions of phospholipases D1 and D2 in platelet α-granule release'.
- Joint Symposium of the SFB 688 and the Comprehensive Heart failure Center Würzburg, Würzburg, Germany, June 2012. 'Redundant functions of phospholipases D1 and D2 in platelet α-granule release'.
- 6th International Symposium of the Graduate School of Life Science, Würzburg, Germany, October 2011, 'Phospholipase D1, but not PLD2, is essential for efficient GPIb-dependent $\alpha IIb\beta 3$ activation'.

6.5 Affidavit

I hereby confirm that my thesis entitled "Function and regulation of Phospholipase D in blood platelets: *in vitro* and *in vivo* studies in mice" is the result of my own work. I did not receive any help or support from commercial consultants. All sources and/or materials applied are listed and specified in the thesis.

Furthermore, I confirm that this thesis has not yet been submitted as part of another examination process neither in identical nor in similar form.

Würzburg, April 2014   _____

6.6 Eidesstattliche Erklärung

Hiermit erkläre ich an Eides statt, die Dissertation „Funktion und Regulation von Phospholipase D in Thrombozyten: *in vitro* und *in vivo* Studien in Mäusen" eigenständig, d.h. insbesondere selbständig und ohne Hilfe eines kommerziellen Promotionsberaters, angefertigt und keine anderen als die von mir angegebenen Quellen und Hilfsmittel verwendet zu haben.

Ich erkläre außerdem, dass die Dissertation weder in gleicher noch in ähnlicher Form bereits in einem anderen Prüfungsverfahren vorgelegen hat.

Würzburg, April 2014   _____